Characterization of the hydantoin-hydrolysing system of *Pseudomonas putida* RU-KM3$_S$

Thesis submitted in fulfilment of the requirements for the degree of

Doctor of Philosophy

of

Rhodes University

by

Gwynneth Felicity Matcher

April 2004

ABSTRACT

The biocatalytic conversion of 5-monosubstituted hydantoin derivatives to optically pure amino acids involves two reaction steps: the hydrolysis of hydantoin to *N*-carbamylamino acid by an hydantoinase or dihydropyrimidinase enzyme, followed by conversion of the *N*-carbamylamino acid to the corresponding amino acid by an *N*-carbamoylase enzyme. This biocatalytic process has been successfully applied in several industrial processes for the production of enantiomerically pure amino acids used in the synthesis of pharmaceuticals, insecticides, hormones, and food additives.

P. putida RU-KM3$_S$ was selected for study based on inherent high levels of hydantoinase and *N*-carbamoylase activity. Subsequent biocatalytic analysis of the enzyme activity within this strain revealed unique properties thus prompting further characterization. The main focus of this research was the isolation of the genes encoding the hydantoin-hydrolysing pathway in RU-KM3$_S$. A genomic library was constructed and screened for heterologous expression of the hydantoin-hydrolysing enzymes. However, this approach was unsuccessful prompting the use of transposon mutagenesis in order to circumvent the drawbacks associated with complementation studies. The enzymes responsible for hydantoin-hydrolysis were identified by insertional inactivation as a dihydropyrimidinase and β-ureidopropionase encoded by *dhp* and *bup* respectively. A third open reading frame, encoding a putative transport protein, was identified between the *dhp* and *bup* genes and appeared to share a promoter with *bup*. Analysis of the amino acid sequence deduced from *bup* and *dhp* substantiated the distinctive properties and potential industrial application of the L-enantioselective β-ureidopropionase and provided targets for potential optimisation of the substrate-selectivity and activity of the dihydropyrimidinase by site directed mutagenesis.

Several transposon-generated mutants with an altered phenotype for growth on minimal medium with hydantoin as the sole source of nitrogen were also isolated. Analysis of the insertion events in these mutants revealed disruptions of genes encoding key elements of the Ntr global regulatory pathway. However, inactivation of these genes had no effect on the dihydropyrimidinase and β-ureidopropionase activity levels. An additional mutant in which the gene coding for the dihydrolipoamide succinyltransferase, which is involved in the TCA cycle, was isolated with reduced levels of both dihydropyrimidinase and β-ureidopropionase activities. These results indicated that the hydantoin-hydrolysis pathway in RU-KM3$_S$ is regulated by carbon rather than nitrogen catabolite repression. This was confirmed by the

reduction of hydantoin-hydrolysis in cells grown in excess carbon as opposed to nitrogen. Identification of a putative CRP-binding site within the promoter region of these enzymes further supported the regulatory role of carbon catabolite repression (CCR). As CCR in Pseudomonads is poorly understood, elucidation of the mechanism by which the hydantoin-hydrolysing pathway in RU-KM3$_S$ is regulated would provide valuable insight into this complex process.

TABLE OF CONTENTS

LIST OF FIGURES

LIST OF TABLES

LIST OF ABBREVIATIONS

5-FU	5-fluorouracil
AMM	Minimal medium with ammonium as sole nitrogen source
ATP	Adenosine triphosphate
BLAST	Basic Local Alignment Search Tool
bp	Base pair
cAMP	Cyclic adenosine monophosphate
CAP	Catabolite activator protein
CCR	Carbon catabolite repression
CFE	Cell-free extract
Crc	Catabolite repression control protein
CRP	cAMP receptor protein
CTAB	Hexadecyltrimethyl-ammonium bromide
dddH_2O	Triple distilled water
DNA	Deoxyribonucleic acid
EMS	Ethylmethane sulfonate
GMM	Minimal medium with glycine as sole nitrogen source
HMM	Minimal medium with hydantoin as sole nitrogen source
IPTG	Isopropyl-β-thiogalactosidase
mRNA	Messenger RNA
Na_2EDTA	Ethylene diamine tetra-acetic acid
***N*-carbamoylase**	*N*-carbamoylamino acid amidohydrolase
NCBI	National Centre for Biotechnology Information
NCG	*N*-carbamylglycine
Ntr	Global nitrogen regulatory system
OD_{600}	Optical density at 600nm
ORF	Open reading frame
PCR	Polymerase chain reaction
RNA	Ribonucleic acid
RNase	Ribonuclease
rpm	Revolutions per minute
SDS	Sodium dodecyl sulphate
TCA	Tricarboxylic acid cycle
TE buffer	Tris-EDTA buffer
Tris	Tris-2-amino-2-(hydroxymethyl)-1,3-propandiol
UMM	Minimal medium with uracil as sole nitrogen source
Vfr	Virulence factor regulator
X-gal	5-bromo-4-chloro-3-indolyl-β-D-galactopyranosidase
Δ	Deletion

ACKNOWLEDGMENTS

My most sincere thanks to my wonderful supervisor Professor Dorrington, whose enthusiasm and dedication to science has been an inspiration and who has guided and encouraged me throughout my studies. Thank you for all your effort in providing a wonderful working environment and for invaluable guidance and critical input into this project.

Thanks are also due to the members of Lab 417, past and present, for their friendship and intellectual stimulation. To my friends Meesbah Jiwaji and Fritha Hennessy who kindly proofread this thesis, provided valuable criticisms, technical assistance, and encouragement where needed. In particular, I would like to thank Carol Hartley for helping me as I started out on this project and Meesbah Jiwaji for her inexhaustible cheerfulness and encouragement. To Dr Bradley for technical assistance with the phylogenetic tree.

For all their love and support, I would like to thank my very special family without whom I would not have completed this project. For picking me up and encouraging me when times were trying and loving me regardless of how difficult life became. I thank God for so richly blessing me with such a wonderful family and some special friends.

For funding of this research, I gratefully acknowledge Rhodes University, AECI (Pty) Ltd. South Africa, and the DACST Innovation Fund.

RESEARCH OUTPUTS

Burton S.G., Dorrington R.A., Hartley C., Kirchmann K., Matcher G, Phehane V. (1998) Production of enantiomerically pure amino acids: characterization of South African hydantoinases and hydantoinase-producing bacteria. *Journal of Molecular Catalysis B: Enzymatic* **5**, 301-305

Buchanan K., Burton S.G., Dorrington R.A., Matcher G.F., Skepu Z. (2001) A novel *Pseudomonas putida* strain with high levels of hydantoin-converting activity, producing L-amino acids. *Journal of Molecular Catalysis B: Enzymatic* **11**, 397-406

Matcher G.F., Burton S.G., Dorrington R.A. (2004) Mutational analysis of the hydantoin hydrolysis pathway in *Pseudomonas putida* RU-KM3$_S$. *Applied Microbiology and Biotechnology*, In Press.

1.1 INTRODUCTION

Natural living systems are intrinsically chiral with stereochemistry a characteristic feature of enzymatic reactions, messenger-receptor interactions and metabolic processes. Consequently, metabolic and regulatory systems within an organism are sensitive to interaction with chiral compounds and often display different responses to the action of a pair of enantiomers. Thus, when considering xenobiotics such as agrochemicals, food additives, pharmaceuticals, flavours, and fragrances, the stereochemistry of the compounds must be taken into account (Maier *et al.* 2001).

Numerous pharmacological studies on the relative activities of enantiomers of a target drug have indicated that the (S)-isomer not only has a greater therapeutic effect than the (R)-isomer (28-fold in the case of ibuprofen) but therapeutic concentrations in the blood are reached more rapidly with optically pure compounds than with the racemic mixture (Zaks and Dodds 1997). Furthermore, the enantioselectivity of drugs has implications in terms of bioavailability, distribution, side-effects and even toxicity (Maier *et al*. 2001). D-enantiomer pharmaceuticals have also been shown to be more stable against decomposition in the liver, kidney, and bloodstream than their L-analogs (Bommarius *et al*. 1998).

The importance of utilizing the more biologically active enantiomer can be applied to agrochemicals and crop-protection as well. Treatment with less- or non-active stereoisomers not only increases the degree of pollution without any reciprocal benefits but may be toxic or counterproductive (Maier *et al.* 2001). In order to produce balanced food or feed, cereals are often supplemented with amino acids such as lysine (Demain 2000). However, addition of D-amino acids results in a nutritionally poor product as mammals are unable to metabolise or use these amino acids (Maier *et al*. 2001).

1.1.1 Chiral amino acids in industry

Chiral precursors are used to synthesize complex enantiomerically pure compounds. Interest in enantiomerically pure amino acids in particular is primarily due to the increasing use of unnatural amino acids in the production of pharmaceuticals or pesticides resulting in novel activity of the substances produced. A few of the chiral amino acids produced industrially and the compounds for which they are used as precursors are listed in Table 1.1.

Table 1.1 Some examples of optically pure amino acids and their applications in industry

Amino acid	Industrial application
D-phenylglycine	Cefaclor (antibiotic)[4]
D-hydroxyphenylglycine	Amoxicillin (antibiotic)[1, 5]
	Cephadroxil (cephalosporins)[5]
D-valine	Fluvanate (pyrethroid insecticide)[1, 2]
D-cysteine	Beta-lactam antibiotics[6]
D-aspartic acid	Beta-lactam antibiotics[6]
D-alanine	Synthetic sweetner[6]
L-homophenylalanine	Benazepril, Lisinopril, Quinapril (angiotensin converting enzyme inhibitor)[3]
L-*tert*-leucine	Sandoz (antiviral)[1, 2]
	Abbott (HIV protease inhibitor)[1, 2]
	Biomega (antiviral)[1, 2]
	BB-2516 (antitumour)[1, 2]
	RO-31-9790 (anti-inflammatory)[1, 2]
	Zeneca (antitumour)[1, 2]
	Marimastat (anticancer)[5]
	Captopril (cardiovascular)[5]
L-valine	Valaciclovir (reverse-transcriptase inhibitor)[2]
L-leucine	Ubestatin, Bestatin (immunostimulant)[2]
	Orlistat (hypolipidemic)[2]
L-methionine	Dorcarpamine, Tanadopa (cardiovascular, antiallergenic)[2]
	Ademethionine, Gumbaral (antiarthritic)[2]

(Bommarius *et al.* 1998[1], Drauz 1997[2], Hu *et al*. 2003[3], Liese and Filho 1999[4], Schulze and Wubbolts 1999[5], Yagasaki and Ozaki 1998[6])

The use of biocatalysts is an attractive alternative to chemical production of enantiomerically pure amino acids. Due to their specific regioselectivity, enzymes do not require substrate functional-group protection thus bypassing the additional steps required to block and unblock substituents required in organic syntheses (Schmid *et al.* 2001). Furthermore, enzymes function at lower temperatures and neutral pH, produce fewer toxic by-products, exhibit broad substrate-range, and are strictly stereospecific (Koeller and Wong 2001, Azerad 1995).

1.1.2 Hydantoin-hydrolysis for the production of enantiopure amino acids

Biocatalytic production of optically pure amino acids is primarily done via dynamic resolutions and asymmetric synthesis (Schulze and Wubbolts 1999). The most prominent example of dynamic kinetic resolution is the production of D-*p*-hydroxyphenylglycine from a benzylic hydantoin derivative by the hydantoinase, *N*-carbamylamino acid amidohydrolase (*N*-carbamoylase) and racemase enzymes (Schultze and Wubbolts 1999). Hydrolysis of hydantoin derivatives to form enantiospecific amino acids has several advantages including a potentially 100% yield with 100% enantiopure amino acid produced from a racemic substrate (Altenbuchner *et al*. 2001). In addition, most D,L-5-monosubstituted hydantoin derivatives can be readily synthesized from inexpensive chemical precursors (Syldatk *et al*. 1992a).

The use of hydantoin-hydrolysing enzymes has been found to be applicable to the production of highly lipophilic, silicon-containing amino acids. This non-natural amino acid offers several advantages including prevention of hydrophobic pocket collapse, higher lipophilicity, and enhanced stability towards proteolytic degradation (Smith *et al*. 2001). D- and L-enantioselective *N*-carbamoylases have also been shown to recognise the configuration of the α-carbon as well as the β-carbon of some *N*-carbamylamino acids (Ogawa *et al.* 1999a,b). This is extremely valuable in the synthesis complex of α,β-diastereomeric amino acids which can be found in four stereoisomers and which makes stereospecific synthesis of these compounds difficult by conventional chemical or enzymatic methodologies (Ogawa *et al.* 1999a,b, 2001).

D-*p*-hydroxyphenylglycine is the most important compound produced by the hydantoinase process to date (Syldatk *et al.* 1999) with approximately 2000 tons produced each year (Ogawa and Shimizu 2002). There are three main processes used by competing industrial companies to produce D-*p*-hydroxyphenylglycine. Kanegafuchi Chemical Industries hydrolyse 5-(4'-hydroxyphenyl)hydantoin with immobilized *Bacillus brevis* cells containing D-hydantoinase while Snamprogetti use immobilized dihydropyrimidinase purified from calf liver. In both processes the resultant *N*-carbamyl-D-*p*-hydroxyphenylglycine is then chemically treated with HNO_2 to produce D-*p*-hydroxyphenylglycine (Syldatk *et al*. 1990b). Recordati and Degussa use resting cells of *Agrobacterium radiobacter* expressing both a D-hydantoinase and D-carbamoylase thereby negating the necessity of treatment with HNO_2 (Syldatk and Pietzsch 1995).

An L-stereoselective industrial process for the production of non-natural aromatic L-amino acids has been developed by Rütgers using whole cells of *Arthrobacter aurescens* DSM 3745 and DSM 3747 both of which express an L-hydantoinase, L-carbamoylase, and racemase enzymes (Syldatk and Pietzsch 1995). Amino acids produced via this method

include L-tryptophan, L-phenylalanine, L-O-benzylserine, *p*-chloro-phenylalanine, *p*-fluorophenyl-alanine, *p*-nitro-phenylalanine, 1'-naphthylalaine, 2'-naphthylalanine, 3,4-dimethoxyphenyl-alanine, and 2'-thienylalanine (Syldatk and Pietzsch 1995).

1.2 HYDROLYSIS OF 5-MONOSUBSTITUTED HYDANTOINS

Hydantoin, also known as imidazolidine-2,4-dione or 2,4-diketotetrahydroimidazole, was first discovered in 1861 by Baeyer as a reduction/hydrogenation product of the naturally occurring cyclic amide allantoin (Syldatk and Pietzsch 1995). Subsequently, hydantoins have been isolated from several natural sources such as white shoots of sugar beet and oriental plane tree buds (Ware 1950). Hydantoin derivatives have long been of interest in industry and are utilized as anticonvulsants in epilepsy treatment, as herbicides, fungicides, antimicrobial, and virucidal agents (Syldatk *et al*. 1992a). However, as discussed above, the microbial hydrolysis of 5-monosubstituted hydantoins resulting in the production of enantiomerically pure D- and L-amino acids has gained in interest in recent years (Syldatk *et al.* 1999).

1.2.1 Enzymatic hydrolysis of hydantoins

Microbial cleavage of hydantoins is widespread in nature and can be catalysed by a variety of enzyme systems. Hydrolysis of 5-monosubstituted hydantoin derivatives to the corresponding amino acids occurs via three reactions (Figure 1.1). Firstly, the ring structure of the hydantoin molecule is opened by cleavage of the cyclic amide bond at position 2 of the hydantoin ring. The resultant *N*-carbamylamino acid is then converted to the corresponding amino acid either chemically or enzymatically. Depending on the stereospecificities of the enzymes involved in these two reactions, the end product is either a D- or L-enantiomer. The third component of the hydrolysis of racemic hydantoins to optically pure amino acids involves spontaneous or enzymatic racemization of the unreacted hydantoin substrate (Syldatk and Pietzsch 1995).

Of the enzymes listed in Figure 1.1, the dihydropyrimidinase, hydantoinase (D-, L-, non-stereospecific), *N*-carbamoylamino acid amidohydrolase (D- or L-stereospecific), and β-ureidopropionase are of particular interest due to the generally high activity levels and broad substrate-selectivities observed.

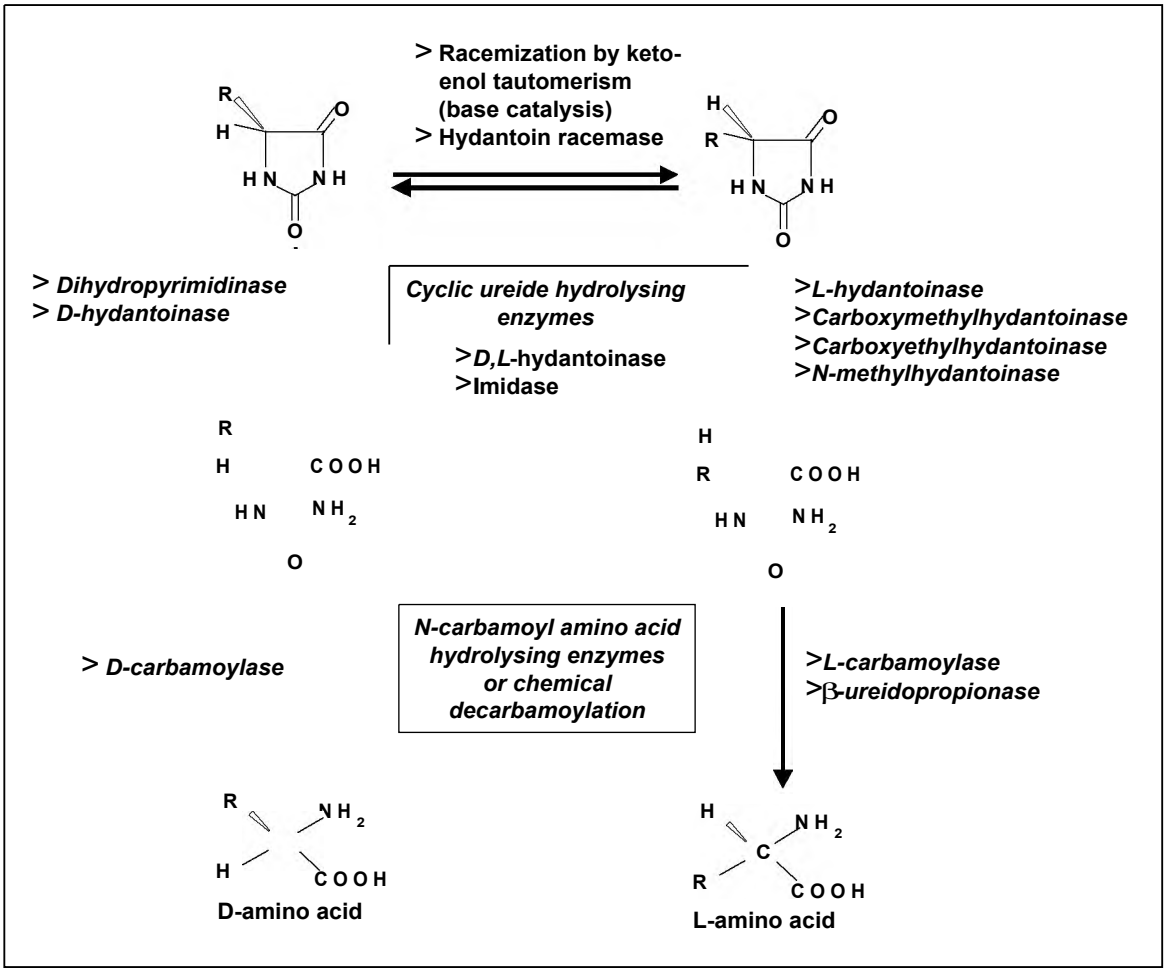

Figure 1.1 Enzymatic hydrolysis of hydantoin to form enantiomerically pure amino acids (modified from Ogawa and Shimizu 1997).

1.2.2 Hydantoin-hydrolysing enzymes

Hydantoinase belongs to the E.C. 3.5.2 group which includes enzymes able to hydrolyse cyclic amide bonds (Syldatk *et al*. 1990b). Enzymes within this category capable of hydrolysing hydantoin include hydantoinase, dihydropyrimidinase, imidase, carboxymethylhydantoinase, carboxyethylhydantionase, *N*-methylhydantoinase, and allantoinase enzymes. Of these, only two enzymes, carboxymethylenehydantoinase (E.C. 3.5.2.4) and allantoinase (E.C. 3.5.2.5), hydrolyse naturally occurring hydantoin derivatives as their natural substrates. The remaining enzymes within this classification, while able to hydrolyse hydantoin derivatives, have unknown natural functions and/or hydrolyse natural substrates which contain no hydantoin ring (Syldatk *et al.* 1990b, Syldatk and Pietzsch 1995).

Allantoinase (allantoin amidohydrolase, 5-ureidohydantoinase), whilst absent in mammals, is found in microorganisms and plants (Syldatk *et al.* 1999) and functions naturally in the purine degradation pathway. However, the allantoinase enzyme has a high substrate specificity

and low enantioselectivity thus biotechnological application of this enzyme is limited (Syldatk *et al*. 1999). The catalytic function of carboxymethylenehydantoinase (L-carboxymethyl-hydantoin amidohydrolase) is postulated to be involved in a side reaction in the metabolism of pyrimidines (Syldatk and Pietzsch 1995) but, besides the ability to hydrolyse carboxy-methylhydantoin to L-aspartic acid, no investigation of the substrate spectrum or enzymatic properties of this enzyme has been done (Syldatk *et al.* 1999). *N*-methylhydantoin amidohydrolase (*N*-methylhydantoinase) is an ATP-dependent enzyme that hydrolyses *N*-methylhydantoin to *N*-carbamoylsarcosine which is part of the creatinine degradation pathway (Ogawa and Shimizu 1997). *N*-methylhydantoinase is able to hydrolyse hydantoin derivatives L-specifically but is unable to hydrolyse dihydropyrimidines (Ogawa *et al.* 1995a), and due to its ATP-dependence it is an unlikely candidate for industrial production of optically pure amino acids (Syldatk *et al*. 1999). Imidase functions in the initial part of the cyclic amide metabolic pathway. Whilst this enzyme was shown to hydrolyse simple cyclic imides and cyclic ureides such as dihydrouracil and hydantoin, bulky imides and 5-monosubstituted hydantoins were not hydrolysed (Soong *et al*. 2001). Lastly, carboxyethylhydantoinase has been shown to be involved in the degradation of histidine and is classified as L-stereoselective. However, very little research has been done on this enzyme to date (Syldatk *et al.* 1999).

Of primary interest when considering enzymes capable of hydrolysing hydantoin derivatives to the corresponding *N*-carbamylamino acids are the dihydropyrimidinase and hydantoinase enzymes. Hydantoinase enzymes have been found in a wide variety of organisms including plants (Eadie *et al.* 1949 cited in Syldatk *et al.* 1999, Morin 1993), animals (Bernheim and Bernheim 1946, Wada 1934 cited in Syldatk *et al*. 1999, Cecere *et al.* 1975) and bacteria. Hydantoinase enzymes have predominantly been characterized from bacterial isolates including species such as *Agrobacterium* (Hils *et al*. 2001, Durham and Weber 1995, Grifantini *et al*. 1998, Hartley *et al.* 1998), *Arthobacter* (Moller *et al*. 1988, Siemann *et al.* 1999, Gross *et al*. 1990, May *et al.* 1998a, Volkel and Wagner 1995), *Bacillus* (Luksa *et al*. 1997, Kim *et al*. 1997, Mukohara *et al*. 1994, Park *et al*. 1998), *Pseudomonas* (Buchanan *et al*. 2001, Gokhale *et al*. 1996, Chien *et al*. 1998, LaPointe *et al.* 1994, Yokozeki *et al*. 1987b, Sudge *et al*. 1998, Ishikawa *et al.* 1997), *Thermus* (Abendroth *et al.* 2000a), *Flavobacterium* (Yokozeki *et al*. 1987d), and *Methanococcus* (Chung *et al*. 2002), and have been shown to hydrolyse 5-monosubstituted hydantoin derivatives effectively.

Traditionally, hydantoinase enzymes have been classified according to their hydrolytic enantioselectivity and grouped as L-, D-, or non-enantioselective hydantoinases respectively. However, this is misleading as it implies that the hydantoinase enzymes differ solely in their enantioselectivities which is not the case. Furthermore, enantioselectivity of hydantoinase enzymes from *Arthrobacter* sp. DSM 3745 and *Flavobacterium* sp. have been shown to be

substrate dependent (May *et al.* 1998a, Yokozeki *et al*. 1987e cited in Syldatk *et al*. 1999). However, for the purposes of this literature review, hydantoinases have been grouped based on their predominant enantioselectivity.

1.2.2.1 D-enantioselective hydantoinases

D-enantioselective hydantoinases are often considered synonymous with dihydropyrimidinases (Syldatk *et al.* 1999). This is due to the finding that isolated dihydropyrimidinases were capable of hydrolysing 5-monsubstituted hydantoin derivatives as well as their natural substrate dihydropyrimidines (Xu and West 1994). Also, several D-hydantoinases which have subsequently been isolated are able to hydrolyse dihydrouracil as a substrate (Lee *et al*. 1995, Sharma and Vohra 1997, Siemann *et al.* 1999, Durham and Weber 1995, Ogawa *et al.* 1995b, Sudge *et al.* 1998). In contrast, the dihydropyrimidinase from *Clostridium uracilicum* has been shown to be unable to hydrolyse hydantoin (Campbell 1958 cited in Syldatk *et al*. 1999) and an hydantoinase was isolated from *Agrobacterium* sp. IP I-671 which was unable to hydrolyse dihydrouracil (Runser and Meyer 1993). Thus, while the names D-hydantoinase and dihydropyrimidinase are often used interchangeably, these are in fact two separate enzymes with different catalytic capabilities. D-hydantoinase enzymes from a wide variety of bacterial species have been described in literature. Some of the characteristics of these enzymes are summarized in Table 1.2.

With the exception of the D-hydantoinases from *Bacillus stearothermophilus* SD-1 and *Burkholderia pickettii*, which are dimeric in structure (Lee *et al.* 1995, Xu *et al.* 2003a), the remaining D-hydantoinases analysed were found to form tetramers (Table 1.2). The optimum temperature for the catalytic activity of these enzymes ranged from 30^{o}C for *Pseudomonas desmolyticum* NCIM 2212 (Gokhale *et al*. 1996) to 75^{o}C for *Bacillus circulans* (Luksa *et al.* 1997) with the majority of the D-hydantoinases functioning optimally at ~60^{o}C (Table 1.2). With respect to optimal pH for hydantoin hydrolysis by D-hydantoinases, the highest activities generally occurred at alkali pH (pH 8-10) (Table 1.2).

In all instances where metal ion dependency has been investigated, D-hydantoinases have been observed to require divalent metal ions as co-factors (Table 1.2). Consequently, these enzymes are sensitive to metal ion chelators and are stimulated by metal ions such as Mn^{2+} and Co^{2+}. This metal ion dependency was verified by crystallographic analysis of D-hydantoinases from *Thermus* sp. (Abendroth *et al*. 2002a), *Burkholderia pickettii* (Xu *et al*. 2003a), and *B. stearothermophilus* SD-1 (Cheon *et al*. 2002) in which two metal ions were identified within the catalytic site. These studies are described in greater detail in Section 1.3.1. In most cases, the co-factor was Zn^{2+} which could be replaced by other divalent transition group metals such as Mn^{2+} or Co^{2+} (Abendroth *et al.* 2002a).

Table 1.2 Biochemical and genetic properties of bacterial D-hydantoinase enzymes.

Source	Substrate selectivity	Opt. Temp.	Opt. pH	Metal ions		Encoding gene	Subunit molecular weight	Total molecular weight	Reference
				Inhibition	Stimulation				
Agrobacterium sp. IP I-671	BeH>HPG>MTH> BuH>IBH>IPH>MH> Hyd (No DHU)	60 °C	10.0	Metal ion chelators	Ni^{2+}, Mg^{2+}	*hyuH* (1374bp)	50kDa	250kDa	Hils *et al.* 2001, Runser and Meyer 1993, Runser and Ohleyer 1990
Agrobacterium tumefaciens 47C	DHU>MH>PH>MTH >IBH>BuH>IPH> HMH>BeH	70 °C	10.0	-	None	-	-	-	Durham and Weber 1995
Agrobacterium tumefaciens NRRL B 11291 (formerly *A. radiobacter*)	THE>MPH>CPH> PH>BH>HPG>MH	60 °C	9.0	Fe^{2+}	Mn^{2+}	ORF2 (1370bp)	50kDa	-	Grifantini *et al.* 1998, Olivieri *et al.* 1981 Achary *et al.* 1997
Agrobacterium tumefaciens RU-OR	MH>HPG>Hyd	40-60 °C	9.0	-	-	-	-	-	Hartley *et al.* 1998, Burton *et al.* 1998
Arthrobacter crystallopoietes AM 2	Hyd>MH=HMH >DHU	50 °C	9.2	No effect with EDTA	-	-	-	-	Moller *et al.* 1988
Arthrobacter crystallopoietes DSM 20117	Hyd>PH>MTH> HPG>BeH>DHU	50 °C	8.0	No effect with EDTA	Zn^{2+} within the subunits	-	60kDa	257kDa	Siemann *et al.* 1999
Bacillus circulans	Hyd>PH>BH> MTH>PrH>IBH	75 °C	8.0-10.0	-	Mn^{2+}, Ni^{2+}, Co^{2+}	-	53kDa	212kDa	Luksa *et al.* 1997
Bacillus sp. AR9	Hyd>PH>DHU >HPG	65 °C	9.5	-	Mg^{2+}, Ni^{2+}, Mn^{2+}, Co^{2+}	-	-	-	Sharma and Vohra 1997

Source	Substrate selectivity	Opt. Temp.	Opt. pH	Metal ions		Encoding gene	Subunit molecular weight	Total molecular weight	Reference
				Inhibition	Stimulation				
Bacillus stearothermophilus SD-1	Hyd>DHU>PH >HPG	65 °C	8.0	-	Mn^{2+}	ORF (1419bp)	54kDa	126kDa	Kim *et al*. 1997, Lee *et al*. 1995
Bacillus stearothermophilus NS1122A	MH>MTH>IBH>IPH> BeH	60 °C	9.5	-	Mn^{2+}, Co^{2+}, Ni^{2+}	ORF (HN) (1416bp)	51.7kDa	200kDa	Mukohara *et al*. 1994, Ishikawa *et al*. 1994
Bacillus thermocatenulatus GH-2	HPG	65 °C	7.5	EDTA	Mn^{2+}	-	56kDa	230kDa	Park *et al*. 1998, Kim *et al*. 1998
Blastobacter sp. A17p-4	Hyd>DHU>MH> MTH	60 °C	9.0-10.0	Hg^{2+}	Ni^{2+}, Co^{2+}, Mn^{2+}	-	53kDa	200kDa	Soong *et al*. 1999, 2001
Burkholderia pickettii	-	50 °C	8.0	-	Co^{2+}, Mn^{2+}, Zn^{2+}, Fe^{2+}, Ni^{2+}	-	52kDa	110kDa	Xu *et al*. 2003a
Pseudomonas desmolyticum NCIM 2112	PH	30 °C	9.5	-	-	-	-	-	Gokhale *et al*. 1996
Pseudomonas putida 7711-2	-	-	-	-	-	*dht* (1440bp)	52.5kDa	-	Chen and Tsai 1998
Pseudomonas putida CCRC 12857	HPG	-	-	-	-	*dht* (1485bp)	53.4kDa	-	Chien *et al*. 1998

Source	Substrate selectivity	Opt. Temp.	Opt. pH	Metal ions		Encoding gene	Subunit molecular weight	Total molecular weight	Reference
				Inhibition	Stimulation				
Pseudomonas putida DSM 84	DHU>methionine >IPH (Hyd=poor)	55 °C	9.0	Cu^{2+}	Mn^{2+}, Fe^{2+}	ORF1 (1104bp)	60kDa	230kDa	Morin *et al*. 1986a,b, LaPointe *et al*. 1994
Pseudomonas putida IFO 12996	DHU>>MH>Hyd	45-55 °C	8.0-9.0	Metal ions chelators	-	-	-	190kDa	Takahashi *et al*. 1978, Ogawa *et al*. 1994c
Pseudomonas sp. AJ-11220	CEH>MTH=hyd>CH >PH>HPG>MH>BeH (very low DHU)	43 °C	8.0	Hg^{2+}	Mg^{2+}, Mn^{2+}, Co^{2+}, Ni^{2+}, Cu^{2+}		-	-	Yokozeki *et al*. 1987b
Pseudomonas sp. KBEL 101	HPG	30 °C	8.0	-	-	-	-	-	Kim and Kim 1993
Pseudomonas sp. NCIM 5109	DHU>Hyd>PH> HPG	30 °C	9.0-9.5	-	-	-	-	-	Sudge *et al*. 1998
Thermus sp.	Prefers 5-phenylic substituted hydantoins	-	-	-	Mn^{2+}, Zn^{2+} within the subunits	-	-	50kDa	Abendroth *et al*. 2000a, 2002a

(BeH= 5-benzylhydantoin; BuH= 5-(sec)-butylhydantoin; CEH= 5-cyanoethylhydantoin; CH= 5-carbamylethylhydantoin; CPH= chlorophenylhydantoin; DHU= dihydrouracil; HMH=hydroxymethylhydantoin; HPG= 5-hydroxyphenylglycine; IBH= 5-isobutylhydantoin; IPH= 5-isopropylhydantoin; MH= 5-methylhydantoin; MPH= methyoxyphenylhydantoin; MTH= 5-(2-methylthioethyl)hydantoin; PH= 5-phenylhydantoin; PrH= propylhydantoin; THE= thienylhydantoin, Opt. : optimal)

The genes encoding D-hydantoinase enzymes have been isolated from *P. putida* DSM 84, *B. stearothermophilus* SD-1, *Agrobacterium* sp. IP I-671, *A. tumefaciens* NRRL B11291, *P. putida* CCRC 12857, *P. putida* 7711-2, and *B. stearothermophilus* NS1122A (Table 1.2). The D-hydantoinase-encoding gene from *Agrobacterium* sp. IP I-671 was isolated by screening a genomic phage library by plaque hybridisation with the previously isolated, DIG-labelled *N*-carbamoylase gene as a probe (Hils *et al*. 2001). The genes encoding the hydantoinase, *N*-carbamoylase and racemase enzymes in this strain were located as a cluster on a native 190kb plasmid (Hils *et al.* 2001). However, the hydantoinase gene isolated was not the only gene encoding for a hydantoin-hydrolysing enzyme present in *Agrobacterium* sp. IP I-671 as inactivation of *hyuH* resulted in 15% residual D-hydantoinase activity (Hils *et al*. 2001).

The amino acid sequence of the D-hydantoinase from *B. stearothermophilus* strains SD-1 (Kim *et al*. 1997) and NS1122A (Mukohara *et al.* 1994) were almost identical with the majority of the few variations observed located in the C-terminal region (Kim *et al*. 1997). However, despite the high similarity between these two enzymes, their biochemical properties differed significantly including variations in oligomeric structure with the hydantoinase from *B. stearothermophilus* SD-1 forming a dimer whilst the *B. stearothermophilus* NS1122A hydantoinase formed a tetramer (Kim *et al*. 1997). This suggested that the C-terminal region has an important role in the structural and/or catalytic properties of these enzymes. The D-hydantoinase encoding gene from *Bacillus thermocatenulatus* GH2, which was found have an identical nucleotide sequence to the corresponding gene in *B. stearothermophilus* NS1122A, was digested with exonuclease III in order to determine if the C-terminal region was important for enzyme activity (Kim and Kim 1998). Enzyme activity was still detected when up to 40 amino acid residues had been deleted implying that the non-homologous C-terminal regions are not involved in the catalysis reaction (Kim and Kim 1998). However, deletion of 11 to 12 amino acids from the C-terminal end of the *B. thermocatenulatus* GH2 D-hydantoinase gave rise to a dimeric protein, as opposed to the parental tetramer, while the dimeric nature of the *B. stearothermophilus* SD-1 hydantoinase remained unchanged (Kim and Kim 1998).

In contrast to the *Bacillus* hydantoinases, the C-terminus of the D-hydantoinase from *P. putida* CCRC 12857 was found to be involved in the catalytic activity of the enzyme as deletion of 32 amino acids from the C-terminal end resulted in loss of hydantoinase activity in this strain (Chien *et al*. 1998). It is interesting that the D-hydantoinases for which the amino acid sequences are known all consist of more than 450 amino acid residues except for the hydantoinase from *P. putida* DSM 84 which was approximately 100 residues shorter in the carboxyl terminus (LaPointe *et al.* 1994, Chien *et al.* 1998).

1.2.2.2. L- and non-enantioselective hydantoinases

Production of L-amino acids from 5-monosubstituted hydantoin derivatives is performed by L-enantioselective *N*-carbamoylases in conjunction with either an L- or non-enantioselective hydantoinase. Significantly fewer L- and non-enantioselective hydantoinases have been isolated in comparison to D-hydantoinases (Table 1.2 vs. Table 1.3). L-hydantoinases have been reported from *Bacillus* (Yamashiro *et al*. 1988 cited in Syldatk *et al*. 1992b), *Flavobacterium* (Yokozeki *et al*. 1987e cited in Syldatk *et al*. 1992b), and *Methanococcus* (Chung *et al*. 2002) species whilst non-enantioselective hydantoinases were found in *Arthrobacter* (Gross *et al*. 1990, Volkel and Wagner 1995, Wagner *et al*. 1996) and *Pseudomonas* (Ishikawa *et al*. 1997) species.

The hydantoinases from *Arthrobacter aurescens* DSM 3745 and *Flavobacterium* sp. cannot be conveniently classified as D-, L-, or non-enantioselective as the enantioselectivity observed in these strains appears to be substrate dependent (May *et al.* 1998a, Yokozeki *et al.* 1987e cited in Syldatk *et al*. 1999). Specifically, the hydantoinase from *Flavobacterium* hydrolysed indolylmethylhydantoin L-enantioselectively and benzyloxymethylhydantoin D-selectively (Yokozeki *et al.* 1987e cited in Syldatk *et al*. 1999). In the case of the *Arthrobacter* hydantoinase, strict L-enantioselectivity was observed with D,L-5-indolylmethyl-hydantoin whilst, when supplied with 5-(2-methylthioethyl)-hydantoin the D-enantiomer intermediate was produced in 3-fold excess to that of the corresponding L-enantiomer (May *et al.* 1998a). The substrate-dependent enantioselectivity of the hydantoinase from *A. aurescens* DSM 3745, along with the inability to hydrolyse unsubstituted hydantoin suggested that this enzyme should be classified as a new member of the EC group 3.5.2 (May *et al*. 1998a). This was substantiated by phylogenetic analysis of this enzyme with dihydropyrimidinases, allantoinases, ureases, and dihydroorotases in which it forms a novel branch of the phylogenetic tree (May *et al.* 1998d). Selected characteristic biochemical and genetic properties of the L- and non-enantioselective hydantoinases reported in literature are summarized in Table 1.3.

As with the D-hydantoinases, the optimum pH for the catalytic activity of L- and non-enantioselective hydantoinases was found to be at slightly alkaline to alkaline pH (Table 1.3). Optimum temperature ranged from 37^{o}C for the non-selective hydantoinase from *Arthrobacter* sp. DSM 9771 through to 80^{o}C for the L-hydantoinase from *Methanococcus jannaschii* (Table 1.3).

Table 1.3 Biochemical and genetic properties of bacterial L- and non-enantioselective hydantoinase enzymes.

Source	Stereo-selectivity	Substrate selectivity	Opt. Temp.	Opt. pH	Metal ions		Encoding gene	Subunit molecular weight	Total molecular weight	Reference
					Inhibition	Stimulation				
Arthrobacter aurescens DSM 3747	non	BuH, BeH, HBH, DHBH, BMEH, IMH	50 °C	8.8-9.25	Metal chelator : EDTA	Mn^{2+}, Co^{2+}	*HyuH* (1376bp)	49.6kDa	232kDa	Gross *et al.* 1990, Syldatk *et al*. 1992b, Wiese *et al.* 2001
Arthrobacter aurescens DSM 3745	Substrate dependent (L for IMH, non for MTEH, D for MH)	ClBH>IMH>MTH> BeH>ABH>MTH>FBH (No Hyd, DHU)	-	-	Metal chelator : EDTA	Co^{2+}, Mn^{2+}, Zn^{2+}	-	49.68kDa	200kDa	May *et al*. 1998a, b, c
Arthrobacter sp. DSM 7330	non	BeH>IMH>MTH>PH	<47 °C	8.0-9.4	Hg^{2+}, Cu^{2+}	Zn^{2+} >Co^{2+}	-	58kDa	120kDa	Volkel and Wagner 1995
Arthrobacter sp. DSM 9771	non	MTH	37 °C	7.5	-	-	-	-	-	Wagner *et al*. 1996, May *et al.* 2000
Bacillus brevis AJ 12299	L	MH, PrH, BuH, MTH, BeH, HBH	50 °C	8.0	-	Mg^{2+}, Mn^{2+}, K^{+}	-	-	-	Yamashiro *et al.* 1988 (cited in Syldatk *et al.* 1992b)

Source	Stereo-selectivity	Substrate selectivity	Opt. Temp.	Opt. pH	Metal ions		Encoding gene	Subunit molecular weight	Total molecular weight	Reference
					Inhibition	Stimulation				
Flavobacterium sp. AJ 3912	Substrate dependent (L for IMH and D for BMH)	H, PrH,BuH, MTH, BeH, HBH, IMH	40	9.7	-	-	-	-	-	Yokozeki *et al.*1987e (cited in Syldatk *et al*. 1992b, 1999)
Methanococcus jannaschii DSM 2661	L	HH>HMH>Hyd>MH> BeH>PH>HBuH No DHU	80 °C	8.0	-	Mn^{2+}, Mg^{2+}, Ni^{2+}, Zn^{2+}	*Mj0963*	62kDa	240kDa	Chung *et al.* 2002
Pseudomonas sp. NS671	Non	MTH, IPH, IBH, BuH, BeH	—	-	-	-	*hyuA* + *hyuB*	75.6kDa + 64.9kDa	-	Ishikawa *et al*. 1993, 1997, Watabe *et al*. 1992a

(ABH=5-(4-aminobenzyl)-hydantoin; BeH= 5-benzylhydantoin; BMEH= 5-benzyloxymethylenehydantoin; BuH= 5-(sec)-butylhydantoin; CEH= 5-cyanoethylhydantoin; CH= 5-carbamylethylhydantoin; ClBH= 5-(4-cholrobenzyl)-hydantoin; CPH= chlorophenylhydantoin; DHBH=5-(3,4-dihydroxybenzyl)hydantoin; DHU= dihydrouracil; FBH= 5-(4-fluorobenzyl)-hydantoin; HBH= 5-*p*-hydroxybenzylhydantoin; HBuH= 5-hydroxybutylhydantoin; HH= 5-hydroxhydantoin; HMH=hydroxymethylhydantoin; HPG= 5-hydroxyphenylglycine; IBH= 5-isobutylhydantoin; IMH= 5-(3'-indolylmethyl)-hydantoin; IPH= 5-isopropylhydantoin; MH= 5-methylhydantoin; MPH= methyoxyphenylhydantoin; MTH= 5-(2'-methylthioethyl)-hydantoin; PH= 5-phenylhydantoin; PrH= propylhydantoin; THE= thienylhydantoin, Opt. : optimal)

Metal ion dependency was also observed for both L- and non-enantioselective hydantoinases (Table 1.3). The hydantoinase from *A. aurescens* DSM 3745 was subjected to atomic adsorption spectrometry and inductive coupled plasma-atomic emission to determine the metal ion content of the enzyme. From this analysis, 10mol zinc ions per 1mol of active enzyme was observed and removal of these zinc ions resulted not only in loss of activity but dissociation of the enzymes into its subunits as well (May *et al*. 1998b,c). Thus zinc was found to be essential not only for catalytic activity but also for the stabilization of the active quaternary structure of the hydantoinase (May *et al*. 1998b). Crystallographic analysis of the *A. aurescens* DSM 3745 hydantoinase verified the presence of the metal ions in the active site of the enzyme as is the case for the D-hydantoinases investigated (Abendroth *et al.* 2002b). The function of the zinc ions within the active site is postulated to be activation of water by lowering its pK_a thus enabling the hydroxyl ion to perform nucleophilic attack on the amide bond resulting in the hydrolytic cleavage of the hydantoin ring (May *et al*. 1998b, Abendroth *et al*. 2002b).

The only L-enantioselective hydantoinase for which the encoding sequence has been determined is that from *M. jannaschii* DSM 2661 (Table 1.3). This gene was amplified from chromosomal DNA using sequence data obtained from the complete genome sequences of *M. jannaschii* available on the NCBI database (Chung *et al*. 2002). *M. jannaschii* is a thermostable methanogen with an optimal growth temperature of 85^{o}C. The hydantoinase from this organism was found to be extremely thermostable with an optimal catalytic activity at 80^{o}C and a half-life of 100 minutes at 90^{o}C (Chung *et al*. 2002).

The nucleotide sequence of the non-enantioselective hydantoinase from *A. aurescens* DSM 3747 was determined by screening a genomic library, prepared in phage λ-RESIII, with a radiolabeled oligonucleotide probe deduced from the N-terminal amino acid sequence of the hydantoinase purified from *A. aurescens* DSM 3745 (Wiese *et al*. 2001). Analysis of the 7,637bp plasmid thus isolated revealed the presence of *hyuP*, *hyuA*, *hyuH*, and *hyuC* genes encoding for a putative permease, hydantoin racemase, hydantoinase, and *N*-carbamoylase respectively. These genes were found to be arranged in an operon and orientated in the same direction. The close proximity of the *hyu* genes to one another indicated that they are co-transcribed into a polycistronic mRNA (Wiese *et al*. 2001).

The hydantoin-hydrolysing enzymes from *Pseudomonas* sp. NS671 were located on a 172Kbp native plasmid on which two genes, *hyuA* and *hyuB*, were found to encode the hydantoinase enzyme (Watabe *et al*. 1992a). Thus, in contrast to all other reported hydantoinases in which the enzymes are homodimers or homotetramers, the hydantoinase from *Pseudomonas* sp. NS671 is comprised of two different subunits. The gene encoding

the L-enantioselective *N*-carbamoylase was located in close proximity to the *hyuA* and *hyuB* genes forming an operon. As with *A. aurescens* DSM 3747, these genes were orientated in the same direction and were closely spaced suggesting that these open reading frames may be translationally coupled (Watabe *et al*. 1992a).

1.2.3 *N*-carbamylamino acid-hydrolysing enzymes

N-carbamylamino acids can be converted to their corresponding amino acids by treatment with HNO_2 (Snamprogetti and Kaneko processes for production of D-*p*-hydroxyphenyl-hydantoin). However, this approach is not viable for amino acids such as tryptophan, citrulline, or pyridylalanine which are unstable when treated with acid (Syldatk and Pietzsch 1995). The enzymatic cleavage of *N*-carbamylamino acids by *N*-carbamoylases (*N*-carbamylamino acid amidohydrolases) provides an alternative approach. In addition, by application of a strictly enantioselective *N*-carbamoylase, enantiopure amino acids can still be produced even if a non-enantioselective hydantoinase is used for the hydrolysis of hydantoin.

N-carbamoylases have been isolated from several bacterial sources (Table 1.4 and Table 1.5) and are classified as L- or D-enantioselective. No substrate dependent or non-enantioselective *N*-carbamoylases have been reported to date. *N*-carbamoylases occur in conjunction with D-, L-, or non-enantioselective hydantoinases with the exception of *Comomonas* sp. E222c in which a D-carbamoylase exists independently of an hydantoinase (Ogawa *et al.* 1993).

As D-carbamoylases were shown to be associated with dihydropyrimidinases, the natural function of these enzymes was originally thought to be that of a β-ureidopropionase which is responsible for the cleavage of *N*-carbamyl-β-alanine (β-ureidopropionic acid) to β-alanine in the pyrimidine degradation pathway (Syldatk and Pietzsch 1995). This did indeed seem to be the case with the D-enantioselective *N*-carbamoylase from *Arthrobacter crytallopoietes* which was able to produce β-alanine from dihydrouracil (Moller *et al*. 1988). However, the D-enantioselective *N*-carbamoylase from *Blastobacter* sp. A17p-4 was unable to hydrolyse β-ureidopropionic acid (Ogawa and Shimizu 1997). Subsequent to this finding, the D-enantioselective *N*-carbamoylases from *Pseudomonas* sp. KNK003A, and *Agrobacterium tumefaciens* AM10 were also shown to be unable to hydrolyse β-ureidopropionic acid (Ikenaka *et al*. 1998a, Sareen *et al*. 2001a). In order to determine if β-ureidopropionase does cleave *N*-carbamylamino acids and with what enantioselectivity, the β-ureidopropionase from *Pseudomonas putida* IFO 12996 was purified and analysed (Ogawa and Shimizu 1994). From these studies, it was found that the β-ureidopropionase not only hydrolysed *N*-carbamyl-α-amino acids but *N*-carbamyl-β- and γ-amino acids as well (Ogawa and Shimizu

1994). Hydrolysis of *N*-carbamyl-α-amino acids by the β-ureidopropionase was shown to be strictly L-enantioselective (Ogawa and Shimizu 1994) suggesting that the natural function of L- rather than D-carbamoylases is in pyrimidine degradation. However, L-enantioselective *N*-carbamoylases from *Alcaligenes xyloxidans* AKU 990, *Arthrobacter aurescens* DSM 3747, *Pseudomonas* sp. NS671, and *Bacillus kaustophilus* CCRC11223 are unable to hydrolyse the natural substrate of β-ureidopropionase (Ogawa *et al*. 1995c, Wilms *et al*. 1999, Ishikawa *et al*. 1996, Hu *et al*. 2003). Furthermore, a β-ureidopropionase recently isolated from *Brevibacillus agri* NCHU1002, while hydrolysing *N*-carbamyl-β-alanine, did not hydrolyse *N*-carbamyl-α-amino acids (Kao and Hsu 2003). Thus the natural function of both L- and D-enantioselective *N*-carbamoylases remains unclear.

1.2.3.1 D-enantioselective *N*-carbamoylases

D-enantioselective *N*-carbamoylases have been found in several *Agrobacterium* isolates, as well as in *Pseudomonas*, *Blastobacter*, *Comamonas*, and *Arthrobacter* species. A selection of the biochemical and genetic properties of these enzymes are listed in Table 1.4. D-carbamoylases are found as homodimers or homotrimers with optimum pH and temperatures for *N*-carbamylamino acid hydrolysis ranging from pH 7 to 9.2, and 40^{o}C to 70^{o}C respectively (Table 1.4). Inhibition of D-carbamoylases by metal ions has been well documented. However, unlike hydantoinases, D-carbamoylases do not appear to be metalloenzymes as indicated by the absence of sensitivity to metal ion chelators and minimal stimulation of enzyme activity subsequent to the addition of metal ions to the biocatalytic reaction (Table 1.4).

The genes encoding for D-carbamoylases in *Agrobacterium* sp. KNK712 and *Agrobacterium tumefaciens* NRRL B11291 were isolated by screening of the relevant genomic libraries (Nanba *et al*. 1998, Buson *et al.* 1996). The gene sequences were observed to be similar with nine residues difference between the amino acid sequences of the two D-carbamoylases (Nanba *et al*. 1998). *Agrobacterium* sp. IP I-671 D-carbamoylase was also found to have a high amino acid sequence identity with the above D-carbamoylases. This was not surprising considering the D-carbamoylase encoding gene was amplified by PCR from the chromosome of *Agrobacterium* sp. IP I-671 using oligonucleotides designed from the aligned sequences of the previously isolated D-carbamoylases from *Agrobacterium* strains NRRL B11291, KNK712 and 80/44-2A (Hils *et al.* 2001). The D-carbamoylases of both *A. tumefaciens* NRRL B11291 and *Agrobacterium* sp. IP I-671 were found to be encoded within the parental strain on 160kb and 190kb plasmids respectively (Hils *et al.* 2001).

Table 1.4 Biochemical and genetic properties of bacterial D-enantioselective *N*-carbamoylase enzymes.

Source	Substrate selectivity	Opt. Temp.	Opt. pH	Metal ions		Encoding gene	Subunit molecular weight	Total molecular weight	Reference
				Inhibition	Stimulation				
Agrobacterium radiobacter	NC-PG> NC-HPG> NC-CPG> NC-A> NC-MPG= NC-PA> NC-TEG> NC-V	60 °C	7.0	-	none	-	-	-	Olivieri *et al.* 1979
Agrobacterium sp.	NC-M> NC-V> NC-PG> NC-HPG> NC-T> NC-PA	70 °C	7.3-7.4	Mg^{2+}, Ba^{2+}, Mn^{2+}, Co^{2+}, Ni^{2+}, Cu^{2+}, Zn^{2+}	none	-	38kDa	-	Louwrier and Knowles 1996
Agrobacterium sp. IP I-671	-	50 °C	7.0	Co^{2+}, Zn^{2+}, Ni^{2+}	-	*hyuC* (915bp)	34kDa	-	Hils *et al.* 2001, Kim and Kim 1995
Agrobacterium sp. KNK712	NC-M> NC-L= NC-NL> NC-PG> NC-HPG> NC-A> NC-NV> NC-IL> NC-S	65 °C	7.0	Cu^{2+}, Hg^{2+}, Ag^{2+}	—	ORF (915bp)	34.285kDa	-	Nanba *et al.* 1998, Ikenaka *et al.* 1999
Agrobacterium tumefaciens AM 10	NC-M> NC-PG> NC-HPG> NC-PA> NC-Trp> NC-V> NC-A> NC-S	-	-	-	-	*dcb* (~1Kb)	38kDa	67kDa	Sareen *et al.* 2001a,b
Agrobacterium tumefaciens NRRL B 11291	NC-HPH	-	-	-	-	*cauA* (912bp)	34.25kDa	-	Buson *et al.* 1996

Source	Substrate selectivity	Opt. Temp.	Opt. pH	Metal ions		Encoding gene	Subunit molecular weight	Total molecular weight	Reference
				Inhibition	Stimulation				
Agrobacterium tumefaciens RU-OR	NC-HPH> NC-MH> NC-G	40 °C	8.0-10.0	-	-	-	-	-	Hartley *et al.* 1998
Arthrobacter crystallopoietes AM2	*N*-carbamylamino acids with charged side chains	50 °C	9.2	-	none	-	-	-	Moller *et al.* 1988
Blastobacter sp. A17p-4	NC-PG> NC-HPG> NC-PA> NC-NL> NC-M> NC-L> NC-V	50-55 °C	8.0-9.0	Co^{2+}, Zn^{2+}, Cu^{2+}, Ag^{2+}, Cd^{2+}, Hg^{2+}	none	-	40kDa	120kDa	Ogawa *et al.* 1994b
Comamonas sp. E222c	NC-PA> NC-M> NC-NL> NC-T> NC-HPG> NC-L> NC-PG> NC-A	40 °C	8.0-9.0	Cu^{2+}, Zn^{2+}, Cd^{2+}, Ag^{2+}, Hg^{2+}, Co^{2+}, Ni^{2+}	none	-	40kDa	120kDa	Ogawa *et al.* 1993
Pseudomonas sp. AJ-11220	NC-M> NC-PG> NC-HPG> NC-DHPA> NC-L> NC-A> NC-Asp> NC-PA (poor hydrolysis of BUP)	55 °C	7.0	-	-	-	-	-	Yokozeki *et al.* 1987c
Pseudomonas sp. KNK003A	NC-MH>> NC-PH> NC-HPH	-	7.0	-	-	*DCase* (936bp)	35kDa	67kDa	Ikenaka *et al.* 1998a

(NC= *N*-carbamyl; A=alanine; Asp= asparagine; CPG=chloro-phenylglycine; DHPA=dihydroxyphenylalanine; G=glycine; HPG=hydroxyphenylglycine; IL=isoleucine; L=leucine; M=methionine; MPG=methoxy-phenylglycine; NL=norleucine; NV=norvaline; PA= phenylalanine; PG=phenylglycine; S=serine; T=tyrosine; TEG=thienylglycine; Trp-tryptophan; V=Valine; Opt.: optimal)

The presence of five cysteine residues were identified in the amino acid sequence of the D-carbamoylase from *A. tumefaciens* NRRL B11291 (Grifantini *et al*. 1996). Chemical derivatization using acrylamide and Ellmans reagent revealed that none of these five cysteines form disulphide bridges. However, Cys^{172} was identified as involved in the catalytic action of the enzyme as site-directed mutagenesis of this residue led to complete inactivation of the enzyme (Grifantini *et al*. 1996). The importance of this residue was verified by crystallographic analysis and protein modelling which identified Cys^{172}, Glu^{47}, and Lys^{127} as the catalytic triad involved in the hydrolysis of *N*-carbamylamino acids by the D-carbamoylases from *Agrobacterium* sp. KNK712 and *A. radiobacter* 14924 (Nakai *et al*. 2000, Wang *et al*. 2001, Chen *et al.* 2003). This is discussed in more detail in Section 1.3.2.

1.2.3.2 L-enantioselective *N*-carbamoylases

L-enantioselective enzymes have been isolated and characterized from *Alcaligenes*, *Bacillus* and *Pseudomonas* species and shown to hydrolyse a wide range of aliphatic and aromatic *N*-carbamylamino acids (Table 1.5). However, due to the highly unstable nature of this enzyme, only L-carbamoylases from *Alcaligenes xylosoxidans* AKU 990, *Arthrobacter aurescens* DSM 3747, and *Pseudomonas* sp. NS671 have been purified (Ogawa *et al*. 1995c, Wilms *et al*. 1999, Ishikawa *et al*. 1996). In all cases the L-carbamoylase was found to be a homodimer (Table 1.5).

Unlike the D-carbamoylases, the optimal pH for hydrolysis of *N*-carbamylamino acid substrates by L-carbamoylases appears to be at a more neutral pH of 7.0 to 8.5 (Table 1.5). Furthermore, metal ions were found to stimulate as well as inhibit L-carbamoylase activities and inhibition by metal ion chelators was observed (Table 1.5) which is in contrast to the results observed for D-carbamoylases (Table 1.4). The presence of metal ion chelators such as EDTA, 8-hydroxyquinoline, and 2,2'-dipyridyl caused considerable inhibition of the β-ureidopropionase from *Pseudomonas putida* IFO12996 indicating that, as is the case with L-carbamoylases, the β-ureidopropionase is a metalloenzyme (Ogawa and Shimizu 1994).

Of the eight L-carbamoylases isolated, four have been shown not to hydrolyse *N*-carbamyl-β-alanine whilst the remaining L-carbamoylases were not tested for the ability to hydrolyse the natural substrate of β-ureidopropionase. This suggests that L-carbamoylases are not synonymous with β-ureidopropionase. The narrow substrate range of the β-ureidopropionase from *Brevibacillus agri* NCHU1002, which hydrolysed *N*-carbamyl-β-alanine but not *N*-carbamyl-α-amino acids (Kao and Hsu 2003) supports this. In contrast, the β-ureidopropionase from *P. putida* IFO 12990 was observed to have a very broad substrate range with hydrolysis of *N*-carbamyl-α,β, and γ-amino acids with strict L-enantioselectivity with respect to *N*-carbamyl-α-amino acid hydrolysis (Ogawa and Shimizu 1994).

Table 1.5 Biochemical and genetic properties of bacterial L-enantioselective *N*-carbamoylase and β-ureidopropionase enzymes.

Source	Substrate selectivity	Opt. Temp.	Opt. pH	Metal ions		Encoding gene	Subunit molecular weight	Total molecular weight	Reference
				Inhibition	Stimulation				
***N*-carbamoylase**									
Alcaligenes xylosoxidans AKU 990	NC-A>NC-G>NC-Asp>NC-V>NC-S	35 °C	8.0-8.3	Cu^{2+}, Zn^{2+}, Cd^{2+}, Hg^{2+}	Mn^{2+}, Ni^{2+}, Co^{2+}	-	65kDa	134kDa	Ogawa *et al.* 1995c
Arthobacter aurescens DSM 3747	Selective for NC with aromatic substituents	50 °C	8.5	-	Mn^{2+}	*HyuC*	44kDa	93kDa	Wilms *et al.* 1999 Syldatk *et al.* 1990a
Arthrobacter sp. DSM 9771	NC-M	34-37 °C	7.5-8.0	-	-	-	-	-	Wagner *et al.* 1996
Bacillus brevis AJ-12299	NC-V, NC-L, NC-IL, NC-M, NC-PA, NC-T	30 °C	7.0-7.5	-	-	-	-	-	Yamashiro *et al.* 1988
Bacillus kaustophilus CCRC11223	NC-Glu= NC-G> NC-HPA> NC-A> NC-V> NC-S> NC-H	70 °C	7.4	EDTA	Mn^{2+}, Co^{2+}, Ni^{2+}	*Inc* (1230bp)	44.315kDa	-	Hu *et al.* 2003
Bacillus stearothermophilus NCIB8224	NC-A> NC-Glu> NC-M> NC-G> NC-L	-	-	-	-	*amaB*	44kDa	-	Batisse *et al.* 1997
Bacillus stearothermophilus NS1122A	NC-A= NC-V> NC-M> NC-L= NC-Thr> NC-S> NC-G> NC-Glu> NC-IL> NC-Asp	60-70 °C	8.0	Cu^{2+}, Zn^{2+}	Co^{2+}, Mn^{2+}, Ni^{2+}	1230bp	44.248kDa	-	Mukohara *et al.* 1993, Ishikawa *et al.* 1994

Source	Substrate selectivity	Opt. Temp.	Opt. pH	Metal ions		Encoding gene	Subunit molecular weight	Total molecular weight	Reference
				Inhibition	Stimulation				
Flavobacterium sp. AJ 3912	NC-G, NC-A, BUP, NG-V, NG-L, NG-IL, NC-S, NC-M, NC-Asp, NC-PA, NC-MPG, NC-Trp, NC-T	40 °C	8.0	-	-	-	-	-	Yokozeki *et al.*1987e (cited in Syldatk *et al*. 1992b)
Pseudomonas sp. NS671	NC-L> NC-V> NC-A> NC-M> NC-IL> NC-PA	40 °C	7.5	-	Mn^{2+}, Co^{2+}, Ni^{2+}	*HyuC*	45kDa	109kDa	Ishikawa *et al.* 1996, Watabe *et al.* 1992a
β-ureidopropionase									
Pseudomonas putida IFO 12996	N-carbamyl-α,β,γ-amino acids	60 °C	7.5-8.2	Cu^{2+}, Ag^{2+}, Hg^{2+}, Zn^{2+}, Sn^{2+}, Pb^{2+}	Co^{2+}, Ni^{2+}, Mn^{2+}	-	45kDa	95kDa	Ogawa and Shimizu 1994
Brevibacillus agri NCHU1002	*N*-carbamoyl-β-alanine, not *N*-carbamyl-α-amino acids	-	-	-	-	*PydC* (890bp)	30.1kDa	-	Kao and Hsu 2003

NC= *N*-carbamyl, A=alanine; Asp= asparagine; CPG=chloro-phenylglycine; DHPA=dihydroxyphenylalanine; G=glycine; Glu = glutamate; HPA = homophenylalanine; HPG=hydroxyphenylglycine; H= histidine; IL=isoleucine; L=leucine; M=methionine; MPG=methoxy-phenylglycine; NL=norleucine; NV=norvaline; PA= phenylalanine; PG=phenylglycine; S=serine; T=tyrosine; Thr=threonine; TEG=thienylglycine; Trp-tryptophan; V=Valine; Opt.: optimal)

Five genes encoding L-carbamoylases have been isolated and found to encode enzymes with similar predicted molecular weights of approximately 44kDa (Table 1.5). The *HyuC* from *Pseudomonas* sp. NS671 was located on a 172Kbp plasmid downstream of the *HyuA* and *HyuB* genes encoding for the hydantoinase (Watabe *et al.* 1992a). The purified enzyme was strictly L-enantioselective with a broad substrate range and shown to be inhibited in the presence of ATP (Ishikawa *et al*. 1996). Sequence analysis of the *HyuC* indicated a 43% similarity to the *HyuA* and *HyuB* genes suggesting that these genes evolved from a common ancestor by gene duplication (Watabe *et al.* 1992a).

The L-carbamoylase gene, *amaB*, from *Bacillus stearothermophilus* NCIB8224 was found to be co-transcribed on a polycistronic mRNA with the *amaA* gene encoding an aminoacylase (Batisse *et al*. 1997). The operon formed by the *amaA* and *amaB* genes in *B. stearothermophilus* NCIB8224 was found, by Southern hybridisation and PCR analysis, to be conserved in other *B. stearothermophilus* strains (Batisse *et al.* 1997).

Analysis of the amino acid sequence of the *Bacillus kaustophilus* L-carbamoylase revealed the presence of six cysteine residues which, by treatment with excess dithiothreitol, were shown to form three disulphide bridges (Hu *et al.* 2003). The amino acid sequence of L-carbamoylases from *Bacillus stearothermophilus* NS1122A, *Pseudomonas* sp. NS671, *A. aurescens* DSM 3747, and *B. stearothermophilus* NCIB8224 were shown to have 93.6, 44.3, 35.5 and 93.6% identity respectively with that of the L-carbamoylase from *B. kaustophilus* (Hu *et al*. 2003). By alignment of the amino acid sequences from these L-carbamoylases, the six cysteine residues found to form disulphide bridges in the *B. kaustophilus* L-carbamoylase were shown to be conserved in the L-carbamoylases from both *B. stearothermophilus* strains (Hu *et al*. 2003). While the L-carbamoylase from *Pseudomonas* sp. NS671 contains five cysteine residues, and inhibition by the SH reagent *p*-chloromercaribenzoate suggested the potential presence of two disulphide bridges (Ishikawa *et al*. 1996), only two of the cysteine residues occur in positions relative to the cysteines in *B. kaustophilus* L-carbamoylase. The L-carbamoylase from *A. aurescens* DSM 3747 does not contain disulphide bridges as only one cysteine residue is present in its primary amino acid sequence. The formation of disulphide bridges is thought to stabilize proteins at high temperatures (Hu *et al.* 2003) and this is reflected in the thermostabilities of the L-carbamoylases from *B. kaustophilus* and *B. stearothermophilus* in comparison to that of *A. aurescens* and *Pseudomonas* sp. NS671 (Table 1.5). Increased overall hydrophobicity and proline substitutions over the entire polypeptide chain were also suggested to contribute to the higher thermostability of the L-carbamoylase from *B. stearothermophilus* NS1122A when compared to *Pseudomonas* sp. NS671 (Mukohara *et al*. 1993).

Surprisingly, the *N*-terminal sequence of the L-carbamoylase from *Alcaligenes xyloxidans* showed no similarity to the L-carbamoylases from *Pseudomonas* sp. NS671 or *B. stearothermophilus* NS1122A but some similarity to the D-carbamoylases from *Comamonas* and *Blastobacter* was observed (Ogawa *et al.* 1995c).

1.2.3 Racemases

In order to achieve the 100% theoretical yield of optically pure amino acids from hydrolysis of hydantoin, the unhydrolysed isomer of the racemic mixture of the hydantoin derivative needs to be racemized. Racemization of 5-monosubstituted hydantoins proceeds via keto-enol-tautomerism (Figure 1.2) and can occur either chemically under basic conditions or by the action of a racemase enzyme. The bulkiness and electronegativity of the substituent in the 5-carbon position affects the rate at which racemization of hydantoins occurs and increased racemization can be observed at more basic pH and at increased temperatures (Syldatk and Pietzsch 1995).

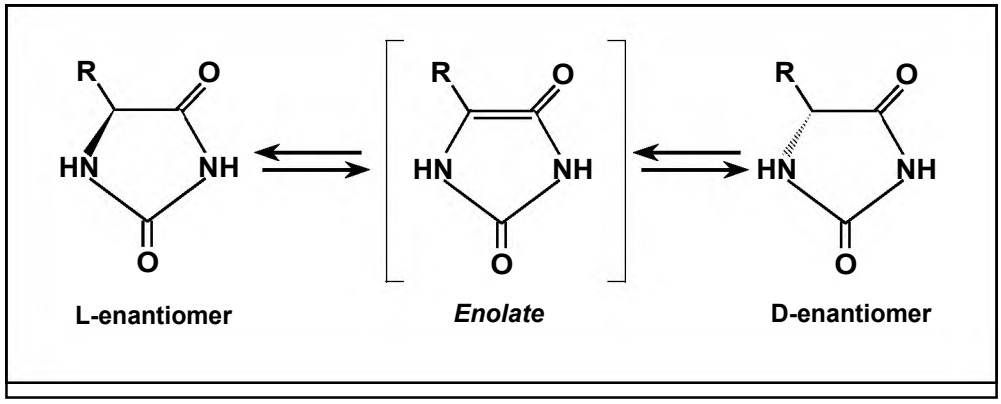

Figure 1.2 Keto-enol-tautomerism of 5-monosubstituted hydantoins (Adapted from Syldatk and Pietzsch 1995)

A gene encoding an hydantoin racemase was first identified in *Pseudomonas* sp. NS671 downstream of the genes encoding the hydantoinase and *N*-carbamoylase enzymes (Watabe *et al.* 1992b). Genes encoding hydantoin racemases have subsequently been isolated from *Agrobacterium* sp. IP I-671 and *Arthrobacter aurescens* DSM 3747 and shown to have 46% and 47.2% amino acid sequence identity with the racemase from *Pseudomonas* sp. NS671 (Hils *et al.* 2001, Wiese *et al*. 2000). The hydantoin racemases from *A. aurescens* DSM 3747 and *Pseudomonas* sp. NS671 have relative molecular masses of approximately 170kDa and 190kDa, with subunits of 25kDa and 32kDa respectively, forming a hexamer, heptamer, or octamer (*A. aurescens* DSM 3747) or a hexamer (*Pseudomonas* sp. NS671) (Wiese *et al*. 2000, Watabe *et al*. 1992c). Most recently, a hydantoin racemase from *Agrobacterium tumefaciens* C58 was purified and found to have a subunit size of 30kDa

and a total molecular mass of 100kDa thus suggesting that the racemase forms a tetramer (Las Heras-Vazquez *et al.* 2003) which is in contrast to the racemases purified from *A. aurescens* and *Pseudomonas*.

The substrate-specificities of the purified hydantoin racemases was found to vary between isolates. The racemase from *Pseudomonas* sp. NS671 was shown to have a preference for hydantoins with aliphatic substituents (Watabe *et al*. 1992c) whereas *A. aurescens* racemized aromatic hydantoin derivatives more efficiently (Wiese *et al*. 2000). *A. tumefaciens* C58 racemase showed a preference for hydantoins with short rather than long aliphatic side chains (Las Heras-Vazquez *et al.* 2003). Unlike the *Pseudomonas* and *A. aurescens* racemases with optimal activity at pH of 9.5 and 8.5 respectively (Watabe *et al*. 1992c, Wiese *et al*. 2000), the racemase from *A. tumefaciens* C58 had an optimal pH of 7.5 for racemase activity (Las Heras-Vazquez *et al.* 2003). Significantly reduced chemical racemization occurs at this pH thus racemization of 5-monosubstituted hydantoins by *A. tumefaciens* C58 is predominantly an enzymatic process (Las Heras-Vazquez *et al.* 2003).

Glutamate racemases from *Lactobacillus fermenti* and *Lactobacillus brevis* were shown to contain two cysteine residues which labilized the proton at the carbon-2 of the substrate (Tanner *et al*. 1993 and Yakasaki *et al.* 1995, cited in Wiese *et al.* 2000). The hydantoinase racemase from *A. aurescens* was rapidly inactivated by mercuric ions and iodoacetamide whilst a two-fold increase in activity was observed on addition of the reducing compound DTT. This indicated that the two cysteine residues, at positions 77 and 182 of the amino acid sequence, may serve as active site base catalysts. These cysteine residues have been found to be highly conserved within hydantoin racemases (Wiese *et al*. 2000).

1.3 STRUCTURAL ANALYSIS

1.3.1 Hydantoinases

The crystal structures of D-hydantoinases from *Thermus* sp. (Abendroth *et al*. 2000b, 2002a), *Bacillus stearothermophilus* SD-1 (Cheon *et al*. 2002), and *Burkholderia pickettii* (Xu *et al.* 2003a), as well as that of the L-hydantoinase from *Arthrobacter aurescens* DSM 3745 (Abendroth *et al.* 2002b) have been solved. By analysis of the crystal structures, as well as modelling based on structurally similar enzymes, explanations for properties such as the catalytic mechanism of hydantoin hydrolysis, enantio- and substrate-selectivity, and thermostability were proposed.

With respect to quaternary structure, the monomeric subunits of the hydantoinase assemble as tetramers when crystallized irrespective of whether the hydantoinase formed dimers or

tetramers in an aqueous environment (Cheon *et al.* 2002, Abendroth *et al.* 2002a, Xu *et al.* 2003a) (Figure 1.3, panel A). Of the crystal structures solved, the hydantoinases and dihydropyrimidinases all exhibited strong structural similarity with the monomers forming a classic, elliptically distorted, $(\alpha/\beta)_8$TIM barrel flanked by a β-sheet domain comprised of both the N- and C-termini (Cheon *et al.* 2002, Abendroth *et al.* 2002a, Xu *et al.* 2003a) (Figure 1.3, panel B).

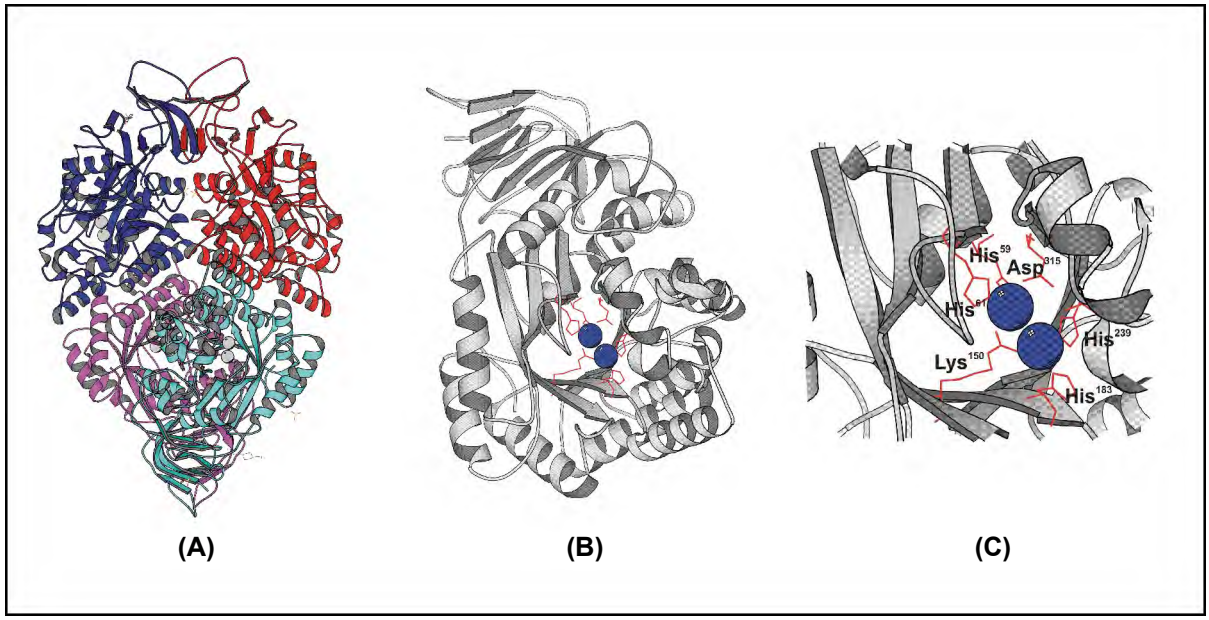

Figure 1.3 Ribbon representation of the *Thermus* sp. D-hydantoinase quaternary structure **(A)**, monomer **(B)**, and catalytic site **(C)** (Panel A: the subunits are individually coloured, Panel B,C: Catalytic residues are depicted in red and the zinc atoms as blue balls) (The accession code for the protein used was 1GKP (Abendroth *et al*. 2002a) and the figures were generated in Molscript (Kraulis 1991)).

The catalytic site is situated in a deep hydrophobic pocket at one end of the TIM barrel distant from the β-sheet domain (Figure 1.3, panel C). It consists of six strictly conserved amino acids involved in coordination of the metal ions. The first zinc ion is coordinated by a carboxylated lysine residue (Lys^{150}), His^{183}, His^{239}, and the oxygen atoms of the hydroxide ion and water while the second zinc ion is coordinated by Lys^{150}, His^{59}, His^{61}, $-OH_3$ and Asp^{315} (Figure 1.3, panel C) (Abendroth *et al*. 2002a). Irrespective of the enantioselectivity of the hydantoinases, these amino acid residues are found to be strictly conserved implying a common mechanism of hydantoin hydrolysis (Cheon *et al*. 2002).

To investigate the substrate- and enantiospecificity of hydantoin hydrolysis, a substrate-bound crystal hydantoinase structure is required. However, due to the lack of a potent inhibitor for hydantoinase, the orientation and interaction of the substrate with the enzyme

could not be determined experimentally. Consequently, the binding and interaction of the substrate with the hydantoinase was modelled on the substrate binding region of the structurally similar enzymes urease and dihydroorotase (Abendroth *et al*. 2002a,b, Xu *et al*. 2003a). There are two components to substrate interaction with the hydantoinase: recognition of the functional amide groups which control the orientation of the substrate, and recognition of the exocyclic substituents which depend on the stereochemistry of the hydantoin substrates (Cheon *et al.* 2002).

Substrate interaction with the hydantoinase is proposed to occur via the formation of several hydrogen bonds between the hydantoin ring and specific amino acids in the hydantoinase including Ser^{288}, Asn^{336}, His^{183} and Tyr^{155} (Figure 1.4, A). Two hydrogen bonds occur with the backbone atoms of Ser^{288}, the importance of which is emphasized by an adjacent hairpin loop supported by *cis*-Pro^{289}, and although the distance is rather long for the potential hydrogen bond with Asn^{336} and the substrate, this bond formation may be important at other stages during catalysis of hydantoins. Tyr^{155}, zinc, and His^{183} are responsible for the stabilization of the oxygen atoms in the tetrahedral transition state (Abendroth *et al*. 2002a). The residues involved in substrate interaction in the D-hydantoinase from *B. pickettii* corresponding to those in the D-hydantoinase from *Thermus* sp. are identical except for Thr^{286} which is a serine in the D-hydantoinase of *B. pickettii*. This change in residue does not however affect the hydrogen bonding interaction with the substrate (Xu *et al*. 2003a).

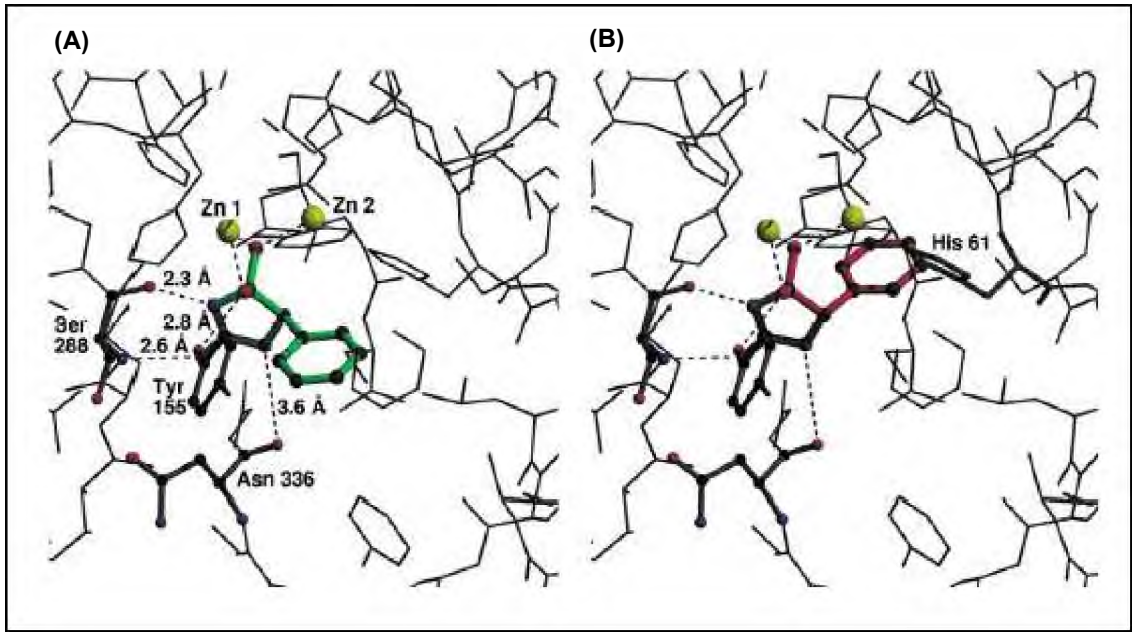

Figure 1.4 Hydrogen bond formation between the D-hydantoinase and D-5-monosubstituted hydantoin substrate **(A)**, and the steric clash occurring when an L-5-monosubstitued hydantoin substrate is modelled into this site **(B)** (from Abendroth *et al.* 2002a).

The pronounced hydrophobic pocket formed by the amino acid residues Leu[64], Cys[95], Phe[152], Tyr[155], and Phe[159] is proposed to be responsible for the enatio- and substrate-specificity exhibited by the D-hydantoinase of *Thermus* sp. (Abendroth *et al*. 2002a). *Thermus* D-hydantoinase readily hydrolyses 5-phenylic substituted hydantoins as these substrates are easily accommodated in the hydrophobic pocket. In contrast, hydantoin derivatives with benzylic or polar substituents were found to be hydrolysed to D-enantiomer intermediates with significantly lower efficiency due to less productive interaction within the hydrophobic pocket. While D-specific hydantoin substrates fit into this model well, the larger side-chains of L-hydantoin derivatives clash sterically with His61 in the catalytic site of D-hydantoinase from *Thermus* (Figure 1.4, panel A vs. B). However, hydantoin derivatives with small side chains are readily hydrolysed but without enantioselectivity as neither enantiomer results in steric clashes with the His[61] residue (Abendroth *et al.* 2002a). The residues proposed to form the hydrophobic pocket in *B. stearothermophilus* D-hydantoinase correspond to that of *Thermus* D-hydantoinase with the exception of Met[63] in place of Cys[95] (Cheon *et al*. 2002).

In contrast to the D-hydantoinases described above, the L-hydantoinase from *A. aurescens* contains no pronounced hydrophobic pocket and subsequent analysis of the structure produced no explanations for the substrate-specificities observed from this enzyme. D/L-5-indolylhydantoin is one of the preferred substrates of the L-hydantoinase. The proposed orientation for the substrate interaction with the hydantoinase would result in no hydrophobic interaction partners for the D-enantiomer of 5-indolylhydantoin whereas the L-enantiomer is able to form hydrophobic interactions with the side chains of His[62] and Ile[95] (Abendroth *et al*. 2002b). Mutation of the L-hydantoinase from *A. aurescens* resulted in increased D-enantiospecificity with respect to 5-methylthioethyl-hydantoin subsequent to a V154A point mutation (May *et al*. 2000). This is most likely due to the increased space for the side chain created by this mutation (Abendroth *et al.* 2002b). The point mutation I95F which resulted in increased L-enantiospecificity of the enzyme (May *et al*. 2000) is most likely due to increased hydrophobicity close to the side chain of L-5-methylthioethyl hydantoin resulting in increased cleavage of the L-enantiomer (Abendroth *et al*. 2002b).

The exocyclic substituent recognition site in the D-hydantoinase from *B. pickettii* is formed by the predominantly hydrophilic amino acid residues Thr[62], Ser[64], Gln[93], Phe[150], Tyr[153], and Asn[157]. This is in contrast to the D-hydantoinases from *Thermus* and *B. stearothermophilus*, which have hydrophobic residues at these positions forming a pronounced hydrophobic pocket. The presence of hydrophilic residues at the exocyclic recognition site of the D-hydantoinase from *B. pickettii* suggest that the enzyme may have a preference for hydantoin substrates with polar substituents (Xu *et al.* 2003a).

Analysis of the crystal structures of hydantoinases not only sheds light on the catalytic properties of these enzymes but also suggests factors likely to contribute toward thermostability of the enzymes. Comparison of the crystal structure of the mesophylic D-hydantoinase from *B. pickettii* with the thermophylic D-hydantoinase from *Thermus* sp. by Xu *et al*. (2003a) revealed that the thermostability of the D-hydantoinase from *Thermus* sp. appears to be due to a combination of several factors. These include the presence of methionine and cysteine residues, which can be readily oxidized at high temperatures, on the surface of the enzymes resulting in decreased thermostability. *B. pickettii* has more methionine and cysteine residues on the surface of its D-hydantoinase than does *Thermus sp*. Increased hydrophilic interactions, such as charged ion pairs and hydrogen-bonding interactions, result in increased thermostability of enzymes. *Thermus* sp. D-hydantoinase was found to contain 44 pairs of salt bridges and 777 hydrogen-bonding interactions compared to the 38 salt bridges and 714 hydrogen bonds in the mesophylic D-hydantoinase. Amino acid composition of the enzyme may also affect thermostability. Proline, for example, has a rigid conformation and thus imposes constraints on the flexibility of proteins. Increased proline content, as is the case in the D-hydantoinase from *Thermus sp.*, results in enzymes which resist unfolding at high temperatures (Xu *et al*. 2003a).

1.3.2 *N*-carbamoylases

The crystal structures of the D-carbamoylases from *Agrobacterium* sp. KNK712 (Nakai *et al*. 2000) and *A. radiobacter* 14924 (Wang *et al.* 2001) have been solved. From these studies, D-carbamoylases are found to consist of monomers with a sandwich of β-sheets surrounded by 2 layers of α-helices (Figure 1.5, panel B). In crystal form, the D-carbamoylases form tetrameric quaternary structures with subunits A+B and C+D forming tightly packed dimers which then interact with one another rather loosely (Nakai *et al*. 2000, Wang *et al*. 2001) (Figure 1.5, panel A). As is the case with the hydantoinase, the D-carbamoylases appear to behave differently in aqueous environments where they form dimers or trimers as opposed to the tetramers formed when crystallized (Nakai *et al*. 2000).

The catalytic residues of the D-carbamoylase enzymes were proposed to be Glu^{46}, Lys^{126}, and Cys^{172} (Nakai *et al.* 2000, Wang *et al*. 2001, Chen *et al*. 2003) (Figure 1.5, panel C). This is supported by site-directed mutagenesis of Cys^{172} resulting in loss of catalytic activity (Grifantini *et al*. 1996, Chen *et al*. 2003). Two helices (α2, α6) and the loops connecting β5 and α4, β7 and α5, and β8 and α6 were found to form the pocket structure of the active site (Nakai *et al*. 2000) (Figure 1.5, panel B). Helix α7 of the adjacent monomer was found to cover the active site pocket thereby narrowing the entrance to the active site (Nakai *et al*. 2000). Further site-directed mutagenesis identified residues His^{129}, His^{144}, and His^{215} as necessary to maintain the stable conformation of the catalytic cleft (Wang *et al*. 2001).

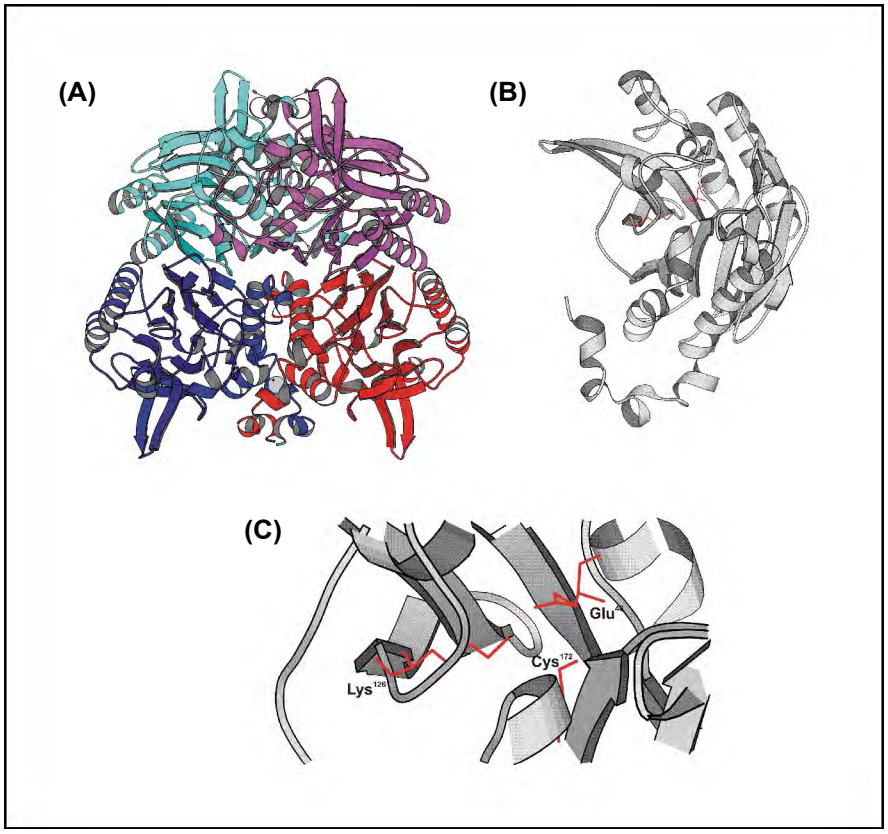

Figure 1.5 Ribbon representation of the D-carbamoylase quaternary structure **(A)**, monomer **(B)**, and catalytic site **(C)**. (Panel A: the subunits are individually coloured, Panel B,C: Catalytic residues are depicted in red) (The accession code for the protein used was 1FO6 (Chen *et al*. 2003) and the figures were generated in Molscript (Kraulis 1991)).

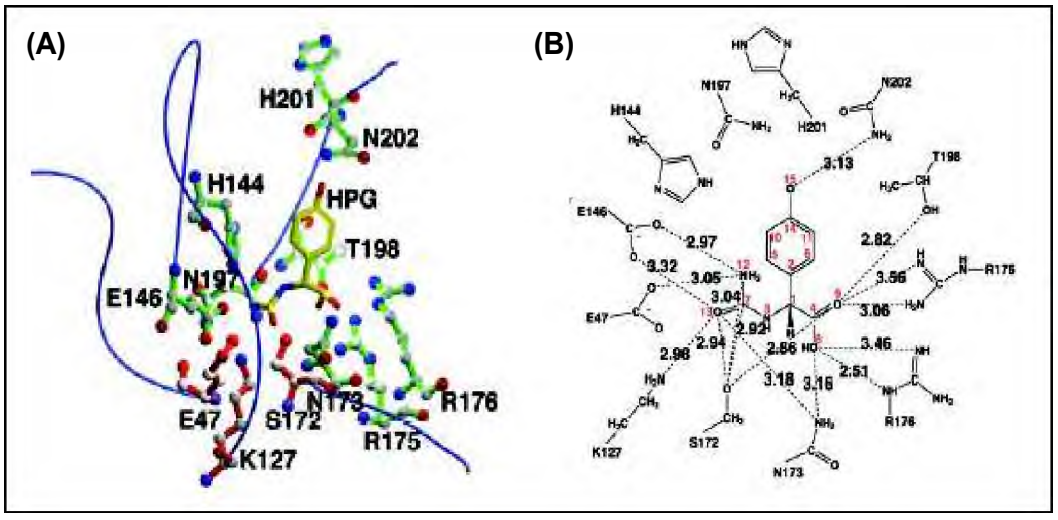

Figure 1.6 Model of the catalytic binding pocket of the D-carbamoylase with hydroxyphenyl-hydantoin substrate **(A)** and the interactions of the substrate with the enzyme **(B)**. (Hydroxyphenyl-hydantoin (HPG) is in yellow; the four loops forming the catalytic pocket shown in blue, the catalytic residues Glu47, Lys127, and Ser172 in red, the remaining residues involved in substrate binding in green, and the interactions of the relevant residues with the substrate are shown by dotted lines). (from Chen *et al*. 2003)

Based on substrate-enzyme modelling of the solved crystal structure of the D-carbamoylase as well as site-directed mutagenesis studies, a mechanism by which *N*-carbamyl-D-amino acids are hydrolysed to their corresponding D-amino acids by the D-carbamoylases was proposed. Based on modelling, the side chains of Glu^{47}, Lys^{127}, and Cys^{172} were proposed to cluster around the carbamoyl moiety of the substrate while the side chains of residues Asn^{173}, Arg^{175}, and Arg^{176} interacted with the carboxyl group resulting in substrate specificity (Figure 1.6, panel B) (Chen *et al.* 2003). Chen *et al*. (2003) also proposed that Cys^{172}, with a nucleophilic Sγ, atom is central in attacking the C7 atom of the carbamoyl group whilst Glu^{47} functions as a general base and Lys^{127} stabilizes the tetrahedral transition state. Based on this data, a possible catalytic mechanism consisting of an acylation reaction with the carbamoyl moiety to cleave the susceptible C-N bond and produce a NH_3, followed by deacylation of the acyl-enzyme intermediate to form the D-amino acid and a CO_2 molecule was suggested (Chen *et al*. 2003).

To date, no crystal structure has been solved for an L-enantioselective *N*-carbamoylase.

1.4 REGULATION OF HYDANTOIN-HYDROLYSING ENZYME ACTIVITY

Overproduction of unwanted enzymes may endow the cell with an energetic burden or result in hydrolytic activity which is detrimental to the cell, as is the case with D-hydantoinases which hydrolyse dihydropyrimidines required for cellular function. In order to protect against such effects, microorganisms possess regulatory mechanisms to control expression of metabolic enzymes. These mechanisms include induction, feedback inhibition, and nutritional regulation by carbon or nitrogen sources (Sanchez and Demain 2002). For industrial applications, deregulation of these mechanisms by classical and genetic manipulations is required such that over-production of the desired metabolite or enzyme is achieved (Sanchez and Demain 2002).

1.4.1 Induction

A wide range of hydantoin and pyrimidine derivatives have been shown to induce expression of genes encoding hydantoin-hydrolysing enzymes with increases in enzyme activities from 5- to 30-fold compared to uninduced cells (Hartley *et al*. 1998, Wiese *et al*. 2001). Table 1.6 provides a summary of the hydantoin-hydrolysing enzymes reported to be subject to inductive regulation and their corresponding inducers. Regulation of expression of the hydantoin-hydrolysing genes by induction ensures that the hydantoinase and *N*-carbamoylase enzymes are produced only when a suitable substrate is available. The D-hydantoinase enzymes from *Pseudomonas fluorescens* DSM84, *Agrobacterium tumefaciens* NRRL B11291, and *Pseudomonas* sp. NCIM 5109 are exceptions with constitutive

expression of the hydantoinase genes in these isolates (Morin *et al.* 1986a, Deepa *et al.* 1993, Sudge *et al.* 1998).

Table 1.6 Inducers of hydantoin-hydrolysing activities in bacterial isolates

Isolate	Inducer	Enzyme affected	Reference
Agrobacterium tumefaciens RU-OR	2-thiouracil	D-hydantoinase D-carbamoylase	Hartley *et al*. 1998
Arthrobacter aurescens DSM 3747	D,L-5-(3-indolylmethyl)-3-*N*-methylhydantoin	Hydantoinase L-carbamoylase	Wiese *et al*. 2001
Arthrobacter crystallopoietes AM2	Hydantoin DL-5-hydroxymethyl-hydantoin	D-hydantoinase D-carbamoylase	Moller *et al*. 1988
Arthrobacter sp. BH20	DL-5-indolylmethyl-hydantoin	Hydantoinase	Syldatk *et al.* 1987
Bacillus brevis AJ-12299	DL-5-isopropyl-hydantoin	D-hydantoinase	Yamashiro *et al*. 1988
Flavobacterium sp. I-3	DL-5-indolylmethyl-hydantoin	Hydantoinase L-carbamoylase	Nishida *et al*. 1987
Pseudomonas putida RU-KM1	Hydantoin	Hydantoinase D-carbamoylase	Burton *et al*. 1998
Pseudomonas putida RU-KM3$_S$	Hydantoin	Hydantoinase L-carbamoylase	Burton *et al*. 1998
Pseudomonas sp. AJ-11220	DL-5-methylthioethyl-hydantoin	D-hydantoinase D-carbamoylase	Yokozeki *et al.* 1987b

The hydantoin hydrolysing enzymes from *Arthrobacter* sp. DSM 3747 were induced by DL-5-(3-indolylmethyl)hydantoin (Syldatk *et al.* 1990a). However, Syldatk *et al*. (1990a) reported a decrease in hydantoin-hydrolysing activities over time due to degradation of the inducer. Addition of higher concentrations of DL-5-(3-indolylmethyl)hydantoin was not feasible as it resulted in significant growth retardation. Thus, in order to obtain optimum levels of hydantoin-hydrolysis with maximum production of biomass, the inducer had to be continuously fed into the growth medium (Syldatk *et al*. 1990a). An alternative is the use of non-metabolizable inducers such as D,L-5-(3-indolylmethyl)-3-*N*-methylhydantoin (*N*-3-CH_3-IMH) (Syldatk *et al.* 1990a). Induction studies of *A. aurescens* DSM 3747 showed a 30-fold increase in hydantoinase activity when *N*-3-CH_3-IMH was supplied in the growth medium as an inducer (Wiese *et al.* 2001). Similar results were obtained in *Agrobacterium tumefaciens*

RU-OR in which the use of the non-metabolizable 2-thiouracil as inducer resulted in a 5- and 10-fold increase in hydantoinase and *N*-carbamoylase activity levels respectively (Hartley *et al*. 1998).

Selection of inducer-independent strains, in order to reduce the costs of industrial production of enantiopure amino acids, has been done in an *Arthrobacter* (Wagner *et al*. 1996) and an *Agrobacterium* strain (Hartley *et al*. 1998). To select for an inducer-independent mutant, *Arthrobacter* sp. DSM 7330 was subjected to extended selection pressure by repeated cycles of growth in minimal medium with *N*-carbamoyl-L-methionine as a sole source of nitrogen. The uninduced cells of the subsequently isolated mutant, DSM 9771, displayed a 3-fold increase in hydantoinase activity but somewhat lower *N*-carbamoylase activity when compared to the induced parental cells. However, on induction, the hydantoinase and *N*-carbamoylase activity in DSM 9771 was 5-fold higher than that of DSM 7330 under corresponding conditions (Wagner *et al*. 1996).

Inducer-independent mutants were also generated from *Agrobacterium tumefaciens* RU-OR wild type. Mutant strains RU-ORL5 and RU-ORLB3 were isolated by growth in the presence of the toxic hydantoin analogue 5-fluorouracil in the absence of an inducer. This selection was based on the principle that unless the cells were able to express the hydantoinase under non-inducing conditions, hydrolysis of the toxic 5-fluorouracil to a non-toxic intermediate by the hydantoinase enzyme would not occur resulting in cell death (Hartley *et al.* 1998). Mutant strain RU-ORL5 showed constitutive expression of both the hydantoinase and *N*-carbamoylase whilst mutant RU-ORLB3 was constitutive only with respect to hydantoinase activity with *N*-carbamoylase activity still inducer-dependent (Hartley *et al*. 2001). This suggested that while induction of hydantoinase and *N*-carbamoylase enzymes in RU-OR are probably mediated by a common regulatory factor, the expression of the genes are not transcriptionally linked (Hartley *et al*. 2001).

1.4.2 Catabolite repression

Numerous studies have reported that the production of hydantoinase and *N*-carbamoylase enzymes in microorganisms occurs only once late logarithmic to stationary phase of growth has been reached (Hartley *et al*. 1998, Syldatk *et al*. 1990a, Sudge *et al*. 1998, Nishida *et al*. 1987, Gokhale *et al*. 1996). Furthermore, supplementation of various carbon and nitrogen sources in the growth medium affects production of hydantoinase and *N*-carbamoylase enzymes (Sudge *et al.* 1998, Morin *et al.* 1986a, Yamashiro *et al.* 1988, Syldatk *et al.* 1990a, Nishida *et al*. 1987, Ishikawa *et al*. 1994). These results indicate that hydantoin-hydrolysing enzymes are subject to catabolite repression in addition to regulation by induction. Catabolite repression is a regulatory mechanism which functions to ensure organised and

sequential utilization of nutrient sources. Nutrient sources which most readily supply carbon or nitrogen and energy for growth are classified as “good” nutrient sources and are metabolised by the cell first. Synthesis of enzymes for the metabolism of other, “poorer” nutrient sources is then repressed until the primary substrate has been exhausted (Sanchez and Demain 2002). Hydantoin derivatives are a poor nitrogen and carbon source and expression of hydantoin-hydrolysing genes is likely to be subject to carbon and/or nitrogen catabolic repression mechanisms.

Upstream of the genes encoding for the hydantoinase (*hyuA* and *hyuB*) and *N*-carbamoylase (*hyuC*) in *Pseudomonas* sp. NS671, ORF1 was identified and found to share strong amino acid similarity with the NifA and NtrC proteins (Watabe *et al*. 1992a) which are involved in control of nitrogen fixation and regulation by functioning as transcriptional activators of σ^{54} RNA polymerase (Morett and Segovia 1993). The gene product of ORF1 may therefore be involved in regulatory control of the hydantoin-hydrolysing gene cluster of *Pseudomonas* sp. NS671 which is preceded by a putative σ^{54}-promoter region (Watabe *et al*. 1992a). A putative σ^{54}-dependent promoter region has also been identified upstream of the hydantoin-hydrolysing gene cluster of *Arthrobacter aurescens* DSM 3747 (Wiese *et al*. 2001). As activation of σ^{54}-dependent promoters occurs via an activator protein which usually belongs to the NtrC family (Snyder and Champress 2003), the presence of these regions upstream of the genes encoding for hydantoin-hydrolysing enzymes suggests that these operons may be regulated by nitrogen catabolite repression (Ntr system).

The production of hydantoinase and *N*-carbamoylase in *Agrobacterium tumefaciens* RU-OR also appeared to be regulated by nitrogen catabolite repression as evidenced by the dramatic decrease in activity in cells cultured with a good nitrogen source such as $(NH_4)_2SO_4$. This is substantiated by mutant strain RU-ORPN1 which was no longer subject to nitrogen catabolite repression as, unlike the wild type, hydantoinase and *N*-carbamoylase activities were observed in mid-log phase of growth (Hartley *et al*. 2001). Subsequent to incubation for 30 minutes in minimal medium with $_{(NH4)2SO4}$ as a nitrogen source, *A. tumefaciens* RU-OR cells retained only a third and a half of the original hydantoinase and *N*-carbamoylase activities respectively. This second regulatory mechanism was termed ammonia shock and was shown to involve the enzymatic action of glutamine synthetase as addition of the glutamine synthetase inhibitor D,L-methionine D,L-sulfoximine protected the hydantoinase from ammonium shock (Hartley *et al.* 2001).

Glutamine synthetase activity is an integral part of the global nitrogen regulatory system in prokaryotic cells (Merrick and Edwards 1995). To verify the importance of glutamine synthetase in the activity of hydantoinase and *N*-carbamoylase enzymes in *A. tumefaciens*

RU-OR, a glutamine auxotrophic mutant of RU-ORPN1, RU-ORPN1F9, was isolated which was not sensitive to ammonia shock (Hartley *et al.* 2001). As a rule, the higher the degree of adenylation of glutamine synthetase, the lower the level of glutamine synthesis (Merrick and Edwards 1995). The adenylation of the glutamine synthetase in mutant strain RU-ORPN1F9 was found to be equivalent pre- and post-ammonia shock whilst in the wild type strain, adenylation of glutamine synthetase occurred only after ammonia shock. Thus the glutamine auxotrophy in RU-ORPN1F9 is due to decreased glutamine synthesis as a result of abnormally high levels of adenylation of the glutamine synthetase enzyme (Hartley *et al*. 2001). The cellular ratio of α-2-ketoglutarate to glutamine reflects the nitrogen status of the cell and affects the regulation of the nitrogen catabolite repression pathway (Merrick and Edwards 1995). Thus a reduction in glutamine synthesis in mutant strain RU-ORPN1F9 resulted in an inability of the cell to detect a high nitrogen status and as a result regulation of the hydantoin-hydrolysing enzymes did not occur (Hartley *et al*. 2001).

1.5 HETEROLOGOUS EXPRESSION OF HYDANTOIN-HYDROLYSING ENZYMES

Increasing interest has been directed at the heterologous expression of hydantoin-hydrolysing enzymes. The reasons for this include: a) decreased costs of catalysis as *Escherichia coli*, in contrast to many wild type organisms, grows rapidly to a high cell density on inexpensive substrates (Baneyx 1999), b) expression of the genes can be readily manipulated in *E. coli* (Weickert *et al*. 1996), c) enzymatic properties such as stability and stereoselectivity can be improved by alteration of the recombinant gene by rational protein design (if the structure and catalytic mechanisms have been elucidated) or by evolutionary protein design (Syldatk *et al*. 1999).

Genes coding for hydantoinase and *N*-carbamoylase enzymes from several bacterial sources have been heterologously expressed in *E. coli* with varying success. The D-hydantoinase from *B. stearothermophilus*, for example, was found to be constitutively expressed from its own promoter in *E. coli* and specific activities 30 times higher than that of the wild type strain observed (Lee *et al*. 1996). Whilst the heterologous expression of *A. radiobacter* D-hydantoinase and D-carbamoylase encoding genes under the control of their corresponding wild type promoters resulted in the conversion of D,L-hydroxyphenylhydantoin to D-hydroxyphenylglycine with a conversion yield of 97% and a productivity five times higher than that obtained from the gene donor strain (Chao *et al*. 1999b). Recombinant expression, also under its native promoter, of the D-carbamoylase from *Pseudomonas* sp. KNK003A in *E. coli* resulted in activity levels 40-fold higher than that of the native strain (Ikenaka *et al*. 1998a).

1.5.1 Expression systems

As an alternative to expression of genes using native promoters, expression of hydantoinase and *N*-carbamoylase in *E. coli* can be placed under the control of a promoter with high-level production of protein but which is regulated, as opposed to constitutive, to minimize the metabolic burden and possible toxic effects that expression of the gene may incur (Weickert *et al*. 1996). Heterologous expression of *P. putida* CCRC 12857 D-hydantoinase under the control of the T5*lac* promoter and lactose induction resulted in activity levels of 200U.L^{-1} which was approximately 20-fold higher than that of the wild type strain (Chien *et al.* 1998). The *cauA* gene, encoding the D-carbamoylase from *A. radiobacter* NRRL B11291, under T7 promoter control resulted in production of D-carbamoylase at 40% of the total protein with a specific activity of 0.7U (Buson *et al*. 1996).

High levels of expression of hydantoinase and *N*-carbamoylase enzymes in *E. coli* was, however, found to result in the formation of insoluble aggregates of inactive proteins, termed inclusion bodies (Buson *et al*. 1996, Chien *et al*. 1998, Hils *et al.* 2001, Chao *et al.* 2000a, Wilms *et al*. 2001b) due to improperly folded proteins (Baneyx 1999). In addition, retarded growth rates were also observed which may be attributed to the unregulated degradation of pyrimidines in the cell by the overproduced hydantoinase enzyme (Mukohara *et al*. 1994, Chien *et al*. 1998). Whilst the formation of inclusion bodies facilitates in the separation of the expressed protein from the rest of the cellular material, the refolding process to resolubilize the protein aggregates varies from case-to-case and costs vary greatly. In addition, the yield of active proteins recovered from the inclusion bodies is usually very low (Hockney 1994).

A substitute for the positively regulated *lac* or T7 promoters, which exhibit high basal expression levels under non-inducing conditions and often result in expression of proteins that are unable to reach their native conformation and either partially or completely segregate within inclusion bodies (Baneyx 1999), is the rhamnose-inducible *rhaBAD* promoter which is one of the most tightly regulated gene promoters described in literature (Wilms *et al*. 2001a). Wilms *et al.* (2001a) used the positively regulated *E. coli rhaBAD* promoter for the heterologous expression of the *A. aurescens* L-carbamoylase gene. This promoter confers two major advantages to the expression system namely, extremely tight regulation of expression under non-inducing conditions and slow induction by L-rhamnose (Altenbuchner *et al*. 2001). These characteristics facilitate in lowering inclusion-body formation and toxicity of the expressed protein. In order to reduce production costs, the host *E. coli* strain used contained a frameshift mutation in the rhamnose operon resulting in an inactive rhamnose kinase. This mutation prevented hydrolysis of the rhamnose inducer by the cell thus reducing the amount of inducer required for expression by a factor of approximately 20 (Wilms *et al*. 2001a).

A further cost in the production of heterologously expressed proteins is the requirement of antibiotics in the fermentations, however, removal of the selection pressure supplied by the antibiotic resulted in dramatic increases in plasmid-free cells. This is partly due to multimerization of the plasmids resulting in a reduction in the copy number available for random distribution to the daughter cells. Thus Wilms *et al.* (2001a) integrated a *cer* site onto the plasmid which is recognised by the chromosomally encoded integrase, XerCD, which catalyses the formation of monomers from the plasmid multimers. As a result, plasmid stability was enhanced and at the end of the fermentation without supplementation of an antibiotic, over 90% of the cells still carried plasmids (Wilms *et al*. 2001a). The combination of the above manipulations resulted in a space time yield of L-carbamoylase of 458U.L^{-1}.h^{-1} with nearly 50g of enzyme produced from a single 13 litre fermentation (Wilms *et al.* 2001a).

1.5.2 Ratio of *N*-carbamoylase to hydantoinase

Expression and activity levels of the enzymes involved in hydantoin-hydrolysis does not occur at equivalent rates with the hydrolysis of *N*-carbamylamino acids to amino acids by *N*-carbamoylase identified as the rate limiting step in the reaction (Chao *et al*. 2000b, Grifantini *et al*. 1998, Burton *et al*. 2001). In order to optimise the reaction cascade, the catalytic efficiency of the *N*-carbamoylase enzyme must be improved or alternatively, the production of *N*-carbamoylase relative to the hydantoinase needs to be increased. Manipulation of the production levels of *N*-carbamoylase and hydantoinase enzymes relative to one another can be achieved by expressing the encoding genes separately and then adjusting the loading ratio of the individual cells according to the enzyme activity levels required. This approach was used by Chao *et al*. (2000b) to express the D-hydantoinase and D-carbamoylase genes from *A. radiobacter* NRRL B11291 under the control of the *tac* promoter in separate cells lines. Optimal productivity was found at a ratio of D-carbamoylase to D-hydantoinase activity of between 1 and 2. When the ratio was increased to 4 or decreased to less than 0.5, the productivity observed dropped to 25% and 50% respectively (Chao *et al*. 2000b).

Equivalent loading of the separate cells expressing the D-hydantoinase and D-carbamoylase genes, from *B. stearothermophilus* SD-1 and *A. tumefaciens* NRRL B11291 respectively, such that the activities were the same (200 units/L) resulted in a product yield of 71% D-hydroxyphenylglycine (D-HPG). However, when the activity of D-carbamoylase was increased to 400 units/L, the production rate of D-HPG increased to 90% (Park *et al*. 2000). Expression of the enzymes in two separate cell lines has a drawback in that the substrate and intermediate have to diffuse across several membranes before complete conversion to amino acids can occur thereby decreasing productivity (Park *et al.* 2000, Chao *et al*. 2000b). In particular, the *N*-carbamylamino acid intermediate is easily transported out of the cell but is not readily taken up, resulting in reduced productivity (Pietzsch *et al*. 2000).

Co-expression of the hydantoinase and *N*-carbamoylase genes within the same *E. coli* strain was studied by Park *et al.* (2000). They expressed the D-hydantoinase gene from *Bacillus stearothermophilus* SD-1 and the *N*-carbamoylase from *Agrobacterium tumefaciens* NRRL B11291 on separate plasmids under the control of the constitutive promoter isolated upstream of the D-hydantoinase gene in *B. stearothermophilus* SD-1. The hydrolytic activity of these co-expressed enzymes resulted in 98% conversion (6.74mM/g-cell/h in 15 hours) of hydroxyphenylhydantoin to hydroxyphenylglycine compared to the 71% conversion (2.57mM/g-cell/h in 15 hours) observed when the genes were expressed in separate cell lines (Park *et al*. 2000).

An alternative approach is the expression of the hydantoinase and *N*-carbamoylase genes from a single recombinant plasmid as a polycistronic mRNA. Consequently, *E. coli* expression vectors were constructed with the genes encoding hydantoinase and *N*-carbamoylase isolated from *Agrobacterium tumefaciens* NRRL B11291 such that these genes were expressed as a polycistronic mRNA under the control of a constitutive promoter. The order in which the hydantoin-hydrolysing genes were placed in relation to the promoter was found to be important as the vector in which the *N*-carbamoylase gene was placed first and the hydantoinase gene distal from the promoter resulted in better conversion of hydroxyphenylhydantoin to hydroxyphenylglycine than when the hydantoinase gene preceded the *N*-carbamoylase gene (Grifantini *et al*. 1998). Expression of the construct in which the hydantoinase preceded the *N*-carbamoylase gene resulted in conversion yields equivalent to that of the wild type *A. tumefaciens* NRRL B11291 with 30% of the substrate converted to hydroxyphenylglycine after 22 hours. In contrast, the heterologous expression of the *N*-carbamoylase and hydantoinase from polycistronic mRNA in which the *N*-carbamoylase gene preceded the hydantoinase led to over 60% conversion of the substrate to the corresponding amino acid (Grifantini *et al.* 1998).

The major limitation of the above heterologous expression systems is an inability to regulate the levels of *N*-carbamoylase relative to the hydantoinase within the cell (Park *et al.* 2000). This can be circumvented by expression of the relevant genes under the control of different promoters with the gene product with the lowest activity combined with the strongest promoter and visa versa. However, this approach requires the use of different inducers. Alternatively, the genes can be placed under the control of the same promoter but encoded on replicons with varying copy numbers (Wilms *et al*. 2001b). This approach was utilized by Wilms *et al*. (2001b) for the expression of the genes encoding the hydantoinase (*hyuH*), *N*-carbamoylase (*hyuC*) and racemase (*hyuA*) from *Arthrobacter aurescens* DSM 3747 under the control of a rhamnose inducible *E. coli* promoter. When all three genes (*hyuA*, *hyuC*, and *hyuH*) were separately coded for on pBR322, which has a copy number of 40-50, and co-

expressed in the same *E. coli* cell, the racemase produced was soluble, the *N*-carbamoylase resulted in the formation of small inclusion bodies, whilst expression of the hydantoinase resulted in high levels of inclusion body formation. As over-expression of proteins often leads to inclusion body formation, the number of *hyuH* gene copies within the cell needed to be reduced.

Expression of the genes from alternative vectors such as pSC101 or pACYC184 which have copy numbers of 5-10 and 10-15 respectively, as well as insertion of the *hyuH* gene into the *E. coli* chromosome was therefore investigated. The optimal expression system was found to consist of the *hyuA* and *hyuC* genes in pBR322 vectors and insertion of the *hyuH* gene into the vector pSC101 resulting in productivity levels of 1.2mmol/h/g, compared to the 0.3mmol/h/g obtained with the wild type *A. aurescens* DSM 3747, with the hydantoinase as the limiting activity. Further optimisation of this system was done by replacing the *hyuH* gene from *A. aurescens* DSM 3747 with the corresponding gene from *A. aurescens* DSM 3745 (Wilms *et al.* 2001b) which differ from one another by 8 amino acid residues (Wilms *et al*. 1999). With this optimised catalytic cascade, a productivity of 1.9mmol/h/g was obtained which is 6-fold higher than that of the wild type (Wilms *et al*. 2001b).

1.5.3 Co-overexpression with molecular chaperones

Despite the optimisation of the heterologous expression of various hydantoinase and *N*-carbamoylases in *E. coli*, a significant proportion of the expressed protein still remains within the insoluble fraction of the cell lysate as inclusion bodies. Many proteins have been found to require the presence of molecular chaperone proteins in order to attain their biologically active native conformation. Molecular chaperones function by temporarily stabilizing the unfolded or partially folded target proteins thus minimizing the formation of incorrect inter- and intra-molecular interactions which result in deposition of the misfolded proteins in inclusion bodies (Hockney 1994). Thus over-expression of hydantoinase and/or *N*-carbamoylase encoding genes in *E. coli* result in high levels of nascent protein formation which, due to their rapid accumulation, may not be adequately chaperoned (Chao *et al.* 2000a). Accordingly, over-expression of molecule chaperones were investigated to determine if an increase in these proteins would facilitate correct folding of the heterologously expressed hydantoin-hydrolysing enzymes.

Co-expression of the *N*-carbamoylase from *Agrobacterium radiobacter* NRRL B11291 in *E. coli* with a plasmid encoding for the GroEL/ES molecular chaperones resulted in a 3-5-fold increase in enzyme activity and a significant reduction in inclusion body formation (Chao et al. 2000a). A similar result was obtained with expression of the *dcb* gene from *Agrobacterium tumefaciens* AM 10 in *E. coli* JM109. Prior to co-expression with the

molecular chaperones GroEL/ES only 10% of the *N*-carbamoylase protein produced was present in the soluble fraction. Subsequent to co-transformation with a plasmid encoding for the GroEL/ES molecular chaperones, 60% solubilization of the total expressed *N*-carbamoylase was observed with a 6.2-fold increase in activity compared to cells grown under the same conditions but without co-expression of the molecular chaperones (Sareen *et al*. 20001b). In contrast, co-expression of the GroEL/ES chaperones with the hydantoinase isolated from *A. radiobacter* NRRL B11291 did not result in any significant improvement in enzyme activity or solubility. However, co-expression with the molecular chaperones DnaK/DnaJ resulted in an increase in hydantoinase activity by a factor of 3.8 and a reduction in inclusion bodies observed (Chao *et al*. 2000a). While co-expression of molecular chaperones was found to increase the solubility and biological activity of the hydantoinase and *N*-carbamoylase enzymes in these cases, it is unlikely to provide a universal solution as the beneficial effect of over-expression of GroEL/ES or DnaK/DnaJ molecular chaperones is highly dependent on the folding pathway of the target protein (Hockney 1994, Baneyx 1999).

1.6 GENETIC MANIPULATIONS FOR IMPROVED BIOCATALYSTS

1.6.1 Fusion proteins

Fusion proteins were originally constructed to facilitate purification and/or immobilization of a target protein by supplying an affinity tag for specific absorption to a matrix. An advantageous side-effect of recombinant fusion proteins is that, in certain instances, the solubility of the target protein, which would normally aggregate in the *E. coli* cytoplasm, was found to be increased (Baneyx 1999). The hydantoinase (HyuH) from *A. aurescens* DSM 3747 was fused to the maltose-binding protein (MalE) resulting in enhanced solubility of the hydantoinase. In addition, the specific activity of the MalE-HyuH fusion protein was found to be equivalent to that of the wild type despite the fact that the protein had approximately doubled in size (Pietzsch *et al*. 2000). In comparison, fusion of the phenylhydantoinase from *E. coli* K12 with the maltose-binding protein resulted in a 350- to 600-fold increase in hydroxyphenylhydantoin hydrolysis when compared to that of the wild type cells (Kim *et al*. 2000c).

The affinity of the fused protein for immobilized ligands can be used to purify the target protein, however, binding usually occurs with low affinity which prohibits the use of stringent wash conditions. This can be remedied by the fusion of polypeptide tags, composed of amino acids such as histidine, which can be efficiently purified by metal affinity chromatography (Baneyx 1999). In addition, the smaller size of the affinity tag (6 His residues of 0.84kDa vs. ~40kDa maltose-binding protein) reduces potential interference of the tag with the structure and function of the recombinant protein (Sheibani 1999). However,

His_6-tagging of the hydantoinase from *A. aurescens* DSM 3747 resulted in high levels of inclusion body formation and a loss of activity of over 80% during elution from the affinity column with imidazole (Pietzsch *et al.* 2000, Ragnitz *et al*. 2001). Loss of activity subsequent to imidazole treatment may have been due to the removal of the zinc ions which are crucial for the biocatalytic activity of hydantoinases (Altenbuchner *et al.* 2001). In contrast, the *N*-carbamoylase containing a His_6-tag could be eluted from the metal affinity column with imidazole as the chelating agent without loss in specific activity. Tagging of the *N*-carbamoylase with six aspartate residues did not affect the specific activity of the enzyme either but in both instances, tagging the *N*-carbamoylase allowed for a one-step purification procedure as apposed to the three steps required for wild type enzyme (Pietzsch *et al.* 2000). A His_6-tag was also fused to the *N*-carbamoylase isolated from *B. kaustophilus* CCRC 11223 and a 430-fold increase in specific activity observed (Hu *et al*. 2003).

An alternative use of fusion protein technology is the construction of bifunctional enzymes in which two enzymes with different catalytic properties are fused together. This has the obvious advantage of only one protein having to be produced and purified as opposed to two in addition to potential increases in reaction kinetics of the fusion enzyme compared to that of the two individual enzymes (Altenbuchner *et al.* 2001). Kim *et al*. (2000a) constructed a bifunctional enzyme (CAB-HYD) by fusion of the *N*-carbamoylase from *A. radiobacter* NRRL B11291 to the N-terminus of the D-hydantoinase from *B. stearothermophilus* SD-1 such that complete conversion of hydantoin derivatives to the corresponding amino acids by a single enzyme could be achieved. Whilst the constructed fusion protein did exhibit bifunctional activity, CAB-HYD was found to be subject to extensive proteolysis. An increase in CAB-HYD protein was detected subsequent to expression of the fusion protein in the protease deficient *E. coli* strain BL21 but over 95% of the detected protein occurred in the insoluble fraction of the cell lysate (Kim *et al.* 2000a). High levels of proteolysis and inclusion body formation may be attributed to low structural stability of CAB-HYD and DNA-shuffling was therefore used to isolate a mutant of CAB-HYD with improved stability. The resultant enzyme, called F11, was isolated with increased resistance to proteolytic degradation and a 6-fold increase in production of D-amino acids compared of CAB-HYD. Sequence analysis of the gene encoding F11 revealed 19 point mutations, distributed predominantly in the hydantoinase domain, of which 8 were silent mutations (Kim *et al.* 2000a).

A related hydantoinase from *B. thermocatenulatus* GH2 was also fused to the *A. radiobacter* *N*-carbamoylase resulting in a bifunctional enzyme (CAB-HYD1) which showed improved catalytic performance when compared to CAB-HYD (Kim *et al*. 2000b). The different properties of CAB-HYD and CAB-HYD1 appear to be as a result of differences in the primary structure of the hydantoinase domain. Sequence analysis of the two hydantoinases revealed

17 amino acid residues difference when conservative substitutions were considered (Kim *et al*. 2000a). The major disadvantage of protein fusion to generate bifunctional enzymes is the lack of flexibility with respect to optimisation of reaction conditions if the two fused enzymes have different optimal conditions of catalytic activity as is often the case with hydantoinase and *N*-carbamoylase enzymes (Altenbuchner *et al*. 2001).

1.6.2 Directed evolution

Optimisation of hydrolysis of hydantoin to optically pure amino acids by hydantoinase and *N*-carbamoylase enzymes by manipulation of culture, expression, and reaction conditions can only be carried to a certain extent. Beyond this, optimisation of the catalytic action of the enzyme itself is required by alteration of the enzymes primary structure such that a desired physical characteristic (e.g. thermostability, etc) is achieved. However, despite enormous developments in research, a complete understanding of the relationship between amino acid sequence, structure, and catalytic mechanism/function is incomplete. Consequently, rational design of new proteins by site-directed mutagenesis is not always successful (Arnold and Moore 1997). By contrast, directed evolution involves the generation of a random library of mutants, via random mutagenesis (e.g. error-prone PCR) or recombination of gene fragments, followed by screening for a representative with the desired altered characteristic (Zhao *et al*. 2002).

The *N*-carbamoylase from *A. tumefaciens* NRRL B11291 has low oxidative and thermostability in comparison to the hydantoinase enzyme. Consequently, directed evolution of the *N*-carbamoylase by DNA shuffling over two evolutionary generations was done. Evolved enzyme 2S3 was selected from the second generation of mutants subsequent to screening of the mutant enzymes for increased thermostability and oxidative stability by incubation at 70^{o}C for 2 hours and treatment with hydrogen peroxide for 30 minutes respectively (Oh *et al*. 2002a). Analysis of the evolved enzyme 2S3 revealed an 8-fold increase in thermostability and an oxidative stability approximately 18-fold higher than that of the wild type enzyme (Oh *et al*. 2002b). Sequence analysis of 2S3 revealed the amino acid residue alterations in 8 positions. In order to determine the significance of each of the amino acid residue alterations, the mutations were individually carried out on the wild type enzyme and the resultant effect on thermostability and oxidative stability observed. Substitutions Q23L, H58Y, M184L, and T262A were found to contribute towards thermostability and oxidative stability with T262A resulting in the most significant increase in stability. Substitutions V40A and G75S were found to enhance oxidative stability alone (Oh *et al*. 2002a). However, the enhanced stability of the evolved enzyme 2S3 appeared to come at the cost of reduced activity levels as the $_{kcat/Km}$ of 2S3 was approximately 70% that of the wild type enzyme (Oh *et al*. 2002b).

Directed evolution was also applied to the hydantoinase from *Arthrobacter* sp. DSM 9771 in order to generate mutant enzymes with increased activity levels and/or inverted enantioselectivity (May *et al*. 2000). The first generation of mutants were produced by random mutagenesis via error-prone PCR and five mutants were isolated with altered levels of activity with D- or L-5-(2-methylthioethyl)hydantoin (MTEH) as substrates. Mutant enzymes 1CF3, 1CG7, and 14CB10 were isolated with significantly increased D-enantioselectivity (90% enantiomeric excess $(ee)_D$ at 30% conversion) than the wild type enzyme. Sequence analysis of these three enzymes revealed a single amino acid substitution of V154A. Mutant enzymes 19AG11 and 11DH7, with the mutation I95L, were slightly more active toward L-MTEH than D-MTEH exhibiting 20% ee_D compared to 40% ee_D for the wild type. In the second generation of random mutagenesis in which 11DH7 was used as the parent, mutant enzyme 22CG2 (carrying the mutation V180A) was isolated and found to be have the same enantioselectivity as the parent but was 4-fold more active (May *et al*. 2000).

However, the number of amino acid substitutions achieved by PCR mutagenesis is limited due to the low error rate obtained. Consequently, May *et al*. (2000) carried out saturation mutagenesis, in which a specific amino acid residue is targeted for mutation, with mutant enzyme 22CG2 as the parent. As the amino acid residue at position 95 had been identified as responsible for a slight shift in enantioselectivity in mutants 19AG11 and 11DH7, saturation mutagenesis was used to generate a library in which all 20 amino acids had been substituted into this position. The subsequently isolated mutant enzyme Q2H4 was found to produce *N*-carbamoyl-L-methionine with an ee_L of 20% compared to the 20% ee_D and 40% ee_D of the parental and wild type enzymes respectively. In addition to inversion of enantioselectivity, the single amino acid substitution of I95F in mutant enzyme Q2H4 also resulted in approximately 1.5-fold increase in activity compared to that of the parent (May *et al.* 2000).

1.7 RESEARCH PROPOSAL

Several hydantoin-hydrolysing microorganisms were isolated from soil samples collected from the Grahamstown and Hogsback area (Eastern Cape, South Africa) by the Rhodes Hydantoinase Research Group. Isolates were screened for the ability to utilize hydantoin as the sole source of nitrogen. Of 146 isolates, six grew well with hydantoin, *N*-carbamylglycine, methylhydantoin, or *N*-carbamylalanine as sole sources of nitrogen and were subjected to biocatalytic assays to determine their hydantoin-hydrolysing enzyme activity levels. One of these six isolates, designated RU-$KM3_S$, exhibited high levels of *N*-

carbamylglycine and glycine production from hydantoin in resting cell assays and was subsequently selected for further investigation (Burton *et al*. 1998). The central objective of this research project was to determine if the hydantoin-hydrolysing enzyme system in RU-KM3$_S$ had potential for industrial application. To achieve this, the following objectives were identified:

Research objectives

1) Identification of the environmental isolate in order to eliminate the possibility of RU-KM3$_S$ being a pathogen. This information will also facilitate in the establishing the potential novelty of the hydantoin-hydrolysing enzyme system.
2) Establishment of potential industrial application of the hydantoin-hydrolysing enzyme system by biochemical characterization of the relevant enzymes.
3) Isolation of the genes coding for the hydantoinase and *N*-carbamoylase enzymes and comparison of the deduced nucleotide/amino acid sequence to those in literature to determine if the enzymes are indeed novel.
4) Investigation of the mechanisms by which the hydantoin-hydrolysing system in RU-KM3$_S$ is regulated.

2.1 INTRODUCTION

The process of developing a biocatalyst involves a series of research phases (Figure 2.1). First, a suitable biocatalyst able to catalyse the desired reaction needs to be selected, either by screening for a potentially novel biocatalyst from the environment or by application of an existing enzyme or organism. The second phase in biocatalyst design entails characterization of the biocatalyst and encompasses several aspects such as selectivity, yield, optimum reaction conditions, stability and co-factor requirement. Once the biophysical parameters of the biocatalyst have been established, the next phase involves optimisation of the reaction by engineering the biocatalyst either directly by cell or enzyme modification, or indirectly by optimisation of the process design. Once the maximum performance has been achieved, the biocatalyst can be applied in the production of the desired end-product provided the system proves to be industrially viable (Schmid *et al*. 2001).

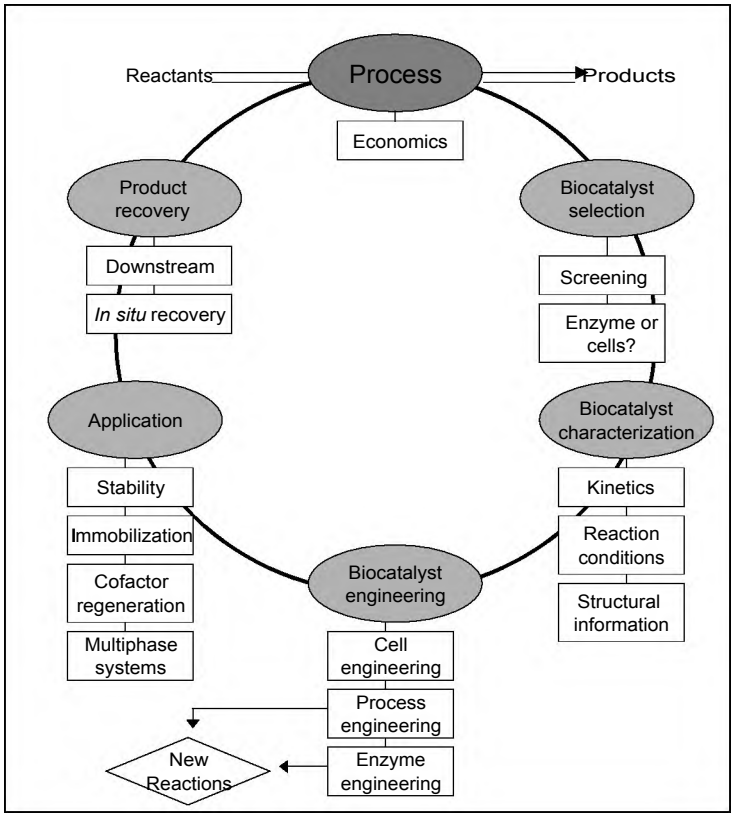

Figure 2.1 Rational development of a biocatalyst for production of industrially important organic compounds (modified from Schmid *et al.* 2001).

When characterising a potential hydantoin-hydrolysing biocatalyst, enantioselectivity is one of the most important properties to be considered. Evaluation of the selected biocatalyst can be achieved by colourimetric assay of the products produced from optically pure substrates (Moller *et al*. 1988, Yokozeki *et al.* 1987a). Alternatively, thin layer chromatography (TLC)

and high performance liquid chromatography (HPLC) using chiral supports (Morin *et al*. 1993, Syldatk *et al*. 1987, Hartley *et al*. 1998) allow for direct enantiomeric analysis of the products. Enantiospecificity of hydantoin-hydrolysis products can also be accurately determined by nuclear magnetic resonance (NMR) studies and infra-red spectroscopy (Yokozeki *et al*. 1987a), or X-ray diffraction patterns of the amino acid products (Sano *et al*. 1977). However, these methods require expensive equipment as well as the purification of the products from the reaction mixtures (Syldatk *et al*. 1990b). Alternatively, elucidation of hydantoinase enantioselectivity can be determined via the reverse hydantoinase reaction: a cell lysate containing hydantoinase activity was subjected to non-denaturing PAGE followed by incubation with D- or L-carbamyltryptophan which is enzymatically converted to insoluble indolymethylhydantoin and visualized as a precipitant (May *et al.* 1998e).

Besides enantioselectivity, factors such as metal ion- and ATP-dependency of hydantoin-hydrolysing enzyme systems are also addressed in this chapter. The requirement of metal ions for hydantoinase and *N*-carbamoylase activity has been well documented, however, which metal ions are stimulatory and which are inhibitory with respect to enzyme activity varies greatly between isolates. There are two major approaches to determining if the hydantoinase or *N*-carbamoylase enzymes of a particular bacterial strain are metal ion dependent or not. Firstly, the metal ions may be removed from the reaction mixture using EDTA to chelate any metal ions present (Louwrier and Knowles 1997) or via dialysis of the reaction mixture against a buffer solution which is free of metal ions (Syldatk *et al.* 1987). The second approach involves the addition of the appropriate metal ion to the reaction mixture and measurement of the effect of the metal on enzyme activity (Ishikawa *et al.* 1994).

Finally, identification of a microbial isolate with biocatalytic potential may provide information as to the potential novelty of the hydantoin-hydrolysing enzyme system. In addition, the potential pathogenicity of environmental isolates will influence the choice between using the native organism or a recombinant host in the development of an industrial biocatalytic process. Traditionally, microbial identification was based on phenotypic characteristics determined by metabolic reactions and microscopy (Brunk *et al.* 1996). However, identification of bacterial strains by these means are not always conclusive due to common phenotypic parameters between several species, as well as expression of the tested characteristics on plasmids which can undergo abrupt and multiple changes or be lost altogether. In contrast, the analysis of the genotype of an organism does not rely on expression of particular genes and is not subject to phenotypic variation (Towner and Cockayne 1993). Due to the fundamental role of ribosomes in protein synthesis, rRNA genes are highly conserved and are not affected by environmental conditions (Rosello-Mora and Amann, 2001) yet sufficient differentiation exists between isolates to allow for unambiguous identification (Brunk *et al.* 1996). In this study, the strain of interest was

initially identified based on phenotypic characteristics. This information was used to select 16S rRNA gene sequences from strains of the same species, from which primers were designed and amplification of the 16S rRNA gene sequence from the environmental isolate was done. The nucleotide sequence analysis of the resultant PCR product was then compared to a comprehensive sequence dataset of approximately 16 277 prokaryotic entries which is readily available on the Ribosomal Database Project (RDP) databases (Cole *et al*. 2003).

As described in Chapter 1, strain RU-KM3$_S$ was isolated from environmental samples and selected due to its relatively high productivity in whole cell biocatalytic assays using hydantoin as a substrate (Burton *et al*. 1998). The aim of the research described in this chapter was to establish the presence of unique properties in the RU-KM3$_S$ hydantoin-hydrolysing enzyme system. This was done through characterization of the RU-KM3$_S$ enzyme system in terms of enantioselectivity, metal ion inhibition/stimulation, ATP-dependence, and the identification of the strain by determining the 16S rRNA gene sequence. Previous and concomitant characterization of RU-KM3$_S$ by Z. Skepu and K. Buchanan with respect to substrate-selectivity, induction, and optimum reaction conditions on hydantoin-hydrolysing activity are also discussed (Buchanan *et al.* 2001).

2.2 METHODS AND MATERIALS

2.2.1 Chemicals and kits

D-L-methylhydantoin was prepared as a 1:1 mixture of D- and L-methylhydantoin (Toronto Research Chemicals Ltd.). Hydantoin, *N*-carbamylglycine, glycine, and alanine were obtained from Aldrich, ICN Biomedicals Inc., Saarchem, and Sigma respectively. Adenosine triphosphate (ATP) was obtained from Boehringer Mannheim. The growth medium nutrient broth was supplied by Merck.

2.2.2 Hydantoinase and *N*-carbamoylase enzyme assays

2.2.2.1 Resting cell biocatalytic assay

A detailed methodology for resting cell biocatalytic assays is described in Appendix 2.1. Unless otherwise stated, a starter culture of strain RU-KM3$_S$ was generated in hydantoin minimal medium (HMM) (Appendix 1) and used to seed nutrient broth supplemented with 0.1% hydantoin as an inducer such that the $_{OD600}$ was 0.02. The seeded cultures were then incubated at 28^{o}C, shaking at 200rpm, until the culture reached stationary phase of growth (after approximately 20 hours). Absorbance readings were determined at 600nm using the Shimadzu UV-visible spectrophotometer with the corresponding uninoculated medium as a blank.

Once optimum $_{OD600}$ was reached, the cells were harvested by centrifugation and resuspended in 0.1M phosphate buffer (pH 8.0). A final concentration of 20mg wet cell mass/ml was aliquoted into each reaction mixture with either 0.1M phosphate buffer (cell blank) or the appropriate substrate in 0.1M phosphate buffer (e.g. 50mM hydantoin or 25mM *N*-carbamylglycine). Following incubation at 40^{o}C for 3 hours, the reaction mixtures were centrifuged in a Heraeus microfuge (13 000rpm unless otherwise stated) and the supernatant analysed for *N*-carbamylamino acids and amino acids using the Ehrlich's and ninhydrin colorimetric assays respectively. The units of activity were measured as µ mol/ml of product and expressed as an average of 3 replicates. Hydantoinase activity was calculated as the total amount of *N*-carbamylamino acid and amino acid produced from an hydantoin substrate whilst *N*-carbamoylase activity was expressed as µ mol/ml amino acid produced from the *N*-carbamylamino acid intermediate.

2.2.2.2 Cell-free extracts

Induced RU-KM3$_S$ cells were cultured and harvested as described above. The resuspended cells were then disrupted by a single pass through a Yeda-press (LINCA Lamon Instrumentations, Tel Aviv) at 15psi., 4^{o}C and at a flow rate of approximately 1 drop per second. The resultant cell-free extract was then utilized in biocatalytic reactions as described above.

2.2.3 Metal ion dependence

To determine the effect of metal ions on hydantoinase and *N*-carbamoylase activities, the metal ions Mg^{2+}, Mn^{2+}, Zn^{2+}, Co^{2+}, Cu^{2+}, Fe^{2+}, or Co^{2+} and Mg^{2+} were added to each biocatalytic reaction triplicate set at a concentration of 2.5mM together with or without 2.5mM Na_2EDTA. To obtain dialysed cell free extracts, the harvested RU-KM3$_S$ cells were disrupted as described above and the cell-free extract subjected to dialysis with Spectrafor^{R} dialysis tubing (MWco 6-8000) against 0.1M phosphate buffer, pH 8.0, with or without 2.5mM Na_2EDTA for 90 minutes at 4^{o}C, changing the buffer every half hour. In order to determine the stimulatory effect of the respective metal ions on hydantoinase and *N*-carbamoylase activities, 2.5mM Mg^{2+}, Mn^{2+}, Zn^{2+}, Co^{2+}, Cu^{2+}, Fe^{2+}, or Co^{2+} and Mg^{2+} were added to the respective biocatalytic reaction sample sets after dialysis against 0.1M phosphate buffer containing 2.5mM Na_2EDTA as described above. Controls were established as undialysed cell-free extract, cell-free extract dialysed without addition of any metal ions, and cell-free extract allowed to stand at 4^{o}C for the time taken for dialysis. Hydantoin was used as a substrate at a final concentration of 50mM and the reactions were incubated at 40^{o}C for 3 hours before carrying out Ehrlich's and ninhydrin assays (Appendix 2.1).

2.2.4 Effect of ATP

In order to determine the ATP requirements of the hydantoinase and *N*-carbamoylase in RU-KM3$_S$, ATP was added to the resting whole cell biocatlytic reactions (prepared as described above) at a final concentration of 1.5mM, 3mM, and 6mM. Hydantoin, at a final concentration of 50mM, was used as a substrate and the reaction mixtures incubated at 40^{o}C for 3 hours before carrying out Ehrlich's and ninhydrin assays to determine levels of *N*-carbamylglycine and glycine production respectively (Appendix 2).

2.2.5 Strain identification

Genomic DNA was extracted from RU-KM3$_S$ by the detergent lysis/CTAB and organic solvent extraction method as described in Appendix 5.2. Polymerase chain reaction (PCR) amplification of the 16S rRNA gene from the prepared genomic DNA was done with universal primers for the 16S rRNA coding region, CH1 and CH3 (Appendix 3, Table A3.1) using Vent DNA Polymerase (New England Biolabs) under standard amplification parameters and an annealing temperature of 63^{o}C (Appendix 5.3). The resultant 1300bp PCR product was cloned into the *Bam* HI site of vector pUC18 (Appendix 3, Figure A3.1) as follows: the PCR product was digested with *Bam* HI restriction endonuclease (flanking sites generated by the primers CH1 and CH3) and ligated with *Bam* HI digested pUC18, that had been treated with Shrimp Alkaline Phosphatase (USB), using T4 DNA Ligase (Promega) as per manufacturers specifications. The resultant plasmid clones were then transformed into competent *E. coli* DH5α (*supE44* Δ*lac*U169(∅80*lacZ*ΔM15)*hsdR17 recA1 endA1 gyrA96 thi-1 relA1*) and colonies hosting insert-containing plasmids selected, using the blue/white selection provided by β-galactosidase activity, on Luria agar plates containing 100μ g/ml ampicillin, 40μ g/ml 5-bromo-4-chloro-3-indolyl-β-D-galactopyranosidase (X-gal) (Biosolve, Ltd), and 50μ g/ml isopropyl-β-thiogalactosidase (IPTG) (Roche).

The High Pure Plasmid Isolation Kit (Roche) was used to purify the correct recombinant clones, pGMS1 and pGMS2 in which the insert was subcloned into the pUC18 vector in both orientations. The nucleotide sequence of the PCR product was determined using the Alf Express Automated DNA Sequencing service (University of Cape Town, South Africa) and ABI Prism Big Dye Terminator (Amersham) procedure. The 5' and 3' end of the 16S rRNA gene was sequenced using primers specific for the pUC18 vector, pUCF and pUCR (Appendix 3, Table A3.1). In order to generate overlapping sequence from both strands, deletion constructs of pGMS1 and pGMS2 were constructed by restriction endonuclease digestion with *Hinc* II (USB), *Sma* I (USB), or *Csp* 451 (Promega) followed by recirculirization using T4 DNA Ligase. The nucleotide sequence of the resultant plasmids (pGMS1Δ*Hinc* II, pGMS1Δ*Sma* I, pGMS2Δ*Sma* I, pGMS2Δ*Csp* 451) was determined as above using primers pUCF or pUCR where applicable.

Sequence data obtained for the 16S rRNA gene from RU-KM3$_S$ was subjected to comparative analysis with the small subunit rRNA gene sequences available on the Ribosomal Database Project II (http://rdp.cme.msu.edu/html/) (Cole *et al*. 2003). The sequence alignment was done using ClustalW software (Thompson *et al.* 1994) located at the BCM Search Launcher website (http://searchlauncher.bcm.tmc.edu) and presented in boxshade format (http://www.ch.embnet.org/software/BOX form.html).

2.3 RESULTS

2.3.1 Growth phase for optimal hydantoin hydrolysis

It has been well documented that maximum hydantoinase and *N*-carbamoylase activities occur in cells during stationary phase of growth. Accordingly, the hydantoinase and *N*-carbamoylase activities of RU-KM3$_S$ were determined in cells harvested at different stages of growth in complete medium containing hydantoin as an inducer. During early (after 4 hours) and mid-logarithmic phase (after 8 hours), low levels of hydantoin-hydrolysing activity were observed (Figure 2.2). Production of glycine reached optimal levels after 14 hours of growth, whilst maximum levels of hydantoinase activity were observed in cells harvested in mid- to late-stationary phase after 21 hours of growth (Figure 2.2). Consequently, all subsequent biocatalytic assays were carried out using cells harvested after 20 hours of growth in nutrient broth at 28^{o}C.

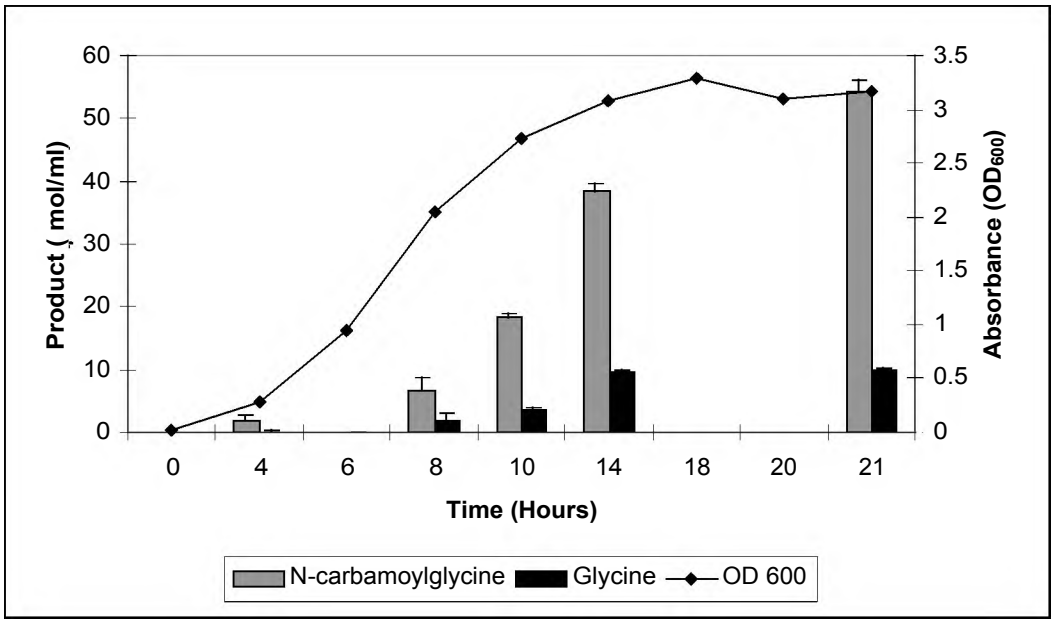

Figure 2.2 Production of *N*-carbamylglycine and glycine from hydantoin by RU-KM3$_S$ at various phases of growth in complete medium. (Error bars represent the standard error of the mean, n=3)

2.3.2 Enantioselectivity

Previous attempts to determine the enantioselectivity of the hydantoin-hydrolysing enzyme system in RU-KM3$_S$ using chiral TLC analysis of the amino acid products obtained from biocatalytic reactions using D,L-methylhydantoin as a substrate were inconclusive as the separation of D- and L-alanine was difficult and the resolution between the two compounds inconclusive. Consequently, biocatalytic assays with optically pure D- and L-methylhydantoin were conducted and the production of *N*-carbamylalanine and alanine from each enantiomer used to determine the stereoselectivity of the RU-KM3$_S$ enzyme system.

Table 2.1 Production of *N*-carbamylalanine and alanine from D/L-methylhydantoin and optically pure L- or D-methylhydantoin by RU-KM3$_S$.

Substrates (50mM)	Hydantoinase activity (μmol/ml NCA)	*N*-carbamoylase activity (μmol/ml alanine)	Ratio of NCA:alanine
D/L-methylhydantoin	25.82 (±1.65)	2.67 (±0.27)	9.67
L-methylhydantoin	23.88 (±1.65)	4.49 (±0.32)	5.32
D-methylhydantoin	27.55 (±1.52)	0.74 (±0.29)	37.23

(NCA : *N*-carbamylalanine, (± SEM): standard error of the mean)

The hydantoinase enzyme of RU-KM3$_S$ catalysed the hydrolysis of both the D- and L-enantiomer of methylhydantoin (Table 2.1), suggesting that the hydantoinase is non-stereoselective. In contrast, the *N*-carbamoylase activity resulted in significant variances in production of alanine depending on the enantiomer supplied as a substrate in the biocatalytic reactions. The production of alanine from L-methylhydantoin was 6-fold higher than that produced from D-methylhydantoin (4.49μ mol/ml vs. 0.74μ mol/ml, Table 2.1). The significantly higher productivity of RU-KM3$_S$ *N*-carbamoylase with L-methylhydantoin indicated that this enzyme is L-stereoselective. The amount of alanine produced from the racemic D/L-methylhydantoin substrate, in which the total concentration of L-methylhydantoin is half that present in reaction supplied with L-methylhydantoin alone, was approximately half that produced from L-methylhydantoin (2.67μ mol/ml vs. 4.49μ mol/ml, Table 2.1). This, along with the lack of production of alanine from D-methylhydantoin suggested that there is no racemase present in this strain.

2.3.3 Metal ion dependence

Hydantoin-hydrolysing enzyme activities have been reported in literature to be affected, either positively or negatively, by the presence of metal ions. Specifically which metal ions result in these stimulatory or inhibitory effects varies significantly between isolates. In order to determine the potential metal ion dependence of the hydantoin-hydrolysing enzymes in RU-KM3$_S$, a range of divalent metal ions were added to the resting cell biocatalytic reactions

and the subsequent hydantoinase and *N*-carbamoylase activities observed. Cell free extracts rather than resting whole cells were used in the assays to ensure that access of the metal ions to the enzymes was not limited due to transport across the cell membrane.

Table 2.2 Effect of metal ions on hydantoinase and *N*-carbamoylase activities in cell free extracts (CFE) of RU-KM3$_S$ in the presence/absence of Na_2EDTA.

Metal ions added	Hydantoinase (μmol/ml NCG)		*N*-carbamoylase (μmol/ml glycine)	
	CFE	CFE + Na_2EDTA	CFE	CFE + Na_2EDTA
-	/	36.36 (±0.99)❖	/	7.46 (±0.69)❖
-	32.99 (±1.72)	21.39 (±3.48)	8.08 (±0.92)	3.07 (±0.79)
Fe^{2+}	26.17 (±3.36)	21.25 (±1.90)	7.41 (±0.75)	4.086 (±0.55)
Mg^{2+}	28.41 (±1.75)	30.73 (±3.02)	9.40 (±1.84)	5.455 (±0.53)
Mn^{2+}	25.29 (±0.63)	27.79 (±2.77)	6.69 (±0.34)	5.19 (±0.93)
Zn^{2+}	32.64 (±3.44)	26.39 (±1.34)	6.97 (±1.59)	4.59 (±0.97)
Co^{2+}	30.58 (±2.53)	30.48 (±4.30)	10.34 (±0.96)	5.75 (±0.42)
Cu^{2+}	0.01 (±1.45)	27.86 (±2.14)	0.53 (±0.07)	3.79 (±0.09)

(NCG: *N*-carbamylglycine, ❖ : No Na_2EDTA was added to this sample , (±SEM) : Standard error of the mean, n=3)

The most noticeable effect on hydantoin-hydrolysis was observed with Cu^{2+} which severely inhibited both the hydantoinase and *N*-carbamoylase in the cell free extracts resulting in almost complete loss of activity (0.01μ mol/ml *N*-carbamylglycine and 0.53μ mol/ml glycine produced, Table 2.2). Slight decreases in hydantoinase activity were noted for the remaining metal ions with the exception of Zn^{2+} which resulted in activity levels equivalent to untreated cells. With respect to *N*-carbamoylase activities (Table 2.2), a 16% and 28% increase in glycine production occurred on addition of Mg^{2+} and Co^{2+} ions respectively with activity levels increasing from 8.08μ mol/ml glycine produced to 9.40μ mol/ml and 10.34μ mol/ml respectively (Table 2.2).

The data obtained for hydantoinase and *N*-carbamoylase activities subsequent to addition of metal ions suggested some dependence of these enzymes on metal ions. To determine if metal ions are required for activity, the effect of addition of the metal ion chelator Na_2EDTA was investigated. There was a significant reduction in hydantoinase and *N*-carbamoylase activities in RU-KM3$_S$ cell free extracts when Na_2EDTA was added to the biocatalytic reactions with *N*-carbamylglycine levels decreasing from 36.36μ mol/ml to 21.39μ mol/ml and glycine dropping from 7.47μ mol/ml to 3.07μ mol/ml (Table 2.2) indicating that these enzymes are metal ion dependent. To determine if the inhibition of hydantoin-hydrolysis caused by the

addition of Na_2EDTA is reversible, various metal ions were added to the biocatalytic reaction. All of the tested metal ions, excepting Fe^{2+} with respect to hydantoinase activity, relieved the negative effect of Na_2EDTA to a certain degree but did not completely restore activity levels.

The increase in activity on addition of metal ions to the biocatalytic reactions containing Na_2EDTA could not, however, be directly attributed to the requirement of the respective enzymes for a particular metal ion. Rather, the reduction in inhibition of enzyme activity was most likely due to interaction of the respective metal ions with the Na_2EDTA thus preventing its interference with the hydantoinase and *N*-carbamoylase enzymes. To determine which metal ions resulted in reactivation of the enzymes subsequent to inactivation due to metal ion removal, dialysis of the cell free extract was done. Thus, when the cell free extract is utilized in biocatalytic reactions to which the metal ions are added, the interference of the metal ion chelating activity of Na_2EDTA is absent. Dialysis also circumvents potential inhibitory effects resulting from direct interaction between Na_2EDTA and the enzymes.

Dialysis of cell free extracts against phosphate buffer alone resulted in a modest decrease in enzyme activity (25.55µ mol/ml to 22.17µ mol/ml *N*-carbamylglycine and 6.9µ mol/ml to 5.34µ mol/ml glycine produced, Figure 2.3, panels A and B). This decrease was most likely due to diffusion of metal ions into the metal ion free buffer as apposed to instability of the enzymes under the conditions used for dialysis since a cell free extract incubated for an equivalent time at $4^{o}C$ showed only a small decrease in activity (Figure 2.3, panel A and B, CFE vs. St). A significant reduction of 25% in hydantoinase (19.27µ mol/ml vs. 25.55µ mol/ml) and 30% *N*-carbamoylase activity (4.8µ mol/ml vs. 6.91µ mol/ml), as compared with undialysed cell-free extract was observed after dialysis against buffer containing Na_2EDTA (Figure 2.3, panels A and B, D+E vs. CFE). This data confirmed earlier results suggesting the importance of divalent cations for hydantoinase and *N*-carbamoylase activities.

The addition of Cu^{2+} to dialyzed cell-free extracts resulted in dramatic loss of hydantoinase and *N*-carbamoylase activity (Figure 2.3, panel A and B), as had been observed with undialysed cell-free extracts (Table 2.2). The addition of Fe^{2+} resulted in a further reduction in production of *N*-carbamylglycine (19.27µ mol/ml to 14.22µ mol/ml), and glycine (4.8µ mol/ml to 2.83µ mol/ml) which accounted for an approximately 30% and 40% reduction in hydantoinase and *N*-carbamoylase activity respectively. While Zn^{2+} increased hydantoinase productivity slightly, it resulted in a 15% reduction in *N*-carbamoylase activity (Figure 2.3). Metal ions Mg^{2+}, Mn^{2+}, and Co^{2+} were all stimulatory with respect to hydantoinase activity with increases of 10%, 36% and 49% in *N*-carbamylglycine produced as compared with dialysed cell-free extract (Figure 2.3, panel A). When considering *N*-carbamoylase activity, Mg^{2+} inhibited the enzyme somewhat while Mn^{2+} and Co^{2+} significantly increased the activity

levels by 67% and 90% respectively relative to dialysed cell-free extract activities (Figure 2.3, panel B).

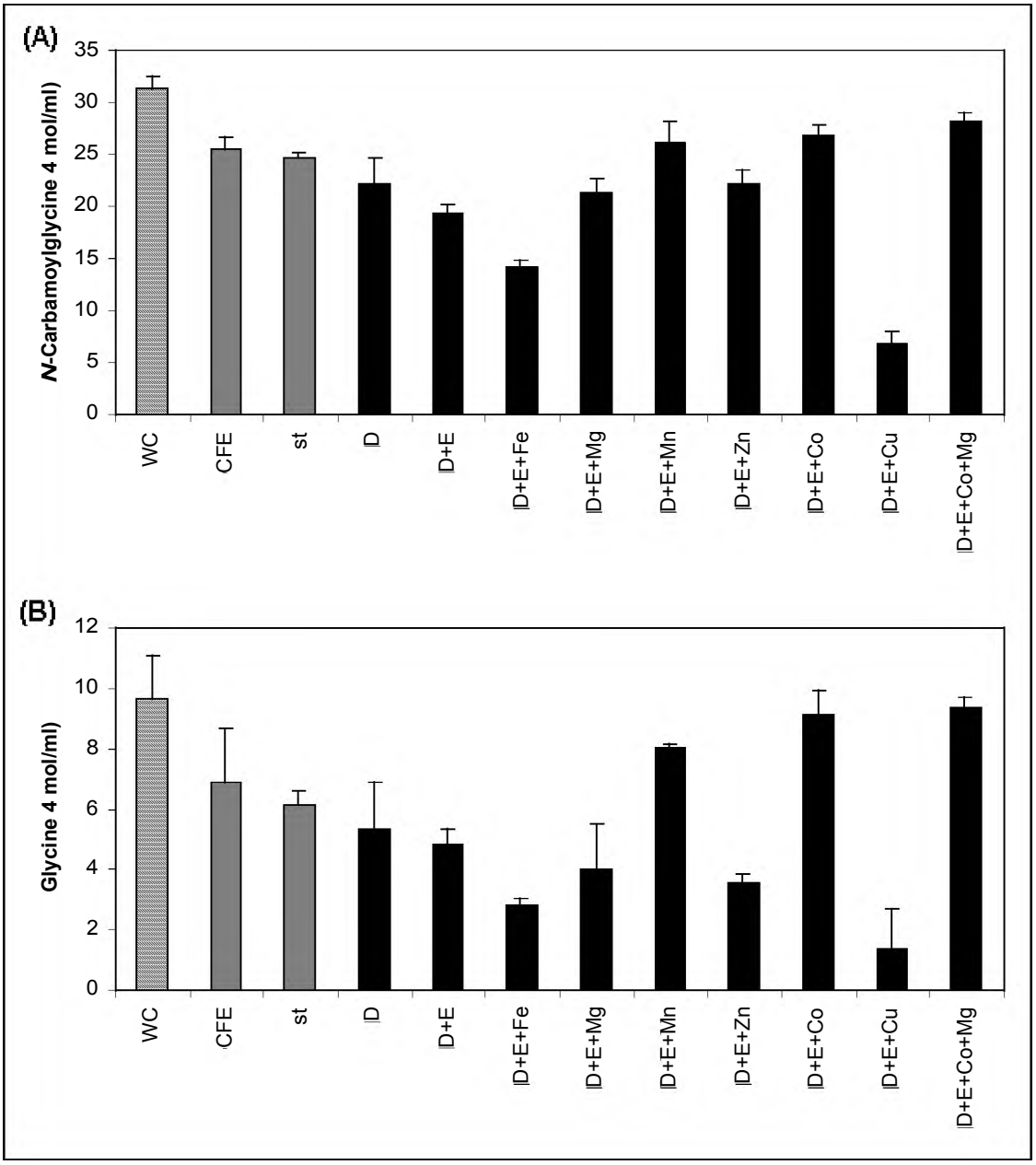

Figure 2.3 The effect of divalent cations on hydantoinase and *N*-carbamoylase activity after dialysis of cell free extracts of RU-KM3$_S$ against phosphate buffer containing Na_2EDTA. [Panel A: Hydantoinase activity, Panel B: *N*-carbamoylase activity, WC: whole resting cells, CFE: cell free extract, st: undialysed sample allowed to stand at 4 ^{o}C for the duration of dialysis on the remaining cells, D: dialysed, D+E: dialysed against buffer containing Na_2EDTA (Error bars represent the standard error of the mean, n=3)]

Maximum reversal of the effect of metal ion leaching as a result of dialysis with Na_2EDTA on hydantoinase and *N*-carbamoylase activity was obtained with co-addition of Co^{2+} and Mg^{2+} in which hydantoinase activity was increased by almost third and *N*-carbamoylase activity

reached almost twice that of the metal ion free cell lysate. The data obtained thus suggested that Mn^{2+}, Mg^{2+}, and Co^{2+} are important co-factors for RU-KM3$_S$ hydantoinase and *N*-carbamoylase enzymes whilst Fe^{2+} and Cu^{2+} severely inhibited hydantoin hydrolysis.

2.3.4 ATP dependence

In several isolates, Mg^{2+} ions have been shown to be stimulatory either for hydantoinase or *N*-carbamoylase activity (Runser and Ohleyer 1990, Sharma *et al*. 1997, Xu and West 1994, Chung *et al*. 2002, Shi *et al*. 2001). In the case of RU-KM3$_S$, addition of Mg^{2+} to cell-free extracts resulted in increased *N*-carbamoylase activity (Table 2.2). This increase in enzyme activity may be due to associated ATP hydrolysis which requires Mg^{2+} or metal dependence by the enzyme itself. Thus the effect of ATP on RU-KM3$_S$ hydantoin-hydrolysing activities required elucidation. Biocatalytic assays were conducted in the presence of ATP at concentrations of up to 6mM to determine potential ATP-dependence of the hydantoin-hydrolysing enzymes in strain RU-KM3$_S$.

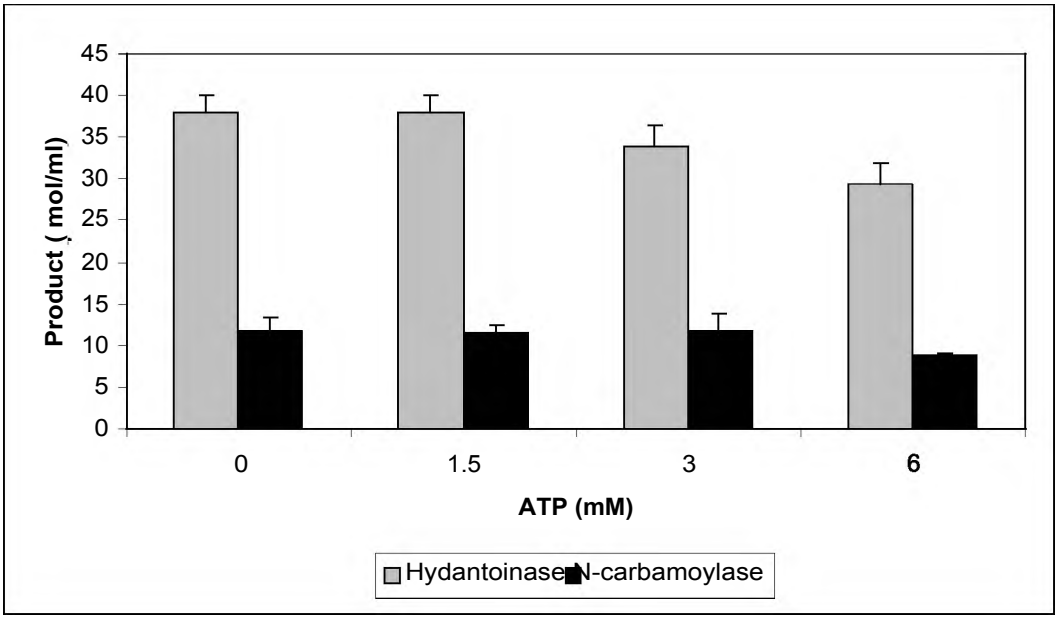

Figure 2.4 Effect of ATP on hydantoinase and *N*-carbamoylase activities in resting whole cell biocatalytic assays of RU-KM3$_S$. (Error bars represent the standard error of the mean, n=3)

No increase in hydantoinase or *N*-carbamoylase activity was noted subsequent to the addition of ATP indicating that the hydrolysis of hydantoin in RU-KM3$_S$ occurs in an ATP-independent manner. Surprisingly, a decrease in enzyme activity was noted subsequent to addition of ATP, particularly at the higher concentration of 6mM (Figure 2.4).

2.3.5 Strain identification

Biochemical identification of strain RU-KM3$_S$ by expanded API test performed by the South African Institute of Medical Research indicated that the isolate was most likely a *Pseudomonas putida*. Analysis of the 16S rRNA gene of RU-KM3$_S$ was done to verify the biochemical identification. A 1300bp DNA fragment was amplified by PCR from genomic DNA of RU-KM3$_S$ using primers corresponding to the conserved regions in the 5' and 3' regions of the 16S rRNA gene sequence of *P. putida*. Restriction endonuclease mapping of the PCR product using expected sites derived from *P. putida* 16S rRNA gene sequences deposited in the RDP database (Table 2.3) was used to confirm the identity of RU-KM3$_S$.

Table 2.3 DNA fragment lengths produced from restriction endonuclease digestion of the 16S rRNA gene from *P. putida* strain BH downloaded from the RDP database.

Restriction endonuclease	-	*Csp* 451	*Hind* II	*Pvu* I	*Sac* II	*Stu* I	*Sma* I
Predicted size of generated fragments	1330	117bp*	53bp*	74bp*	488bp	12bp*	574bp
		409bp	494bp	1256bp	842bp	936bp	756bp
		804bp	783bp			381bp	

(* : Fragments too small to visualize on an agarose gel)

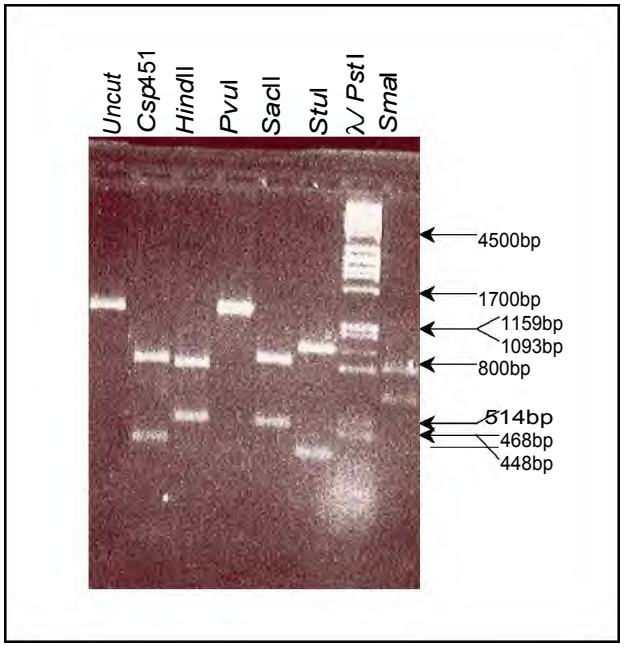

Figure 2.5 DNA fragments generated by restriction endonuclease digestion of the 16S rRNA gene of RU-KM3$_S$ and separated electophoretically through an agarose gel.

No restriction fragment length polymorphisms (RFLPs) were observed (Table 2.3 vs. Figure 2.5), as all predicted fragments (Table 2.3), barring those too small to visualize on an

agarose gel, occurred subsequent to digestion of the 16S rRNA gene of RU-KM3$_S$ with the corresponding restriction endonucleases (Figure 2.5).

The 16S rRNA genes of different species of *Pseudomonas* have a relatively high degree of conservation, however, and thus RFLP analysis is not sufficient to distinguish between different *Pseudomonas* isolates. The PCR amplification product was therefore cloned into the vector pUC18 and two recombinant clones, in which the DNA fragments was orientated in opposite directions, namely pGMS1 and pGMS2 (Figure 2.6, panel A), were selected. These recombinant plasmids together with deletion plasmids pGMS1ΔHinc II, pGMS1ΔSma I, pGMS2ΔCsp 451, and pGMS2ΔSma I, were used to determine the nucleotide sequence of the PCR amplification product derived from the 16S rRNA gene of RU-KM3$_S$ (Figure 2.6, panel B).

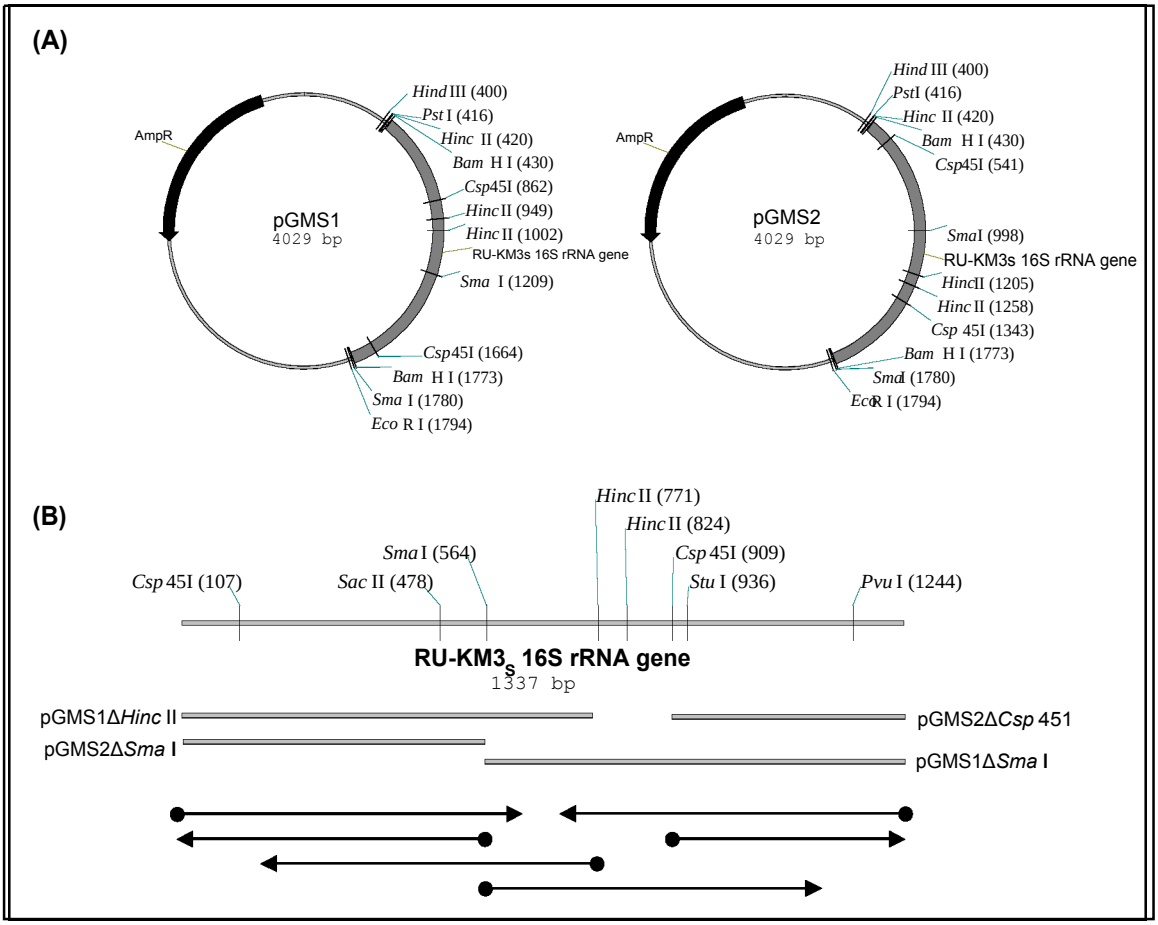

Figure 2.6 Restriction endonuclease map of the 16S rRNA gene from *P. putida* RU-KM3$_S$ constructed from sequence data obtained from the parental and deletion constructs of the PCR product in pUC18. [Panel A: 16S rRNA gene amplified from RU-KM3$_S$ in pUC18 vector, Panel B: Schematic diagram of the 16S rRNA gene from RU-KM3$_S$ constructed from nucleotide sequences (arrows) determined from template DNA (grey lines)]

The nucleotide sequence obtained was entered into the Ribosomal Similarity Ranking facility (Maidek *et al.* 2001) and aligned with the 10 most similar 16S rRNA sequences in the RDP database. The Sequence Match Version 2.7 program quantifies the number of unique oligomers in the submitted sequence which is common to each sequence in the database. The result (S_ab) was expressed as the number of shared oligomers divided by either the number of unique oligomers in the submitted sequence or the data base sequence, depending on which is lower. This ensured that a good match between partial sequences, or partial and complete sequences, was scored higher than a less efficient match between complete sequences. High S_ab scores were obtained primarily with *P. putida* strains although homology of the RU-KM3$_S$ 16S rRNA gene was observed with a *P. plecoglossicida* and a *P. monteilli* strain (Table 2.4). Based on 16S rRNA gene sequence, RU-KM3$_S$ is most closely related to *Pseudomonas putida* strain BH, thus verifying the biochemical identification previously done.

Table 2.4 Similarity rank of the 16S rRNA gene from strain RU-KM3$_S$ with corresponding gene sequences submitted to the Ribosomal Database Project

S_ab	Organism
0.964	*Pseudomonas putida* strain BH
0.964	*Pseudomonas plecoglossicida* strain FPC951
0.961	*Pseudomonas putida* strain A10L
0.956	*Pseudomonas putida* strain mt-2 JMC6156
0.955	*Pseudomonas monteilli* strain CFML 90-60 CIP 104883
0.953	*Pseudomonas putida* strain PB4
0.950	*Pseudomonas putida* strain K23-1
0.949	*Pseudomonas putida* strain F1
0.945	*Pseudomonas putida* strain mt-2
0.945	*Pseudomonas putida* strain IFO 14671

The nucleotide variances between *P. putida* strains RU-KM3$_S$ and BH can be seen in Figure 2.7 in which the sequence alignment of the 16S rRNA gene from these two isolates are depicted in boxshade format. The nucleotide sequence of the terminal ends of the 16S rRNA gene from RU-KM3$_S$ are not present in the alignment (Figure 2.7). This is due to the fact that ion exchange columns, with a size exclusion of 75bp, were used to purify the extension products of the cycle sequencing reaction before analysis in the ABI Prism 3100 Genetic Analyser. Thus the first 75bp from the end of the primer utilized in the cycle sequencing reaction will not be represented in the sequence data.

```
RU-KM3s    1  - - - - GCCTAACACATGCAAGTCGAACGGATGACGGGAGCTTGCTCCTTGATTCAG
BH         1 TGGCGGCAGGCCTAACACATGCAAGTCGAGCGGATGACGGGAGCTTGCTCCTTGATTCAG


RU-KM3s 52 CGGCGGACGGGTGAGTAATGCCTAGGAATCTGCCTGGTAGTGGGGGACAACGTTTCGAAA
BH        61 CGGCGGACGGGTGAGTAATGCCTAGGAATCTGCCTGGTAGTGGGGGACAACGTTTCGAAA


RU-KM3s 112 GGAACGCTAATACCGCATACGTCCTACGGGAGAAAGCAGGGGACCTTCGGGCCTTGCGCT
BH       121 GGAACGCTAATACCGCATACGTCCTACGGGAGAAAGCAGGGGACCTTCGGGCCTTGCGCT


RU-KM3s 172 ATCAGATGAGCCTAGGTCGGATTAGCTAGTTGGTGGGGTAATGGCTCACCAAGGCGACGA
BH       181 ATCAGATGAGCCTAGGTCGGATTAGCTAGTTGGTGGGGTAATGGCTCACCAAGGCGACGA


RU-KM3s 232 TCCGTAACTGGTCTGAGAGGATGATCAGTCACACTGGAACTGAGACACGGTCCAGACTCC
BH       241 TCCGTAACTGGTCTGAGAGGATGATCAGTCACACTGGAACTGAGACACGGTCCAGACTCC


RU-KM3s 292 TACGGGAGGCAGCAGTGGGGAATATTGGACAATGGGCGAAAGCCTGATCCAGCCATGCCG
BH       301 TACGGGAGGCAGCAGTGGGGAATATTGGACAATGGGCGAAAGCCTGATCCAGCCATGCCG


RU-KM3s 352 CGTGTGTGAAGAAGGTCTTCGGATTGTAAAGCACTTTAAGTTGGGAGGAAGGGCAGTAAG
BH       361 CGTGTGTGAAGAAGGTCTTCGGATTGTAAAGCACTTTAAGTTGGGAGGAAGGGCAGTAAG


RU-KM3s 412 CTAATACCTTGCTGTTTTGACGTTACCGACAGAATAAGCACCGGCTAACTCTGTGCCAGC
BH       421 CTAATACCTTGCTGTTTTGACGTTACCGACAGAATAAGCACCGGCTAACTCTGTGCCAGC


RU-KM3s 472 AGCCGCGGTAATACAGAGGGTGCAAGCGTTAATCGGAATTACTGGGCGTAAAGCGCGCGT
BH       481 AGCCGCGGTAATACAGAGGGTGCAAGCGTTAATCGGAATTACTGGGCGTAAAGCGCGCGT


RU-KM3s 532 AGGTGGTTCGTTAAGTTGGATGTGAAAGCCCCGGGCTCAACCTGGGAACTGCATCCAAAA
BH       541 AGGTGGTTCGTTAAGTTGGATGTGAAAGCCCCGGGCTCAACCTGGGAACTGCATCCAAAA


RU-KM3s 592 CTGGC-AGCTAGAGTACGGTAGAGGGTGGTGGAATTTCCTGTGTAGCGGTGAAATGCGTA
BH       601 CTGGCGAGCTAGAGTACGGTAGAGGGTGGTGGAATTTCCTGTGTAGCGGTGAAATGCGTA


RU-KM3s 651 GATATAGGAAGGAACACCAGTGGCGAAGGC-ACCACCTGGACTGATACTGACACTGAGGT
BH       661 GATATAGGAAGGAACACCAGTGGCGAAGGCGACCACCTGGACTGATACTGACACTGAGGT


RU-KM3s 710 GCGAAAGCGTGGGGAGCAAACAGGATTAGATACCCTGGTAGTCCACGCCGTAAACGATGT
BH       721 GCGAAAGCGTGGGGAGCAAACAGGATTAGATACCCTGGTAGTCCACGCCGTAAACGATGT


RU-KM3s 770 CAACTAGCCGTTGGAATCCTTGAGATTTTAGTGGCGCAGCTAACGCATTAAGTTGACCGC
BH       781 CAACTAGCCGTTGGAATCCTTGAGATTTTAGTGGCGCAGCTAACGCATTAAGTTGACCGC


RU-KM3s 830 CTGGGGAGTACGGCCGCAAGGTTAAAACTCAAATGAATTGACGGGGGCCCGCACAAGCGG
BH       841 CTGGGGAGTACGGCCGCAAGGTTAAAACTCAAATGAATTGACGGGGGCCCGCACAAGCGG


RU-KM3s 890 TGGAGCATGTGGTTTAATTCGAAGCAACGCGAAGAACCTTACCAGGCCTTGACATGCAGA
BH       901 TGGAGCATGTGGTTTAATTCGAAGCAACGCGAAGAACCTTACCAGGCCTTGACATGCAGA
```

Figure 2.7 Boxshade of the aligned 16S rRNA gene sequences of *P. putida* strains BH and RU-KM3$_S$.

Alignment of the 16S rRNA gene sequence from RU-KM3$_S$ and BH indicated very little variation between these two species with only six nucleotide differences observed (Figure 2.7), three of which occur at the end of the 16S rRNA gene sequence. Two deletions of a guanine nucleotide in RU-KM3$_S$ can be seen at bases 597 and 681 when compared to BH. The last difference between these two sequences occurs at nucleotide 21 where an adenosine base has replaced a guanine base (Figure 2.7). Thus, based on 16S rRNA gene sequence similarity of RU-KM3$_S$ with that from BH, RU-KM3$_S$ was correctly classified as a *Pseudomonas putida* strain.

2.4 DISCUSSION

To determine if the hydantoin-hydrolysing enzyme system of RU-KM3$_S$ differed from those reported in literature, thereby validating in depth analysis and potential industrial application of RU-KM3$_S$, general characterization of the isolate and its hydantoin-hydrolysing properties was done (reported in Buchanan *et al.* 2001). Strain RU-KM3$_S$ was identified as a *Pseudomonas putida* isolate by comparative analysis of the 16S rRNA gene. This has important implications when considering biosafety, both in the laboratory and industry (if the natural host is utilized in the fermentations), as some isolates from this taxon are plant pathogens or can cause opportunistic human infections (Stover *et al.* 2000). However, this is

not the case for *P. putida*. In addition, *P. putida* KT2440 has been certified as a biological safety strain by the Recombinant DNA Advisory Committee (Nelson *et al*. 2002).

With respect to hydantoin-hydrolysing activities, initial characterization of RU-KM3$_S$ by Buchanan (1996) revealed an optimum pH, temperature and incubation period for catalysis of hydantoin by resting whole cells to be pH 8.0, 40^{o}C, and 3 hours respectively after which 100% conversion of hydantoin to *N*-carbamylglycine and an average of 20% conversion to glycine occurred. Induction of the hydantoinase and *N*-carbamoylase enzymes with hydantoin, dihydrouracil, dimethylhydantoin, and thiouracil was investigated with hydantoin being the best inducer (Buchanan, 1996). The substrate selectivity of the hydantoin hydrolysing enzyme in RU-KM3$_S$ revealed high levels of hydantoin converting activity, with the aliphatic but not necessarily short-chain 5-monosubstituted hydantoin derivatives as the preferred substrates (Skepu, 2000). The hydantoinase enzyme appeared to be non-stereoselective, whilst the *N*-carbamoylase is strictly L-stereoselective when supplied with methylhydantoin as a substrate. The enzyme system from RU-KM3$_S$ appeared to be ATP-independent but metal-ion dependent as significant reduction in the production of *N*-carbamylglycine and glycine occurred after dialysis of crude cell extracts against buffer containing the metal ion chelator Na_2EDTA. Of the metal ions tested, Cu^{2+} severely inhibited both enzymes whilst Co^{2+}, Mg^{2+}, and Mn^{2+} stimulated hydantoin-hydrolysing activities.

Expression of the hydantoinase and *N*-carbamoylase enzymes in RU-KM3$_S$ cells requires the presence of an inducer and, when cultured in complete medium, optimal enzyme activities were detected at early stationary growth phase. This observation corresponds to data in literature where hydantoinase and *N*-carbamoylase enzymes are optimally produced after log phase of growth (Gokhale *et al*. 1996, Sudge *et al*. 1998, Ishikawa *et al*. 1993, Hartley *et al.* 1998, Syldatk *et al*. 1990a, Lee *et al.* 1994, Hils *et al.* 2001). The increase in hydantoin-hydrolysing enzyme activities late in the growth cycle of RU-KM3$_S$ suggests that the hydantoinase and *N*-carbamoylase are subject to catabolite repression. Typically, a medium with readily metabolizable nutrient sources will promote rapid biomass production but simultaneously cause repression of enzymes involved in utilization of poorer sources of nitrogen or carbon such as hydantoin. Both carbon and nitrogen catabolite repression have been reported to regulate hydantoin-hydrolysing activity (Sudge *et al*. 1998, Hartley *et al.* 2001). The extent to which catabolite repression regulates hydantoinase and *N*-carbamoylase activities in RU-KM3$_S$ cells will be examined in detail in Chapter 5.

Hydantoinase and *N*-carbamoylase enzymes have been reported in a wide diversity of bacterial strains with the biocatalytic characteristics varying considerably between isolates. The bulk of research with respect to hydantoin-hydrolysing bacterial strains has been carried out on *Agrobacterium*, *Arthrobacter*, and *Bacillus* isolates. Of the *Pseudomonas* species with

hydantoin-hydrolysing abilities, only *Pseudomonas* sp. NS671 (Watabe *et al*. 1992a) is reported to express a non-enantioselective hydantoinase. The hydantoinases from remaining isolates all exhibit D-enantiospecificities (Ogawa and Shimizu 1994, LaPointe *et al*. 1994, Gokhale *et al*.1996, Kim and Kim 1993, Sudge *et al*. 1998, Yokozeki *et al*. 1987c, Chien *et al*. 1998, Shi *et al*. 2001). *N*-carbamoylase enzyme activities are not reported for most of the *Pseudomonas* sp. listed above. *Pseudomonas* sp. KNK003A (Ikenaka *et al.* 1998a) and AJ-11220 (Yokozeki *et al*. 1987b) are reported to have a D-stereoselective carbamoylases whilst *Pseudomonas* sp. NS671 expresses an L-enantioselective *N*-carbamoylase (Watabe *et al*. 1992a) and *Pseudomonas putida* IFO 12996 expresses a β-ureidopropionase with L-enantioselective *N*-carbamoylase activity (Ogawa and Shimizu 1994). Thus, with respect to enantioselectivities of the hydantoinase and *N*-carbamoylase enzymes, RU-KM3$_S$ seems most similar to *Pseudomonas* sp. NS671 and *P. putida* IFO 12996 with a non-enantioselective hydantoinase and L-enantioselective *N*-carbamoylase. However, the non-stereoselective hydantoinase from *Pseudomonas* sp. NS671 has been shown to be ATP-dependant which is not the case for the hydantoinase from RU-KM3$_S$. On the other hand, the *N*-carbamoylase from this strain displays several similarities with the corresponding enzyme in RU-KM3$_S$ with similar optimum pH and temperature profiles, L-enantiospecificity, and inhibition by ATP at high concentrations (5mM-10mM) in crude extracts (Ishikawa *et al*. 1993). The β-ureidopropionase from *P. putida* IFO 12996 (Ogawa and Shimizu 1994) whilst sharing L-enantioselectivity with RU-KM3$_S$, differs in terms of optimal pH and temperature for biocatalytic activity. In addition, IFO 12996 β-ureidopropionase does not hydrolyse *N*-carbamyl-L-leucine (Ogawa and Shimizu 1994) which is readily hydrolysed by the *N*-carbamoylase from RU-KM3$_S$ (Buchanan *et al*. 2001). However, characterization of the β-ureidopropionase from *P. puitda* IFO 12996 was done using purified enzymes whilst characterization of the *N*-carbamoylase activity in RU-KM3$_S$ was done with whole cells or cell-free extracts which may account for some of the differences noted between these two enzymes.

The effect of metal ions, either positive or negative, on hydantoinase and *N*-carbamoylase enzyme activities has been documented for almost all isolates reported to exhibit hydantoin-hydrolysing activity. Which metal ions are stimulatory and which are inhibitory varies between species and even between strains. However, many of the reported enzymes are inhibited by Cu^{2+} as is the case with RU-KM3$_S$ (Morin *et al.* 1986b, Syldatk *et al*. 1987, Ogawa and Shimizu 1994, Ogawa *et al*. 1993, Xu *et al*. 1994, Ishikawa *et al*. 1994, Louwrier and Knowles 1996, 1997, Nanba *et al*. 1998). Exceptions to this are *Ochobactrum anthropi* 245 in which the addition of Cu^{2+} resulted in stimulation of the hydantoinase (Pozo *et al.* 2002), and *B. stearothermophilus* NS1122A hydantoinase which was unaffected by Cu^{2+} ions (Mukohara *et al.* 1994).

Specific comparison of the effect of metal ions on hydantoinase (Shi *et al*. 2001), L-carbamoylases (Ishikawa *et al.* 1994), and β-ureidopropionase (Ogawa and Shimizu 1994) from *Pseudomonas* sp. with the corresponding enzymes in *P. putida* RU-KM3$_S$ demonstrates some similarities and differences between these isolates. Both the L-carbamoylase and β-ureidopropionase from *Pseudomonas* sp. NS671 and *P. putida* IFO 12996 respectively, were stimulated by the addition of Mn^{2+}, Co^{2+}, and Ni^{2+}. Whilst Ni^{2+} was not tested for RU-KM3$_S$, Mn^{2+} and Co^{2+} were also stimulatory with respect to the *N*-carbamoylase activity in this strain. However, *P. putida* IFO 12996 β-ureidopropionase activity was reported to be restored by Fe^{2+} subsequent to treatment with EDTA (Ogawa and Shimizu 1994), whereas Fe^{2+} was shown to significantly inhibit enzyme activity in RU-KM3$_S$. The D-hydantoinase from *Pseudomonas* sp. 2262 (Shi *et al*. 2001) was reported to be activated by addition of Mn^{2+} and Mg^{2+} which is consistent with what occurs in RU-KM3$_S$. However, the *Pseudomonas* sp. 2262 hydantoinase enzyme is inhibited by Zn^{2+} which has a slight stimulatory effect on the hydantoinase from RU-KM3$_S$.

In conclusion, whilst some similarities exist between the hydantoin-hydrolysing enzymes system in RU-KM3$_S$ and those characterized in other *Pseudomonas* isolates, sufficient variability was observed for the enzymes from RU-KM3$_S$ to be considered different. The most conclusive method to determine if an enzyme is unique or not is by comparison of the nucleotide sequence of the encoding gene with those reported in literature. Thus isolation of these genes from RU-KM3$_S$ and determination of their nucleotide sequence was investigated.

3.1 INTRODUCTION

Isolation of the genes encoding the enzymes responsible for hydantoin hydrolysis in RU-KM3$_S$ would be beneficial for a variety of reasons. Not only would it verify that the enzymes are indeed different to those reported in literature but it would also provide insight into the regulation of expression of the genes and, by comparison to crystallographic and mutational analysis done on previously isolated enzymes, provide an opportunity to optimise the catalytic function of the enzymes.

Several hydantoinase and *N*-carbamoylase enzymes have recently been cloned and heterologously expressed in *E. coli*. The methodologies used to isolate the genes encoding these enzymes include screening of genomic libraries or amplification of the relevant genes from genomic DNA by PCR using primers designed from the N-terminal amino acid sequence of the purified protein (Chen and Tsai 1998) or degenerate primers designed based on sequences of related enzymes in literature (Chao *et al*. 1999b, Hils *et al*. 2001, Hu *et al.* 2003). Genomic libraries created for the isolation of hydantoin-hydrolysing genes have been constructed in plasmid vectors such as pUC18 (Mukohara *et al.* 1993, Mukohara *et al.* 1994, Ikenaka *et al.* 1998a, Nanba *et al.* 1998), pBR322 (Lee *et al.* 1996) and pBluescript (Chien *et al*. 1998), or by construction of cosmid DNA libraries (Buson *et al.* 1996) and phage libraries (Hils *et al.* 2001, Wiese *et al*. 2001). A critical step in the isolation of genes from genomic libraries is the screening methodology utilized. With respect to hydantoinase and *N*-carbamoylase encoding genes, this has been achieved by screening for the ability of cells carrying recombinant plasmids to utilize hydantoins and/or *N*-carbamylamino acids as sole sources of nitrogen for growth (Mukohara *et al.* 1993, Mukohara *et al*. 1994, Ikenaka *et al.* 1998a, Nanba *et al*. 1998), by detection of *N*-carbamoylase activity via a change in pH as a result of *N*-carbamylamino acid production using phenol red indicator (Lee *et al*. 1996, Kim *et al.* 1997), or by direct screening for hydantoin-hydrolysing activity using colorimetric assays (LaPointe *et al.* 1994, Buson *et al.* 1996, Chien *et al*. 1998). In addition, screening of genomic libraries by hybridisation to probes derived from the *N*-terminal amino acid sequence of the purified protein (Wiese *et al*. 2001) or a gene involved in the same catalytic pathway (Hils *et al.* 2001) has also been used.

With respect to *Pseudomonas* isolates, the genes encoding D-hydantoinases have been isolated from *P. putida* strains 7711-2, CCRC 12857, and DSM 84 by screening of genomic libraries by hybridisation with an oligonucleotide designed from the N-terminal amino acid sequence of the purified protein or by detection of hydrolysis of dihydrouracil or hydantoin in microtitre plates (Chen and Tsai 1998, Chien *et al.* 1998, LaPointe *et al.* 1994). A D-enantioselective *N*-carbamoylase from *Pseudomonas* sp. KNK003A was isolated from a genomic library with growth in minimal medium containing methlyhydantoin as the sole

nitrogen source as the selection method (Ikenaka *et al.* 1998a). The only L-enantiospecific *N*-carbamoylase isolated from a *Pseudomonas* sp. was located on a native plasmid in *Pseudomonas* sp. NS671 with a non-specific hydantoinase located downstream (Watabe *et al.* 1992a).

Isolation of the genes encoding the hydantoinase and *N*-carbamoylase enzymes in RU-KM3$_S$ was desirable for several reasons. Most importantly, the differences in the biocatalytic properties of the RU-KM3$_S$ hydantoin-hydrolysing enzymes as compared to those reported in literature (discussed in chapter 2) needed to be confirmed by characterization and comparative analysis at the nucleotide and primary amino acid sequence level. In addition, since only five L-enantioselective *N*-carbamoylases have been isolated to date (Wilms *et al.* 1999, Batisse *et al*. 1997, Mukohara *et al.* 1993, Watabe *et al.* 1992a, Hu *et al.* 2003), characterization of the gene from RU-KM3$_S$ would contribute to our understanding of L-stereoselective *N*-carbamoylase enzymes.

In some instances, the genes encoding the hydantoin-hydrolysing enzyme system have been localized on large native plasmids in the wild type strains. *Agrobacterium* sp. IP I-671, *A. tumefaciens* NRRL B11291 (Hils *et al.* 2001), and *Pseudomonas* sp. NS671 (Watabe *et al.* 1992a) were each shown to contain native plasmids of 190kb, 160kb, and 172kb in size respectively, on which the genes of interest were encoded. Thus the potential existed that the hydantoin-hydrolysing enzymes in strain RU-KM3$_S$ might also be located on a large plasmid, which would obviate the necessity to generate a complete genomic library to isolate the genes.

This chapter describes attempts to isolate the hydantoinase and *N*-carbamoylase encoding genes from the RU-KM3$_S$ genome. While at least one large plasmid was identified in this strain, it did not appear to be required for hydantoinase or *N*-carbamoylase activity. Thus, construction of a genomic library of RU-KM3$_S$ and subsequent screening of the library for genomic fragments encoding the hydantoinase and/or *N*-carbamoylase enzymes was done. Screening methodologies including direct screening for hydantoinase and *N*-carbamoylase activity using hydantoin or *N*-carbamylglycine as substrates as well as growth of recombinant *E. coli* with hydantoin or *N*-carbamylglycine as sole sources of nitrogen.

3.2 METHODS AND MATERIALS

3.2.1 Large plasmid extraction and curing

The extraction protocol recommended for the Bac-to-Bac Baculovirus Expression System (Invitrogen), which is reputedly capable of isolating plasmids >100kb, was modified for plasmid extraction from RU-KM3$_S$. The cells were cultured overnight at 28^{o}C in 5ml Luria broth of which the cells in 1.5ml were pelleted by centrifugation in a Heraeus microfuge (13,000rpm unless otherwise stated). The pellet was then resuspended in 0.3ml solution P1 (15mM Tris-HCl (pH 8), 10mM Na_2EDTA, 100µ g/ml RNase A), to which 0.3ml solution P2 (0.2N NaOH, 1% SDS) was added and the mixture incubated at room temperature for 5 minutes such that the cells were lysed. In order to precipitate the protein and genomic DNA, 0.3ml solution P3 (3M potassium acetate, pH 5.5) was mixed gently with the cell lysate and incubated for 5-10 minutes on ice. The resultant white precipitate was pelleted by centrifugation for 10 minutes in a Heraeus microfuge and the supernatant transferred to a fresh eppendorf tube containing 0.8ml isopropanol. The eppendorf was inverted a few times to ensure complete mixing of the solutions and then placed on ice for a further 5 – 10 minutes followed by incubation at –20^{o}C for 2 hours. After centrifugation for 15 minutes, the supernatant was removed and the pellet washed twice with 0.5ml ice cold 70% ethanol with 5 minutes centrifugation in between. The resultant pellet was dried by vacuum centrifugation with the Speedvac concentrator (Savant) and resuspended in 40µ l TE buffer of which 20µ l was subjected to electrophoresis through a 0.7% agarose gel containing 0.5µ g/ml ethidium bromide and visualized by UV light using the Kodak 120 Digital Imaging System.

Curing RU-KM3$_S$ of its native plasmid was accomplished by growth in nutrient broth containing 150µ g/ml acridine orange overnight at 28^{o}C. As antibiotic resistance is often coded for on plasmids, an isolate of RU-KM3$_S$ cured of its plasmid was selected for based on acquired sensitivity to ampicillin, and subjected to the plasmid extraction procedure described above. An isolate, which no longer contained the native RU-KM3$_S$ plasmid, was then tested for loss of hydantoinase and/or *N*-carbamoylase activity by whole cell biocatalytic assay as described in Appendix 2.1.

3.2.2 Isolation and preparation of chromosomal DNA

Total genomic DNA was extracted from RU-KM3$_S$ by the detergent lysis/CTAB and organic solvent extraction method as described in Chapter 2, section 2.2.4 (Appendix 5). Partial digestion of the genomic DNA was performed by digestion with restriction endonuclease *Sau* 3AI at varying concentrations such that suitably sized fragments of between 5 and 10kb were obtained. The resultant fragments were then purified by addition of 1 volume of phenol:chloroform:isoamyl alcohol (25:24:1) and centrifuged for 5 minutes in a Heraeus

microfuge. The aqueous phase was removed and the DNA fragments precipitated with 2 volumes ice cold 96% ethanol and 0.1 volumes sodium acetate (pH 5.2).

3.2.3 Construction of an RU-KM3$_S$ genomic library

The genomic library of RU-KM3$_S$ was constructed using the ZAP Express™ system (Stratagene). The *Sau* 3AI-digested genomic fragments were ligated into ZAP express phage vector, predigested with *Bam* HI and treated with Calf Intestinal Alkaline Phosphatase, at a vector:insert ratio of 1:2. The ligated phage constructs were then packaged into recombinant lambda phage using the Gigapack III Gold packaging extract in order to optimise packaging efficiency and library representation. The packaged particles were amplified to produce a high-titre phage library with an estimated titre of 10^8 pfu/ml. This was then followed by *in vivo* excision of the pBK-CMV phagemid vector (Figure 3.4) from the ZAP Express recombinant phages by co-infection with ExAssist helper phage. The mass-excision supernatant was stored at –20^{o}C until required.

The mass-excision supernatant containing the RU-KM3$_S$ genomic library was transformed as described in Appendix 4 into *E. coli* XLOLR (Δ(*mcrA*)183Δ(*mcrCB-hsdSMR-mrr*)173 *endA1 thi-1 recA1 gyrA96 relA1 lac*[F'*proAB lacI*^{q}ZΔM15 Tn10(Tet^r)] Su$^-$ (nonsuppressing) λ^r (Lambda resistant)) and plated onto Luria agar plates containing 50μ g/ml kanamycin, 40μ g/ml X-gal, and 50μ g/ml IPTG in order to isolate insert-containing recombinants by selection for inactivated *lacZ* gene resulting in white colonies. A representative selection of white colonies were then individually cultured in 5ml Luria broth with 50μ g/ml kanamycin to confluence overnight at 37^{o}C. The recombinant plasmids were isolated by the Easyprep method (Berghammer and Auer 1993) and the size of the insert determined by electrophoresis of diagnostic restriction endonuclease digests through a 1% agarose gel stained with 0.5μ g/ml ethidium bromide and visualized under UV light. The average insert size of these clones was utilized to estimate the number of clones, containing random fragments of genomic DNA, required such that the entire genome of RU-KM3$_S$ would be represented in the library. The probability of the representation of any given DNA sequence in the genomic library was calculated using the following equation :

$$N = \ln (1 - P) / \ln [1 - (I / G)] \qquad \textbf{Eq. 1}$$

Where "N" is the number of independent clones which must be screened when the average size of the cloned fragment, "I", of a total genome size "G" to isolate a particular gene with probability "P" (Ausubel *et al.* 1983).

3.2.4 Screening of the genomic library

3.2.4.1 Microtitre plate biocatalytic assays

A set of master cultures were first generated in 96-well microtitre plates with each well containing approximately 40 insert-containing recombinant clones. To do this, appropriate dilutions of the mass excision supernatant transformed into *E.* coli XLOLR were aseptically aliquoted into each well of a 96-well microtitre plate with Luria broth containing 50µ g/ml kanamycin to a final volume of 200µ l. The microtitre plates were then incubated at 37^{o}C overnight before addition of 60µ l 50% glycerol (in Luria broth) and storage of the plates at - 70^{o}C. A total of ten master plates were generated to ensure complete representation of the genomic library.

To screen the library, the master plates were thawed slightly and 20µ l of the culture from each well was inoculated into the corresponding wells of four duplicate plates of which two contained 180µ l Luria broth plus 50µ g/ml kanamycin and two contained 180µ l Luria broth plus 50µ g/ml kanamycin and 1mM IPTG. These plates were incubated at 37^{o}C with shaking overnight until late log to early stationary growth phase had been reached. The cells were pelleted by centrifugation at 5000rpm for 15 minutes using a Eppendorf A-2MTP rotor and Eppendorf centrifuge. The supernatant was discarded by gently flicking the plates and the pellets resuspended in 200µ l 0.1M phosphate buffer (pH 8.0) containing 50mM hydantoin or 25mM *N*-carbamylglycine and incubated at 40^{o}C for 4-24 hours with shaking (100rpm). The microtitre plates were then centrifuged as before to pellet the cells and the supernatant analysed for the presence of *N*-carbamylglycine and glycine using a modified Ehrlich's and ninhydrin assay respectively (Appendix 2.2).

Wells in which production of *N*-carbamylglycine or glycine was detected in duplicated biocatalytic assays, were selected for further screening. The master plate was again thawed slightly and 20µ l from selected wells inoculated into 5ml Luria broth containing 50µ g/ml kanamycin. The inoculated culture was grown at 37^{o}C for approximately 5 hours before being diluted and plated onto Luria agar plate containing 50µ g/ml kanamycin, 1mM IPTG, and 40µ g/ml X-gal such that single colonies were obtained. White, insert-containing colonies were isolated and grown to stationary phase in 5ml Luria broth plus 50µ g/ml kanamycin with/without 1mM IPTG at 37^{o}C. The confluent culture was then placed in 200µ l aliquots in 4 duplicate wells of a fresh microtitre plate and the cells pelleted as before. After removal of the supernatant, 200µ l 0.1M phosphate buffer (pH 8.0) was added to one of the four duplicate wells and 200µ l of either 50mM hydantoin or *N*-carbamylglycine in 0.1M phosphate buffer was used to resuspend the cells in the remaining three wells. The biocatalytic reactions were carried out as described above and the presence of *N*-carbamylglycine and glycine detected as in Appendix 2.2.

3.2.4.2 Selective growth media

Recombinant phagemid clones containing genomic fragments of RU-KM3$_S$ were screened in *E. coli* XLOLR for growth on minimal medium agar plates (Appendix 1) with 1% hydantoin or 1% *N*-carbamylglycine as sole sources of nitrogen, supplemented with 0.01% thiamine hydrochloride. In addition, growth of recombinant cells on nutrient agar plates containing 0.02% 5-fluorouracil (5-FU), a toxic structural analogue of hydantoin, was also investigated. Colonies able to grow on these nutrient sources were selected and cultured overnight in 5ml Luria broth, with 50µ g/ml kanamycin, at 37^{o}C with shaking. Biocatalytic assays were conducted on selected recombinant *E. coli* strains as follows: cells were cultured in 5ml Luria broth with 50µ g/ml kanamycin and grown to confluence overnight at 37^{o}C. The 5ml overnight culture was then used to inoculate 100ml Luria broth, containing 50µ g/ml kanamycin, to a final $_{OD600}$ of 0.02, followed by incubation at 37^{o}C overnight with and without the addition of 1mM IPTG after which biocatalytic assays on the harvested resting cells was done as describe in Appendix 2.1. Alternatively, the cultures were grown to early log phase of growth (OD_{600} ~ 0.5) before induction with 1mM IPTG for 15 minutes to 4 hours followed by harvesting of the cells and analysis by biocatalytic reaction with resting cells.

3.2.5 *E. coli* plasmid isolation and manipulation

Plasmid screening, isolation and manipulation was done as described in Appendix 5. Nested deletions of recombinant clones pGMlib15 were created utilizing Exonuclease III from Erase-a-Base system (Promega) which specifically digests 5' protruding or blunt ended DNA (Henikoff 1984). Protection of the sequencing primer binding site from digestion by the exonuclease was achieved by digestion with *Kpn* I (USB) whilst an exonuclease sensitive overhang was generated by restriction digestion with *Xho* I (Roche). In order to generate nested deletions from the opposite end of the insert, restriction endonuclease *Pst* I (USB), generating exonuclease-resistant 3' overhangs, and *Hind* III (USB), to allow for exonuclease digestion, were used. Ten colonies from each time interval were grown to confluence overnight at 37^{o}C in 5ml Luria broth containing 50µ g/ml kanamycin and the extracted plasmids analysed by appropriate diagnostic digestion with restriction endonucleases as described in Appendix 5.

3.2.6 DNA sequence determination and analysis

Nucleotide sequences were determined from double stranded plasmid DNA by ABI Prism Big Dye Terminator Cycle Sequencing as described in Appendix 5 using sequencing primers, pUCR and pUCF (Appendix 3). Preliminary analysis of raw sequence data was carried out using Vector NTI DeLuxe v4.0 or v5.0 software (Informax Inc.). Identification of known genes to which acquired sequence data exhibits a high degree of similarity was performed using the

Basic Local Alignment Search Tool (BLASTX, BLASTP) (Altschul *et al*. 1990) hosted by the National Centre for Biotechnology Information (NCBI) website (http://www.ncbi.nlm.nih.gov).

3.2.7 Southern hybridisation

Chromosomal DNA, extracted from RU-KM3$_S$ as previously described, as well as selected plasmid DNA, were digested with various combinations of *Pst* I, *Sal* I , and *Hind* III. The resultant fragmented chromosomal and plasmid DNA were separated by electrophoresis on 0.7% and 1% agarose gels respectively and visualization achieved by UV illumination after briefly staining the gel for 5-10 minutes in TAE buffer containing 50µ g/ml ethidium bromide. The DNA was transferred to Hybond^{TM} N+ nylon membrane (Amersham) by alkali capillary transfer using 0.4M NaOH as per manufacturers specifications. A radioactive probe was prepared by PCR amplification of the insert of pGMlib15 using pUCF and pUCR primers and the Expand High Fidelity PCR system (Roche) under standard amplification parameters (Appendix 5.3) with an annealing temperature of 57^{o}C and 50µ Ci α32P dCTP added to the reaction. The resultant radioactive PCR product was purified using High Pure PCR Product Purification columns (Roche). Southern hybridisation of the probe to the immobilized DNA on the prepared membrane was done as described by Ausubel *et al.* (1983) at 42^{o}C in a Hybaid Omnigene Hybridisation oven. High stringency washes were carried out as follows: two 10 minute washes at room temperature with 2X SSPE (20X SSPE:3.6M NaCl, 0.2M sodium phosphate, 0.02M Na_2EDTA pH 7.7) and 0.1% SDS, one 15 minute wash at room temperature with 0.5X SSPE and 0.1% SDS, one 30 minute wash at 42^{o}C and one 10 minute wash at 62^{o}C with 0.5X SSPE and 0.1% SDS. To increase stringency, an additional wash with 0.1X SSPE and 0.1% SDS at 62^{o}C for 10 minutes was done for the plasmid DNA blot. The presence of the membrane-bound radioactive probe was detected using BioMax light film (Kodak), or Agfa medical X-ray film, incubated overnight at –70^{o}C with an intensifying screen. Development of the film was done using standard photographic developing techniques with solutions obtained from Kodak.

3.3 RESULTS

3.3.1 Curing RU-KM3$_S$ of plasmids

A large plasmid of approximately 30Kb in size was successfully isolated from RU-KM3$_S$ cells subsequent to treatment with the modified Bac-to-Bac large plasmid isolation procedure (Figure 3.1, panel A). Accurate estimation of the size of this native plasmid could not be determined as large DNA molecules cannot be efficiently separated by standard agarose electrophoresis and require techniques such as pulse field electrophoresis.

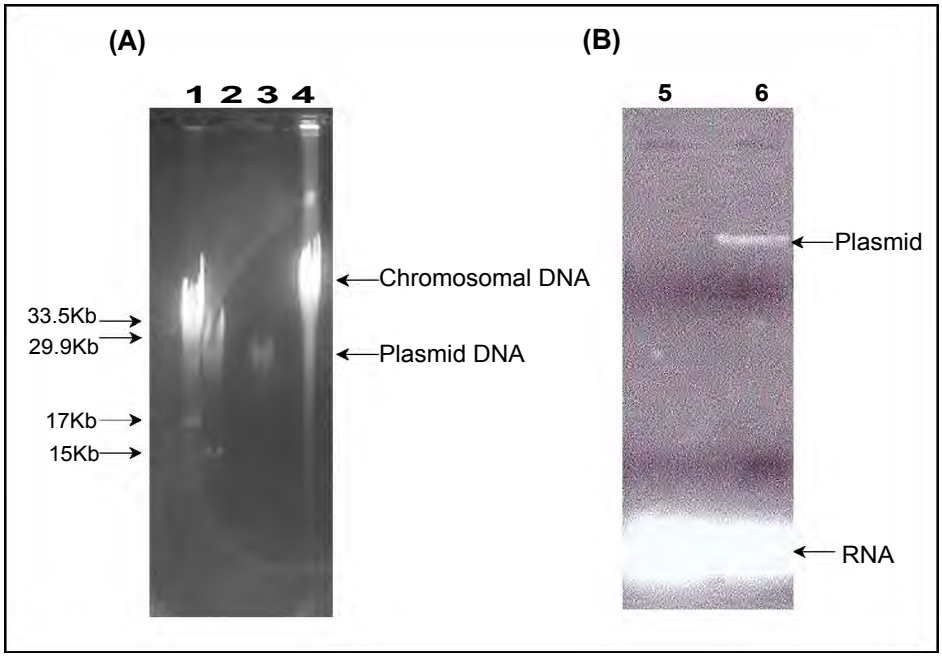

Figure 3.1 Electrophoresis of the native plasmid extracted from RU-KM3$_S$ as well as RU-KM3$_S$ chromosomal DNA **(A)** and plasmid extraction supernatant for RU-KM3$_S$ and GMPpc **(B).** (Lane 1: λ/*Xho* I marker, lane 2: λ/*Kpn* I marker, lane 3: native plasmid, lane 4: chromosomal DNA, lane 5: plasmid extraction from GMPpc, lane 6: plasmid extraction from wild type RU-KM3$_S$).

Curing RU-KM3$_S$ of its native plasmid was done by treating the cells with acridine orange and selecting for an acquired sensitivity to ampicillin. A strain of RU-KM3$_S$, called GMPpc, was isolated and shown to have lost the plasmid present in the wild type strain (Figure 3.1, panel B). The plasmid cured GMPpc strain was then tested for loss of hydantoinase and/or *N*-carbamoylase activity by whole cell biocatalytic assay. As the enzymes involved in pyrimidine degradation within the cell have been found to have hydantoin-hydrolysing capabilities (Chapter 1), hydrolysis of dihydrouracil as well as hydantoin was determined.

Table 3.1 Hydantoin-hydrolysing activity of wild type RU-KM3$_S$ and plasmid cured strain GMPpc. (Hydantoinase activity was calculated as the amount (μ mol/ml) of *N*-carbamylglycine and glycine produced and *N*-carbamoylase activity as the μ mol/ml glycine produced.) (±SEM)

Strain	Hydantoinase activity (μ mol/ml)		*N*-carbamoylase activity (μ mol/ml)	
	Hydantoin	Dihydrouracil	Hydantoin	Dihydrouracil
Wild type	38.42 *(±1.57)*	38.31 *(±2.01)*	5.64 *(±0.07)*	8.98 *(±0.24)*
GMPpc	39.59 *(±0.37)*	39.62 *(±1.14)*	6.66 *(±0.09)*	8.99 *(±0.97)*

The loss of the plasmid did not result in a concomitant decrease in hydantoinase or *N*-carbamoylase activity thus indicating that the gene(s) involved in the hydrolysis of hydantoin are not encoded on the plasmid isolated from RU-KM3$_S$ (Table 3.1).

3.3.2 Construction of RU-KM3$_S$ genomic library

Chromosomal DNA extracted from RU-KM3$_S$ was subjected to partial digestion with varying concentrations of restriction endonuclease *Sau* 3A1 in order to generate random chromosomal DNA fragments of between 2 and 10kb in size. Thus 1µ g of chromosomal DNA was digested with 0.8 to 0.002 units of *Sau* 3A1 and an aliquot of each digest was sized by agarose gel electrophoresis (Figure 3.2).

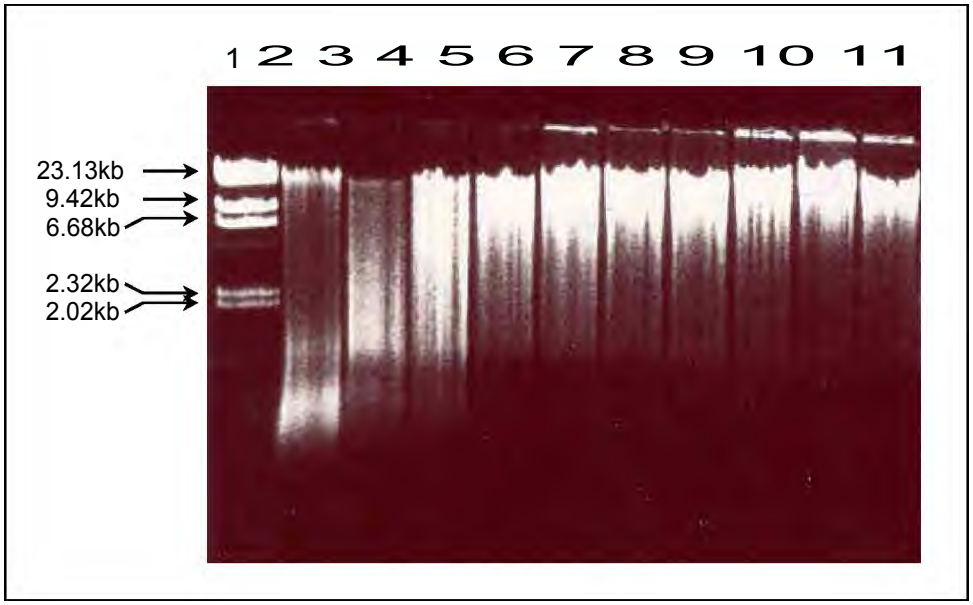

Figure 3.2 Partial digestion of RU-KM3$_S$ chromosomal DNA by addition of varying concentrations of *Sau* 3A1. [Lane 1: Phage λ / *Hind* III marker, lanes 2-11: chromosomal DNA digested with 0.8, 0.08, 0.04, 0.02, 0.013, 0.01, 0.008, 0.006, 0.004, and 0.002 units of *Sau* 3A1 per µ g of genomic DNA respectively]

Chromosomal fragments generated by partial digestion with 0.06 units of *Sau* 3A1/1µ g chromosomal DNA (Figure 3.2, lane 9) were used to produce the genomic library in pBK-CMV using the ZAP Express procedure with a 60 to 80% insertion frequency after mass excision. Recombinant plasmids contained an average insert size of approximately 5kb (Figure 3.3).

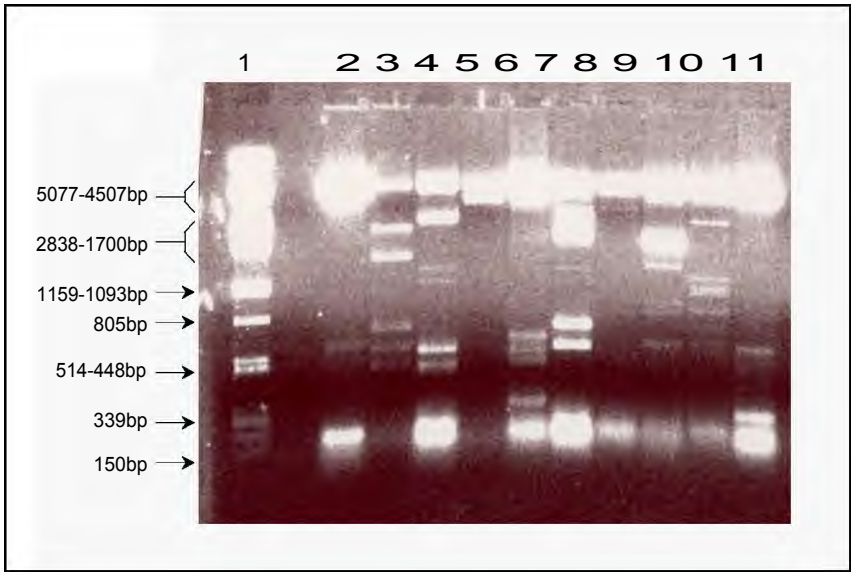

Figure 3.3 Estimation of insertion frequency and average size of insert of the recombinant clones in the constructed genomic library of RU-KM3$_S$. (Lane 1 : λ/*Pst* I marker, lanes 2-11 randomly selected plasmids subjected to restriction endonuclease digestion with *Pst* I and *Xho* I.)

3.3.3 Screening of the genomic library for biocatalytic activity in microtitre plates

The total genomic library of RU-KM3$_S$ expressed in *E. coli* XLOLR was aliquoted into 96-well microtitre plates such that each well contained approximately 40 insert-containing recombinant plasmids with a total of about 38 000 recombinant plasmids spread over 10 microtitre master plates. The recombinant clones in these master plates were screened over four rounds for those plasmids encoding for proteins capable of hydrolysing hydantoin or *N*-carbamylglycine as outlined in Table 3.2. First, duplicate subcultures of each master plate were grown in the presence and absence of IPTG (for induction of the vector *lac* promoter) and assayed for hydantoinase and *N*-carbamoylase activity with hydantoin and *N*-carbamylglycine as substrates. Detection of *N*-carbamylglycine production was not very accurate however, due to the cross reaction of the Ehrlichs reagent with an unknown component of the *E. coli* cells resulting in the production of a pink colour which interfered with the absorbance readings at 420nm.

E. coli carrying the expression vector, pBK-CMV, without insert was used as a negative control and positive results were scored as those pools in which activity levels of >1μ mol/ml were detected. The activity levels of the 84 pools selected (Table 3.2) ranged from ~1 to ~6μ mol/ml and ~1 to ~4μ mol/ml for *N*-carbamylglycine and glycine production respectively. Pools in which hydantoinase or *N*-carbamoylase activity was observed in both duplicate assays were selected for the second phase of screening in which selected wells in the

master plates were sub-cultured in 5ml Luria broth, with and without IPTG, and assays carried out in microtitre plates with hydantoin or *N*-carbamylglycine as substrates. Levels of hydantoin and *N*-carbamylglycine hydrolysis by the plasmid encoded proteins ranged from 2.3 to 3µ mol/ml and 2.25 to 9.52µ mol/ml for *N*-carbamylglycine and glycine production respectively. Single, insert-containing (white) colonies, obtained by dilution and spread plating of cells originating from those pools with positive results in the second phase of the screening procedure, were then selected and individually analysed with respect to insert size and hydantoinase and *N*-carbamoylase activity in microtitre plates in the third phase of screening of the genomic library of RU-KM3$_S$. The results for each round of screening are summarized in Table 3.2.

Table 3.2 Summary of the screening process for the genomic library of RU-KM3$_S$ in microtitre plates

Screening phase	Pools entering each phase	Recombinants entering each phase	Pools/ clones selected
Phase 1 Assay of replicate pools in microtitre plate	960	~38 000	84 pools
Phase 2 Subculture of cells from selected pools in 5ml Luria broth and assay for hydantoinase and *N*-carbamoylase activity in microtitre plates	84	~3 360	33 pools
Phase 3 Serial dilution and isolation of individual clones from wells selected from screening phase 2. Homogenous cells cultured in 5ml Luria broth and assayed in microtitre plates	33	~1 320	38 recombinant clones

Of the 38 recombinant plasmids selected for at the end of phase 3, ten were chosen for further characterization based upon their enzyme activity (Table 3.3). However, the hydantoin-hydrolysing activities of these recombinant plasmids were highly variable and in the final stage in the screening process, involving full-scale assays of potential plasmids from the previous round of screening expressed in *E. coli* strain XLOLR and DH5α, no activity was detected at all. Sonication and reduced induction times were also explored as possible methods to increase activity levels and decrease potential toxicity of the enzymes encoded on the recombinant plasmids. These measures did not, however, result in detectable enzyme activity.

Table 3.3 Biocatalytic activity of recombinant clones selected from the genomic library of RU-KM3$_S$ as determined in microtitre plates

Recombinant plasmid	Hydantoinase activity (μmol/ml)		*N*-carbamoylase activity (μmol/ml)		Insert size (kb)
	+IPTG	-IPTG	+IPTG	-IPTG	
pGMlib24	3.68 *(0.50)*	-	-	-	7.3
pGMlib23	1.85 *(2.22)*	4.6 *(1.45)*	-	-	6.4
pGMlib22	2.93 *(0.37)*	-	1.01 *(0.28)*	-	4.9
pGMlib21	1.77 *(0.44)*	-	3.04 *(0.11)*	1.11 *(0.12)*	1.9
pGMlib20	2.33 *(0.23)*	-	-	-	4.3
pGMlib19	-	2.27 *(0.61)*	2.196 *(0.68)*	-	1.7
pGMlib18	6.17 *(1.40)*	1.14 *(1.74)*	2.31 *(0.75)*	-	3.4
pGMlib17	9.56 *(0.74)*	-	2.47 *(0.73)*	-	6.3
pGMlib16	2.32 *(2.17)*	-	2.19 *(1.31)*	-	4
pGMlib15	-	-	-	3.44 *(2.92)*	2

(Standard error in italicised brackets, - : no detectable activity)

3.3.4 Southern hybridisation analysis

As detection of hydantoinase and/or *N*-carbamoylase activity resulted in inconsistent results and mapping of the restriction endonuclease sites of each of the recombinant plasmids did not reveal any obvious common fragments (data not shown), Southern hybridisation was done to assess whether the clones contained overlapping inserts. Recognition sites for the restriction endonucleases *Pst* I, *Sal* I and *Hind* III are located in the cloning cassette of the parental pBK-CMV vector (Figure 3.4) and digestion of the recombinant plasmids a using combination of *Pst* I and *Hind* III or *Sal* I and *Hind* III resulted in excision of the insert from the vector backbone.

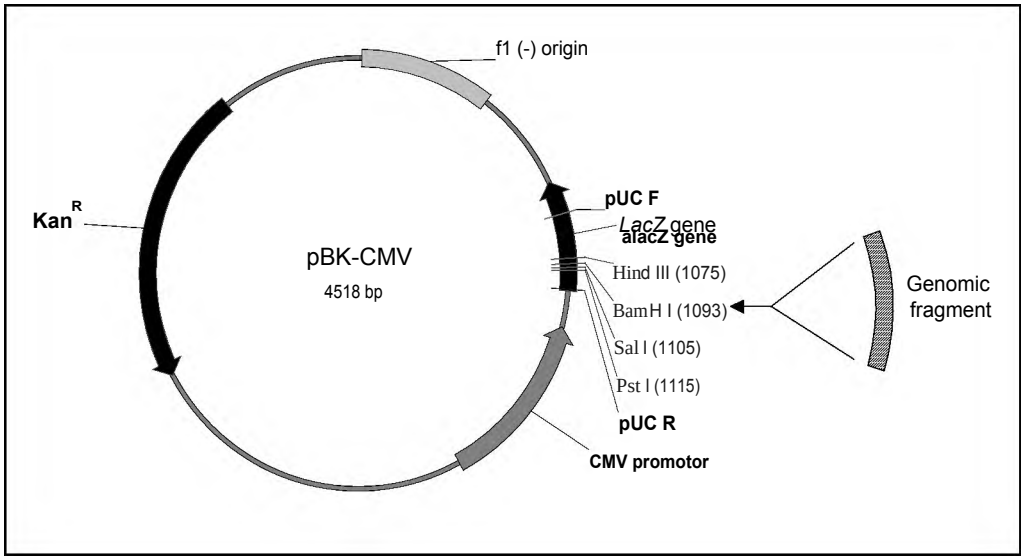

Figure 3.4 Schematic diagram of the pBK-CMV vector in which the genomic library of RU-KM3$_S$ was constructed. (Insertion of genomic fragments occurred at the *Bam* HI site as illustrated above, Kan^R : Gene encoding for kanamycin resistance, pUCF+pUCR : primers used to amplify probe for Southern blotting).

The DNA fragments of the recombinant plasmids generated by a double digest with either *Pst* I and *Hind* III, or *Sal* I and *Hind* III restriction endonucleases were separated by electrophoresis through an agarose gel (Figure 3.5, panel A). Due to its small size and thus ease of amplification, the insert from pGMlib15 was used as the probe in the Southern blotting procedure. As the probe was generated using the primers pUCF and pUCR (Figure 3.4), some of the pBK-CMV vector sequence was amplified in addition to the RU-KM3$_S$ genomic fragment coded for in pGMLib15. Consequently, DNA fragments corresponding to the vector backbone of the recombinant plasmids in the Southern blot also hybridised to the probe (Figure 3.5, panel B). Five of the eight potential clones selected from the genomic library of RU-KM3$_S$, namely pGMLib17, pGMlib24, pGMlib20, pGMlib18, and pGMlib23, appeared to contain DNA fragments homologous to sequences in the probe (pGMLib15) (Figure 3.5, panel B). This suggested that the recombinant plasmids isolated contained chromosomal fragments from a common encoding region of the genome of RU-KM3$_S$.

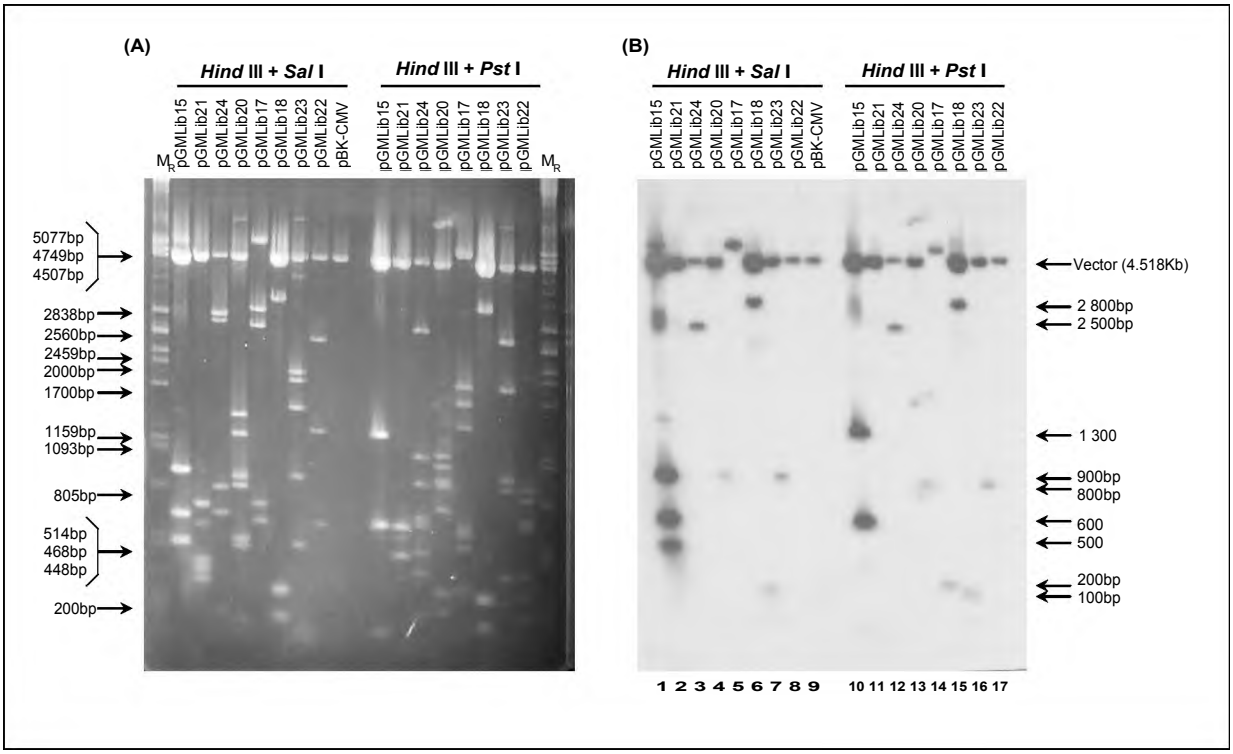

Figure 3.5 Endonuclease digestion of plasmid preparations **(A)** probed with radioactive PCR product of the insert from pGMLib15 **(B).** (M_R = λ/*Pst* I marker, lanes 1-9 and 10-17 : pGMLib15, pGMlib21, pGMlib24, pGMlib20, pGMlib17, pGMlib18, pGMlib23, pGMlib22, V : pBK-CMV parental vector.)

Restriction endonuclease digestion of pGMLib20 and pGMLib23 with *Hind* III and *Sal* I produced an 900bp DNA fragment for both clones which was found to hybridise to the probe (Figure 3.5, panel B, lanes 4 and 7). A fragment of similar size was also generated by the equivalent restriction endonuclease digestion of pGMLib15 (Figure 3.5, panel B, lane 1). This suggested that these three recombinant clones encode at least 900bp sequence which is common between them. Due to the lack of hybridisation to any of the other DNA fragments of pGMLib20 and pGMLib23 generated by *Hind* III/*Sal* I digestion, the 900bp fragment is most likely located toward the end of the genomic DNA fragment coded for by these recombinants with the terminal sequence for the inserts from pGMLib20 and pGMLib23 overlapping with that of pGMLib15. This was supported by the hybridisation of the probe to DNA fragments of pGMLib15 versus pGMLib20 and pGMLib23, generated by *Hind* III/*Pst* I restriction endonuclease digest, which were of different sizes (Figure 3.5, panel B, lanes 10 vs. lanes 13 and 16). Hydrolysis of *N*-carbamylglycine was detected for recombinant clone pGMLib15 in microtitre plates whilst only hydantoin-hydrolysis was observed for pGMLib20 and pGMlib23 (Table 3.3). This indicated that the hydantoinase and *N*-carbamoylase may be found as a gene cluster in RU-KM3$_S$ with pGMLib15 encoding for a *N*-carbamoylase while pGMLib20 and pGMLib23 may encode a hydantoinase with the positive bands produced on the Southern blot representing the DNA sequence between the two genes or a fragment of either gene in the opposite recombinant.

Hybridisation of the probe also occurred with the DNA fragments from recombinant clones pGMLib24 and pGMlib18 (Figure 3.5, panel B, lanes 3, 6, 12, and 15). Despite positive results for *N*-carbamylglycine hydrolysis by cells expressing both pGMLib15 and pGMlib18 in microtitre plates (Table 3.3), no DNA fragments of equivalent sizes from these two recombinants hybridised to one another (Figure 3.5, panel B, lanes 10 vs. 15). This suggested that the sequence encoded within these two clones followed on from one another with an overlap in the middle of the combined genomic sequence of the clones and that no *Pst* I, *Hind* III, or *Sal* I recognition sites occurred within the overlapping region. Hydantoin-hydrolysing activity in microtitre plates was observed for cells expressing both pGMLib18 and pGMLib24 (Table 3.3). The insert encoding RU-KM3$_S$ genomic DNA in pGMLib18 was calculated to be ~3.4Kb in size whilst that of pGMLib24 was ~7.3Kb in size (Figure 3.5, panel A). The sizes of the fragments to which the probe hybridised were ~2.5Kb and ~2.8Kb in size for pGMLib24 and pGMLib18 respectively (Figure 3.5, panel B, lanes 12 and 15). This suggested that either the sequences coded for by these two fragments are identical and represent genomic sequence running concurrent to one another with significant overlap, or that the genomic fragments may be orientated on the chromosome with no overlap except for that provided by the genomic DNA encoded by the probe (pGMLib15). However, hydantoin-hydrolysing activity was observed in cells expressing both pGMLib24 and pGMLib18 (Table 3.3) suggesting that the former is true.

The inability to detect *N*-carbamoylase activity in cells expressing pGMLib24 in contrast to pGMLib18 (Table 3.3) may be due to the truncation of at least 300bp of the pGMLib24 insert closest to the potential *N*-carbamoylase encoding gene. In addition, hydantoinase activity in pGMLib18 was detected in uninduced and induced cultures suggesting that expression of the enzyme responsible for hydantoin-hydrolysis is under the control of a native, as opposed to vector, promoter. Thus, either the gene was orientated in the opposite direction to that of the vector promoter or sufficient DNA lies between the *lacZ* promoter and the encoded gene to prevent expression under the control of the *lacZ* promoter. In contrast, hydantoin-hydrolysing activity in cells expressing pGMLib24 was detected only in the presence of IPTG (Table 3.3) suggesting that the encoded enzyme is located close to and in the same orientation as the *lacZ* promoter in the vector.

Hybridisation of the probe to a ~200bp DNA fragment of pGMLib17, generated by *Hind* III/*Pst* I digestion, was observed (Figure 3.5, panel B, lane 14). However, subsequent to digestion of this plasmid with *Hind* III and *Pst* I, the DNA fragment corresponding to the vector was larger than expected indicating that complete excision of the insert from the vector backbone had not occurred (Figure 3.5, panel B, lane 14). Consequently, complete analysis of the Southern blot of pGMLib17 was difficult.

Whilst sequence similarity between five of the selected clones had been established (Figure 3.5, panel B), restriction endonuclease mapping of the clones relative to one another remained inconclusive (data not shown). In order to facilitate mapping of the recombinant clones relative to one another, the chromosomal region on the genome from which the insert encoded in pGMLib15 was derived was analysed by digestion of the chromosomal DNA with *Hind* III, *Sal* I, and *Pst* I restriction endonucleases and generation of a Southern blot with the pGMLib15 insert as the probe (Figure 3.6).

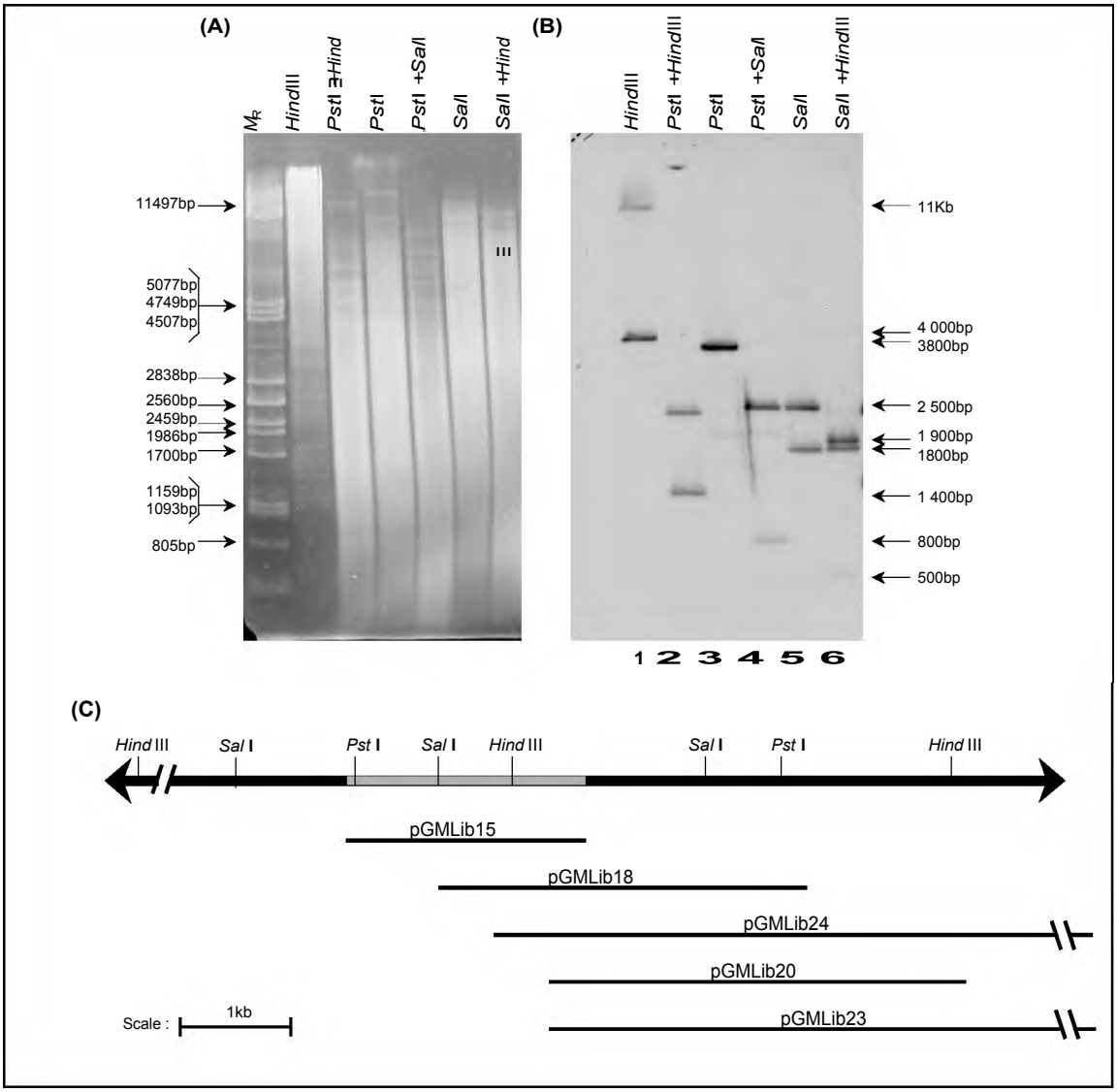

Figure 3.6 Southern analysis of the chromosomal DNA flanking the sequence encoded by the insert in pGMLib15. Restriction digest of chromosomal DNA from RU-KM3$_S$ **(A)** probed with radioactive PCR product of the insert from pGMlib15 **(B)** as well as mapping of the restriction endonuclease recognition sites on the genomic DNA (coloured black) flanking pGMlib15 (coloured grey) and suggested relative location of the genomic fragments contained in the recombinant clones **(C)**. (Lane 1: λ/*Pst* I marker, lane 2-7: genomic DNA digested with *Hind* III, *Pst* I+*Hind* III, *Pst* I, *Pst* I+*Sal* I, and *Sal* I respectively.)

By analysis of the chromosomal fragments to which the probe hybridised, the *Hind* III, *Pst* I and *Sal* I recognition sites located on the genome could be mapped beyond the known sites within the genomic fragment encoded by the pGMLib15 insert (Figure 3.6, panel C). The approximately 2 500bp *Pst* I/*Hind* III generated chromosomal fragment to which the probe hybridised (Figure 3.6, panel B, lane 2) was of a similar size to that of pGMLib24 subjected to digestion and hybridisation with the equivalent restriction endonuclease enzymes and probe respectively (Figure 3.5, panel B, lane 12). Based on this, the genomic fragment encoded by the insert of pGMLib24 was aligned downstream of that encoded by the probe pGMLib15 with approximately 750bp overlap in sequence between the two (Figure 3.6, panel C). The minimal overlap between these two genomic fragments was supported by the hydantoin-hydrolysing activity of cells expressing pGMLib24 but not those expressing pGMLib15 whilst the opposite was observed for *N*-carbamylglycine-hydrolysing activity (Table 3.3). However, Southern blot analysis of chromosomal DNA digested with *Hind* III and *Sal* I resulted in bands corresponding to DNA fragments of approximately 1.9Kb and 1.8Kb in size (Figure 3.6, lane 6) which were not mirrored by the corresponding restriction endonuclease digest of pGMLib24 (Figure 3.5, panel B, lane 3). From the data obtained from the Southern blot of pGMLib18 and pGMLib24, these two recombinants appeared to overlap to a large degree but with pGMLib18 encoding more sequence corresponding to the pGMLib15 insert than pGMLib24 as suggested by the additional positive hybridisation band at ~500bp (Figure 3.5, panel B, lane 15). A faint band of corresponding size was observed in the Southern blot of the chromosomal DNA also digested with *Sal* I and *Hind* III (Figure 3.6, panel B, lane 6), However, if pGMLib18 is aligned as depicted in Figure 3.6 (panel C) as suggested by the data, a DNA fragment from the *Hind* III/*Pst* I digest, of ~2.5Kb should have been hybridised by the probe but a band of ~2.9Kb was observed instead (Figure 3.5, panel B, lane 15).

Hybridisation of the probe to ~900bp and ~800bp DNA fragments of pGMLib20 and pGMLib23 digested with *Hind* III/*Sal* I and *Hind* III/*Pst* I respectively (Figure 3.5, panel B, lanes 4, 7, 13, and 16) indicated an overlap of the inserts of pGMLib23 and pGMLib20 with pGMLib15 toward the end of the pGMLib15 insert. However, mapping of the pGMLib20 and pGMLib23 inserts relative to the chromosomal map generated from the Southern blot of digested chromosomal DNA (Figure 3.6, panel C) was unsuccessful as restriction endonuclease digestion with *Hind* III/*Pst* I and *Hind* III/*Sal* I would be expected to form fragments which hybridised to the probe with minimum sizes of 2.1Kb and 1.1Kb or 1Kb respectively. As hydantoin-hydrolysing activity was observed in *E. coli* cells expressing pGMLib20 and pGMLib23, as was the case for pGMLib18 and pGMlib24, the inserts encoded in pGMLib20 and pGMLib23 most likely overlapped with that of pGMLib18 and pGMLib24 (Figure 3.6, panel C). The possibility of loss of restriction endonuclease recognition sites due to instability of the insert DNA will be discussed later in this chapter and may explain the variations in fragment sizes obtained.

From analysis by Southern blotting, the genomic DNA fragments contained in at least five recombinant clones appeared to form overlapping segments from the same region on the chromosome of RU-KM3$_S$. To determine if the genomic fragment used as the probe in the Southern blots encoded an *N*-carbamoylase gene, as suggested by initial activity assays (Table 3.3), nested deletions of pGMlib15 were created by varying exposure to exonuclease digestion thus enabling sequence analysis of the entire 2Kb genomic fragment.

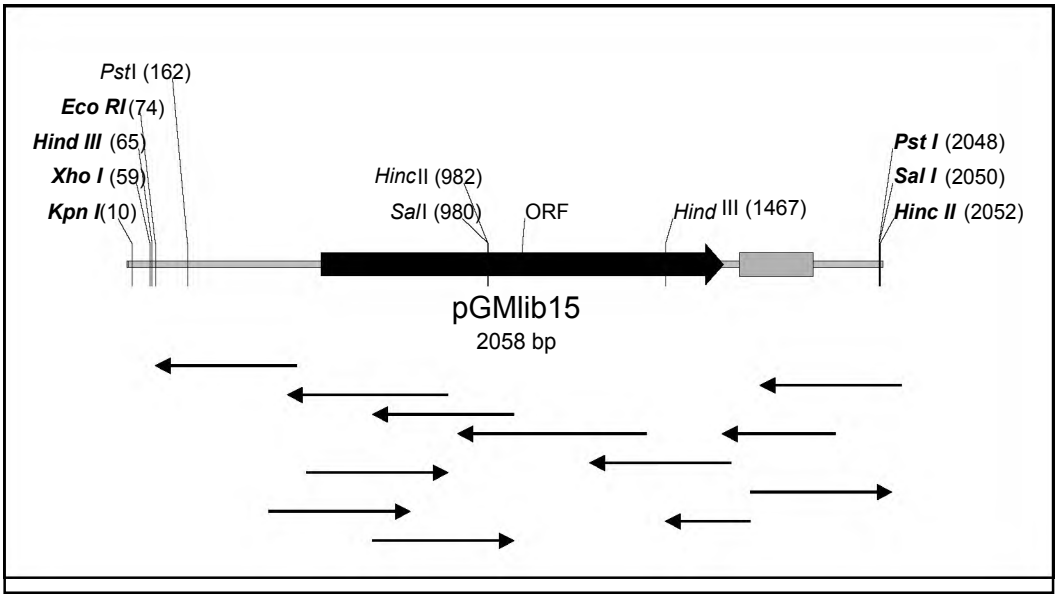

Figure 3.7 Graphical representation of the strategy used to determine the nucleotide sequence of the RU-KM3$_S$ genomic fragment contained in pGMlib15. (Arrows represent sequenced regions and the direction of sequencing, the block arrow represents the putative open reading frame, restriction endonuclease recognition sites located within the cloning cassette of the vector are written in bold).

The complete nucleotide sequence of the insert of pGMLib15 was determined except for a region of approximately 100bp (indicated by the grey bar in Figure 3.7) for which no data could be obtained on either strand. Addition of DMSO, a detergent which facilitates separation of DNA strands and denaturation of secondary structures, did not facilitate sequencing of this region.

An open reading frame (ORF) of 1.141Kb in size was identified within the insert contained in pGMLib15 orientated in the opposite direction to the pBK-CMV *lac* promoter (Figure 3.7). The orientation of the ORF relative to the *lac* promoter correlated with activity data in which *N*-carbamoylase activity was detected in the absence of IPTG (Table 3.3). The putative ORF was translated and the amino acid sequence compared to *N*-carbamoylase sequences reported in literature (listed in Table 1.4 and 1.5), however, no significant similarity was observed. The entire pGMLib15 insert sequence was therefore used for a BLASTX search

on the NCBI database system. The only sequences to which the genomic fragment encoded in pGMLib15 exhibited any nucleotide sequence similarity was that from the total genomes of *Pseudomonas putida* KT2440 (Nelson *et al*. 2002), *Pseudomonas aeruginosa* PAO1 (Stover *et al*. 2000), and *Pseudomonas syringae* DC3000 (Buell *et al*. 2003) (Table 3.4). The putative proteins, annotated on the total genome sequences of these organisms, on either side of the genes to which pGMLib15 exhibited similarity did not allow identification of the potential genes encoded within the genomic fragments of the recombinant clones isolated from RU-KM3$_S$ genomic library (Table 3.4).

Table 3.4 Encoded proteins to which the genomic fragment contained in the recombinant clone pGMLib15 showed similarity and the gene products flanking the homologous protein on the total genome sequences of *P. putida*, *P. aeruginosa*, and *P. syringae*.

Organism	Gene product to which the pGMLib15 insert exhibited similarity	Identity (%)	Encoded gene product located downstream	Encoded gene product located upstream
P. putida KT2440	Putative oxidoreductase, FAD binding	91%	Rieske 2Fe-2S family protein	Putative methyl-accepting chemotaxis transducer
P. aeruginosa PAO1	Probable ferredoxin	81%	Probable ring hydroxylating dioxygenase	Hypothetical protein
P. syringae DC3000	Putative iron-sulphur cluster-binding protein	81%	Iron-sulphur cluster-binding protein, Rieske family	Hypothetical protein

3.3.5 Screening of the genomic library by growth on agar plates

The genomic library of RU-KM3$_S$ was also screened for *E. coli* containing recombinant clones expressing proteins with hydantoin- and/or *N*-carbamylglycine-hydrolysing activity by selection for growth on nutrient agar plates containing the toxic hydantoin analogue, 5-FU or minimal medium plates with *N*-carbamylglycine (NCG-MM) or hydantoin (H-MM) as sole sources of nitrogen.

The total genome size of *P. aeruginosa* PAO1, which was the only complete genome sequence for a *Pseudomonas* species available at the time of screening, is 6.264Mb (Stover *et al.* 2000). By using the equation described in Section 3.2.3, the number of recombinant clones to be screened with an average insert size of 5Kb for a 99% chance of isolating the genes encoding the hydantoinase and/or *N*-carbamoylase was calculated as 5 767

recombinant clones. Over 16 700 recombinant clones were screened on nutrient agar plates containing 5-FU and over 12 500 were screened on NCG-MM and H-MM plates thus ensuring complete representation of the genome of RU-KM3$_S$ in the screening processes.

No colonies were isolated from H-MM or 5-FU plates, however, two transformants were able to grow on NCG-MM plates. Recombinant plasmids pGMLib1 and pGMLib2 were isolated from these two colonies and found to have insert sizes of approximately 10.7Kb and 6.3Kb respectively (Figure 3.8, panel A). Initial restriction endonuclease digestion (Figure 3.8, panel A) of pGMLib1 and pGMLib2 resulted in DNA fragments of similar sizes of approximately 5100bp, 4000bp, and 1800bp generated as a result of *Pst* I digestion and DNA fragments of approximately 5100bp, 4100bp and 1600bp subsequent to digestion with *Hind* III (Figure 3.8, panel A). This suggested that these clones might contain fragments of genomic DNA from the same section of the RU-KM3$_S$ genome. However, subsequent to sub-culturing of the *E. coli* cells containing pGMLib1 in Luria broth, restriction digestion of the plasmid extracted from these cells resulted in the formation of only a single band of approximately 4500bp, which corresponded to that of the vector, as opposed to the four DNA fragments generated by the equivalent restriction endonuclease digestion before sub-culturing (Figure 3.8, lanes 2 and 4 vs. lanes 6 and 8). The insert in pGMLib1 was therefore unstable.

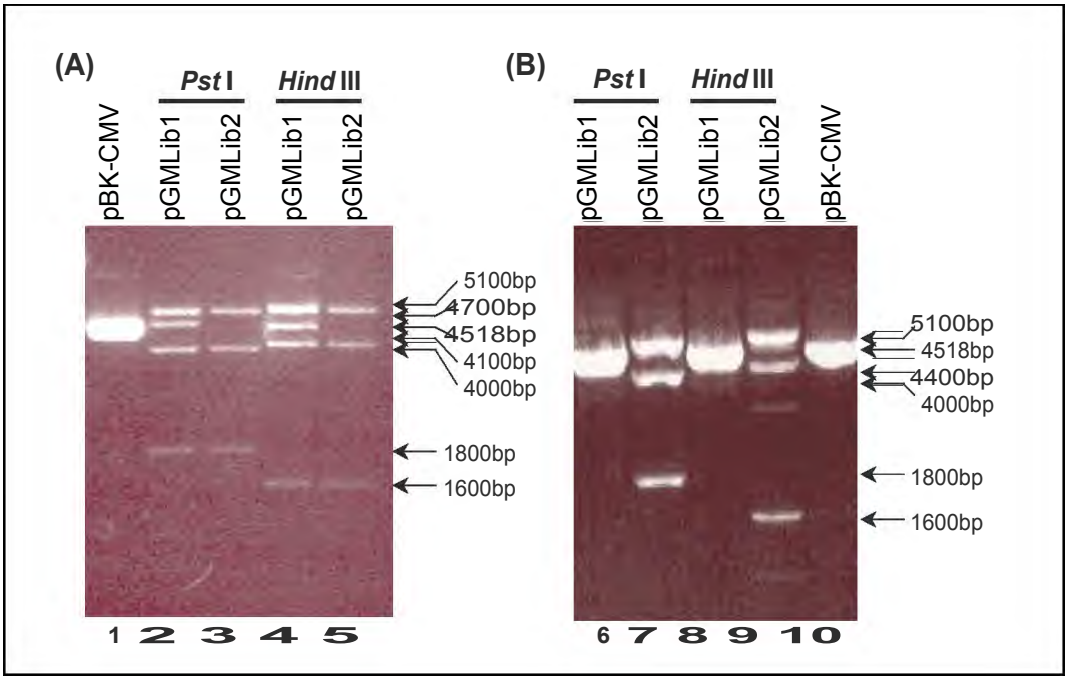

Figure 3.8 Restriction endonuclease digestion of pGMlib1 and pGMlib2 from initial culture of the recombinant directly from the NCG-MM plate **(A)**, and subsequent to sub-culturing in Luria broth **(B)**.

Not surprisingly, biocatalytic assays of pGMlib1 and pGMlib2 in *E. coli* XLOLR cultured to confluence overnight at 37^{o}C in Luria broth with IPTG as an inducer showed no detectable *N*-carbamoylase activity. To reduce potential toxicity, cells expressing the recombinant clones were cultured to mid-log growth phase before addition of IPTG and induction for 15 minutes or 2 hours prior to harvesting for biocatalytic assays. However, this did not result in detectable *N*-carbamoylase activity either.

As *E. coli* DH5α cells were routinely being used to express other *N*-carbamoylase enzymes in the laboratory, pGMLib1 and pGMLib2 were transformed into this strain and the cells assayed for activity. However, no positive result was observed. Analysis of the growth characteristics of *E. coli* strain DH5α containing the parental vector pBK-CMV versus recombinant clones pGMlib1 and pGMlib2 showed retarded growth for those cells expressing the recombinant clones compared to the control expressing the vector alone (Figure 3.9). This suggested that the expression of the genes encoded by pGMLib1 and pGMLib2 might be toxic to the cells. No difference in growth rates was noted between induced and uninduced cultures indicating that the expression of the potentially toxic gene products was constitutive (Figure 3.9).

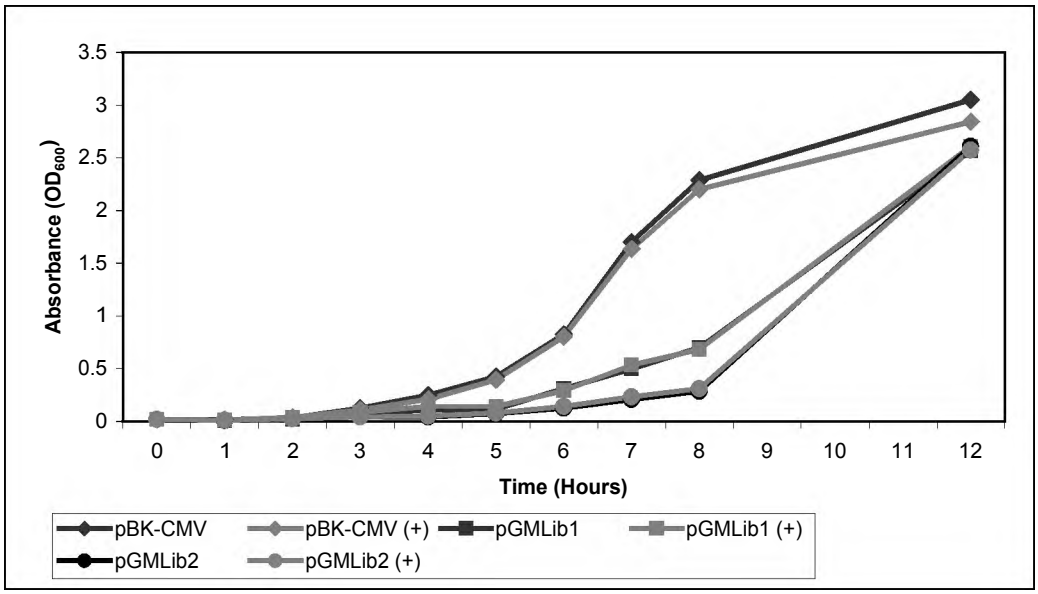

Figure 3.9 Comparison of the growth of *E. coli* DH5α transformants expressing pBK-CMV, pGMlib1, or pGMlib2 over time. [(+) : culture induced with 1mM IPTG].

Sequence analysis of the 5' and 3' regions of the insert encoded by pGMlib2 using primers pUCF and pUCR (Figure 3.4) yielded no significant similarity to any known hydantoinase or *N*-carbamoylase genes. BLASTX analysis (NCBI database) of the sequence data revealed a high degree of similarity to sequences in the total genomes of *P. putida* KT2440 (Nelson *et*

al. 2002), *P. aeruginosa* PAO1 (Stover *et al*. 2000), and *P. syringae* DC3000 (Buell *et al*. 2003) (Table 3.5).

Table 3.5 Gene loci to which the genomic fragment of RU-KM3$_S$ contained within pGMLib2 had a high degree of similarity

Nucleotide sequence of pGMLib1	Gene locus	Strain	Identity (%)
NCG6F*	Putative penicillin-binding protein	*P. putida* KT2440	84% over 756bp
		P. aeruginosa PAO1	79% over 722bp
		P. syringae DC3000	77% over 754bp
NCG6R†	Ketol-acid reductoisomerase	*P. putida* KT2440	91% over 885bp
		P. syringae DC3000	85% over 889bp
		P. aeruginosa PAO1	88% over 740bp

*Nucleotide sequence obtained using pUCF as the sequencing primer

†Nucleotide sequence obtained using pUCR as the sequencing primer

The open reading frames between the putative penicillin-binding protein and the ketol-acid reductoisomerase loci on the total genome database of *P. putida* KT2440 were annotated as a putative acetolactate synthase (small and large subunit), a conserved hypothetical protein, and a putative lipoprotein.

3.4 DISCUSSION

The aim of the work described in this chapter was to isolate the genes encoding the hydantoinase and *N*-carbamoylase enzymes in RU-KM3$_S$. To this end, the potential location of the hydantoin-hydrolysing genes on a native plasmid within RU-KM3$_S$ was investigated. A plasmid of approximately 30Kb was isolated from RU-KM3$_S$, however, loss of this plasmid did not result in a concomitant loss of hydantoin-hydrolysing activity implying that the relevant genes are encoded on the chromosome or that there are multiple genes encoding hydantoin-hydrolysing proteins (discussed in Chapter 5). This is in contrast to data from *Agrobacterium* sp. IP I-671 and *Pseudomonas* sp. NS671 in which the hydantoin-hydrolysing operons were located on 190kB and 172Kb native plasmids respectively (Hils *et al*. 2001, Watabe *et al.* 1992a).

Amplification by PCR has been used to isolate the genes encoding D-enantioselective hydantoinases and *N*-carbamoylases from *P. putida* 7711-2, *A. radiobacter* NRRL B11291 and *Agrobacterium* sp. IP I-671 (Chen and Tsai 1998, Chao *et al*. 1999b, Hils *et al*. 2001). The primers used for the amplification procedure were either designed based on the N-terminal amino acid sequence, determined by Edman degradation, of the purified protein (Chen and Tsai 1998) or by alignment of related sequences reported in literature to produce degenerate primers (Chao *et al*. 1999b, Hils *et al*. 2001). However, the only non-enantioselective hydantoinases (from *A. aurescens* DSM 3747 and *Pseudomonas* sp. NS671) for which the encoding genes have been isolated to date have no similarity to one another (Wiese *et al*. 2001, Watabe *et al*. 1992a). With respect to L-enantioselective *N*-carbamoylases, only four gene sequences were available at the time of this study (Watabe *et al*. 1992a, Mukohara *et al*. 1993, Batisse *et al*. 1997, Wilms *et al*. 1999). While the amino acid sequence of the L-carbamoylases from *B. stearothermophilus* NCIB8224 and NS1122A had a high degree of similarity, the remaining enzymes did not (data not shown). Thus design of degenerate primers for PCR amplification of the non-stereoselective hydantoinase and L-stereoselective *N*-carbamoylase of RU-KM3$_S$ could not be attempted. Furthermore, the genome sequence for *P. aeruginosa* PAO1 was the only complete genome available for comparative analysis at the time of this study (Stover *et al*. 2000). Moreover, a search of the annotated database of *P. aeruginosa* PAO1 did not reveal any genes annotated as a *N*-carbamoylase (data not shown). Consequently, screening of a genomic library of RU-KM3$_S$ was approached in order to isolate the genes encoding the hydantoin-hydrolysing enzymes in this strain. A genomic library of RU-KM3$_S$ was successfully constructed, using the λ-phage ZAP Express system, with an average insert size of 5Kb and 60 to 80% insertion frequency. To ensure that the entire genome of RU-KM3$_S$ was represented in the screening procedures, the number of recombinant clones screened was 2- to 4-fold in excess to that required as calculated using equation 1 (Section 3.2.3).

Initial screening of recombinant *E. coli*, containing fragments of the RU-KM3$_S$ genome in the pBK-CMV vector, was based on detection of *N*-carbamylglycine and glycine production from hydantoin or *N*-carbamylglycine as substrates in microtitre plates. Whilst positive results were obtained in the first three phases of the screening process, the hydantoin-hydrolysing activity of the recombinant *E. coli* selected was highly variable and activity was completely lost by screening phase 4 which entailed full-scale biocatalytic reactions. The variations observed may in part be due to the inability to standardize recombinant cell concentration in the microtitre plate biocatalytic reactions as growth of recombinants varied depending on the metabolic burden placed on the cell by the expression of the foreign proteins encoded on the genomic fragments. Also, low activities, obtained as a result of dilution in the mixed population of clones (40 clones per well) in the early phases of screening, may have been

obscured by background readings. Furthermore, the pink colour resulting from cross-reaction of the Ehrlichs reagent with components of the *E. coli* cell also affected absorbance readings with respect to the detection of *N*-carbamylglycine. Loss of hydantoin- and *N*-carbamylglycine-hydrolysing activity by the fourth phase of screening may be due to either false positives in the microtitre plate assay or due to instability of the insert DNA. However, Southern analysis of eight of the clones revealed at least five which contained apparently homologous fragments of DNA suggesting that a common or overlapping region of genomic DNA was encoded within the genomic fragment inserts. If the loss of activity was solely due to false positive results, random fragments of genomic DNA as opposed to fragments from a common region of the genome would have been isolated. The loss of activity was therefore most likely due to instability of the insert DNA. Sequence analysis of the probe, generated from the insert in pGMlib15, yielded no significant similarity to *N*-carbamoylase or hydantoinase sequences reported in literature.

Screening of the genomic library by growth on minimal medium plates with hydantoin or *N*-carbamylglycine as sole sources of nitrogen had advantages over screening for activity for two reasons. Firstly, by culturing the recombinant *E. coli* on medium with hydantoin/*N*-carbamylglycine as a sole source of nitrogen, a selection pressure was applied that would promote insert stability. Secondly, the recombinant plasmid could be isolated directly after transformation and culture of the recombinant plasmid without the necessity of sub-culturing the *E. coli* through several rounds of screening during which the integrity of the plasmid could not be monitored. Restriction analysis of the two recombinant clones isolated from NCG-MM indicated the presence of common, overlapping sequences, suggesting that the inserts may be from the same region on the RU-KM3$_S$ genome. However, as was the case with the previously isolated clones, no hydantoinase or *N*-carbamoylase activity was observed in the biocatalytic assays irrespective of the temperature at which the cells were cultured, induction time, or sonication. The insert in pGMLib1 was found to be highly unstable as a single sub-culture of the recombinant *E. coli* resulted in complete loss of the insert when cultured in *E. coli* XLOLR. *E. coli* strain DH5α was therefore investigated as an alternative host for the isolated recombinant clones. While the gross structural integrity of the recombinant plasmids was maintained within this strain (data not shown), a significant reduction in growth was noted when pGMlib1 and pGMlib2 were expressed suggesting that the expression of the foreign proteins was either toxic to the cell or placed a high metabolic burden on the cell resulting in slower growth.

The pBK-CMV vector utilized in the construction of the genomic library of RU-KM3$_S$ relies on expression from the *lacZ* promoter. There are two negative feedback controls associated with the lac operon. The first is carbon catabolite repression and the second involves the lac

repressor protein (LacI), encoded by the *lacI* gene, which controls transcription by binding to the operator region and preventing RNA polymerase action. However, when present, lactose or a structural analogue thereof (i.e. IPTG) binds to LacI resulting in a conformational change thus preventing binding of the repressor to the operator region consequently resulting in expression of *lacZ* (Snyder and Champness 2003). This repression of *lacZ* expression is however incomplete and "leaky" (Freifelder 1987). "Leaky" lac promoters can be completely repressed by expression of the plasmids in host strains carrying the *lacI´* allele. This mutation of the chromosomal promoter region for *lacI* results in increased production of LacI repressor molecules from 10-20 to over 100 molecules per cell (Baneyx 1999). *E. coli* strain XLOLR contains this mutated allele whilst strain DH5α does not, thus biocatalytic assays of β-galactosidase expressed from the lac promoter encoded within pBK-CMV results in constitutive expression of the *lacZ* when in *E. coli* DH5α (Pers. Comm. M. Jiwaji). This "leakiness" of the *lac* promoter when in *E. coli* DH5α due to an unequal supply of repressor protein LacI, leads to instability of plasmids and/or low induction levels (Wilms *et al.* 2001a). However, XLOLR, which contains the *lacI´* mutant allele, did not result in stable maintenance of recombinant plasmids encoding genomic fragments of RU-KM3$_S$ either. Thus plasmid instability may be attributed to the fact that pBK-CMV is derived from a high copy number ColE1 based plasmid. High copy number plasmids burden the metabolic capacity of the host cell resulting in a starvation-like condition. This in turn leads to the accumulation of uncharged tRNAs which, due to sequence homologies, tend to interact with the plasmid-replication mechanisms resulting in excessive replication of the plasmid up to the point where the metabolic capacity of the cell is completely exhausted (Grabherr and Bayer 2002). In addition, strong promoters, such as T7 found in pBK-CMV, also result in such high levels of expression that the expressed protein is often unable to achieve its native conformation and segregates in inclusion bodies (Baneyx 1999).

The toxic effect of heterologous expression of hydantoin-hydrolysing genes in *E. coli* has been well documented as resulting in the formation of inclusion bodies (Chien *et al.* 1998, Chao *et al*. 2000a , Hils *et al*. 2001, Wilms *et al*. 2001b), reduced growth rates (Mukohara *et al*. 1994, Chien *et al.* 1998) and low levels of activity (Wilms *et al*. 2001a, Hils *et al*. 2001). As hydantoinases and *N*-carbamoylases are associated with pyrimidine catabolism, the unregulated degradation of pyrimidines in the cells by over-expression of the hydantoinase may provide a possible explanation for the toxicity observed (Mukohara *et al*. 1994, Chien *et al.* 1998). Furthermore, *Pseudomonas* proteins are well-known in literature for poor expression in *E. coli* and further examples are continually being published (Schweizer 2001). The shortcomings of screening for heterologous expression of the RU-KM3$_S$ hydantoinase and *N*-carbamoylase encoding genes in *E. coli* are numerous thus necessitating an alternative approach.

4.1 INTRODUCTION

Optimisation of hydantoin-hydrolysing enzyme systems in native organisms has been accomplished by spontaneous mutation (Syldatk *et al*. 1990a) or via chemically induced mutagenesis (Wagner *et al*. 1996, Hartley *et al*. 1998, 2001). Mutant strains thus generated exhibit phenotypes such as increased hydantoin-hydrolysing activity (Syldatk *et al.* 1990a), inducer-independent expression (Hartley *et al*. 1998, Wagner *et al*. 1996), as well as mutants which are no longer subject to nitrogen catabolite repression (Hartley *et al*. 2001).

In the case of chemically induced mutagenesis, alklating agents ethylmethane sulfonate (EMS) or N-methyl-N-nitro-N-nitrosoguanidine (MNNG) were utilized. The mutagenic action of alklyating agents involve addition of ethyl groups to the nucleotide bases in DNA, with O^6-alkyl guanine being the prime cause of mutations *in vivo*, resulting in mispairing of thymine with guanine. Consequently, G:C→A:T transitions are the primary point mutations which occur (Miller 1992).

An alternative mutagenesis methodology involves the use of transposons. In contrast to chemical mutagenesis, where subtle changes in the target gene may occur, complete inactivation of the gene can result when utilizing transposons. Transposons are broadly classified as segments of DNA that can move, termed transposition, from one location on a genome or plasmid to another (Judson and Mekalanos 2000). While transposons may contain several genes (Malay *et al.* 1994), the components essential for transposition are the transposase gene and two inverted repeat sequences flanking the DNA encoding the selectable phenotype (de Lorenzo and Timmis 1994). The transposase enzyme is responsible for recognition of the inverted repeats and integration of the DNA located between these repeats into the bacterial genome (Malay *et al*. 1994). Placement of the gene encoding the transposase outside of the inverted repeats results in the formation, after the insertional event, of a non-replicating DNA fragment containing the transposase gene which is lost in subsequent cell replication (Dennis and Zylstra 1998). This ensures that transposition occurs once only and that further movement or rearrangement of DNA due to the transposase is negated resulting in a stable, inheritable insertional mutation which can then be analysed (de Lorenzo and Timmis 1994). Furthermore, the presence of a conditional origin of replication within the integrated DNA sequence allows for rapid identification of the sequence flanking the transposon site of insertion. This is achieved by digestion of the total genomic DNA of a selected insertional mutant strain with a restriction endonuclease non-specific for the inserted foreign DNA, followed by circularisation of the resultant fragments by self-ligation. Transformation of the ensuing circular DNA fragments into *E. coli* and selection for the phenotype, such as an antibiotic resistance marker, inserted into the target genome by the transposon allows for the isolation of the genomic fragment interrupted by the

transposon DNA. The chromosomal DNA flanking the inserted transposon DNA can then be sequenced with primers specific for the terminal ends of the inserted DNA (Snyder and Champress 2003).

Dennis and Zylstra (1998) utilized the above characteristics to create a construct called a "plasposon", derived from the terms 'plasmid' and 'transposon', which was utilized in this study. Plasposons consist of Tn5 inverted repeats, a conditional origin of replication (pMB1 oriV), Tn5 transposase gene for random insertion events, origin of transfer (RP4 oriT) responsible for the movement of the plasposon into the target organism, and exchangeable antibiotic resistance genes (Figure 4.1)

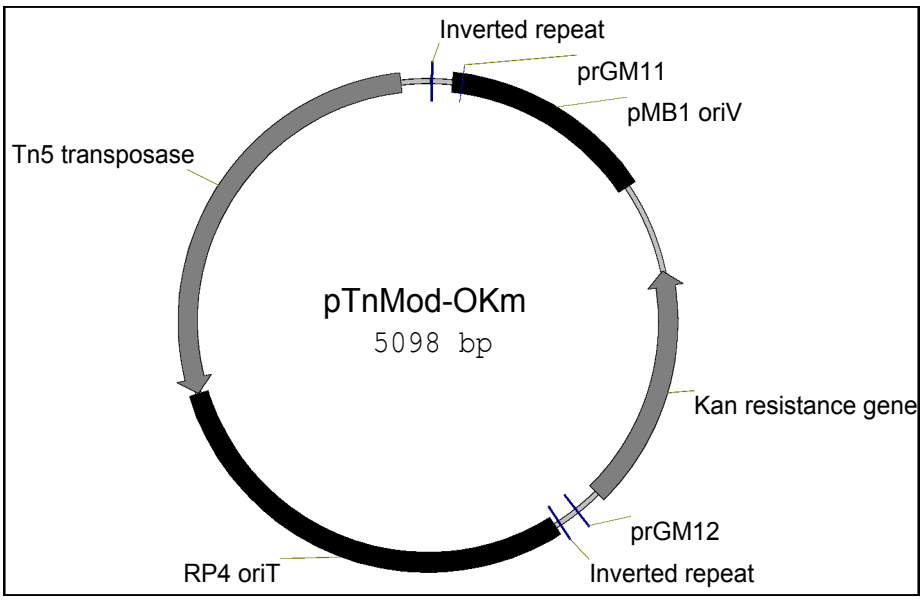

Figure 4.1 Schematic map of the plasposon pTnMod-OKm. [pTnMod-OTc differs only in that the antibiotic resistance gene codes for tetracycline resistance rather than kanamycin resistance]

A major advantage of mutagenesis over complementation studies in *E. coli* is that screening for the desired gene involves detection of loss of activity of the gene product under optimised and well-known conditions rather than attempting to detect activity in a heterologous host such as *E. coli* where factors such as toxicity and production of functionally active protein may be problematic. In addition, screening for reduction as well as elimination of the target protein in mutant strains allows for identification of genes and/or metabolic pathways involved in the regulation of the expression or activity of the specific enzymes.

In this chapter, the use of chemical and transposon mutagenesis to produce mutant libraries of RU-KM3$_S$ is discussed. Mutants generated by chemical mutagenesis were screened for inducer-independence, while plasposon generated mutants were screened for decreased or

loss of hydantoin-hydrolysing capabilities, indicating inactivation of genes involved in the hydantoin-hydrolysing enzyme system of RU-KM3$_S$.

4.2 METHODS AND MATERIALS

4.2.1 Chemical mutagenesis of RU-KM3$_S$

RU-KM3$_S$ cells were subjected to random chemical mutagenesis with EMS (Sigma) as described in Miller (1992). A confluent culture of RU-KM3$_S$ in 5ml nutrient broth, incubated overnight at 28^{o}C, was used to seed 30ml of nutrient broth which was incubated at 28^{o}C, shaking at 200rpm, until an $_{OD600}$ of 0.3 to 0.5 was achieved. The culture was then centrifuged at 5 000rpm (Beckman centrifuge, JA20 rotor) for 10 minutes at 4^{o}C. All subsequent steps were carried out on ice. The pellet was washed in 30ml minimal buffer A (per litre: 10.5g K_2HPO_4, 4.5g KH_2PO_4, 1g $(NH_4)_2SO_4$, 0.5g sodium citrate.$2H_2O$) and centrifuged again as above. The pellet was then resuspended in 15ml minimal buffer A and 2ml removed as a control. EMS was added to the remaining cells at a concentration of 15µ l/ml and the flask placed at 28^{o}C, 200rpm. At 10 minute intervals, 2ml aliquots of the culture were removed, the cells pelleted by centrifugation in a Heraeus microfuge (13,000rpm), washed with minimal buffer A, and resuspended in a final volume of 1ml of minimal buffer A.

In order to calculate the percentage survival, a serial dilution in minimal buffer A was done for each EMS-treated time interval, 10^{-5} and 10^{-6} dilutions plated onto nutrient agar plates, and incubated overnight at 28^{o}C. A 1:20 dilution of the mutagenized cells in 5ml nutrient broth was grown overnight at 28^{o}C, 200rpm, as the outgrowth. Serial dilutions of the cells from the outgrowth were plated onto nutrient agar plates with and without rifampicin in order to determine the rate of mutation. The remaining outgrowth culture was stored by mixing 1ml of the culture with 0.45ml 50% glycerol in Luria broth and placing at –70^{o}C. Selection for inducer-independent mutant strains was based on growth on nutrient agar supplemented with 0.1% 5-flourouracil (5-FU) (Sigma) or minimal medium (Appendix 1) with 0.25% ammonium sulphate as the sole nitrogen source and 0.1% 5-FU. Hydantoinase and *N*-carbamoylase activities in the subsequently isolated mutants were assayed as described in Appendix 2.1.

4.2.2 Tri-parental conjugal mating for transposon mutagenesis

The suicide plasmid pTnMod-OKm, hosted in *E. coli* DH5α, was introduced into the target strain RU-KM3$_S$ by conjugal transfer during tri-parental mating with *E. coli* HB101 (*SupE44 hsdS20*($r_B^- m_B^-$)*recA13 ara-14 proA2 lacY1 galK2 rspL20 xyl-5 mtl-1*) hosting the mobilizing plasmid pRK2013 (RK2-Tra$^+$ RK2-Mob$^+$ Km^R ColE1) (Santos *et al.* 2001) as follows. Single

colonies of each strain were inoculated into 5ml Luria broth (50µ g/ml kanamycin was added to the Luria broth to ensure maintenance of the plasmids), and incubated overnight at optimum growth temperatures of 37^{o}C, for the *E. coli* strains, and 28^{o}C, for RU-KM3$_S$. These confluent cultures were used to seed 40ml Luria broth cultures containing no antibiotic. The strains were grown separately at their respective optimum growth temperatures to mid-log phase as determined by their optical densities at $_{OD600.}$ 1ml aliquots of each of the cultures were then combined in an eppendorf tube at a ratio of 1:1:1, 1:5:5, and 1:10:10 of *P. putida* RU-KM3$_S$, *E. coli* (pTnMod-OKm), and *E. coli* (pRK2013) respectively and the cells pelleted by centrifugation (13 000rpm). The pellet was then resuspended in approximately 150µ l Luria broth and the suspension pipetted onto Luria agar plates as a pool. The plates were allowed to dry and then incubated overnight at 28^{o}C. The mated cultures were scraped off the agar plates using a sterile loop and resuspended in 1ml filter sterilized 10% glycerol (in dddH_2O), and plated onto Luria agar plates containing 25µ g/ml chloramphenicol (Boehringer Mannheim), to select against the *E. coli* strains, and 50µ g/ml kanamycin (USB), to select against untransposed RU-KM3$_S$ strains. In order to determine the operational transpositional frequency, six 10-fold serial dilutions of the mated suspension were plated onto Luria broth containing either 25µ g/ml chloramphenicol, or 25µ g/ml chloramphenicol and 50µ g/ml kanamycin, and incubated at 28^{o}C for one to two days to allow colonies to grow to a workable size. All tri-parental matings entering the screening process used an optimal ratio of 1:1:1 of RU-KM3$_S$ (wild type or mutant strain GMP1), *E. coli* (pTnMod-OKm) and *E. coli* (pRK2013) respectively. (Plasposon vectors and helper plasmids were kindly donated by Dr Dennis and Dr Zylstra)

4.2.3 Screening of GMP1 transposon mutants

Transconjugants of RU-KM3$_S$ mutant strain GMP1 were spread plated to single colonies on Luria agar plates containing 50µ g/ml kanamycin and 25µ g/ml chloramphenicol and grown at 28^{o}C for 2 days. Approximately 12 000 transposon mutants were then aseptically transferred into individual wells of sterile 96-well microtitre plates containing 150µ l Luria broth, 50µ g/ml kanamycin, and 25µ g/ml chloramphenicol. The microtitre plates were then incubated at 28^{o}C, gently shaking, for 2 days and the resultant cultures replica plated onto selective media using an 96-pin microtitre plate aseptic replicator or “frog” (Omeg Scientific). Nutrient agar plates containing 0.1% 5-FU were utilized as the selective media whilst growth on nutrient agar plates without 5-FU provided the positive control. Transposon mutants which grew on the control plates but not on the selective medium were assayed for hydantoinase and *N*-carbamoylase activity in microtitre plates (Appendix 2.2). Full-scale biocatalytic assays of hydantoinase and *N*-carbamoylase activities in the subsequently isolated mutants was done as described in Appendix 2.1.

4.2.4 Enrichment and screening of RU-KM3$_S$ transposon mutants

An enrichment for mutants unable to use hydantoin as a nitrogen source was performed by resuspending 38 pools of plasposon mutants, generated by triparental mating with RU-KM3$_S$, and *E. coli* carrying plasmids pRK2013 or pTnMod-OKm, in minimal medium (Appendix 1) with 1% hydantoin as a sole source of nitrogen. The culture was then grown at 28^{o}C, shaking, for 8 hours after which 1mg/ml ampicillin was added followed by incubation at 28^{o}C for a further 16 hours. The cells were harvested by low speed centrifugation (5 000rpm, JA20 rotor in a Beckman centrifuge), washed with 10mM HEPES and the combined pellets were resuspended in 1ml 10% filter-sterilized glycerol (in dddH_2O) before being plated onto minimal medium agar plates (Appendix 1) containing 0.25% $(NH4)2SO_4$ as nitrogen source supplemented with 50µ g/ml kanamycin and 25µ g/ml chloramphenicol.

Screening of transposon mutants of wild type RU-KM3$_S$, after enrichment with hydantoin as a sole source of nitrogen, was done as described for strain GMP1 but with different selective media. Minimal medium (Appendix 1) with either 0.25% $(NH4)2SO4$ or 1% hydantoin as a nitrogen source was used as the positive control and selective medium respectively. Ultrapure agar (USB) was utilized to ensure no nutrient sources other than those supplied in the minimal medium were available to the mutants. Approximately 6 600 mutants surviving the enrichment process were replica plated and isolates unable to hydrolyse hydantoin as a sole source of nitrogen were then patched onto minimal medium with either 1% hydantoin or 0.25% $(NH4)2SO4$ as sole sources of nitrogen in order to verify the phenotype noted. In addition, these strains were also patched onto minimal medium plates with 1% uracil or 1% glycine as sole sources of nitrogen and preliminary microtitre plate assays for hydantoinase and *N*-carbamoylase activity were carried out (Appendix 2.2). Full-scale biocatalytic assays of hydantoinase and *N*-carbamoylase activities in the subsequently isolated mutants were done as described in Appendix 2.

4.3 RESULTS

4.3.1 Chemical mutagenesis of RU-KM3$_S$

Before screening for inducer-independent mutants, the optimal period for which RU-KM3$_S$ cells should be exposed to the chemical mutagen EMS had to be established. Optimal mutagenic conditions are reflected by high mutational frequencies whilst maintaining survival rates of at least 50%. Survival rates were determined by cell counts before and after treatment with EMS whilst mutational frequencies were calculated as the frequency of a single mutation of the gene encoding the β-subunit of the RNA polymerase. These mutations were detected by selecting for acquired resistance of mutant isolates to rifampicin (Rif^R). Rifampicin functions by inhibiting transcription by binding to the β-subunit of the RNA

polymerase, thus changes in one amino acid due to mutation of the RNA polymerase gene results in an inability of rifampicin to bind and inhibit RNA synthesis (Miller 1992). The optimal mutation frequency was observed after 50 minutes treatment with EMS with a survival percentage of 51.5% where Rif^R mutants were generated at a frequency of 2×10^{-4} (Figure 4.2). Screening for inducer-independent mutants was subsequently carried out using this EMS-treatment time interval.

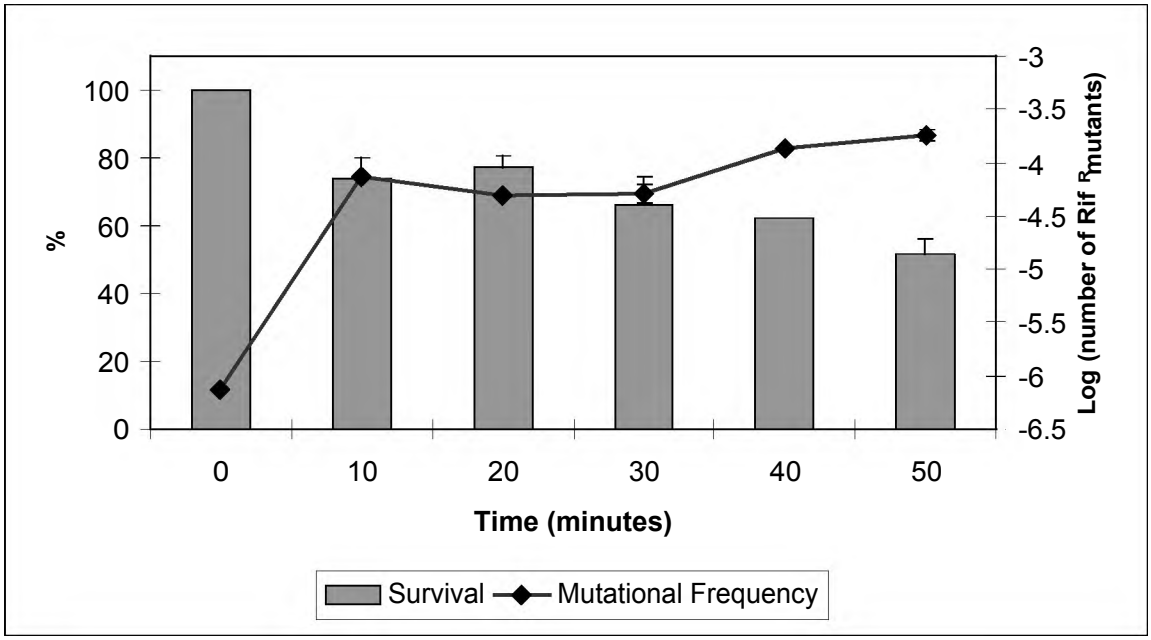

Figure 4.2 Optimisation of EMS mutagenesis treatment of RU-KM3$_S$ cells. (Error bars represent the standard error of the mean)

Mutant strains in which constitutive expression of the hydantoinase gene occurs were selected for using the toxic structural analogue of hydantoin, 5-flourouracil (5-FU) (Hartley *et al.* 1998). An active hydantoinase enzyme is able to cleave the cytotoxic 5-FU at the α-carbon producing the non-toxic 5-fluoroureidopropionic acid. Thus, expression of the hydantoinase gene in the absence of an inducer would result in growth on agar plates containing 5-FU whilst strains requiring induction for expression would be unable to grow. Mutants were grown in complete medium as well as minimal medium with ammonium sulphate as the sole nitrogen source. Several mutants were isolated with resistance to 5-FU in the absence of inducer in the growth medium (Figure 4.3), all of which exhibited equivalent phenotypes with respect to hydantoin-hydrolysing activity levels. Of these mutants, GMP1, isolated from complete medium, and GMP2, isolated from defined medium, were selected as representatives for further analysis. The ability of uninduced GMP1 and GMP2 isolates to grow in the presence of 5-FU, unlike the wild type, implied that the hydantoinase activity of these strains was no longer dependent on the presence of hydantoin in the growth medium

(Figure 4.3). A brown compound was secreted into the medium by GMP1 at stationary phase of growth in complete medium which was not observed with GMP2 (Figure 4.3). The isolation of a 5-FU-sensitive mutant producing the same brown pigment as GMP1 suggested that the production of the pigment was not directly related to the expression of hydantoinase activity in RU-KM3$_S$ cells and this phenotype was not pursued any further.

Figure 4.3 Phenotypes of RU-KM3$_S$ wild type (WT) and corresponding chemically induced mutant strains GMP1 and GMP2 on nutrient agar plates supplemented with and without 0.005% 5-FU, in the presence and absence of hydantoin as inducer.

Resting cell biocatalytic assays for hydantoinase and *N*-carbamoylase activities in mutant strains GMP1 and GMP2 relative to wild type activity levels were done with induced and uninduced cultures in order to determine if the mutant strains required induction for expression of the hydantoinase and *N*-carbamoylase genes. In addition to hydantoin and D-methylhydantoin, dihydrouracil was also supplied as a substrate as several hydantoinase enzymes reported in literature are capable of hydrolysing this substrate (Chapter 1, Section 1.2.2.1).

With respect to hydantoinase activity, uninduced GMP1 and GMP2 cells exhibited elevated levels of activity in comparison to that of the wild type strain under the same conditions with a four-fold increase in *N*-carbamylglycine production from hydantoin substrate (3.22μ mol/ml vs. 12.83μ mol/ml and 11.93μ mol/ml for GMP1 and GMP2 respectively, Figure 4.4, panel A). However, the uninduced hydantoinase activities of GMP1 and GMP2 did not reach levels equivalent to that of the induced wild type. In addition, the hydrolysis of hydantoin by the mutant strains increased when cultured with, as opposed to without, inducer (Figure 4.4, panel A). When considering hydrolysis of hydantoin, dihydrouracil, and D-methylhydantoin by cells cultured under uninduced conditions, RU-KM3$_S$ wild type strain hydrolyses these substrates at efficiency levels 25%, 42%, and 63% that of the mutants strains for each of the substrates respectively (Figure 4.4, panel A).

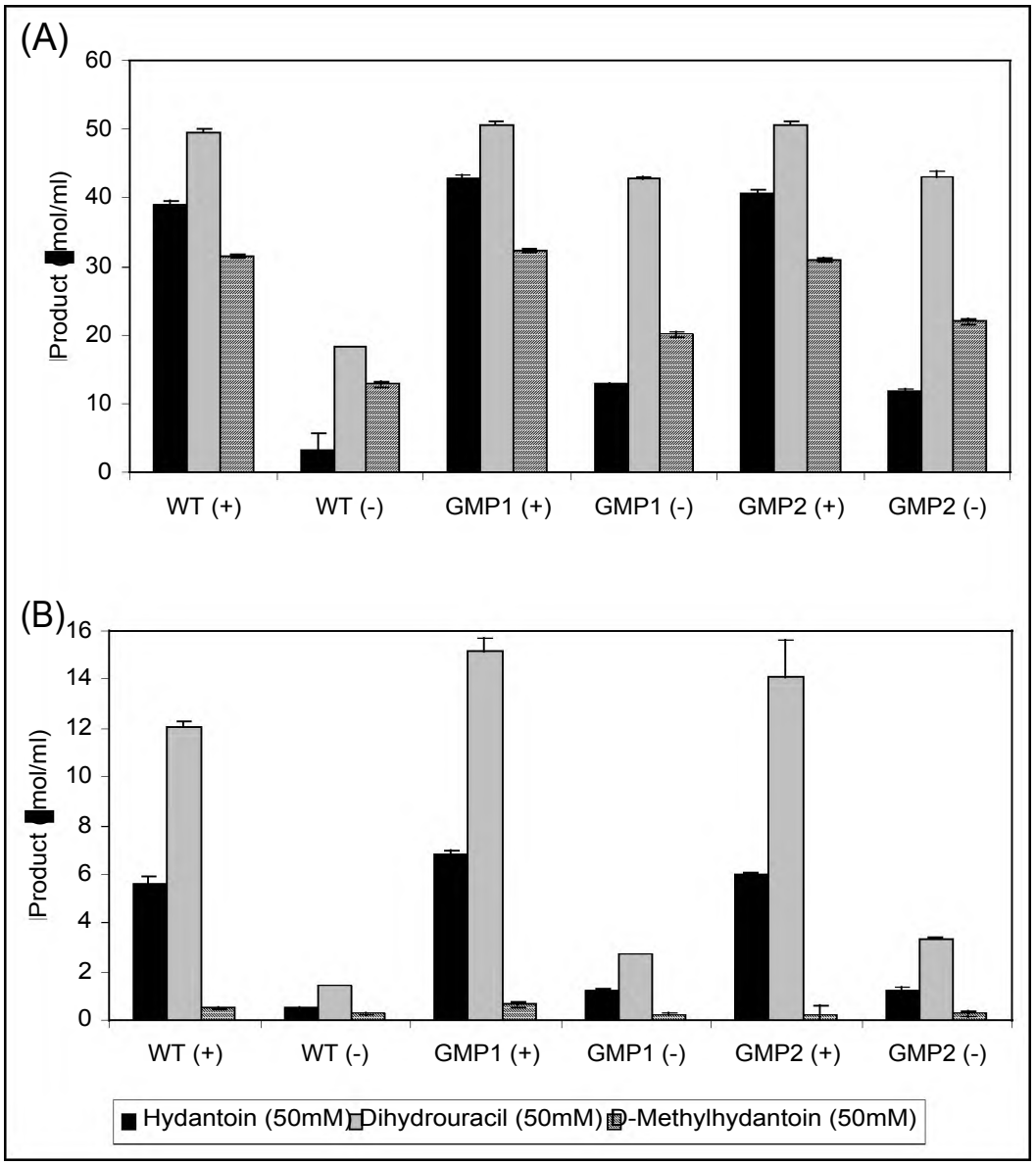

Figure 4.4 Hydantoinase and *N*-carbamoylase activities, of induced and uninduced resting cells, of wild type RU-KM3$_S$ and mutant strains GMP1 and GMP2. [Panel A: Hydantoinase activity, Panel B: *N*-carbamoylase activity, (+): induced, (-): uninduced, WT: wild type. Whole cell biocatalytic reactions were done with 50mM hydantoin, dihydrouracil, or D-methylhydantoin as substrates. (Error bars represent the standard error of the mean, n=3)].

The *N*-carbamoylase in the wild type and mutant strains exhibited similar trends in activity levels with negligible production of amino acids by uninduced cultures (Figure 4.4, panel B). The low levels of D-alanine production in induced cells (an average of 0.46μ mol/ml D-alanine produced vs. an average of 6.13μ mol/ml glycine and 13.75μ mol/ml β-alanine produced) was expected as the *N*-carbamoylase of RU-KM3$_S$ is L-enantioselective (Figure 4.4, panel B). Subsequent to induction during growth, slight increases in *N*-carbamoylase activity were observed for GMP1 and GMP2 in comparison to the wild type strain (Figure 4.4, panel B).

4.3.2 Optimisation of RU-KM3$_S$ transposon mutagenesis

Insertional mutation by transposons required that the target chromosome be accessible to the transposable element which, in this study, was the plasposon pTnMod-OKm. This could be achieved by electroporation or via conjugal transfer of the plasposon into the target organism. Electroporation of DNA into RU-KM3$_S$ was tested but was found to be very inefficient (data not shown) necessitating the development of a conjugal mating system optimised for RU-KM3$_S$ cells. Plasposons, whilst encoding an *oriT* site, do not encode the *tra* genes needed for pilus formation and plasmid mobilization which must therefore be supplied by an alternate source. Some *E. coli* strains, such S17-1, encode these proteins on their chromosomes. However, attempts to utilize *E. coli* strain S17-1 harbouring pTnMod-OTc in bi-parental matings with strain RU-KM3$_S$ were unsuccessful. Consequently, tri-parental mating with an *E. coli* strain containing a helper plasmid, such as pRK2013, encoding the proteins required for conjugal transfer to occur was investigated. Tri-parental mating with *P. putida* RU-KM3$_S$, pTnMod-OKm in *E. coli* strain DH5α, and pRK2013 in *E. coli* strain HB101 was successful and is reflected by the operational transposition frequencies.

The operational transposition frequency, calculated as the ratio of exconjugants with non-lethal insertions to the total number of recipient cells, was optimised by varying the ratios of RU-KM3$_S$ to *E. coli* cells containing pTnMod-OKm, and pRK2013. The highest operational transposition frequency was obtained with the ratio of 1:1:1 (RU-KM3$_S$:pTnMod-OKm:pRK2013) (Table 4.1) which was applied to all subsequent tri-parental mating procedures.

Table 4.1 Optimisation of the operational transposition frequencies by varying the ratio of RU-KM3$_S$ cells to *E. coli* cells containing pTnMod-OKm and pRK2013.

Ratio			Frequency
RU-KM3$_S$	***E. coli* (pTnMod-OKm)**	***E. coli* (pRK2013)**	
1	1	1	4.8×10^{-5}
1	5	5	1.6×10^{-4}
1	10	10	1.98×10^{-4}

4.3.3 Isolation of 5-FU sensitive insertional mutants of GMP1

Mutant strain GMP1, isolated by chemical mutagenesis using EMS, was utilized as the parental strain due to the high levels of dihydrouracil hydrolysis as well as increased levels of hydantoinase activity exhibited by this strain in uninduced cultures resulting in resistance to the toxic effect of 5-FU. Consequently, insertional mutant strains of GMP1 with sensitivity to

5-FU suggest that insertion of the plasposon DNA has interrupted either the hydantoinase enzyme or the control thereof.

Two tri-parental matings with strain GMP1, pTnMod-OKm in *E. coli* DH5α, and pRK2013 in *E. coli* HB101 were carried out with operational transpositional frequencies of 1.87×10^{-5} and 2.7×10^{-5}, respectively. Approximately 12 000 mutant strains from these tri-parental matings were inoculated into 96-well microtitre plates containing Luria broth. Once grown to confluence, the mutant strains were replica plated onto Luria agar plates supplemented with (selection medium) and without (control) 0.1% 5-FU. Mutants which exhibited reduced or no growth in the presence of 0.1% 5-FU were assayed for hydantoinase and *N*-carbamoylase activity in microtitre plates. Of these, mutant strain GMP5 was found to have reduced levels of hydantoin and dihydrouracil hydrolysis.

Initial full-scale resting cell biocatalytic assay of this mutant along with the parental strain GMP1 and wild type strain of RU-KM3$_S$ showed that hydrolysis of dihydrouracil occurred rapidly in the wild type and that the substrate quickly became a limiting factor in the production of the intermediate, β-ureidopropionate. Thus in order to provide an accurate reflection of the hydrolysis of dihydrouracil, the production of catalytic products was determined after 1 and 2 hours incubation at 40^{o}C as well as the standard 3 hours.

A significant reduction in the hydantoinase activity of mutant strain GMP5, particularly with regard to hydrolysis of hydantoin (33.91μ mol/ml vs. 49.53μ mol/ml), when compared to that of the parental strain GMP1 was observed (Figure 4.5, panel A). In addition, the reduction in activity noted in uninduced cultures of GMP5 was not equivalent to, but rather much lower, than that of uninduced wild type strain of RU-KM3$_S$ (Figure 4.5, panel A). This suggests that the mutation in GMP5 is probably not an inactivation or nullification of the chemical mutation in GMP1 which resulted in increased levels of activity. The reduction in *N*-carbamoylase activity was even more pronounced than the hydantoinase activity levels with almost total loss of production of glycine or alanine (0.58μ mol/ml glycine and 0.35μ mol/ml β-alanine vs. 9.53μ mol/ml and 15.81μ mol/ml glycine and β-alanine production in GMP1, Figure 4.5, panel B). The presence, albeit reduced, of hydantoinase and *N*-carbamoylase activity in GMP5 indicated that the genes responsible for hydrolysis of hydantoin and dihydrouracil have not been directly inactivated and that the insertional mutation in this strain is most likely in a regulatory pathway affecting the expression or activity of these enzymes.

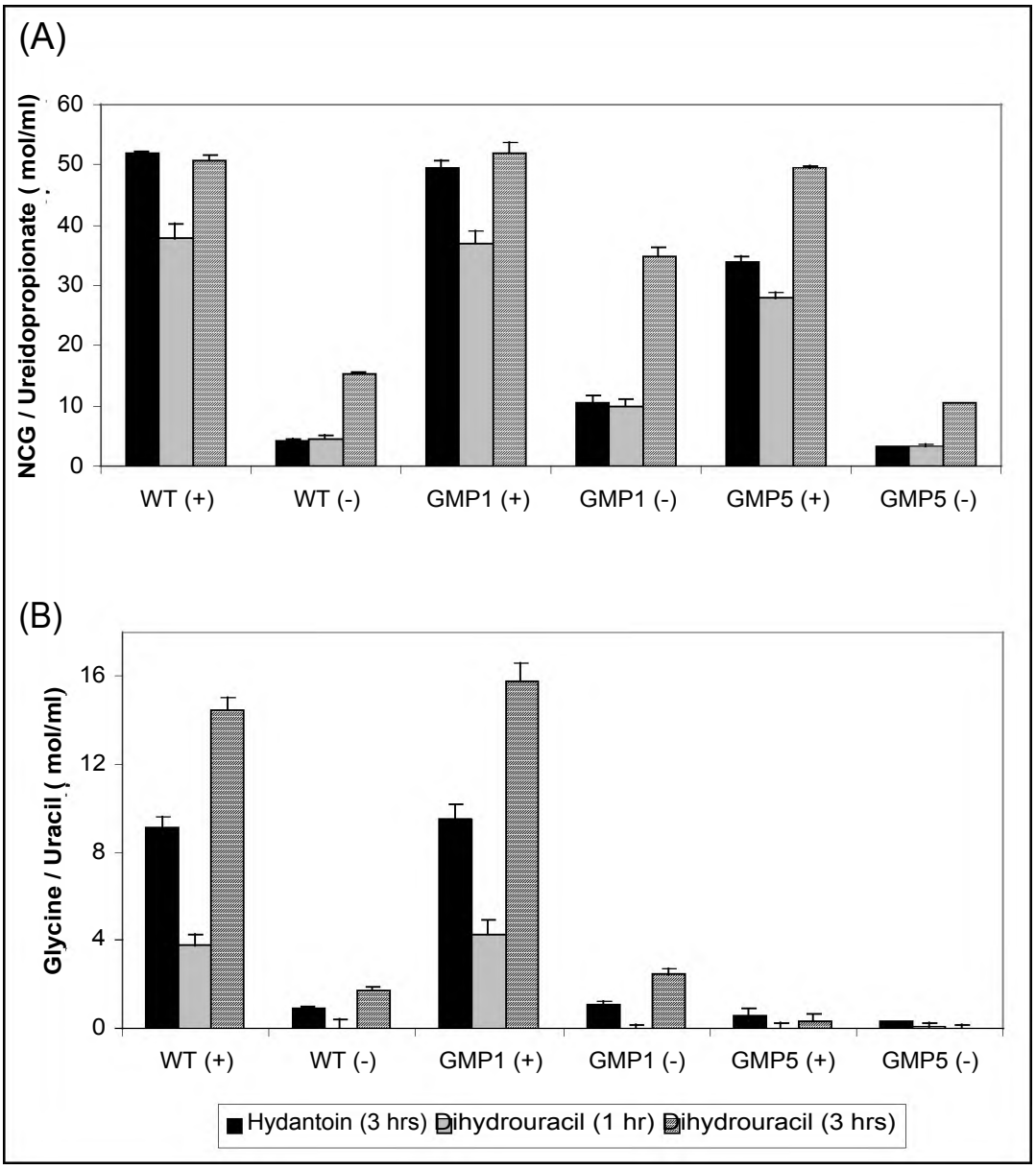

Figure 4.5 Hydantoinase and *N*-carbamoylase activities in wild type RU-KM3$_S$, parental strain GMP1, and insertional mutant GMP5. [Panel A: Hydantoinase activity, Panel B: *N*-carbamoylase activity. Whole cell biocatalytic reactions were carried out with 50mM hydantoin for 3 hours or 50mM dihydrouracil for 1, 2, and 3 hours at 40 °C. Strains were cultured in nutrient broth with (+) and without (-) 0.1% hydantoin as an inducer. (Error bars represent the standard error of the mean, n=3)]

4.3.4 Screening and phenotypic analysis of transposon mutants of wild type RU-KM3$_S$

In order to generate a sufficient number of mutants such that a comprehensive library of mutants carrying random insertional mutations could be obtained, the tri-parental mating procedure was scaled up to 40ml of each culture type rather than 1ml. The enrichment procedure utilized in this study was based on that used by Janssen *et al.* (1981) for the

isolation of glutamine-requiring mutants and modified to select for hydantoinase and/or *N*-carbamoylase minus mutants of RU-KM3$_S$ as described in the methods and materials.

The bactericidal effect of ampicillin provides the basis on which the enrichment procedure was developed. Ampicillin is a β-lactam antibiotic which severely inhibits bacterial cell wall synthesis by inhibiting the transpeptidase enzyme responsible for cross-linkage of the glycan-linked peptide chains essential for the formation of a strong cell wall in bacteria (Madigan *et al.* 1984). In the absence of the transpeptidase activity, the cell wall continues to be formed but gets progressively weaker until cell lysis occurs. If the cells are dormant, however, no cell growth occurs thus no weak cell wall is synthesized and no cell lysis occurs (Snyder and Champress 2003).

Enrichment of plasposon generated mutants in minimal medium with hydantoin as a sole source of nitrogen therefore selected for those mutants which are unable to utilize hydantoin as a source of nitrogen. Thus mutant strains encoding an inactivated hydantoinase and/or *N*-carbamoylase gene were unable to grow and consequently survived treatment with ampicillin, whilst the remaining mutants actively divided and eventually lysed due to weak cell wall formation. In addition to hydantoinase and *N*-carbamoylase minus mutants, auxotrophic mutants unable to grow in minimal medium, irrespective of the nitrogen source supplied, also survived the enrichment. In order to eliminate these from the screening process, the mutant strains surviving enrichment were plated onto minimal medium with ammonium sulphate as a nitrogen source.

A large scale tri-parental mating with RU-KM3$_S$, pTnMod-OKm in *E. coli* DH5α, and pRK2013 in *E. coli* HB101 was carried out and an operational transposon frequency of 7.1×10^{-6} achieved. Approximately 107 000 insertional mutants entered the enrichment process of which approximately 7 000 survived indicating a survival rate of 6.5%. Not all insertional mutants could be entered into the subsequent screening process as colonies which overlapped one another could not be individually processed. Thus 6 624 mutants were inoculated into 96-well microtitre plates and grown to confluence in Luria broth containing chloramphenicol (resistance conferred by RU-KM3$_S$) and kanamycin (resistance conferred by inserted plasposon sequence). These isolated mutants were replica plated onto minimal medium with hydantoin (HMM) or ammonium sulphate (AMM) as sole sources of nitrogen to ensure that only mutants which grew well on ammonium sulphate, and are therefore not auxotrophic for nutrients other than hydantoin, were analysed further. A total of 144 mutants were isolated that were able to hydrolyse ammonium sulphate (*amm*$^+$) but not hydantoin (*hyd*$^-$) as nitrogen sources.

Hydantoin is hydrolysed to *N*-carbamoylglycine and glycine by the hydantoinase and *N*-carbamoylase enzymes respectively. Thus the inability to grow on HMM can be attributed to either direct or indirect inactivation of the hydantoinase and/or *N*-carbamoylase enzymes or an inability to utilize glycine as a nitrogen source. Furthermore, hydantoinase enzymes are often associated with hydrolysis of pyrimidines (Syldatk *et al.* 1999), the end product of which is uracil. Thus mutant strains unable to grow on HMM were scored for growth on minimal medium with glycine (GMM) or uracil (UMM) as sole sources of nitrogen. In addition, the hydantoin-hydrolysing activity of these mutants was evaluated using the modified microtitre plate assay with hydantoin as a substrate. The 144 mutant strains previously isolated as auxotrophic for hydantoin could thus be subdivided into 3 groupings (Table 4.2) based on their growth with hydantoin, ammonium sulphate, uracil, or glycine as sole nitrogen sources and the hydrolysis of hydantoin as determined by microtitre plate assays.

Table 4.2 Insertional mutants of RU-KM3$_S$ auxotrophic with respect to hydantoin, grouped phenotypically based on the ability to utilize various sources of nitrogen, as well as the presence or absence of hydantoinase and *N*-carbamoylase activity.

Group	Number of mutants	Representative isolates	Nitrogen utilization				Enzyme activity	
			amm	*hyd*	*gly*	*ura*	HYDN	NCAAH
WT	——	-	+	—■—	—■—	—■—	—■—	—■—
A	122	GMP6	+	-	+	-	+	+
		GMP7						
		GMP9						
		GMP10						
		GMP15						
		GMP21						
B	14	GMP8	+	-	-	±	+ / nd*	+ / nd*
C	8	GMP3	+	-	+	± / -	+	-
		GMP4						
		GMP16						
		GMP17						
		GMP18						
		GMP19						
		GMP20						

(*amm, hyd, gly, ura*: minimal medium with 0.25% ammonium sulphate, 1% hydantoin, 1% glycine, or 1% uracil respectively as sole sources of nitrogen; WT : wild type RU-KM3$_S$; HYDN: Hydantoinase; NCAAH: *N*-carbamoylase; nd* : The majority of mutants in phenotype group B exhibited retarded growth rates and could therefore not be comparatively assayed)

The majority of the mutants unable to use hydantoin as a sole nitrogen source (122 out of 144) were also unable to grow on uracil but showed hydantoinase and *N*-carbamoylase activities in microtitre plates (Table 4.2, Group A). By comparison, mutants in phenotypic Group B were unable to efficiently utilize uracil, hydantoin or glycine as nitrogen sources (Table 4.2). In addition, poor growth was observed for several of the mutants in Group B suggesting that the mutation carried by these strains is detrimental. Inability to utilize hydantoin as a nitrogen source and poor growth on uracil by mutants in Group C was observed (Table 4.2). However, what differentiates these mutants from those in Group A was the absence of *N*-carbamoylase activity as determined by microtitre plate assay (Table 4.2). As microtitre plate assays are not quantitatively accurate and do not reflect variations in the levels of enzyme activities, full-scale assays of mutants from Group A and C, under optimised conditions to accurately determine activity levels were done.

Resting biocatalytic assays of the mutants in Group C revealed a consistent deficiency in *N*-carbamoylase activities throughout. The activity levels of two representatives of this group, GMP3 and GMP4 are illustrated in Figure 4.6 in which a complete absence of *N*-carbamoylglycine hydrolysing activity (0.01µ mol/ml and 0.97µ mol/ml vs. 8.67µ mol/ml for the wild type, Figure 4.6) was observed. The hydantoinase activity by comparison was equivalent to that of the wild type in all mutants in this grouping.

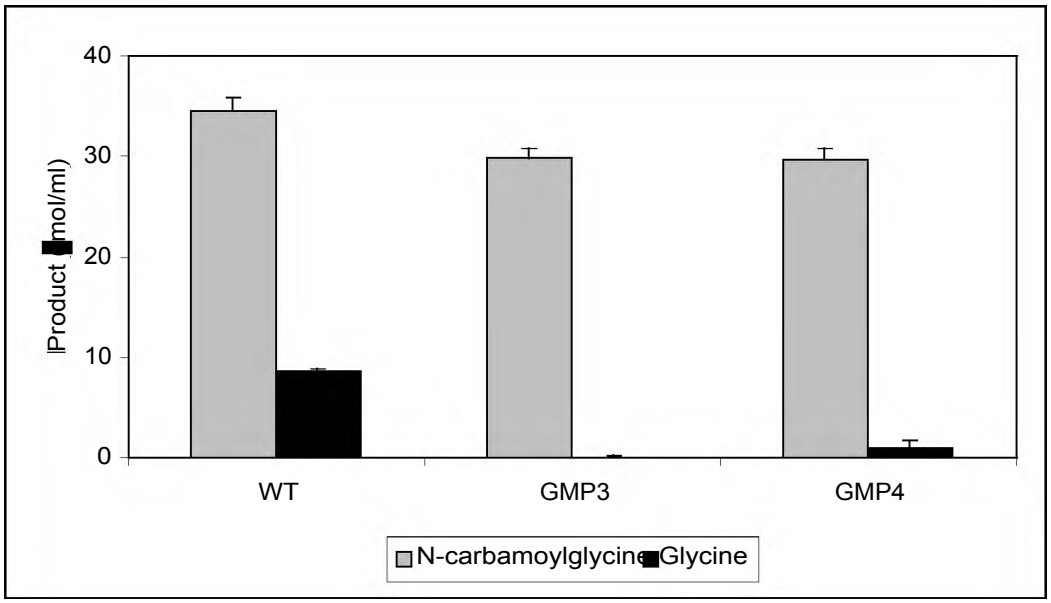

Figure 4.6 Hydantoin-hydrolysing activity of wild type RU-KM3$_S$ and mutant strains GMP3 and GMP4 (from phenotype grouping C). (WT: wild type, Error bars represent the standard error of the mean, n=3)

Full-scale assays of mutant strains GMP6, GMP7, GMP9, and GMP21 selected as representatives of Group A, with a *hyu* $^-$, *gly* $^+$, and *ura* $^-$ phenotype, were done. The hydantoinase and *N*-carbamoylase activities of these mutants were uniformly comparable to that of the wild type (Figure 4.7) suggesting that the inability to use hydantoin as a sole source of nitrogen was due to inactivation of a gene involved in nitrogen metabolism as the enzymes responsible for hydantoin-hydrolysis, viz. hydantoinase and *N*-carbamoylase, were functional (Figure 4.7).

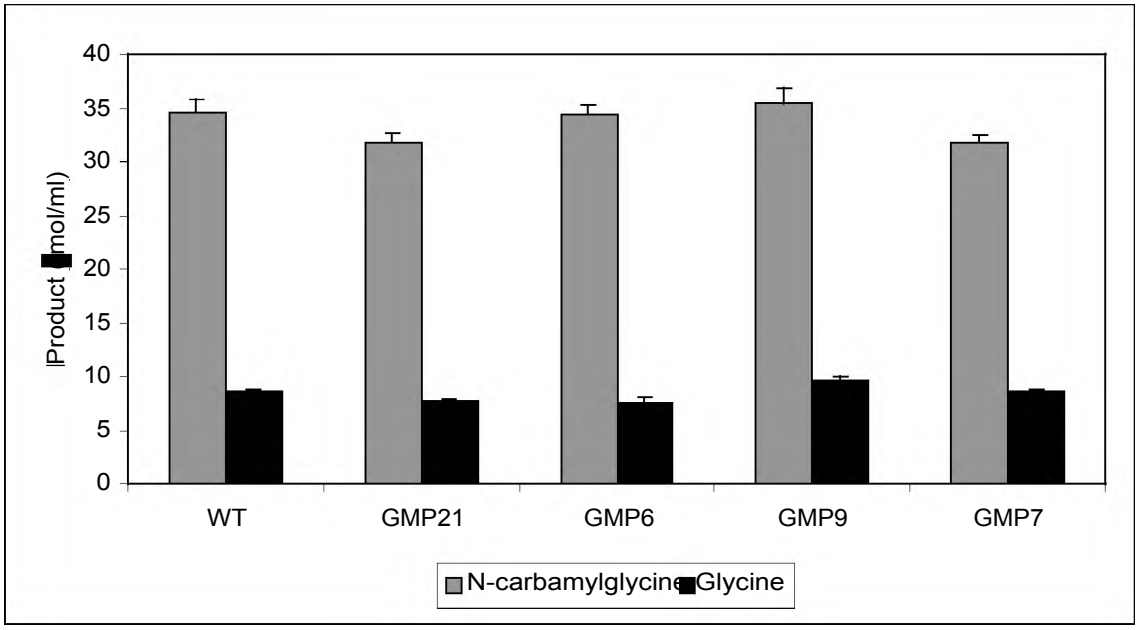

Figure 4.7 Hydantoin-hydrolysing activity of wild type RU-KM3$_S$ and mutant strains GMP6, GMP7 and GMP21 (from phenotype grouping A). [Strains were cultured in nutrient broth containing 0.1% hydantoin as an inducer. (Error bars represent the standard error of the mean, n=3)]

4.4 DISCUSSION

The main objectives of this chapter were two-fold: a) isolation of mutants with constitutive hydantoin-hydrolysing activities and, b) isolation of mutants with loss of hydantoinase and/or *N*-carbamoylase activity due to insertional inactivation by the plasposon pTnMod-OKm so that the genes encoding the enzymes involved in hydantoin-hydrolysis in RU-KM3$_S$ could be identified.

4.4.1 Chemically induced mutants

Mutant strains of RU-KM3$_S$, GMP1 and GMP2, were isolated by screening EMS-treated cells using 5-FU as previously described. However, unlike *A. tumefaciens* RU-ORL5 in which expression of the hydantoinase is constitutive (Hartley *et al*. 1998), the hydantoinase activities in GMP1 and GMP2, whilst elevated in uninduced cells to allow for growth in the

presence of 5-FU, were not equivalent to wild type induced activity levels. In addition to this, an increase in hydantoin-hydrolysis from uninduced to induced cells of GMP1 and GMP2 was also observed.

In addition to the elevated but still inducible hydantoinase activity in GMP1 and GMP2, the discrepancy between the conversion of dihydrouracil and D-methylhydantoin versus hydantoin raised the possibility of the presence of a second hydantoinase in RU-KM3$_S$ cells whose activity was not affected by the mutation in strain GMP1 and GMP2. The point mutation generated by EMS may therefore have been in the promoter region of one of the potential hydantoinase genes resulting in constitutive expression of one of the hydantoinases whilst the remaining enzyme is inducible. Alternatively, the mutation may have occurred in the gene itself such that increased levels of hydrolysing activity of one of the hydantoinases resulted. The presence of two hydantoinases within a single bacterium has been reported for *Agrobacterium* sp. IP I-671 (Hils *et al.* 2001). A third possibility is that the mutation has occurred in a regulatory pathway which exerts repression with variable effects on hydrolysis of different substrates. The latter is more likely as evidenced by the brown pigment produced by GMP1 as regulatory pathways in bacteria often function on a global cellular scale thus modification of a single pathway may have a pleiotrophic effect.

4.4.2 Transposon-generated mutants

With respect to transposon generated mutants, the utilization of an enrichment procedure proved to be successful. Where traditional direct screening was utilized, such as that used for mutant strains of GMP1, over 12 000 plasposon-generated mutants had to be screened in order to yield a single mutant strain (GMP5) of interest. In contrast, by processing mutant strains through an enrichment step before entering the screening procedure, the number of mutants exhibiting the desired phenotype (i.e. *hyd* $^-$) was significantly increased (144 vs. 1) whilst the number of mutants screened by replica plating was almost halved (6,600 vs. 12,000).

As identification of the genes encoding the hydantoin-hydrolysing enzymes in RU-KM3$_S$ by complementation studies with a genomic library (Chapter 3) was unsuccessful, plasposons were used as an alternative approach. Screening plasposon-generated mutants in which the genes encoding the hydantoin-hydrolysing enzymes were inactivated was done based on an inability to utilize hydantoin as a sole source of nitrogen. The plasposon-generated mutant strains thus isolated could be subdivided, based on phenotypic characteristics, into three groupings.

The inability of Group A mutant strains to utilize hydantoin as a sole nitrogen source cannot be attributed to inactive hydantoinase or *N*-carbamoylase enzymes as biocatalytic assays of these mutants showed hydrolytic activities equivalent to that of the wild type strain. Similarly, an inactivation/blockage of the transport of hydantoin into the cells, which may have resulted in a *hyd* $^-$ phenotype, can also be ruled out as the biocatalytic assays were done with intact resting cells. The positive growth score with glycine minimal medium by mutant strains of this grouping furthermore eliminates the possibility of the *hyd* $^-$ phenotype being due to an inability to utilize the end-product of hydantoin hydrolysis as a nitrogen source. The absence of growth on uracil minimal medium plates (*ura* $^-$) suggest insertional mutations affecting pyrimidine catabolism or the utilization of the end product of uracil degradation, β-alanine (Michal 1999). As the hydantoinase and *N*-carbamoylase enzymes of RU-KM3$_S$ are able to hydrolyse pyrimidines (i.e. dihydrouracil), the *ura* $^-$ phenotype observed is most likely due to an failure to utilize alanine as a sole source of nitrogen.

Operons encoding genes responsible for utilizing specific amino acids as nitrogen sources are not only regulated by individual induction pathways, but are often part of larger regulatory mechanisms. Ntr regulation in particular, where expression of certain genes are repressed in the presence of a more suitable nitrogen source such as NH_3, affects expression of many such operons (Snyder and Champness 2003). Thus a mutation in the Ntr regulatory pathway would disrupt utilization of poorer nitrogen sources. This may provide an explanation for the large number of mutants in phenotype Group A, which were found to be hydantoin auxotrophs but do not have altered enzyme activities.

Resting cell biocatalytic assays of mutant strains belonging to phenotypic Group C indicated a complete lack of *N*-carbamoylase activity within these mutants. The majority of hydantoin-hydrolysing enzymes systems investigated to date contain a single enzyme responsible for the conversion of *N*-carbamylglycine to glycine, with a few notable exceptions where two *N*-carbamoylase enzymes have been isolated from a particular strain (Yamanaka *et al.* 1997, Yokozeki *et al.* 1987c). The loss of *N*-carbamoylase activity by a single insertional event in mutant strains in Group C suggests that only one *N*-carbamoylase enzyme is present in *P. putida* strain RU-KM3$_S$. The lack of *N*-carbamoylase activity would explain the absence of growth on hydantoin minimal medium and possibly the poor growth on uracil (if hydantoin-hydrolysis in RU-KM3$_S$ cells is synonymous with pyrimidine degradation).

The majority of the insertional mutants in the phenotypic Group B exhibited retarded growth rates in complete medium indicating a detrimental though sub-lethal mutation. Thus their inability to grow under nitrogen-limiting conditions was not surprising. The few mutant strains with normal growth rates in complete medium, while displaying hydantoinase and *N*-

carbamoylase activity and growth in the presence of good nitrogen sources such as ammonium sulphate, were unable to utilize poorer nitrogen sources suggesting the presence of a mutation in the regulation of nitrogen assimilation by the cells under conditions of nitrogen limitation.

No loss of hydantoinase activity due to insertional inactivation of the relevant genes was observed for any of the mutants described above. Acquired sensitivity to 5-FU by transposon-generated mutants with 5-FU resistant GMP1 as the parental strain, provided an alternative approach to isolation of hydantoinase-inactivated mutants. Whilst a mutant in which an absence of hydantoinase activity was observed was not isolated, mutant strain GMP5 was isolated with significantly reduced levels of both hydantoinase and *N*-carbamoylase enzyme activities. The reduction in both the hydantoinase and *N*-carbamoylase enzyme activities in mutant strain GMP5 is most likely due to a mutation in a regulatory mechanism responsible for the control of expression or activity of both these genes. However, the mutation in GMP5 was probably not a repressor of the original mutation in GMP1 as reversion from GMP1 to wild type RU-KM3$_S$ uniniduced activity levels was not achieved.

In conclusion, mutant strains GMP1 and GMP2 were isolated and shown to have elevated, but not constitutive, levels of hydantoin-hydrolysing activities. As discussed above, this may be due to the presence of two hydantoinase enzymes or as a result of a mutation in a regulatory pathway affecting hydantoin-hydrolysis in RU-KM3$_S$. Inactivation of the hydantoinase gene, once isolated, followed by biocatalytic assay to determine if any residual hydantoin-hydrolysing activity remained would indicate if two hydantoinases are indeed present in RU-KM3$_S$ or not. This is addressed in Chapter 5.

The loss of *N*-carbamoylase activity in mutant isolates from phenotype Group C suggested that the gene interrupted may be that encoding for the *N*-carbamoylase enzyme itself. Group A mutants on the other hand showed wild-type levels of hydantoin-hydrolysing activity but were unable to grow on a poor nitrogen source. This implied that a regulatory pathway involved in nitrogen metabolism but which does not affect expression of the hydantoinase and *N*-carbamoylase genes was interrupted in these mutants. By contrast, the gene inactivated in mutant strain GMP5 resulted in decreased, but not complete loss, of both enzyme activities indicating that a regulatory pathway which regulates expression of the hydantoinase and *N*-carbamoylase genes was affected. Identification of the genes inactivated by transposon insertion, resulting in the phenotypes discussed above, would provide greater insight into the enzymes responsible for hydantoin-hydrolysis in RU-KM3$_S$ and the control thereof and is addressed in the following chapter.

5.1 INTRODUCTION

In order to be competitive, bacteria employ complex regulatory mechanisms to control gene expression to ensure that energy expensive production of catabolic enzymes occurs only in the presence of the corresponding catabolite and absence of a more readily metabolizable nutrient source. For maximum efficiency, many of these regulatory mechanisms function at the level of transcription by elevating/inhibiting promoter activity. These mechanisms include induction and feedback inhibition, as well as global regulatory pathways that reflect the metabolic and energy status of the cell resulting in silencing of energetically less favourable catabolic pathways (Sanchez and Demain 2002).

P. putida strain RU-KM3$_S$ was originally selected for based on the ability to utilize hydantoin as a sole source of nitrogen in defined medium (Chapter 1, Section 1.7). As hydantoin is catabolized in order to supply the nitrogen demand of the cells in defined medium, the hydantoin-hydrolysing enzymes may well be controlled by the global nitrogen regulatory system (Ntr) which is responsible for the coordinated expression of catabolic pathways involved in nitrogen metabolism (Merrick and Edwards 1995, Hartley *et al.* 2001). Support for this hypothesis includes the identification of putative σ^{54}-dependent promoter regions located upstream of the genes encoding the hydantoin-hydrolysing enzymes in *Arthrobacter aurescens* DSM 3747, *Bacillus agri* NCHU1002, and *Pseudomonas* sp. NS671, as well as mutational analysis of the regulation of the hydantoin-hydrolysing enzyme system of *Agrobacterium tumefaciens* RU-OR in which Ntr is implicated (Watabe *et al*. 1992a, Kao and Hsu 2003, Wiese *et al*. 2001, Hartley *et al*. 2001).

Regulation of gene expression in response to the nitrogen status of the cell has been extensively characterized in enteric bacteria (Reitzer 2003). In this system, the Ntr system regulates gene expression at the level of transcription by interaction of the RNA polymerase containing the sigma factor σ^{54} and the NtrC protein. In its phosphorylated form, NtrC acts as a transcriptional activator of σ^{54}-dependent promoters. The phophorylation state of the NtrC is in turn regulated by the bifunctional NtrB which can either phosphorylate or dephosphorylate NtrC (Figure 5.1). The negative/positive phophorylation activity of NtrB is dependent on the state of the regulatory protein $_{PII}$ which occurs in an uridylylated or deuridylylated form catalysed by the UTase/UR (uridylyltransferase/uridylyl-removing) enzyme. The ratio of glutamine to α-ketoglutarate reflects the nitrogen status of the cell. Thus stimulation of UR by glutamine or UTase by α-ketoglutarate, affecting the uridylylation status of $_{PII}$ and subsequent cascade reactions, result in transcriptional repression and activation of the σ^{54}-dependent catabolic enzymes respectively (Merrick and Edwards 1995, Eberl *et al*. 2000).

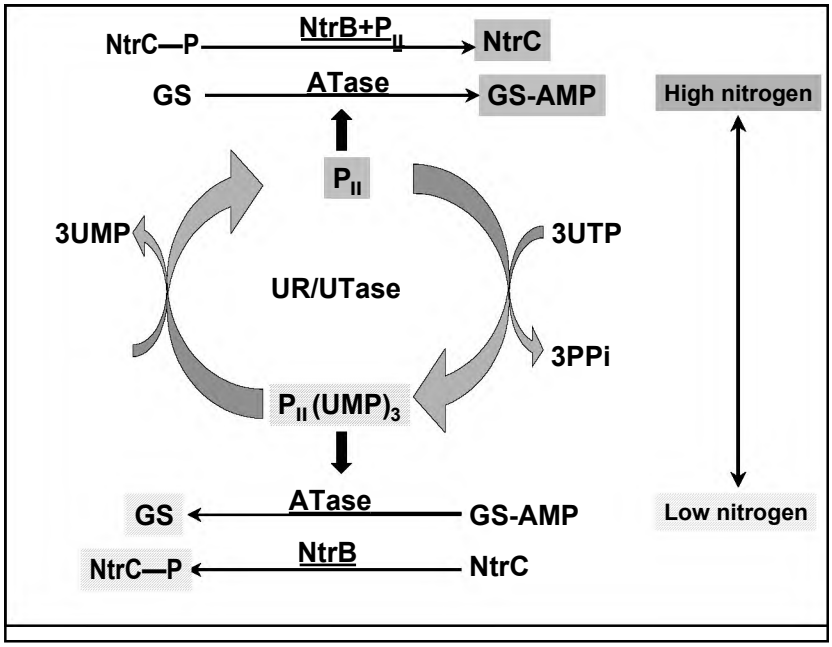

Figure 5.1 Schematic summary of the Ntr regulatory system in response to the nitrogen status of the cell. [UR/UTase: uridylyltransferase/uridyl-removing enzyme, GS: Glutamine synthase, UMP: uridyl-monophosphate, AMP: adenosine-monophosphate, ATase: adenyltransferase, P: phosphate (adapted from Merrick and Edwards 1995).]

In contrast to enteric bacteria, the regulation of gene expression by nitrogen catabolite repression in *Pseudomonas* has not been well characterized. However, the Ntr regulatory system has been found to be surprisingly similar in gram-negative bacteria, including *Escherichia*, *Klebsiella*, *Salmonella,* and *Rhizobium* (Synder and Champress 2003). Furthermore, the regulation of the synthesis and inactivation of glutamine synthase (GS) in *P. aeruginosa* has been shown to be very similar to *E. coli* (Janssen *et al*. 1980). In addition, glutamine levels have been shown to be involved in the expression of allantoinase, which belongs to the same EC grouping as hydantoinase, in *Pseudomonas aeruginosa* by the generation of GS$^-$ mutants in which repression of allantoinase expression is relieved (Janssen and Van der Drift 1983).

Some hydantoin-hydrolysing enzyme systems, however, appear to be sensitive to carbon, as opposed to nitrogen, catabolite repression. Specifically, the hydantoinase and/or *N*-carbamoylase enzyme activities in *Flavobacterium*, *Bacillus brevis*, *Arthrobacter* sp., and *Pseudomonas* have been shown to vary depending on the carbon source supplied (Nishida *et al*. 1987, Yamashiro *et al*. 1988, Syldatk *et al*. 1990a, Sudge *et al*. 1998).

The mechanism of carbon catabolite repression (CCR) has been extensively characterized in the gram-negative enteric bacterium *E. coli* and the gram-positive *Bacillus subtilis* (Warner and Lolkema 2003). CCR involves components of the phosphoenolpyruvate-dependent transport system (PEP-PTS) which is responsible for the transport of glucose across the

membrane and drives the sequential transfer of phosphate from PEP to EI to HPr then EIIA^{glc} and ultimately glucose (Figure 5.2, panel A) (Warner and Lolkema 2003). In *E. coli* CCR is regulated by controlling the cellular cyclic AMP (cAMP) concentrations via adenylate cyclase activity which in turn is affected by the phosphorylation state of EIIA^{glc} (Collier *et al*. 1996). Thus in high concentrations of glucose, which is the preferred carbon source in *E. coli*, EIIA^{glc} is unphosphorylated due to PEP-PTS which in turn lowers the adenylate cyclase activity resulting in reduced production of cAMP from ATP (Collier *et al*. 1996) (Figure 5.2, panel A). In the absence of glucose, EIIA^{glc} remains phosphorylated and stimulates the adenylate cyclase to produce cAMP from ATP (Figure 5.2, panel B). The cAMP produced then interacts with a cAMP receptor protein (CRP) and the resultant complex binds to the promoter region and interacts with the RNA polymerase promoting or repressing transcription depending on the location of the CRP-binding site (Snyder and Champress 2003).

CCR in *Pseudomonas,* however, exhibits major differences to that of *E. coli*. Not only are tricarboxylic acid cycle (TCA) cycle intermediates often stronger repressing agents than glucose, but adenylate cyclase activity, PEP activity, and cellular cAMP pools do not fluctuate with the carbon sources supplied nor does addition of cAMP relieve CCR in *Pseudomonas* strains (Hester *et al*. 2000). The precise mechanism of CCR in *Pseudomonas* strains has not been completely elucidated and appears to be far more complex than that of *E. coli* (Collier *et al*. 1996). The only protein thus far shown to be involved in CCR in *Pseudomonas* strains is Crc. While Crc shows some sequence similarity (25-32% identity) to DNA repair enzymes, it does not appear to have endonuclease activity or DNA-binding abilities suggesting an alternative function (Hester *et al*. 2000). Crc has been implicated in the repression of a number of genes involved in the metabolism of sugars and nitrogenated compounds in *P. aeruginosa* and *P. putida* (Collier *et al.* 1996, Yuste and Rojo 2001, Hester *et al*. 2000). However, not all genes subject to catabolite repression are influenced by Crc (Yuste and Rojo 2001). This is clearly illustrated by the catabolite repression of *PalkB* and *PalkS2* promoters (Yuste and Rojo 2001). When cultured in complete medium, Crc plays a significant role in CCR of *PalkB* and *PalkS2* expression during exponential phase of growth. However, observation of Crc-null mutants revealed that Crc has no significant role in CCR in the expression of these genes in defined medium containing lactate or succinate as carbon sources. This suggests that CCR occurs via two different systems (Yuste and Rojo 2001). The presence of two CCR pathways is seen in *P. aeruginosa* in which the *hut* operon is Crc-independent whilst expression of amidases, *mdh*, and various other genes are controlled by Crc-dependent pathways (Collier *et al.* 2001). Furthermore, the regulation of catabolic pathways appears to vary not only between different *Pseudomonas* species but also between various strains of *Pseudomonas* (Petruschka *et al*. 2002, Hester *et al*. 2000, Yuste and Rojo 2001).

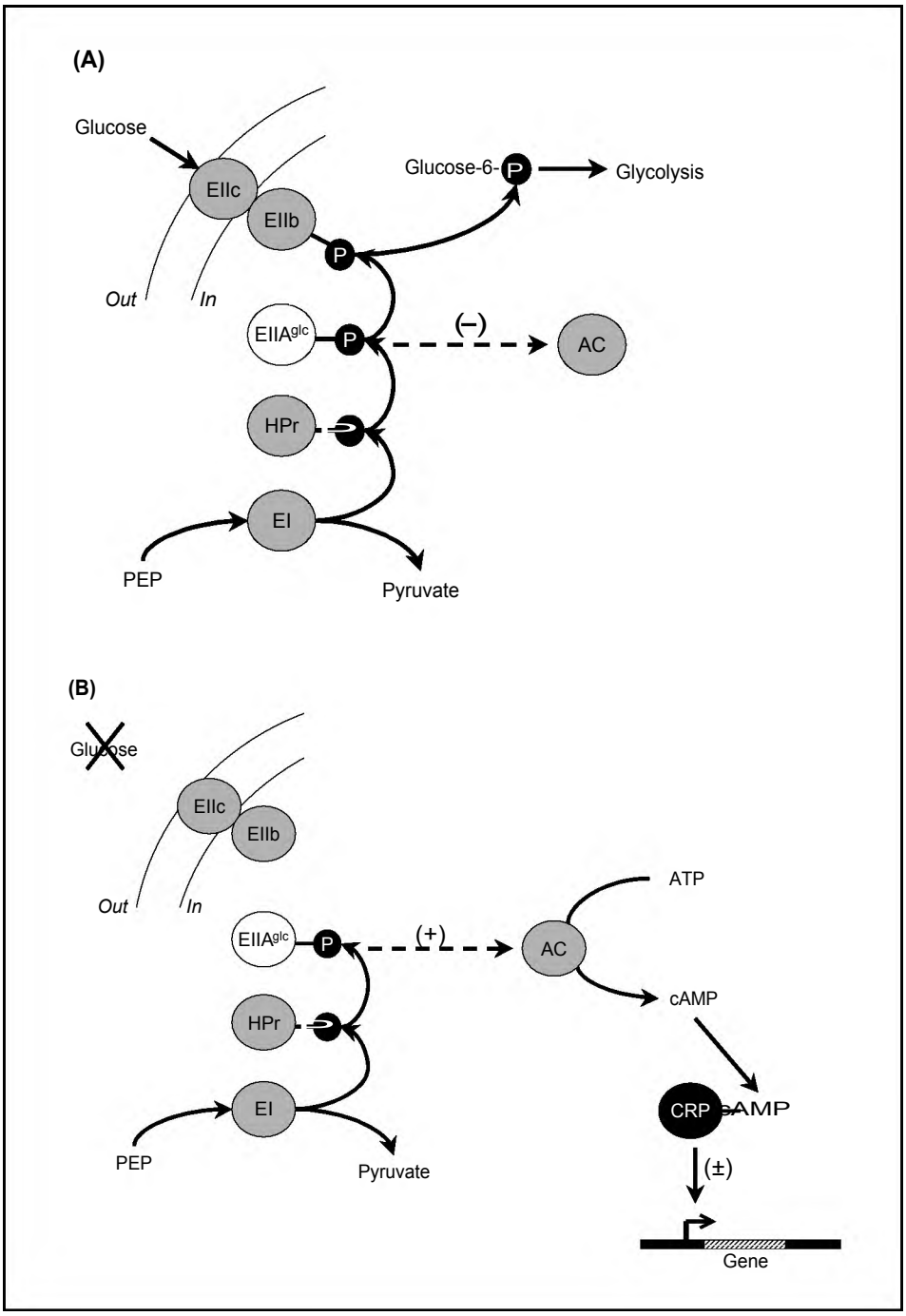

Figure 5.2 Schematic summary of the CCR regulatory system in *E. coli*. (AC: adenylate cyclase, PEP: phosphoenolypyruvate, P: phosphate) (adapted from Warner and Lolkema 2003).

As discussed in Chapter 4, several mutant strains of *P. putida* RU-KM3$_S$ with phenotypes such as reduction or complete loss of hydantoinase and/or *N*-carbamoylase activity, as well as mutant strains unable to utilize hydantoin as a nitrogen source but still exhibiting wild type levels of hydantoin-hydrolysing activity, were isolated. Identification of the locus inactivated by insertional mutation in each mutant strain would facilitate a) isolation of the structural

genes involved in the hydrolysis of hydantoin in RU-KM3$_S$ cells, b) identification of genes whose products are involved in the regulation of hydantoinase and *N*-carbamoylase expression, and c) by use of the collective data, elucidation of the regulatory pathways that control the hydantoin-hydrolysing operon in RU-KM3$_S$ cells. This chapter describes the isolation and characterization of the genomic sequences flanking the transposon insertion in 14 selected mutants and the subsequent analysis of the structural and regulatory components of hydantoin-hydrolysis in RU-KM3$_S$ cells.

5.2 METHODS AND MATERIALS

5.2.1 Identification of plasposon disrupted genes in RU-KM3$_S$ mutants

Genomic DNA was extracted as described in Appendix 5.2 and approximately 1µ g of genomic DNA was digested to completion with either *Bam* HI, *Eco* RI, *Csp* 451, or *Pst* I restriction endonucleases, according to the manufacturers specifications, in a reaction volume of 60µ l. After heat inactivation of the restriction endonuclease, 10µ l of the DNA fragments were self-ligated using T4 DNA Ligase (Promega) in a total reaction volume of 50µ l, incubated at 4^{o}C for 2 to 3 days. Transformation of 10µ l aliquots of the ligation with 150µ l competent *E. coli* DH5α cells was done (Appendix 4) and colonies exhibiting antibiotic resistance conferred by the inserted plasposon DNA were selected by growth on Luria agar plates containing 50µ g/ml kanamycin. Selected colonies were individually isolated and screened for the presence of recombinant plasmids using the Easyprep method (Berghammer and Auer 1993) and diagnostic restriction endonuclease digestion (Appendix 5.1). The High Pure Plasmid Isolation Kit (Roche) was used according to manufacturers instructions to extract selected plasmids for subsequent sequence analysis. The nucleotide sequence of the chromosomal DNA flanking the inserted plasposon DNA was determined from double stranded plasmid DNA by the dideoxy-chain termination method (Sanger 1987) using the ABI Prism Big Dye Terminator Cycle Sequencing Ready Reaction Kit (PE Applied Biosystems) (Appendix 5.4). The primers utilized for the sequencing reactions, prGM11 and prGM12 (Appendix 3), correspond to the terminal ends of the plasposon insertion sequence (Figure 4.1).

5.2.2 DNA sequence analysis

Preliminary analysis of raw sequence data was carried out using Vector NTI DeLuxe v4.0 or v5.0 software (Informax Inc.). Identification of known genes to which acquired sequence data exhibits a high degree of similarity was done using the Basic Local Alignment Search Tool (BLASTX, BLASTP) (Altschul *et al*. 1990) hosted by the National Centre for Biotechnology Information (NCBI) website (http://www.ncbi.nlm.nih.gov).

5.2.3 Construction of *dhp* knockout mutants

Maps of plasmids used in this chapter are contained in Appendix 3. The knockout vector, pGMKdhp, utilized to generate a mutant strain of *P. putida* RU-KM3$_S$ encoding an inactivated dihydropyrimidinase (*dhp*) gene, was constructed using the plasmid pTnMod-OTc and a 5'/3' truncated fragment of the *dhp* gene. The transposase gene was removed from pTnMod-OTc by restriction endonuclease digestion with *Xho* I and *Pvu* II as per manufacturers specifications. The *dhp* fragment truncated at both the 3' and 5' end was obtained by digestion of the *dhp* gene in pGMdhp.a with *Sal* I and *Pvu* II. The 4162bp backbone of pTnMod-OTc and 712bp fragment of the *dhp* gene were purified from an agarose gel using the GFX^{TM} PCR DNA and Gel Band Purification Kit (Amersham). These purified fragments were then ligated with T4 DNA Ligase (Promega) as per manufacturers specifications, incubated overnight at 4^{o}C, and transformed into *E. coli* DH5α. The resultant tetracyline resistant colonies were screened for the properly constructed pGMKdhp vector. The pGMKdhp vector was then introduced into *P. putida* RU-KM3$_S$ by tri-parental mating with *E. coli* DH5α containing the correct pGMKdhp vector, *E. coli* HB101 containing pRK2013, and wild type RU-KM3$_S$ as described in Section 4.2.1 (Chapter 4). The cells were plated onto Luria agar containing 25μ g.ml^{-1} chloramphenicol (to select against the *E. coli* strains) and 50μ g.ml^{-1} tetracyline (to select against RU-KM3$_S$ cells lacking the integrated vector) in order to isolate mutant strains of RU-KM3$_S$ in which conjugal transfer and homologous recombination of the pGMKdhp into the chromosome of RU-KM3$_S$ had occurred rendering the dihydropyrimidinase gene inactive.

To confirm the disruption of the *dhp* gene, the recombinant genomic DNA was extracted as described previously and subjected to PCR analysis using Expand High Fidelity PCR system (Roche) or Taq polymerase (Bioline) using standard amplification parameters (Appendix 5.3) with annealing temperatures of 60^{o}C and 45^{o}C. Primers corresponding to internal sequences of the *dhp* (prGM21, prGM28) and specific for pGMKdhp (prGM19, prGM20, prGM11) (Appendix 3) were utilized. The products of the PCR reactions were then separated by electrophoresis with 1% agarose gel containing 0.5μ g/ml ethidium bromide, and visualized using the Kodak DC 120 gel imaging system.

5.2.4 Analysis of the promoter regions of *bup* , ORF1, and *dhp*

The intergenic region between ORF1 and the dihydropyrimidinase gene was amplified from genomic DNA from *P. putida* RU-KM3$_S$ and GMP1, by PCR using the Expand High Fidelity PCR system (Roche) with primers prGM22, specific for the terminal end of the *dhp* gene, and prGM30, specific for the start of ORF1 (Appendix 3) using standard amplification parameters (Appendix 5.3) with an annealing temperatures of 55^{o}C. The PCR product was then purified (High Pure PCR Product Purification Kit, Roche) and ligated into the pGEM-T Easy vector

(Promega) to form the constructs pGMIRwt and pGMIR1 containing the 2076bp PCR product obtained with wild type and GMP1 genomic DNA as templates respectively. In order to determine the nucleotide sequence of the entire intergenic region, a 1198bp fragment was excised from pGMIRwt and pGMIR1 by restriction digestion with *Sac* II and recircularisation by ligation to form pGMIRwtΔ*Sac* II and pGMIR1Δ*Sac* II respectively. Using primers prGM30, with pGMIRwt and pGMIR1 as templates, and pUCF with pGMIRwtΔ*Sac* II and pGMIR1Δ*Sac* II as templates the nucleotide sequence of the promoter region was sequenced.

5.2.5 Biocatalytic assays

Resting cell biocatalytic reactions were carried out with RU-KM3$_S$ as described in Appendix 2.1, except that the culture medium used was nutrient broth supplemented with and without 1% ammonium sulphate, 1% glucose, or 1% succinate. With respect to the biocatalytic assay of pGMIRwt (Section 5.2.4) in *E. coli* strain DH5α, the cultures were grown to confluence overnight, at 37^{o}C, in Luria broth with 100μ g/ml ampicillin as well as Luria broth supplemented with 100μ g/ml ampicillin and 1% ammonium sulphate, 1% glucose or 1% succinate, and the assays carried out as described in Appendix 2.1. *E. coli* DH5α not expressing the *dhp* gene was utilized as a negative control.

5.3 RESULTS

5.3.1 Sequence analysis of insertional mutants

Chromosomal extractions from the selected mutant strains were digested to completion with restriction endonucleases *Pst* I, *Csp* 451, or *Bam* HI. The recognition sites for these restriction endonucleases are not present within the plasposon DNA sequence inserted into the chromosomes of the mutant strains. This ensured that the plasposon origin of replication and the gene conferring kanamycin resistance remained intact whilst the chromosomal DNA was digested by the selected enzymes. Restriction endonuclease digestion with *Pst* I or *Csp* 451 resulted in small, easily manipulated chromosomal fragments (data not shown). *Bam* HI, in contrast, cut less frequently resulting in larger fragments which, whilst more difficult to ligate and transform into *E. coli*, would potentially provide additional chromosomal DNA flanking the plasposon inserted DNA thereby allowing for inclusion of larger genomic fragments upstream and downstream of the site of insertion.

Once digested, the chromosomal fragments were circularised by self-ligation and transformed into *E. coli* DH5α. By selecting for kanamycin resistance, only the chromosomal fragment containing the inserted plasposon DNA was isolated and primers specific for the terminal ends of the inserted DNA were used to confirm the presence of the plasposon

fragment and then to determine the nucleotide sequence of the chromosomal DNA flanking the point of insertion. The nucleotide sequence data obtained was subjected to BLASTX analysis using the NCBI database to facilitate in the identification of the interrupted genes based on similarity to known genes on the database. The sequence data obtained from each of these mutants showed significant similarity to the corresponding genes annotated in the total genome sequence of *Pseudomonas aeruginosa* PAO1 and *Pseudomonas putida* KT4420 with nucleotide sequence percentage identities of greater than 85% as indicated by BLAST analysis (Section 5.3.2, Table 5.1 and Section 5.3.3, Table 5.2).

5.3.2 Identification of the genes encoding the structural proteins of the hydantoin-hydrolysing pathway in RU-KM3$_S$ cells

Of the seven mutants classified in Group C (*amm*$^+$, *hyd*$^-$, *gly*$^+$, *ura*$^\pm$, wild type hydantoinase but no *N*-carbamylglycine-hydrolysing activity), two (GMP3 and GMP16) arose as a result of insertion of plasposon DNA into a region corresponding to a hypothetical ORF on the *P. aeruginosa* PAO1 genome designated as a probable transporter. The remaining five mutants (GMP4, GMP17, GMP18, GMP19, GMP20) all resulted from insertion of plasposon DNA into sequence corresponding to a β-ureidopropionase (designated *bup* in this study) on the *P. aeruginosa* PAO1 genome sequence. These sequences were also present in the *P. putida* KT2440 genome sequence that was released subsequent to this work.

Table 5.1 Gene locus of insertional inactivation by pTnMod-OKm of mutant strains lacking *N*-carbamoylase activity

Mutant strain	Parental strain	Phenotypic grouping *	TnMod Insertion site	
			Locus	Gene product
GMP3	WT	C	ORF1	Probable transporter
GMP16	WT	C		
GMP4	WT	C	*bup*	β-ureidopropionase
GMP17	WT	C		
GMP18	WT	C		
GMP19	WT	C		
GMP20	WT	C		

(*: As described in Table 4.2)

The *bup* and ORF1 genes in the mutants described above (Table 5.1) were insertionally inactivated at exactly the same location within the gene. This is due to the method by which the cells underwent mutagenesis and enrichment as both procedures provided some opportunity for the cells to divide and form identical daughter cells.

The inability of mutant GMP5, in which the *bup* gene had been interrupted by insertion of plasposon-derived sequences, to hydrolyse *N*-carbamylamino acid (Figure 4.7, Chapter 4) strongly suggested that this locus encoded the enzyme responsible for *N*-carbamylamino acid-hydrolysing activity in RU-KM3$_S$ cells.

Further analysis revealed that the ORF corresponding to a putative transporter was adjacent to the *bup* locus in both *Pseudomonas* genomes, with a gene encoding a dihydropyrimidinase (designated *dhp* in this study) upstream of the ORF. As the genes encoding hydantoin-hydrolysing enzymes often occur in an operon, the region upstream of the *bup* and ORF1 coding regions in RU-KM3$_S$ was isolated to confirm the presence of a *dhp* gene in the RU-KM3$_S$ genome. This was accomplished by extending the sequence analysis of the chromosomal fragments, generated using restriction endonuclease digestion with *Bam* HI, *Pst* I, and *Csp* 451, from mutants GMP4 and GMP3 (Figure 5.3). Analysis of the sequence data obtained revealed the presence of a *dhp* upstream of and in the opposite orientation to ORF1 and *bup*.

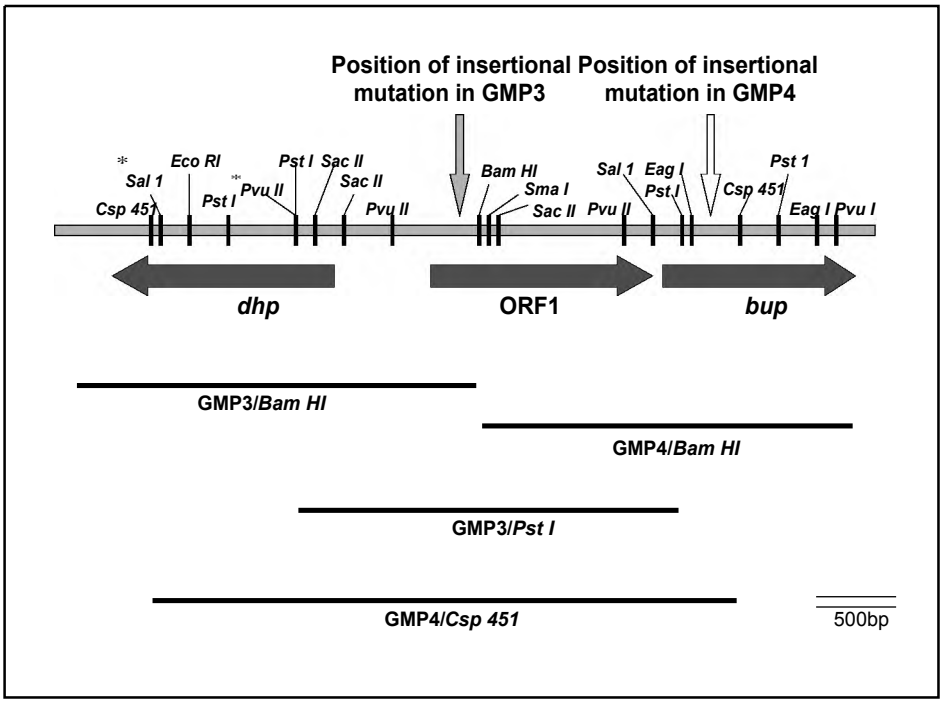

Figure 5.3 Chromosomal map of *P. aeruginosa* PAO1 containing the genes encoding for the dihydropyrimidinase, β-ureidopropionase, and probable transporter as well as relative alignment of the genomic fragments isolated from mutants GMP4 and GMP3. [*dhp*: dihydropyrimidinase; *bup*: β-ureidopropionase; ORF1: probable transporter. The location of the insertion site where the plasposon DNA integrated into the chromosomes of GMP3 and GMP4 are depicted as grey or white arrows respectively. The chromosomal fragments, generated by digestion with restriction endonucleases *Pst* I, *Csp* 451, or *Bam* HI, of GMP3 and GMP4 are illustrated as solid black lines labelled with the mutant strain and the endonuclease utilized to generate the DNA fragment.]

Unlike the *N*-carbamylamino acid-hydrolysing activity, direct assignment of hydantoin-hydrolysing activity to a specific locus on the RU-KM3$_S$ genome was not possible due to the absence of insertional mutants with a hydantoin-hydrolysing minus phenotype. However, the presence of a putative dihydropyrimidinase-encoding ORF upstream of the ORF1 and β-ureidopropionase genes on the RU-KM3$_S$ genome raised the possibility that the hydantoin-hydrolysing activity in RU-KM3$_S$ might be attributable to a dihydropyrimidinase. In addition, results discussed in Chapter 4 (Section 4.3.3 and 4.4) suggested the possibility of a second hydantoinase in the RU-KM3$_S$ genome. Consequently, a strategy was developed to inactivate the *dhp* gene in wild type and mutant RU-KM3$_S$ cells (Figure 5.4, panel A). To this end, a suicide knockout plasmid containing a 5' and 3'-truncated fragment of the *dhp* gene was introduced into wild type RU-KM3$_S$, as well as mutant strains GMP1 and GMP2, by tri-parental mating. Integration of the plasmid, pGMKdhp, into the chromosome of the target strains was selected for by growth of cells on tetracyline agar plates resulting in the isolation of mutant strains GMP11, GMP12, and GMP13 generated from parental strains RU-KM3$_S$, GMP1 and GMP2 respectively.

The disruption of the chromosomal *dhp* was confirmed by PCR analysis of the chromosomal DNA of the respective parental and *dhp*-knockout strains with different combinations of primers such that the vector, wild type chromosomal *dhp*, and truncated chromosomal *dhp* could be distinguished from one another (Figure 5.4, panel B). Primers prGM21 (A1) and prGM28 (A2) amplified a 1048bp DNA fragment corresponding to the 5' end of the *dhp* present in the parental strains (RU-KM3$_S$, GMP1, GMP2) and Δ*dhp* (GMP11, GMP12, GMP13) but not pGMKdhp (Figure 5.4Bi, lanes 1-6 vs. lane 7). Primers prGM19 (B1) and prGM20 (B2) amplified the tetracyline gene to produced a 1350bp DNA fragment from pGMKdhp and Δ*dhp*, but not from parental chromosomal templates (Figure 5.7Bii, lanes 4-7 vs. lanes 1-3). Lastly, to confirm that integration of pGMKdhp into the chromosome of RU-KM3$_S$, GMP1, and GMP2 had occurred as predicted, primer prGM11 (C1) corresponding to pGMKdhp and a second primer specific for the 3' end of the *dhp* were used to produce a 1800bp DNA fragment from the Δ*dhp* strains only (Figure 5.4Biii, lanes 4-6 vs. lanes 1-3 and 7).

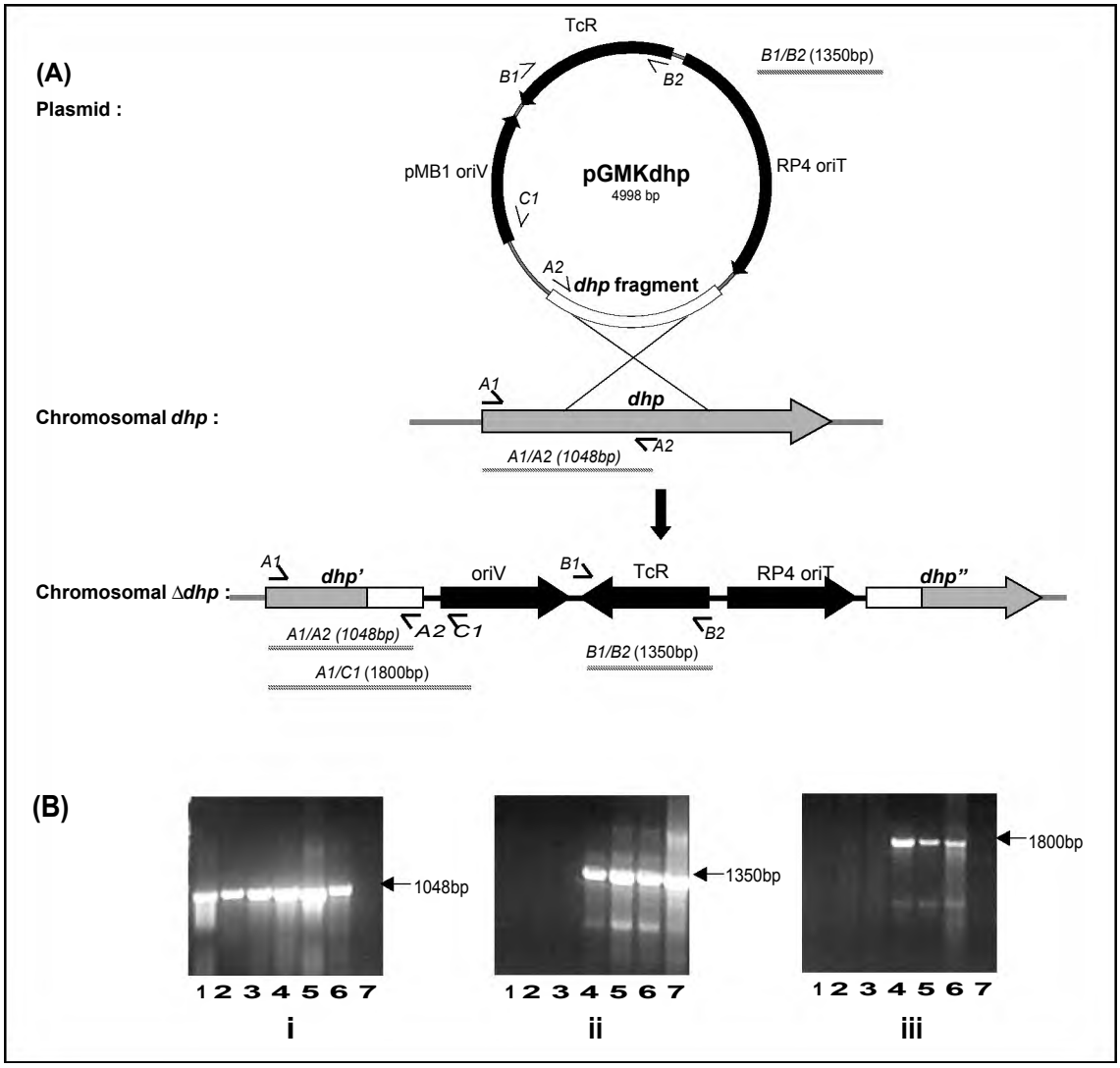

Figure 5.4 Construction of dihydropyrimidinase knockout mutants by homologous recombination of pGMKdhp with the chromosomal dihydropyrimidinase to produce truncated, non-functional *dhp* genes. **(A)** Strategy used to inactivate the *dhp*, and **(B)** confirmation of the knockout by PCR. PCR products, eletrophoresed on 1% agarose gels, obtained with primers A1/A2 **(Bi)**, B1/B2 **(Bii)**, and C1/A1 **(Biii)** using pGMKdhp (lane 7), genomic DNA from RU-KM3$_S$ wild type (lane 1), GMP1 (lane 2), GMP2 (lane 3) and their corresponding *dhp*-knockout mutants GMP11 (lane 4), GMP12 (lane 5), GMP13 (lane 6) as templates. (PCR products are schematically represented as thin lines and primers as half-arrows).

Biocatalytic assays for hydantoinase activity were performed on the resting cells of the *dhp* knockout mutants. No hydantoinase activity was detected in any of the three mutant strains (Figure 5.5). This confirmed that dihydropyrimidinase, encoded by *dhp*, was responsible for hydantoinase activity in RU-KM3$_S$ cells and that there was no second hydantoinase present in this strain.

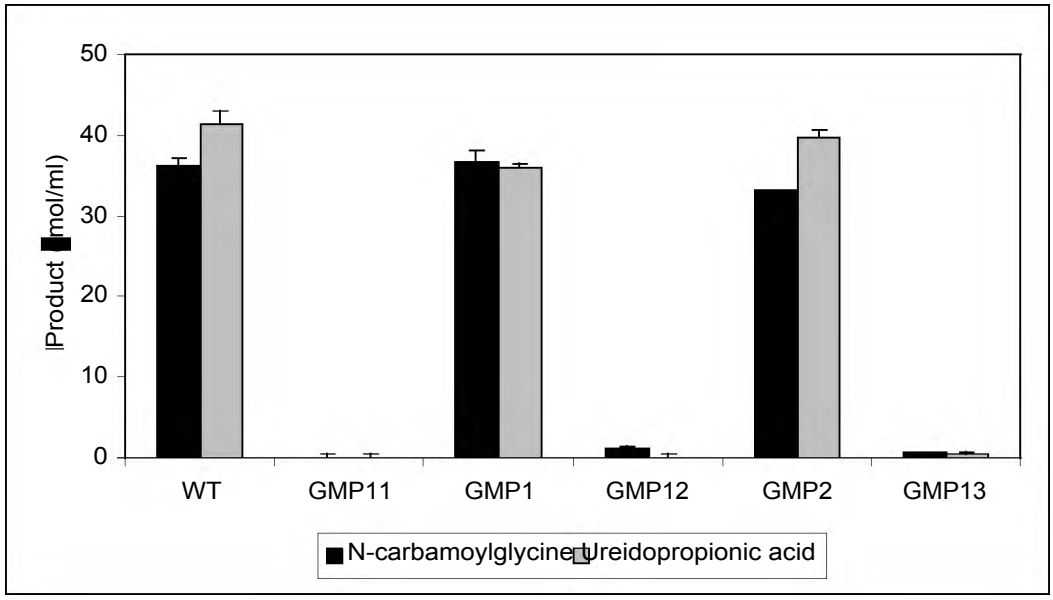

Figure 5.5 Hydantoinase activity of RU-KM3$_S$ wild type, GMP1, GMP2 and their corresponding mutants (GMP11, GMP12, GMP13) in which the gene encoding the dihydropyrimidinase has been inactivated by targeted insertional mutation. [WT: wild type. Enzyme activities were determined as *N*-carbamoylglycine + glycine and β-ureidopropionic acid + alanine produced with 50mM hydantoin and 50mM dihydrouracil respectively as substrates. Error bars represent the standard error of the mean, n=3]

5.3.3 Analysis of Ntr regulatory mutants

In addition to mutants from phenotype Group C (Section 5.3.2), seven mutants were isolated with wild-type levels of hydantoin- and *N*-carbamylglycine-hydrolysis but which were unable to utilize hydantoin or uracil as sole sources of nitrogen (Chapter 4, Section 4.3.3). Analysis of the genomic DNA flanking the point of insertion in these mutant strains revealed sequences similar to the genes annotated on the *P. aeruginosa* PAO1 genome as *glnD*, *ntrC*, and *ntrB* encoding pII uridyltransferase, NtrC, and NtrB respectively (Table 5.2). These three enzymes are key components of the Ntr regulatory pathway which is responsible for regulation of gene expression in response to the nitrogen status of the cell (Figure 5.1). This suggested that the hydantoin-hydrolysing pathway in RU-KM3$_S$ cells is not regulated by the Ntr global regulatory pathway. However, disruption of this regulatory pathway would result in an inability of the cell to respond correctly to the nitrogen status of the cell which may explain why mutants GMP6, GMP15, GMP7, GMP9, GMP10, and GMP21 were unable to grow on poor nitrogen sources such as hydantoin or uracil but showed normal growth rates with good nitrogen sources such as ammonium and glycine.

Table 5.2 Gene locus of insertional inactivation by pTnMod-OKm of mutant strains unable to utilize hydantoin as a sole source of nitrogen

Mutant strain	Parental strain	Phenotypic grouping ∗	TnMod Insertion site	
			Locus	Gene product
GMP6	WT	A	*glnD*	pII uridyltransferase
GMP15	WT	A		
GMP7	WT	A	*ntrC*	NtrC
GMP9	WT	A		
GMP10	WT	A	*ntrB*	NtrB
GMP21	WT	A		
GMP8	WT	B	*gltB*	Glutamate synthase

(∗: As described in Chapter 4, Table 4.2)

Mutant strain GMP8, from phenotype Group B, also exhibited wild-type levels of hydantoin- and *N*-carbamylglycine-hydrolysis but was unable to grow on defined medium with glycine or hydantoin as the sole source of nitrogen (Chapter 4, Section 4.3.3). This mutant arose as a result of insertion of plasposon DNA into a region corresponding to a putative *gltB* gene, encoding for the major subunit of the glutamate synthase enzyme, on the *P. aeruginosa* PAO1 genome sequence. Although the precise role of glutamate synthase in the global Ntr regulatory pathway is unclear, deficiency of this enzyme has been shown to cause pleiotrophic nitrogen assimilation defects in *P. putida* KT2442 which was found to be unable to grow on poor nitrogen sources as well as several amino acids as nitrogen sources (Eberl *et al.* 2000). This reinforces that the hydantoin-hydrolysing pathway in RU-KM3$_S$ cells, while able to supply nitrogen by degradation of hydantoin, is not regulated by the global Ntr regulatory pathway.

5.3.4 Regulation of hydantoin-hydrolysis in RU-KM3$_S$ cells

The only mutation potentially linked to the regulation of the hydantoin-hydrolysing enzymes in RU-KM3$_S$ occurred in mutant GMP5 isolated due to reduced levels of hydantoin-hydrolysis when compared to the wild type (Chapter 4, Figure 4.5). The inactivated gene resulting in this phenotype was found to encode a dihyrolipoamide succinyltransferase enzyme. Dihydrolipoamide succinyltransferase forms part of the α-ketoglutarate dehydrogenase enzyme complex (Palmer *et al.* 1991) which is responsible for the conversion of α-ketoglutarate to succinyl co-A in the tricarboxylic acid cycle (TCA) cycle (Michal 1999). Interruption of the TCA cycle, by inactivation of the dihydrolipoamide succinyltransferase,

would result in subsequent disruption in the concentrations of the intermediates. This, together with the fact that none of the mutants with inactivation of loci encoding Ntr proteins had any effect on enzyme activity, raised the possibility that expression of hydantoin-hydrolysing enzymes in RU-KM3$_S$ cells might be regulated by carbon catabolite repression. Thus the effect of the TCA cycle intermediate succinate as well a readily metabolizable carbon (viz. glucose) or good nitrogen (viz. ammonium sulphate) source on hydantoin-hydrolysing enzyme activity in RU-KM3$_S$ was investigated. The presence of a good nitrogen source did not inhibit the hydrolysis of hydantoin but surprisingly resulted in a slight increase in hydantoinase enzyme activity levels (Figure 5.6). In contrast, cells grown in the presence of glucose or succinate exhibited a significant decrease in both the hydantoinase and *N*-carbamoylase activities such that only 25% *N*-carbamylglycine and 14% glycine was produced when compared to cells grown in complete medium without supplementation with glucose or succinate (Figure 5.6). This indicated that regulation of the hydantoin-hydrolysing enzymes in RU-KM3$_S$ cells involved carbon catabolite repression as opposed to nitrogen catabolite repression.

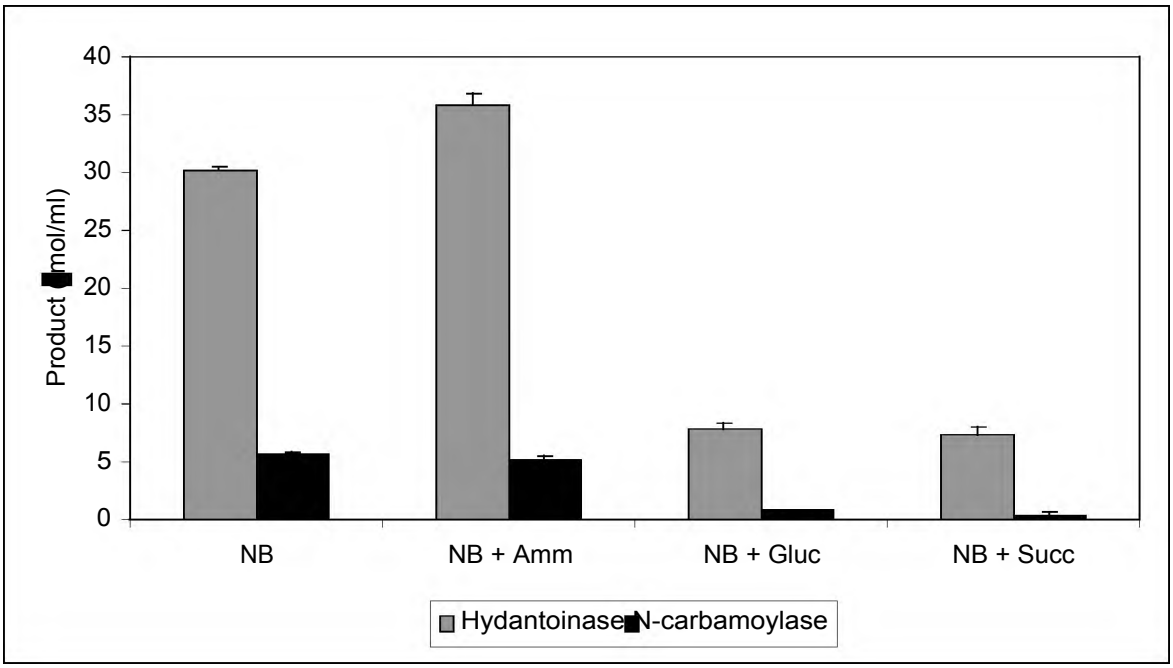

Figure 5.6 The effect of ammonium sulphate, glucose and succinate on the hydantoin-hydrolysing activity of RU-KM3$_S$. [Hydantoinase activity was calculated as the amount of *N*-carbamoylglycine and glycine produced (µ mol/ml) and *N*-carbamoylase activity as the amount of glycine (µ mol/ml) produced from hydantoin substrate. (NB: nutrient broth, Amm: 1% ammonium sulphate, Gluc: 1% glucose, Succ: 1% succinate) (Error bars represent the standard error of the mean, n=3)

5.3.5 Analysis of the promoter regions of *bup* and *dhp*

The genetic characterization and analysis of the *dhp*, *bup,* and ORF1 genes are discussed in detail in Chapter 6, however, analysis of the intergenic region between *dhp* and ORF1 in RU-KM3$_S$ will be discussed here. Insertional inactivation of the open reading frame upstream of *bup*, designated ORF1, resulted in complete loss of β-ureidopropionase activity in mutant strain GMP3 (Figure 4.7) suggesting that these two genes are transcribed as a polycistronic mRNA. The short intergenic region that exists between the *bup* and ORF1 substantiates this. Analysis of the 5' region flanking ORF1 revealed a putative ribosome binding site (Shine-Dalgarno) at nucleotides 8 to 13, a possible Pribnow box at nucleotides 25 to 29, and a sequence similar to the prokaryotic –35 consensus sequence at nucleotides 66-72 (Figure 5.7). Analysis of the promoter region of *dhp* revealed a putative Shine-Dalgarno at nucleotides 609 to 614 and sequences corresponding to the prokaryotic –10 and –35 consensus sequences at nucleotides 40-48 and 380-385 respectively (Figure 5.7). Interestingly, a region with high similarity to an *E. coli* CRP-binding site was also identified at nucleotides 392 to 422 (Figure 5.7).

Alignment of the corresponding intergenic regions from *P. putida* KT2440 and *P. aeruginosa* PAO1 using ClustalW software was done to determine if similar promoter sequences existed in these strains. In addition, the promoter region for the gene coding for the D-hydantoinase from *P. putida* DSM 84 (LaPointe *et al*. 1994) was aligned with the promoter regions for the dihydropyrimidinase encoding genes from RU-KM3$_S$, *P. putida* KT2440, and *P. aeruginosa* PAO1. The promoter region for the putative hydantoin-hydrolysing genes from *P. aeruginosa* PAO1 was found to be similar to that of RU-KM3$_S$ and also contained the putative CRP-binding site (Figure 5.7). However, the corresponding nucleotide sequence in *P. putida* KT2440 was observed to be significantly shorter than that of *P. putida* RU-KM3$_S$ and *P. aeruginosa* PAO1 and, in addition, did not exhibit the same degree of similarity with respect to the putative CRP-binding site (Figure 5.7). The disparity between the locus encoding the hydantoin-hydrolysing enzymes in RU-KM3$_S$ and that of *P. putida* KT2440 is further demonstrated by the gene encoding the *P. putida* KT2440 dihydropyrimidinase containing an authentic frameshift, which is not the result of a sequencing artefact, rendering the gene inactive. Interestingly, the nucleotide sequence from *P. putida* DSM 84 which corresponded to that of the putative CRP-binding site in the promoter region for RU-KM3$_S$ exhibited little similarity (Figure 5.7). The fact that the levels of D-hydantoinase activity in *P. putida* DSM 84 decreased by a factor of 4 when the cells were cultured with glucose (Morin *et al*. 1986a) suggested that although the enzymes from *P. putida* DSM 84 and RU-KM3$_S$ both appeared to be subject to carbon catabolite repression, the mechanism by which the repression took place is most likely different.

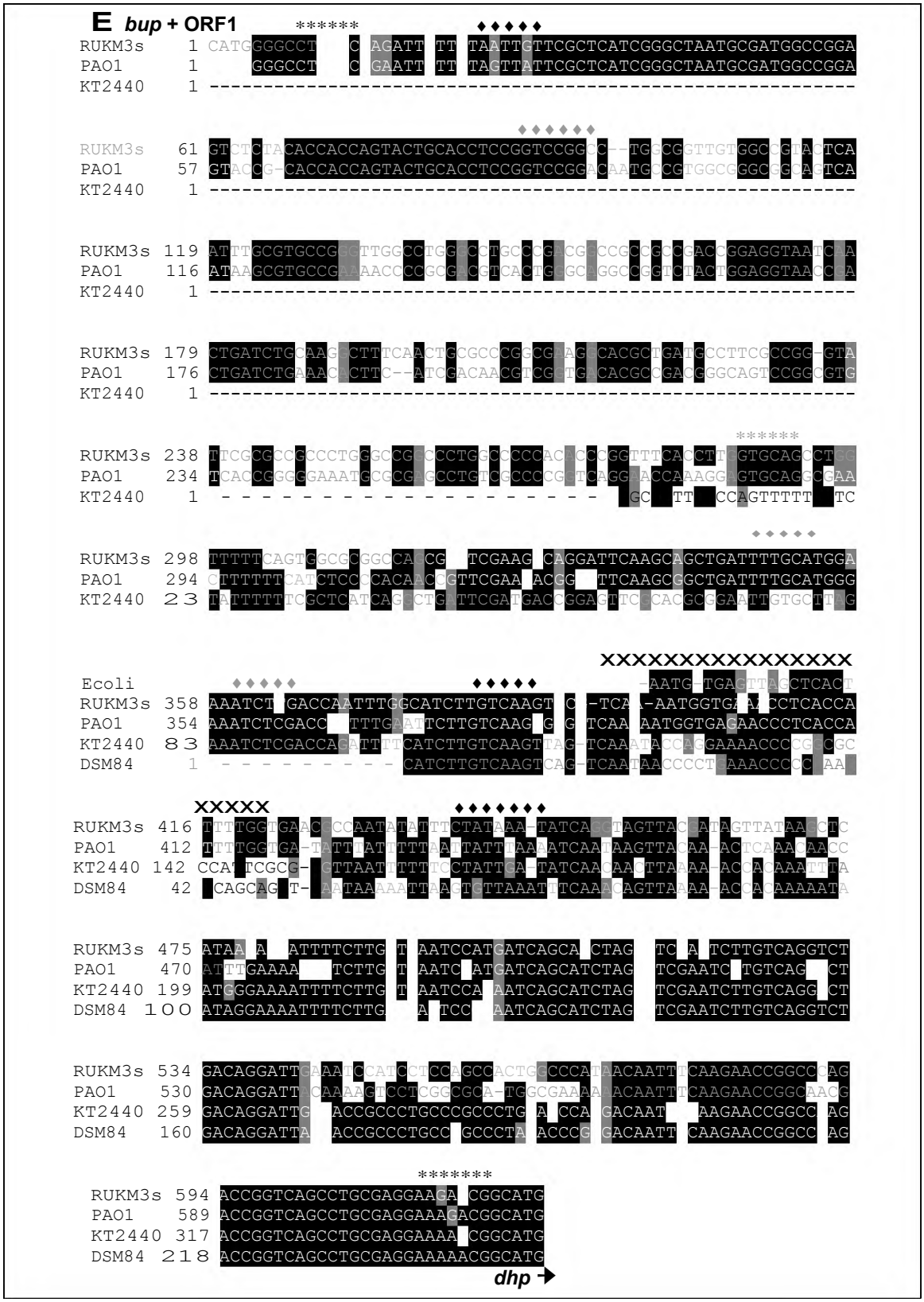

Figure 5.7 Multiple alignment of the nucleotide sequences of the intergenic regions between the *dhp* and ORF1 of RU-KM3$_S$, *P. putida* KT2440, and *P. aeruginosa* PAO1 with the putative CRP binding site highlighted by alignment of a typical *E. coli* CRP-binding site. (x: putative CRP-binding site, *: putative Shine-Dalgarno, ♦: putative –10 and –35 consensus sequences, grey symbols: putative promoter elements for the *bup* of *P. putida* KT2440)

To determine whether the putative CRP site identified upstream of the *dhp* gene in RU-KM3$_S$ was functional, the *dhp* gene and its native promoter region were cloned into pGEM-T-Easy vector in the opposite direction to the *lac* promoter (pGMIRwt) thereby ensuring that any expression of the *dhp* would be due to the native promoter activity only. *E. coli* strain DH5α containing the recombinant plasmid was cultured in Luria broth with and without glucose and resting cell biocatalytic assays were done. In addition, to determine if the inhibitory effect of succinate on *dhp* activity levels in RU-KM3$_S$ cells (Figure 5.6) occurred in *E. coli* as well, cultures were grown in Luria broth supplemented with succinate. Since the natural function of dihydropyrimidinase is catabolism of pyrimidine nucleotide bases which is linked to nitrogen metabolism in the cell, the effect of a good nitrogen source on expression of *dhp* in *E. coli* was also investigated.

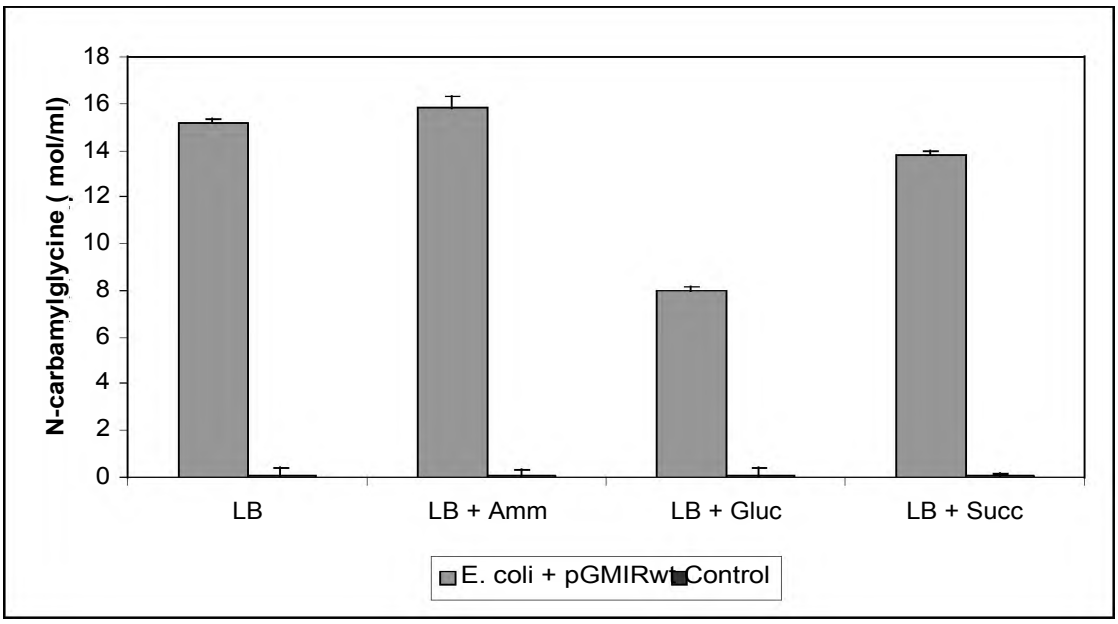

Figure 5.8 Conversion of hydantoin to *N*-carbamylglycine by dihydropyrimidinase from RU-KM3$_S$ expressed in *E. coli* from its native promoter sequence from cultures grown in Luria broth supplemented with ammonium sulphate, succinate, or glucose. (LB: Luria broth, Amm: 1% ammonium sulphate, Gluc: 1% glucose, Succ: 1% succinate, control: *E. coli* without pGMIRwt) (Error bars represent the standard error of the mean, n=3)

Supplementation of ammonium sulphate to the culture medium did not affect the expression or hydantoin-hydrolysing activity of the dihydropyrimidinase in *E. coli* cells (Figure 5.8). Glucose on the other hand resulted in significant reduction in the hydrolysis of hydantoin with a loss of almost half the dihydropyrimidinase activity (15.18μ mol/ml vs. 7.96μ mol/ml) (Figure 5.8). Interestingly, in contrast to RU-KM3$_S$ cells, in *E. coli*, the presence of succinate in the growth medium resulted in only a modest decrease in dihydropyrimidinase activity

(15.18µ mol/ml vs. 13.78µ mol/ml) (Figure 5.8). This data suggested differences in the mechanisms of carbon catabolite repression of this promoter in RU-KM3$_S$ and *E. coli*.

5.4 DISCUSSION

The major objective of this chapter was to identify the genes encoding for the structural proteins responsible for hydantoin-hydrolysis in RU-KM3$_S$ cells by analysis of the genes inactivated in mutant derivatives unable to utilize hydantoin as a sole source of nitrogen. This approach also allowed for elucidation of the regulatory mechanisms affecting the hydantoin-hydrolysing pathway in this strain.

The data presented in this chapter show that the enzymes responsible for the hydantoinase and *N*-carbamoylase activities in *P. putida* RU-KM3$_S$ are a single dihydropyrimidinase, encoded by *dhp*, and a single β-ureidopropionase, encoded by *bup*, respectively. The presence of two hydantoinases, as occurs in *Agrobacterium* sp. IP I-671 (Hils *et al.* 2001), or two carbamoylases, as occurs in *Blastobacter* sp. A17p-4 (Ogawa *et al.* 1994c) and *Pseudomonas* sp. AJ-11220 (Yokozeki *et al.* 1987c) does not apply to RU-KM3$_S$ as complete absence of hydantoin-hydrolysing activity is observed subsequent to inactivation of the *bup* and *dhp* genes.

A third open reading frame, designated ORF1, was located between the *bup* and *dhp* genes. It is tempting to propose that ORF1, which exhibits significant similarity to a putative transport protein in the *P. aeruginosa* genome, could be involved in the transport of hydantoin. However, the observation that insertional inactivation of ORF1 did not affect hydrolysis of hydantoin to *N*-carbamylglycine in whole cell biocatalytic assays suggested otherwise. The inability to convert *N*-carbamoylglycine to glycine when ORF1 is interrupted by insertion of foreign plasposon DNA can be attributed to expression of ORF1 and *bup* from a common promoter as a polycistronic mRNA. This is supported by the very short intergenic region between the *bup* and ORF1 genes. The amino acid sequence and bioinformatic analysis of the β-ureidopropionase, ORF1 and dihydropyrimidinase will be discussed in greater detail in Chapter 6.

With respect to regulation of hydantoin-hydrolysis in RU-KM3$_S$ cells, the data presented conclusively demonstrated that expression of RU-KM3$_S$ *dhp* and *bup* genes is regulated by carbon catabolite repression and is not affected by the nitrogen status of the cell as has been shown in studies of *Agrobacterium tumefaciens* RU-OR (Hartley *et al.* 2001). Firstly, growth of RU-KM3$_S$ cells in complete medium supplemented with ammonium sulphate had no effect on hydantoin-hydrolysis. Furthermore, mutant strains of RU-KM3$_S$ in which key components

of the Ntr regulatory cascade, namely NtrC, NtrB, and $_{PII}$ uridyltransferase encoding genes (Figure 5.1), were inactivated exhibited wild type levels of hydantoin-hydrolysing enzyme activities. Thus expression of *dhp* and *bup* genes in RU-KM3$_S$ occurs independently of the nitrogen catabolite repression control.

Support for the regulation of hydantoin-hydrolysis by CCR is provided by three observations: first, addition of glucose or succinate to the growth medium resulted in significant reductions in both *N*-carbamylglycine and glycine production. Succinate and other TCA cycle intermediates have been shown to impose severe carbon catabolite repression on several metabolic pathways in *Pseudomonas* (Collier *et al*. 1996), and the negative effect of glucose on hydantoinase activities has been documented for *Pseudomonas* sp. NCIM 5109 and *P. putida* DSM 84 (Sudge *et al*. 1998, Morin *et al*. 1986a). Second, the significant reduction in mutant strain GMP5 enzyme activities in which an enzyme within the TCA cycle, namely dihydrolipoamide succinyltransferase, was inactivated supports the proposed CCR regulation of *dhp* and *bup* in RU-KM3$_S$ cells. And thirdly, the presence of a putative CRP-binding site in the promoter region is further evidence for CCR.

As discussed in the introduction to this chapter (Section 5.1), carbon catabolite repression in *Pseudomonas* species varies significantly from that of *E. coli* in which carbon catabolite repression involves binding of the CRP protein to a CRP site in the promoter region thereby stimulating/inhibiting transcription of the gene. To determine if the putative CRP-binding site identified actually functions as one, the *dhp* gene, under control of its natural promoter containing the CRP-binding site, was expressed in *E. coli*. In this strain, glucose functions as a stimulus for CCR by resulting in elevated cAMP levels which complex with CRP and bind to the CRP-binding site resulting in repression of gene expression. The reduction of hydantoin-hydrolysis in the *E. coli* when cultured in the presence of glucose indicated that the cAMP-CRP complex had successfully bound to the CRP-binding site thereby preventing transcription of the *dhp.* The fact that succinate did not result in an equivalent decrease in activity levels, as was the case in the wild type strain, is expected as TCA cycle intermediates are not directly involved with the activity of the CRP protein. As cAMP levels in *Pseudomonas* do not vary, regardless of the carbon source supplied, and CRP does not function in *Pseudomonas* as it does in *E. coli* (Collier *et al*. 1996), the functional CRP-like site upstream of *dhp* in RU-KM3$_S$ suggests the presence of an alternative protein which functions in a manner similar to that of CRP (discussed in Chapter 7).

Surprisingly, the putative CRP-binding site upstream of the *dhp* in *P. putida* RU-KM3$_S$ is not present in the corresponding nucleotide sequences of *P. putida* KT2440 or *P. putida* DSM 84. In contrast, the corresponding promoter region from *P. aeruginosa* PAO1 was very similar to that of RU-KM3$_S$. The hydantoin-hydrolysing activities in both *P. putida* DSM 84

and RU-KM3$_S$ decreased when the cells were cultured in the presence of a readily metabolizable carbon source suggesting that these enzymes are regulated by CCR, however, the fact that the corresponding promoter regions differed implies separate mechanisms of CCR in these two *P. putida* strains. Differences with respect to CCR of a particular gene between *P. putida* isolates and between *P. putida* and *P. aeruginosa* isolates have been observed for the *bkd* operon (encodes the multienzyme complex branched-chain keto acid dehydrogenase), the *zwf-pgl-eda* operon (encoding glucose-6-phosphate dehydrogenase, 6-phosphoglucolactonase, 2-keto-3-deoxy-6-phosphogluconate-aldolase), as well as the expression of amidase (Hester *et al*. 2000, Petruschka *et al*. 2002). In addition, while the Crc protein has been implicated in CCR for numerous enzymes in *Pseudomonas*, several enzymes have been identified as sensitive to CCR but which are unaffected by Crc-null mutations thus implying the presence of a second CCR mechanism in *Pseudomonas* species (Yuste and Rojo 2001, Collier *et al*. 2001, Dinamarca *et al*. 2002).

In conclusion, the *bup* and *dhp* genes have been identified, by insertional inactivation, as encoding proteins responsible for hydantoin-hydrolysis in RU-KM3$_S$. Furthermore, regulation of expression of these genes in RU-KM3$_S$ has been shown to be controlled by the carbon catabolite repression pathway, as apposed to nitrogen catabolite repression which does not affect the dihydropyrimidinase or β-ureidopropionase enzyme activities. This has important implications when considering culture conditions for RU-KM3$_S$ such that maximal expression of the *dhp* and *bup* genes can be achieved.

6.1 INTRODUCTION

The amino acid sequence of a protein provides invaluable information and can be used to predict secondary structure using protein modelling, to identify conserved domains with potential structural or catalytic functions, as well as providing information about the molecular evolution of the proteins investigated. In the previous chapter, the genes involved in the hydrolysis of hydantoin in RU-KM3$_S$ cells were identified as a dihydropyrimidinase and a β-ureidopropionase. An open reading frame, termed ORF1, was located between the *bup* and *dhp* genes and proposed to be co-expressed with *bup* as a polycistronic mRNA. In this chapter, elucidation of the complete nucleotide and amino acid sequence of the β-ureidopropionase and dihydropyrimidinase enzymes from RU-KM3$_S$ as well as comparative analysis of the amino acid sequences with those in literature are discussed. In addition, the protein encoded by ORF1 was aligned with annotated amino acid sequences in order to identify the potential function of this protein.

6.2 METHODS AND MATERIALS

6.2.1 DNA manipulation

Genomic DNA was extracted by detergent lysis/CTAB and organic solvent extraction method as described in Appendix 5. The nucleotide sequence of the *bup* and *dhp* genes was determined from double stranded plasmid DNA by the dideoxy-chain termination method (Sanger 1977) using the ABI Prism Big Dye Terminator Cycle Sequencing. The primers used for sequencing are listed in Appendix 3.

6.2.2 Analysis of DNA sequence generated

Preliminary analysis of raw sequence data was carried out using Vector NTI DeLuxe v4.0 or v5.0 software (Informax Inc.). Identification of known genes to which the acquired sequence data exhibits a high degree of similarity was performed using BLASTX and BLASTP (Altschul *et al*. 1990) hosted by the NCBI (http://www.ncbi.nlm.nih.gov). Sequence alignments were carried out using ClustalW software (Thompson *et al.* 1994) located at the BCM Search Launcher website (http://searchlauncher.bcm.tmc.edu) and are presented in Boxshade (version 3.21) format (http://www.ch.embnet.org/software/BOX form.html). The phylogenetic trees were constructed with amino acid sequences aligned with ClustalW and, after being manually revised, imported into Treeview software (Page 1996) and the tree generated using the neighbour-joining algorithm.

6.3 RESULTS

6.3.1 Sequence analysis of the hydantoin-hydrolysing operon from RU-KM3$_S$

The complete nucleotide sequence of the RU-KM3$_S$ β-ureidopropionase was initially obtained by sequencing the genomic fragment, GMP4/*BamHI* (Figure 5.3) isolated from mutant strain GMP4, as a template. Insertion of plasposon DNA in mutant GMP4 had occurred 170bp into the *bup* gene (Figure 6.1) and thus primers specific for the inserted plasposon DNA resulted in the generation of sequence data for the 5' half of the gene. The sequence data thus obtained was used to design primers which would allow for the extension of the known nucleotide sequence (Figure 6.1). The nucleotide sequence of *bup* was verified by sequence analysis of the PCR product obtained with Expand High Fidelity PCR System, utilizing primers specific for the 5'- and 3'-terminal sequence of the open reading frame and wild type RU-KM3$_S$ genomic DNA as the template (Figure 6.1, double lines).

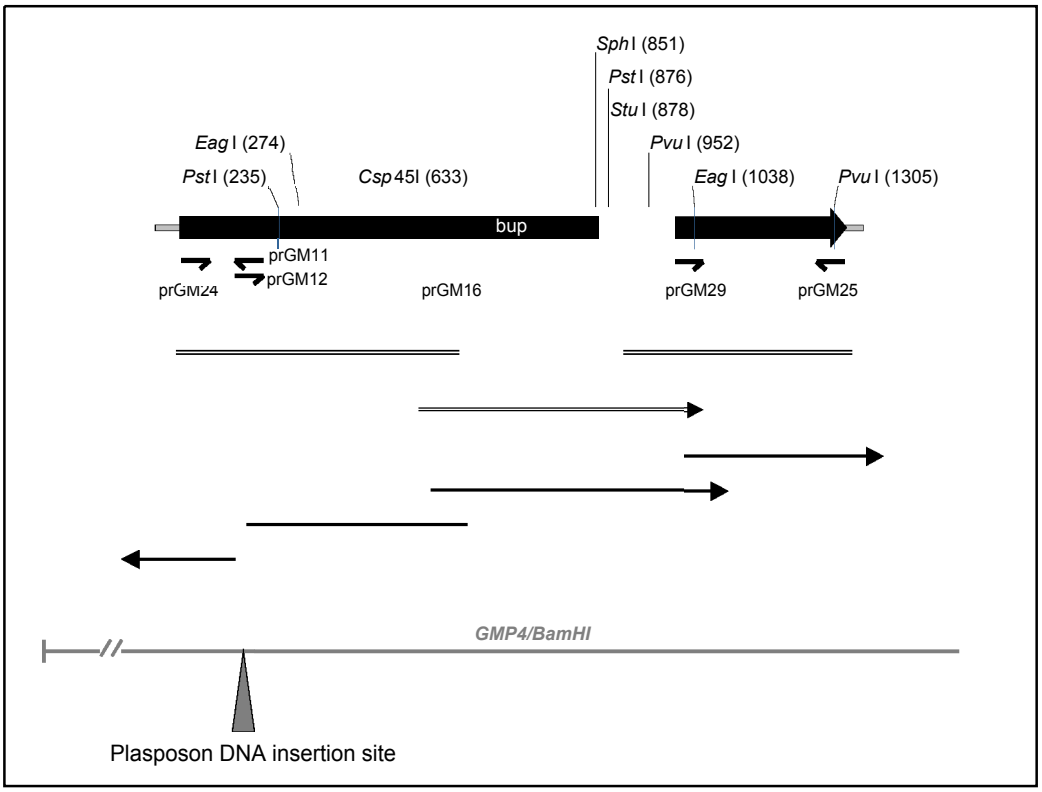

Figure 6.1 Approach for determining the nucleotide sequence of the gene encoding the β-ureidopropionase enzyme. (The grey lines depict the genomic fragment GMP4/*BamHI*. Line arrows represent sequenced regions and the direction thereof: solid and double lines where chromosomal DNA from GMP4 and wild type strains were used as templates respectively. Half-arrows depict the primers utilized and their corresponding locations for annealing.)

The nucleotide and amino acid sequences of the β-ureidopropionase from RU-KM3$_S$ are depicted in Appendix 6.1. Bioinformatic analysis of the sequence data revealed an open reading frame of 1284bp encoding 427 amino acids that was designated *bup.* The

calculated molecular mass of the protein encoded by *bup* was 52 833Da. The nucleotide sequence data obtained from the chromosomal fragment GMP4/*Bam*HI extended 334bp beyond the termination codon for the *bup* gene. However, analysis of this sequence with BLASTX did not reveal any significant identity to sequence data available on the database.

An additional open reading frame was identified directly upstream of the *bup* gene and was called ORF1. The nucleotide sequence of OFR1 was determined from chromosomal fragments of mutants GMP3 and GMP4 digested with *Pst* I and *Csp* 451 respectively (Figure 6.2, grey lines). However, the nucleotide sequence data obtained did not extend far enough such that the sequences overlapped thus small regions (± 20-70bp) of the nucleotide sequence of ORF1 was not determined (Figure 6.2). The size of the regions of ORF1 for which no nucleotide sequence data was obtained was therefore estimated by alignment of the acquired sequences with the probable transporter sequences from *P. putida* KT2440 and *P. aeruginosa* PAO1. The potential transport function of the protein encoded by ORF1 was identified by comparison of the amino acid sequence with sequences submitted to the NCBI database (Table 6.1).

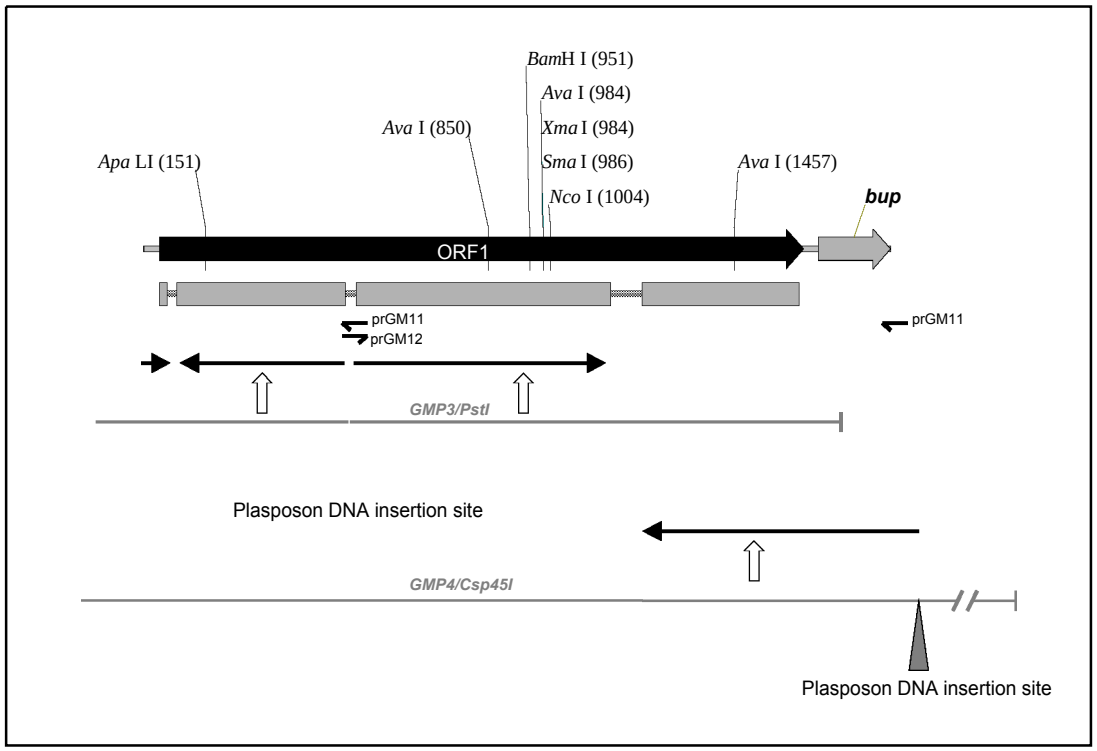

Figure 6.2 Approach for determining the nucleotide sequence of the gene encoding ORF1. (The grey lines depict the genomic fragments from which nucleotide sequence data was obtained while line arrows represent sequenced regions and the direction thereof. Half-arrows depict the primers utilized and their corresponding locations for annealing. The grey boxes represent the portions of ORF1 for which the nucleotide sequence was obtained.)

Table 6.1 Proteins from total genome projects to which the amino acid sequence of ORF1 had a high degree of similarity.

Organism	Protein to which ORF1 exhibited similarity	Identities (%)	Positives (%)	Amino acids*
Pseudomonas putida KT2440	NCS1 nucleoside transporter family	63	67	373
Pseudomonas aeruginosa PAO1	Probable transporter	83	88	190
Arabidopsis thaliana	Permease, cytosine/purines, uracil, thiamine, allantoin family	41	61	162
Streptomycetes avermitilis MA-4680	Putative allantoinase permease	39	54	198
Streptomyces coelicolor A3(2)]	putative integral membrane transporter	38	54	193
Burkholderia fungorum-	Cytosine/uracil/thiamine/allantoin permease	35	62	201

(* Number of amino acids over which similarity was observed, - direct submission to NCBI Microbial Genomes Annotation Project)

The amino acid sequence of ORF1 showed similarity to sequences annotated as putative transport proteins on the total genomes of *P. putida* KT2440, *P. aeruginosa* PAO1, *A. thaliana*, *S. avermitilis* MA-4680, *S. coelicolor* A3(2), and *B. fungorum* (Nelson *et al*. 2002, Stover *et al*. 2000, Haas *et al*. 2002, Omura *et al*. 2001, Bentley *et al*. 2002) (Table 6.1). This suggested that the function of the protein encoded by ORF1 might be linked to transport of pyrimidines and/or allantoin (which is a derivative of hydantoin).

The presence of a gene encoding a putative dihydropyrimidinase upstream of ORF1 was determined from sequence data obtained from chromosomal fragments of mutant strain GMP3, generated by *Pst* I and *Bam* HI restriction endonuclease digestion (Figure 6.3, grey lines). These chromosomal fragments were utilized to determine the complete nucleotide sequence for the dihydropyrimidinase gene as illustrated in Figure 6.3. Primers prGM21 and prGM22, designed based on the sequence data generated, were used to amplify the coding region of *dhp* and the PCR product sequenced to ensure no errors had occurred during amplification (Figure 6.3). The nucleotide and amino acid sequence of the dihydropyrimidinase from RU-KM3$_S$ are depicted in Appendix 6.2.

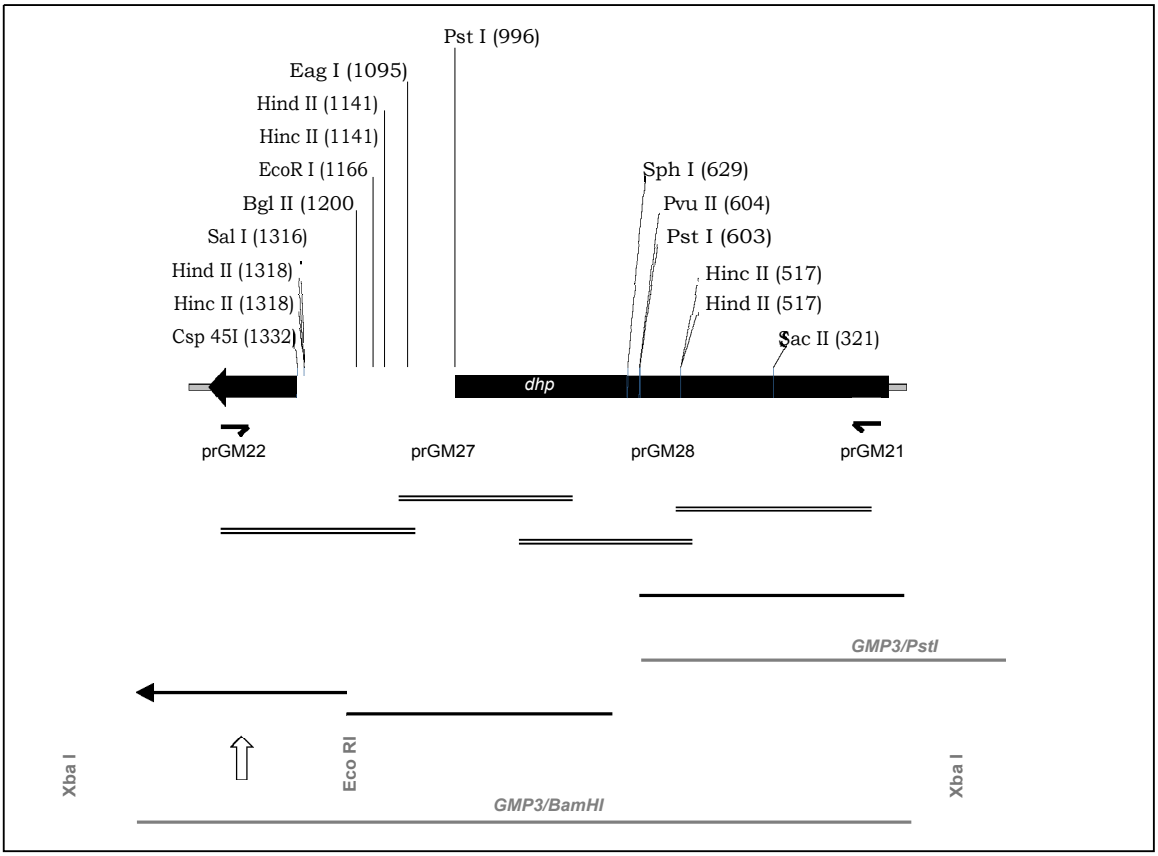

Figure 6.3 Approach for determining the nucleotide sequence of the gene encoding the dihydropyrimidinase enzyme. (Grey lines depict genomic fragments of mutant strain GMP3 isolated by complete digestion of the chromosomal DNA of GMP3 with restriction endonuclease *Bam* HI or *Pst*I. Arrows represent sequenced regions and the direction thereof: solid and double lines where chromosomal DNA from GMP3 and wild type strains were used as templates respectively. Hollow arrows indicate the chromosomal fragment of GMP3 from which the sequence was generated and half-arrows depict the primers utilized and their corresponding locations for annealing.)

Bioinformatic analysis of the sequence data revealed an open reading frame of 1140bp encoding 479 amino acids that was designated *dhp.* The calculated molecular mass of the protein encoded by *dhp* was 61 196Da. Analysis of the nucleotide sequence, of approximately 400bp, flanking the terminal end of *dhp* revealed similarity to putative oxidoreductases or dihydroorotate dehydrogenase proteins annotated on the total genome databases of *Pseudomonas putida* KT2440 (Nelson *et al*. 2002), *Pseudomonas aeruginosa* PAO1 (Stover *et al*. 2000), *Mesorizobuim loti* (Kaneko *et al*. 2000), *Sinorhizobium meliloti* 1021 (Capela *et al.* 2001), and *Brucella suis* 1330 (Paulsen *et al*. 2002) (Table 6.2).

Table 6.2 Gene loci from total genome projects to which the nucleotide sequence upstream of the *dhp* exhibited a high degree of similarity.

Organism	Gene loci	Identity (%)	Base pairs*
P. aeruginosa PAO1	Probable oxidoreductase	90	367
P. putida KT2440	Putative dihydroorotate dehydrogenase	90	367
M. loti	Probable oxidoreductase	82	281
B. suis 1330	Dihydroorotate dehydrogenase family protein	81	267
S. meliloti 1021	Putative oxidoreductase iron-sulphur protein	80	302

(* Number of base pairs over which similarity was observed)

The open reading frame for the probable oxidoreductase annotated in the total genome of *P. aeruginosa* PAO1 is located next to the open reading frame annotated as a dihydropyrimidinase gene. However, on the total genome sequence for *P. putida* KT2440, the open reading frame flanking the dihydropyrimidinase was annotated as glutamate synthase.

6.3.2 Chromosomal arrangement of microbial hydantoin-hydrolysing enzymes

The genes encoding L-enantioselective (Watabe *et al.* 1992a, Wiese *et al.* 2001) and D-enantioselective (Hils *et al.* 2001, Grifantini *et al.* 1998, Nanba *et al.* 1998) hydantoin-hydrolysing enzymes have been shown to occur in clusters, as depicted in Figure 6.4, panels B and C respectively. In addition, a genetic organisation of a pyrimidine catabolism gene cluster from *Brevibacillus agri* NCHU1002 (Kao and Hsu 2003), illustrated in panel D of Figure 6.4, has also been identified.

The D-specific hydantoinase and *N*-carbamoylase encoding genes, *hyuH* and *hyuC* respectively, from *Agrobacterium tumefaciens* NRRL B11291 and *Agrobacterium* sp. IP I-671 have a high degree of similarity to each other with 83% and 94% amino acid sequence identity for the *hyuH* and *hyuC* genes respectively. In all three organisms, *hyuH* and *hyuC* are divergently orientated (Figure 6.4, panel C) and proposed to be transcribed from a common inter-cistronic promoter region (Grifantini *et al.* 1998, Wiese *et al.* 2001).

The L-enantioselective *N*-carbamoylases of *Pseudomonas* sp. NS671 and *Arthrobacter aurescens* DSM 3747 have 37% identity at the amino acid level, however, the hydantoinase enzymes for these two strains differ considerably. The *Pseudomonas* sp. NS671 hydantoinase consists of two distinctly different subunits, encoded by *hyuA* and *hyuB* (Ishikawa *et al.* 1997) and exhibits similarity to *N*-methylhydantoinase whilst the *A. aurescens*

DSM 3747 hydantoinase is encoded by a single gene (Watabe *et al.* 1992a) and shows very little similarity to the hydantoinase from *Pseudomonas* sp. NS671. In contrast to the D-specific organisms described above, the hydantoinase and L-specific *N*-carbamoylase genes of *Pseudomonas* sp. NS671 and *A. aurescens* DSM 3747 are orientated in the same direction and are suggested to be translated from a polycistronic mRNA (Figure 6.4, panel B).

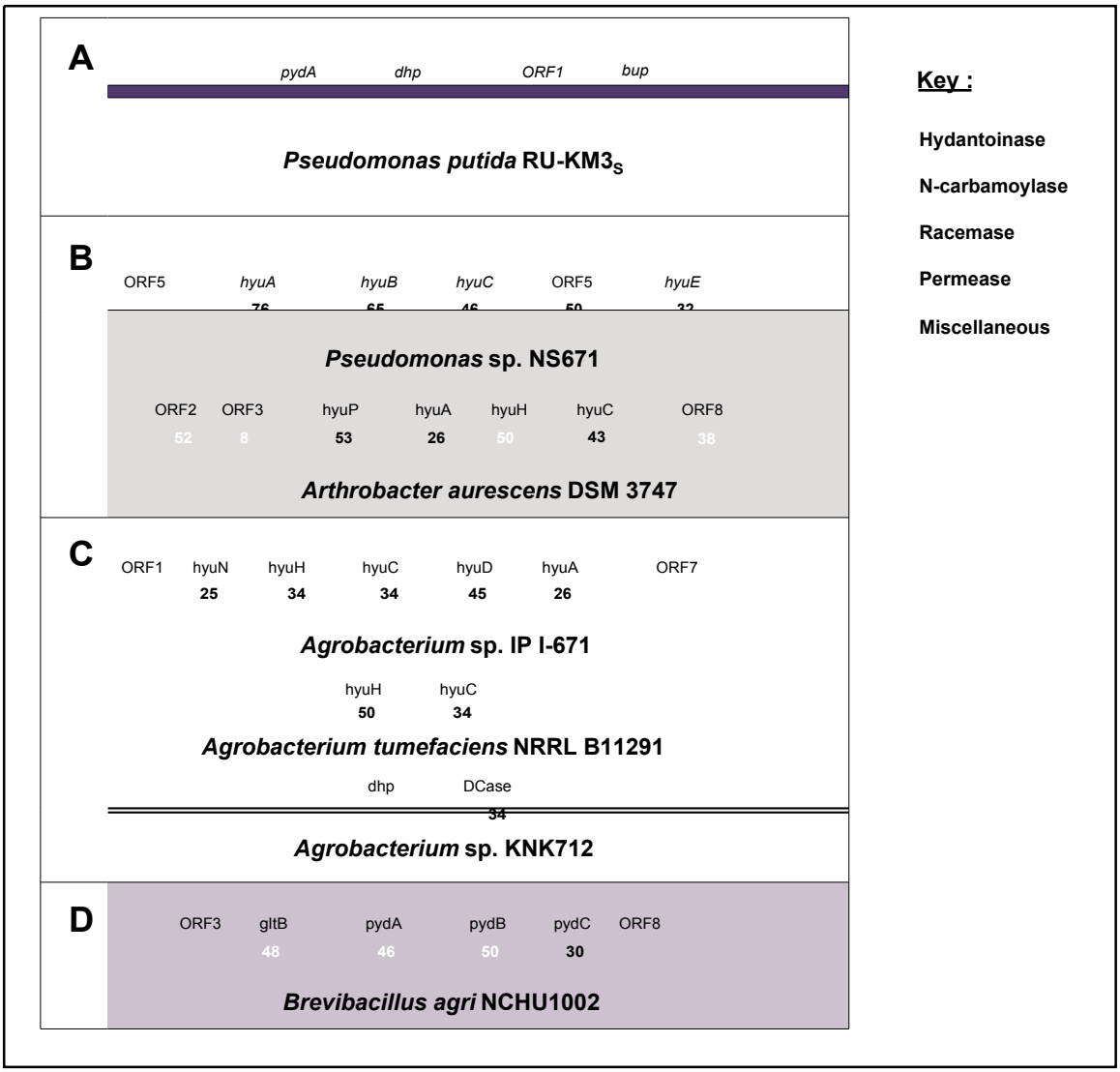

Figure 6.4 Organisation of the gene clusters encoding enzymes involved in hydantoin- and dihydropyrimidine-hydrolysis. [Gene cluster from *P. putida* RU-KM3$_S$ (panel A), L-enantiospecific hydantoin-hydrolysing (panel B), D-enantiospecific (panel C) gene clusters, and dihydropyrimidine catabolic gene cluster (panel D).]

The cluster of genes encoding the hydantoin-hydrolysing enzymes in *P. putida* RU-KM3$_S$, whilst exhibiting similarities to both the D-specific and L-specific gene clusters illustrated in panel B and C, is conspicuously unique. While the *dhp* shows greater amino acid sequence

identity (37%) with the D-hydantoinases of the *Agrobacterium* strains than with the *hyuH* of *A. aurescens* DSM 3747 (28%), the *bup* exhibits no significant similarity to either of the D-specific *hyuC* genes. In contrast, the *bup* from RU-KM3$_S$ has 24% identity at the amino acid level with the L-carbamoylase of DSM 3747, however, the *bup* and *dhp* in RU-KM3$_S$ are divergently orientated. Furthermore, the orientation of the dihydropyrimidinase and β-ureidopropionase encoding gene from RU-KM3$_S$ differ significantly from the only other bacterial pyrimidine catabolism gene cluster reported to date (Kao and Hsu 2003). Not only are the *dhp* and *bup* divergently expressed in RU-KM3$_S$ as apposed to both being expressed off a polycistronic mRNA as is the case for *B. agri* (Kao and Hsu 2003), but an additional ORF is located between these two genes.

6.3.3 Molecular analysis of the gene encoding β-ureidopropionase in RU-KM3$_S$

N-carbamoylase and β-ureidopropionase enzymes from several sources in literature were subjected to comparative analysis at the amino acid level with the β-ureidopropionase isolated from RU-KM3$_S$ using BLASTP.

Comparative amino acid sequence analysis of the β-ureidopropionase with L-enantioselective *N*-carbamoylases from *Bacillus*, *Arthrobacter*, and *Pseudomonas* species showed identities of between 34 and 39% (Table 6.3), whilst no similarity was noted between the amino acid sequences of RU-KM3$_S$ β-ureidopropionase and D-carbamoylases. The β-ureidopropionase from RU-KM3$_S$ was also compared to β-ureidopropionases from a wide variety of organisms in order to determine if these enzymes are at all homologous. BLASTP analysis showed no significant amino acid sequence similarity between the RU-KM3$_S$ β-ureidopropionase and the β-ureidopropionases of *Lycopersicon esculentum* or *Arabidopsis thaliana* (plants), *Drosophila melanogaster* (insect), *Dictyostelium discoideum* (slime mold), *Pyrococcus abyssi* (Archea), *Homo sapiens* or *Rattus norvegicus* (animals), and bacterial species *Streptococcus pneumoniae* R6, *Brucella melitensis* or *Brevibacillus agri.* However, β-ureidopropionase amino acid sequences from yeast strain *Saccharomyces kluyveri* and bacterial strains *Agrobacterium tumefaciens, Mesorhizobium loti, Rhodopseudomonas palustris,* and *Bradyrhizobium japonicum* had amino acid sequence identities to that of RU-KM3$_S$ ranging from 39 to 48% (Table 6.3). The amino acid sequence with the highest percentage identity to that of the RU-KM3$_S$ β-ureidopropionase were the *Pseudomonas putida* and *Pseudomonas aeruginosa* β-ureidopropionase amino acid sequences (Table 6.3). The majority of the β-ureidopropionase sequences mentioned above were obtained from total genome projects and as such are putative proteins assigned as β-ureidopropionases based on structural similarities to purified and characterized β-ureidopropionases.

Table 6.3 Comparison of the primary amino acid sequences of L-stereoselective *N*-carbamoylase and β-ureidopropionase enzymes with the β-ureidopropionase isolated from *P. putida* RU-KM3$_S$.

Strain	Enzyme	Identity (%)	Similarity (%)	NCBI Accession number	Reference
P. putida KT2440	BUP	87	92	NP-746162	Nelson *et al.* 2002
*P. aeruginosa P*AO1	BUP	84	89	NP-249135	Stover *et al.* 2000
R. palustris CGA009	BUP	48	61	CAE27186	Larimer *et al*. unp*
M. loti	BUP	45	60	NP_103174	Kaneko *et al*. 2000
A. tumefaciens C58	BUP	40	53	NP_357528	Goodner *et al*. 2001
S. kluyveri	BUP	39	54	AAK60518	Gojkovic *et al*. 2001
B. japonicum USDA 110	BUP	39	53	BAC48588	Kaneko *et al*. 2002
B. stearothermophilus NCIB8224	NCAAH	39	52	CAA69999	Batisse *et al*. 1997
B. stearothermophilus NS1122A	NCAAH	38	51	JN0885	Mukohara *et al*. 1993
Pseudomonas sp. NS671	NCAAH	37	51	Q01264	Watabe *et al.* 1992a
B. kaustophilus CCRC11223	NCAAH	37	50	AAN31517	Hu *et al*. 2003
A. aurescens DSM 3747	NCAAH	34	47	AAG02131	Wiese *et al*. 2000

* unp : Unpublished (database source – accession BX572598.1)

(BUP: β-ureidopropionase, NCAAH: *N*-carbamoylase)

The N-terminal amino acid sequence of the only purified *P. putida* β-ureidopropionase (from *Pseudomonas putida* strain IFO 12996) reported in literature (Ogawa and Shimizu 1994), showed 80% identity to the corresponding enzyme isolated from RU-KM3$_S$ (Figure 6.5). The total amino acid composition of the β-ureidopropionase from IFO12296 (Ogawa and Shimizu 1994) showed a similar profile to the of the RU-KM3$_S$ β-ureidopropionase with the exception of tryptophan (BUP_{IFO}:13 vs $_{BUPKM3s:4)}$, valine (BUP_{IFO}:28 vs $_{BUPKM3s:34)}$, and glutamine/glutamate (BUP_{IFO}:44 vs BUP_{KM3s}:38).

Figure 6.5 Alignment of the N-terminal amino acid sequence of the β-ureidopropionase enzymes from *P. putida* IFO 12996 and RU-KM3$_S$

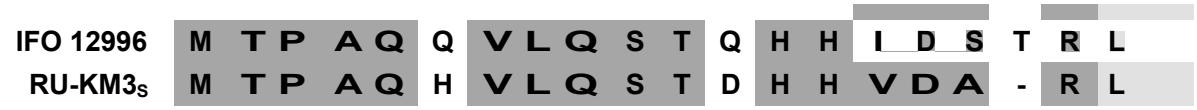

The degree of identity observed between the amino acid sequences of the β-ureidopropionase from RU-KM3$_S$ with L-carbamoylases and some, but not all, β-ureidopropionases from other sources, prompted the construction of a phylogenetic tree in order to determine the evolutionary relationship between β-ureidopropionases, D-carbamoylases, and L-carbamoylases (Figure 6.6). (An L-amino acylase from *Bacillus stearothermophilus* was used as the outgroup). The generally high bootstrap values indicate the reliability of the phylogenetic tree particularly with respect to the two major monophyletic groups which have bootstrap values of 100% (Figure 6.6).

Interestingly, two clear sub-families can be seen (Figure 6.6) with the D-carbamoylases in the one sub-family and the L-carbamoylases in the other. The β-ureidopropionases with amino acid sequence identity to the L-carbamoylases include seven bacterial species and one eukaryote (*Saccharomyces kluyveri*) (Figure 6.6). In contrast, the β-ureidopropionases to which the D-carbamoylases showed identity at the amino acid sequence level originate primarily from eukaryotic organisms including plants, mammals, and insects. In addition, β-ureidopropionases from four bacterial and one archeal source also fall into this clade (Figure 6.6).

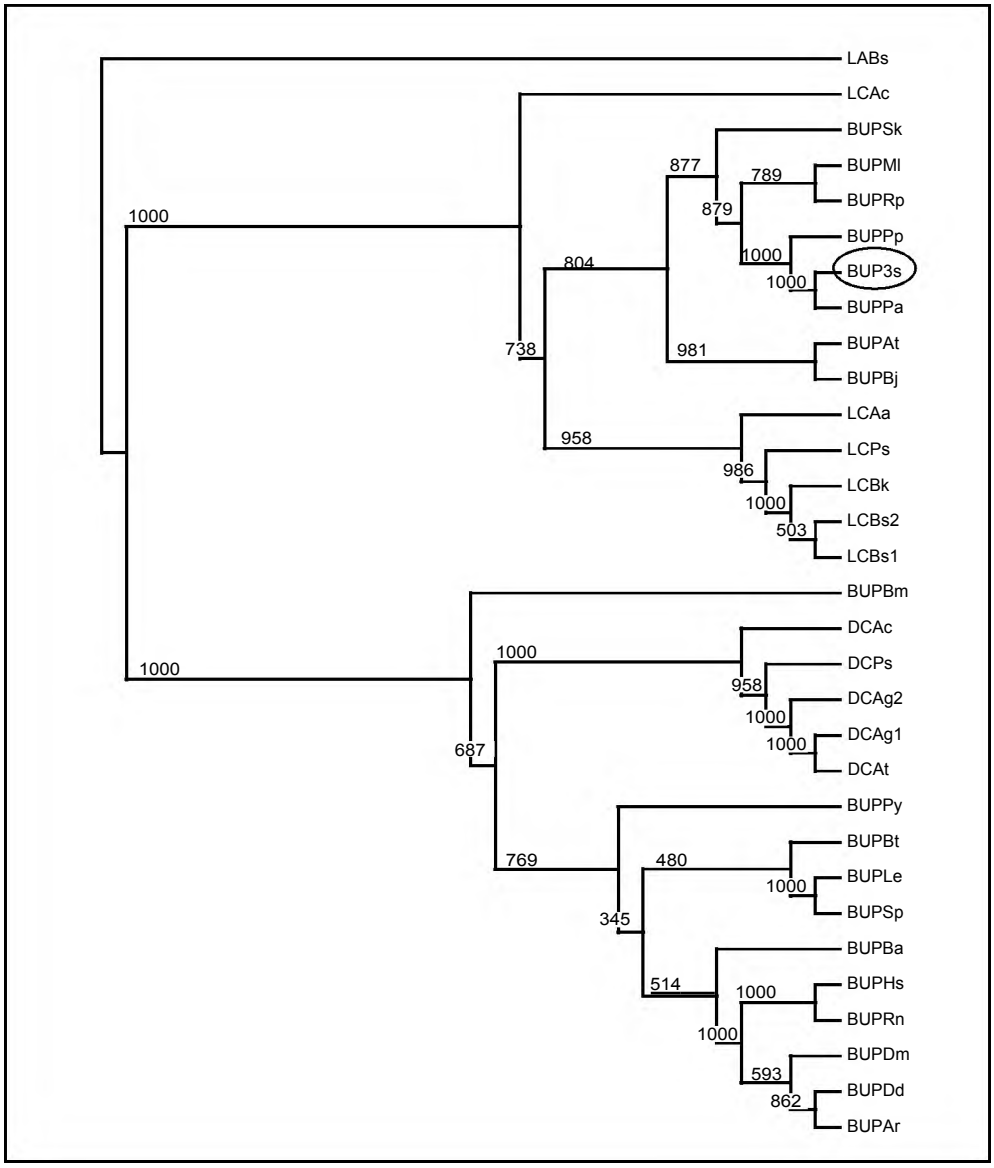

Figure 6.6 Phylogenetic tree of β-ureidopropionases, as well as L- and D-enantioselective *N*-carbamoylases. [LC: L-carbamoylase; BUP: β-ureidopropionase; DC: D-carbamoylase; LA: L-aminoacylase; 3s: *P. putida* RU-KM3$_S$; Aa: *Arthrobacter aurescens* DSM 3747; Ac: *Arthrobacter crystallopoietes* DSM 20117; Ag1: *Agrobacterium* sp. KNK712; Ag2: *Agrobacterium* sp. IP I-671; Ar: *Arabidopsis thaliana;* At (DC): *A. tumefaciens* NRRLB11291; At (BUP): *A. tumefaciens* C58; Ba: *Brevibacillus agri* NCHU1002; Bj: *Bradyrhizobium japonitum* USDA110; Bk: *B. kaustophilus* CCRC11223; Bm: *Brucella melintensis;* Bs1: *B. stearothermophilus* NS1122A; Bs2: *B. stearothermophilus* NCIB8224; Bt: *Bacteroides thetaiotaomicron* VPI-5482; Dd: *Dictyostelium discoideum;* Dm: *Drosophila melanogaster;* Hs: *Homo sapiens;* Le: *Lycopersicon esculentum;* Ml: *Mesorhizobium loti;* Pa: *P. aeruginosa* PAO1; Pp: *P. putida* KT2440; Ps (DC): *Pseudomonas* sp. KNK003A; Ps (LC): *Pseudomonas* sp. NS671; Py: *Pyrococcus abyssi;* Rn: *Rattus norvegicus;* Rp: *Rhodopseudomonas palustris* CGA009; Sk: *S. kluyveri;* Sp: *Streptococcus pneumoniae* R6) (Accession numbers and references for these sequences are listed in Appendix 7).

The amino acid sequence of RU-KM3$_S$ β-ureidopropionase was aligned using ClustalW software with three L-enantiospecific *N*-carbamoylases and three β-ureidopropionases to which the β-ureidopropionase from RU-KM3$_S$ exhibited similarity (Table 6.3). Despite the

relatively low percentage identities between some of these amino acid sequences, five significantly conserved domains can be readily identified from the alignment of these sequences relative to one another (Figure 6.7, depicted by * above the aligned amino acid sequences).

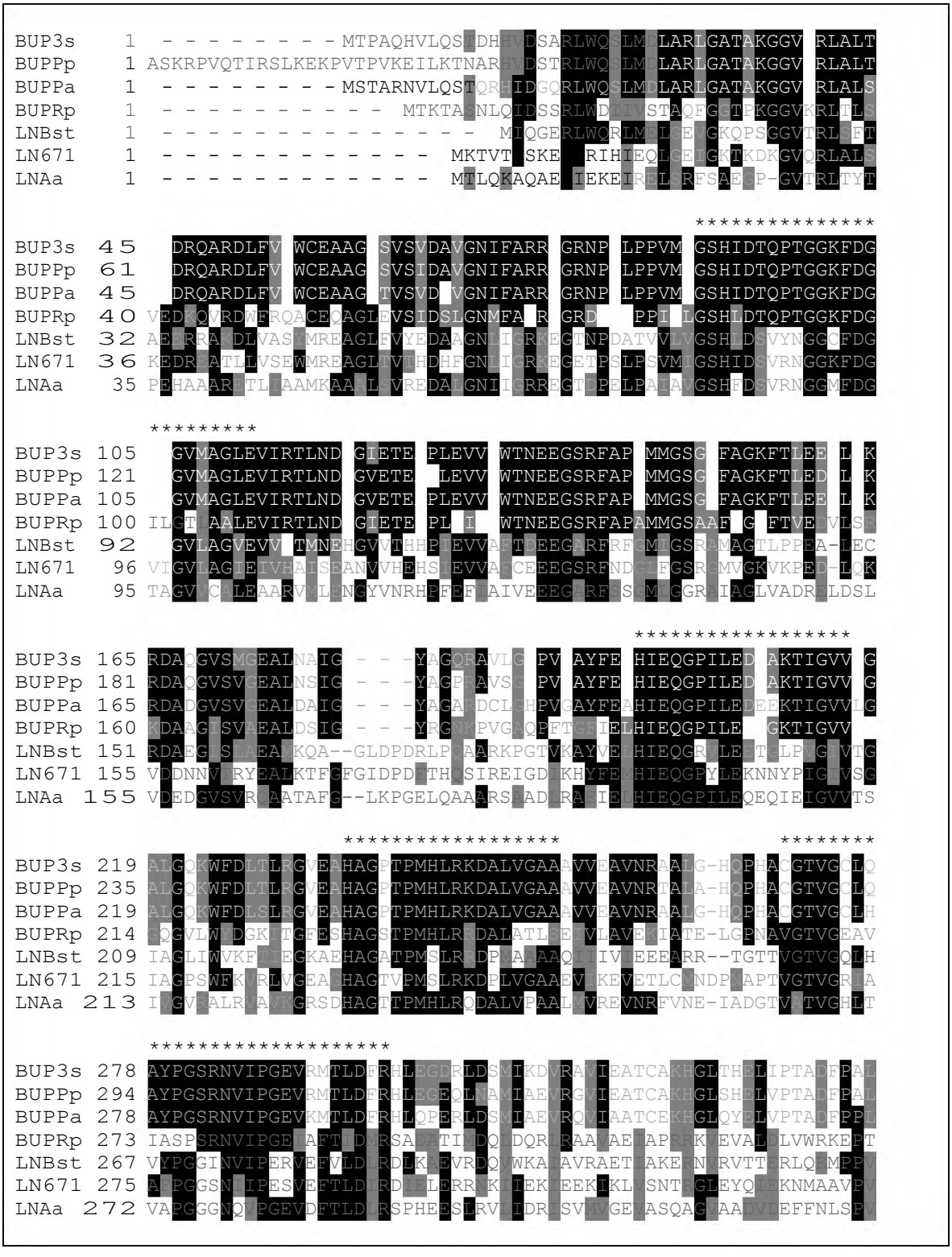

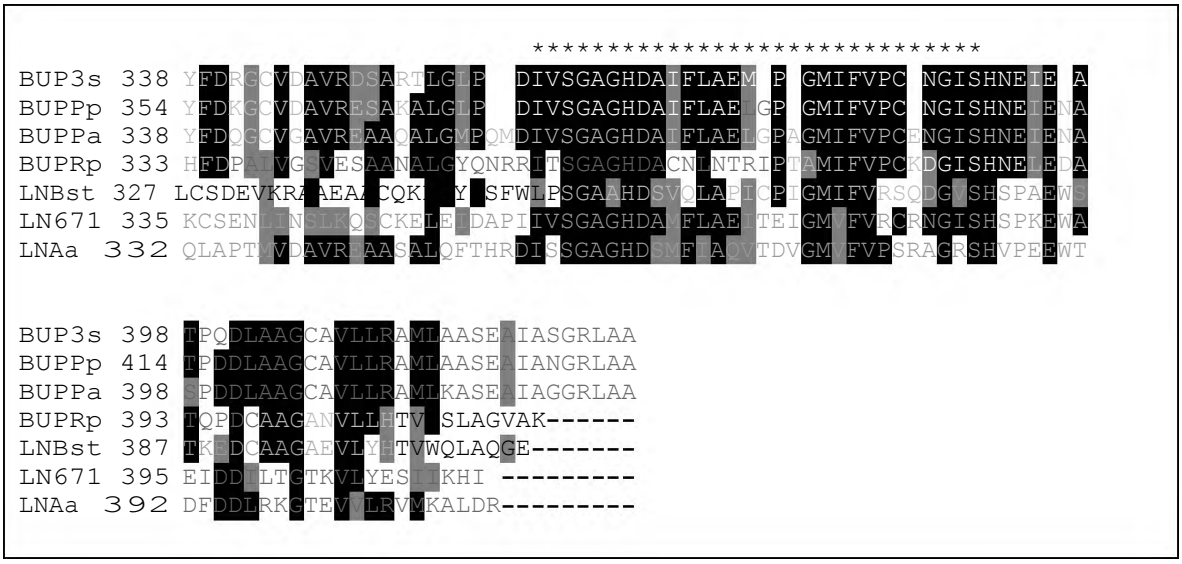

Figure 6.7 Multiple alignment of the primary amino acid sequence of L-enantiospecific N-carbamoylases and β-ureidopropionase enzymes produced by ClustalW software. (L-carbamoylases from *Bacillus stearothermophilus* NS1122A (LNBst), *Pseudomonas* sp. NS671 (LNP671), and *Arthrobacter aurescens* DSM 3747 (LNAa), and β-ureidopropionases from *Pseudomonas putida* RU-KM3$_S$ (BUKM), *Pseudomonas putida* KT2440 (BUPp), *Pseudomonas aeruginosa* PAO1 (BUPa), and *Rhodopseudomonas palustris* CGA009 (BUPRp). * : regions of high similarity.)

6.3.4 Molecular analysis of the gene encoding dihydropyrimidinase in RU-KM3$_S$

Comparative analysis of the amino acid sequence of the dihydropyrimidinase from RU-KM3$_S$ with D-enantiospecific hydantoinases reported in literature yielded identities ranging from 36% to 92% (Table 6.4). The highest percentage identity corresponded with hydantoinases from *Pseudomonas putida* strains. The extremely high similarity, 92% identity and 94% similarity at the amino acid level, with *P. putida* CCRC 12857 suggests that these two enzymes are almost identical. The hydantoinase to which the dihydropyrimidinase from RU-KM3$_S$ had the second highest percentage identity was also a *P. putida* species, DSM 84. It is interesting to note that despite a high degree of identity of 74%, the D-hydantoinase gene from *P. putida* DSM 84 was only 1104bp (encoding 368 amino acid residues) in length compared to 1440bp (encoding 479 amino acid residues) for *dhp* from RU-KM3$_S$. Somewhat lower, but still significant percentage identities to the RU-KM3$_S$ dihydropyrimidinase were observed for the remaining D-hydantoinases (Table 6.4).

Table 6.4 Comparison of the primary amino acid sequences of hydantoinase enzymes with the dihydropyrimidinase isolated from *P. putida* RU-KM3$_S$

Strain	Enantio-selectivity	Identity (%)	Similarity (%)	Accession number	Reference
P. putida CCRC 12857	D	92	94	AAC00209	Chien *et al*. 1998
P. putida DSM 84	D	74	77	AAA21752	LaPointe *et al.* 1994
B. stearothermophilus NS1122A	D*	44	63	JC2310	Mukohara *et al.* 1994
Brevibacillus agri NCHU1002	-	45	63	AAO66292	Kao and Hsu 2003
B. stearothermophilus SD-1	D	43	62	1K1D_H	Cheon *et al*. 2002
Thermus sp.	D	40	55	IGKQ_D	Abendroth *et al.* 2002a
Agrobacterium sp. IP I-671	D	37	58	AAL73199	Hils *et al.* 2001
A. tumefaciens NRRLB11291	D	37	57	CAA62549	Grifantini *et al.* 1998
Burkholderia pickettii	D	36	58	1NFG_D	Xu *et al.* 2003a
A. aurescens DSM 3745	L	28	45	AAG02130	Abendroth *et al.* 2002b
A. aurescens DSM 3747	L	28	45	AAG02130	Wiese *et al*. 2000

* : Hydrolytic activity of this hydantoinase was 10-fold higher for D-enantiomers however some degradation of L-enantioselective substrates did occur (Mukohara *et al.* 1994).

To date, amino acid sequences of four L- or non-enantiospecific hydantoinases have been reported in literature. These include hydantoinases from *Arthrobacter aurescens* DSM 3747 (Wiese *et al*. 2001), *Arthrobacter aurescens* DSM 3745 (Abendroth *et al*. 2002b), *Pseudomonas* sp. NS671 (Watabe *et al*. 1992) and *Methanococcus jannaschii* (Chung *et al*. 2002). The primary amino acid sequence of RU-KM3$_S$ dihydropyrimidinase did not share any significant amino acid sequence similarity with the hydantoinases from *Pseudomonas* sp. NS671 or *Methanococcus jannaschii*. On the other hand, the L-enantiospecific hydantoinases from *Arthrobacter aurescens* strain DSM 3745 and 3747 exhibited 96% amino acid sequence similarity with respect to one another and 28% identity with the dihydropyrimidinase from RU-KM3$_S$ (Table 6.4).

In order to understand the structure, and consequently the function, of hydantoinases, the crystal structures of D-hydantoinases from *Thermus* sp. ($Dhyd_{Th}$) (Abendroth *et al.* 2002a), *B. stearothermophilus* SD-1 ($Dhyd_{Bs}$) (Cheon *et al*. 2002) and *Burkholderia pickettii* ($Dhyd_{Bp}$) (Xu *et al.* 2003a) in addition to an L-hydantoinase from *Arthrobacter aurescens* DSM 3745 ($Lhyd_{Aa}$) (Abendroth *et al*. 2002b) have been solved. Based on studies of these crystal structures, amino acid residues involved in the stereospecific recognition, substrate binding, and catalytic cleavage of 5-monosubstituted hydantoin derivatives have been identified (summarized in Chapter 1). To determine if these residues are conserved in the dihydropyrimidinase from RU-KM3$_S$ $_{(DHPKM3s)}$, a multiple alignment of the amino acid sequences for the hydantoinases whose crystal structures have been solved was constructed (Figure 6.8). A D-hydantoinase from *Pseudomonas putida,* exhibiting high amino acid sequence similarity (94%) to the *dhp* of RU-KM3$_S$, and a dihydropyrimidinase from *Brevibacillus agri* were also included (Figure 6.8).

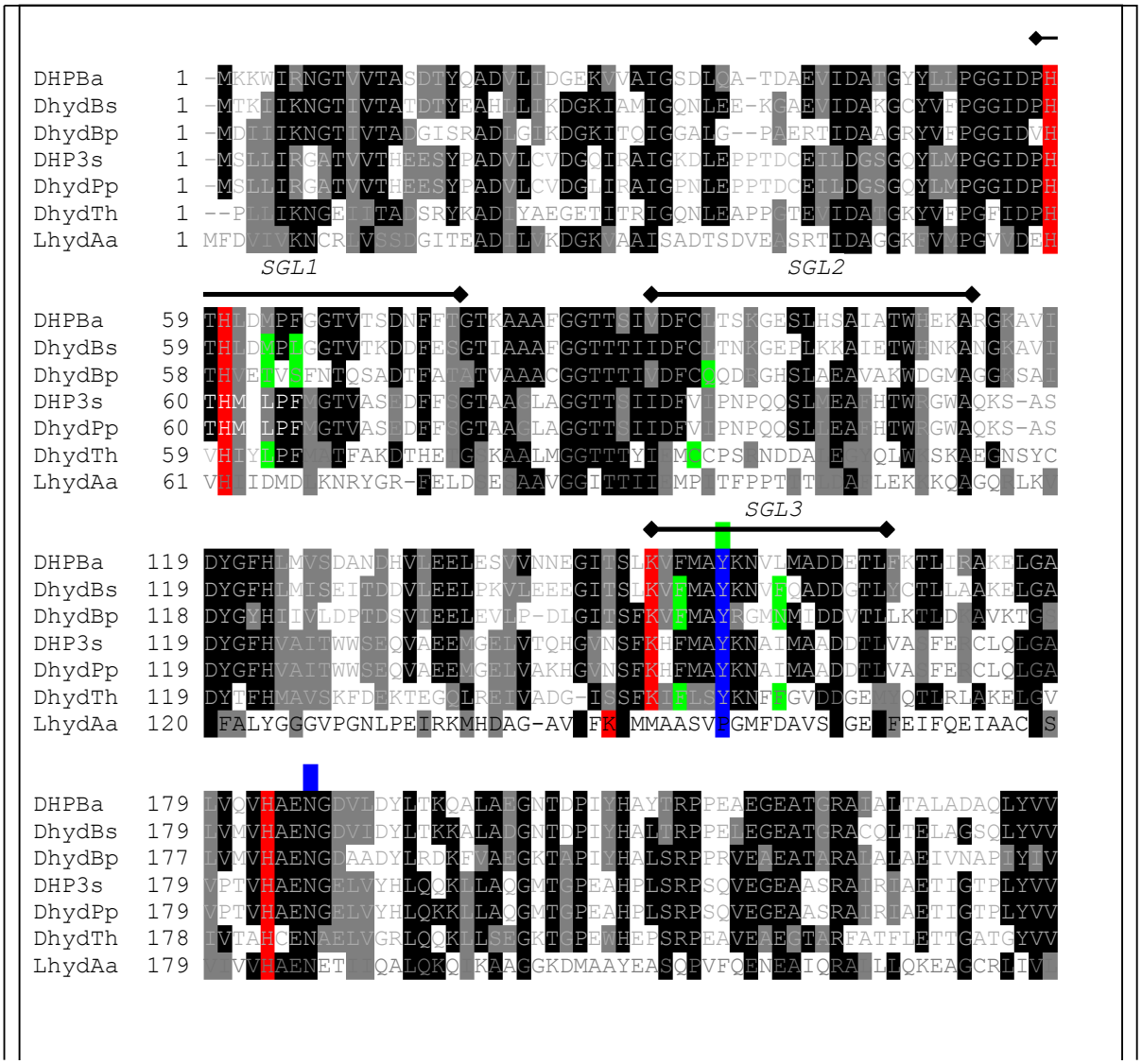

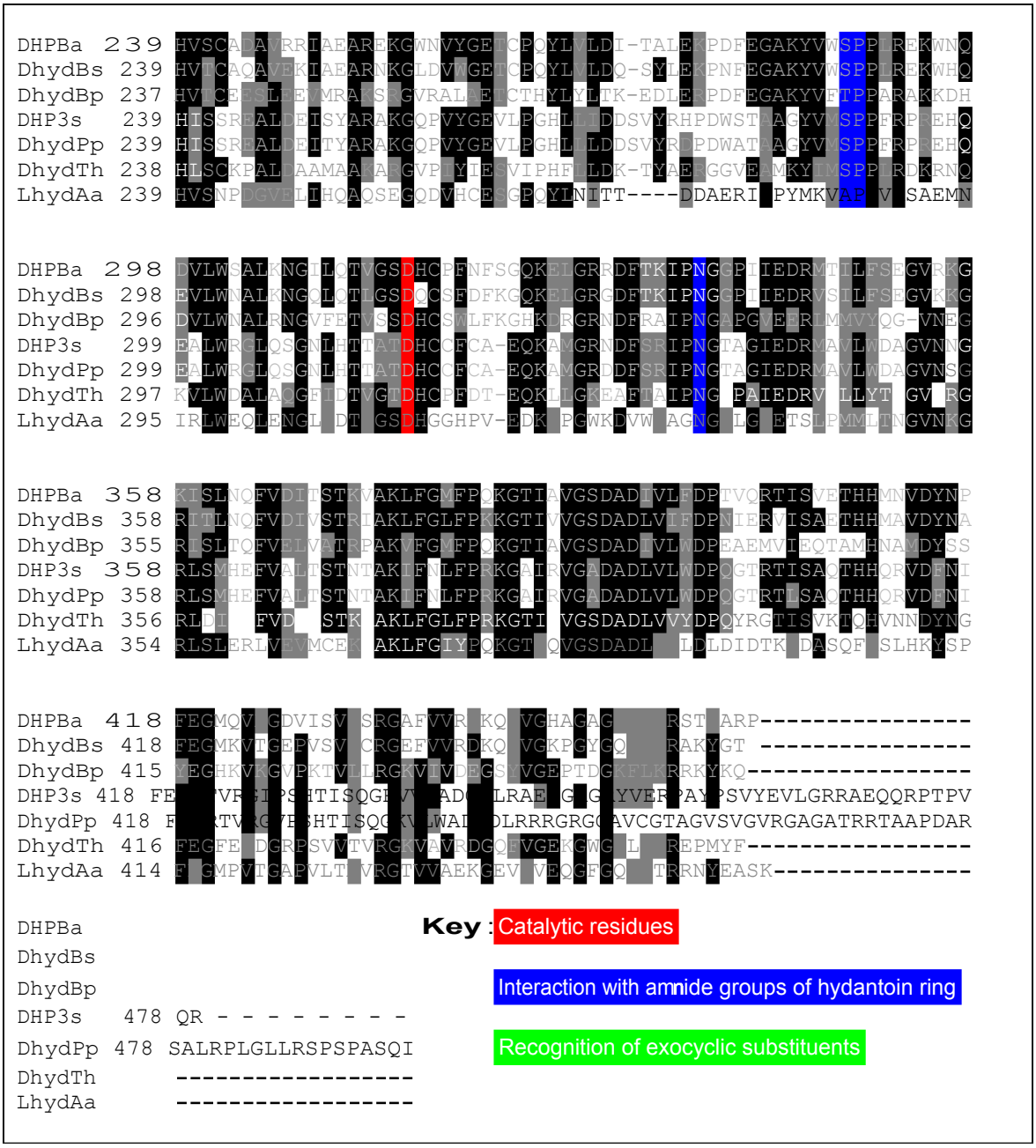

Figure 6.8 Multiple sequence alignment of the primary amino acid sequence of D-enantiospecific hydantoinases and dihydropyrimidinases. Putative catalytic residues deduced from the crystal structures of hydantoinases from *Thermus* sp., *Bacillus stearothermophilus* SD-1, and *A. aurescens* DSM 3745 are highlighted. (D-hydantoinases from *B. stearothermophilus* SD-1 (DhydBs), *B. pickettii* (DhydBp), *P. putida* CCRC 12857 (DhydPp), and *Thermus* sp. (DhydTh), as well as an L-hydantoinase from *A. aurescens* DSM 3745 (LHydAa) and dihydropyrimidinases from *P. putida* RU-KM3$_S$ (DHP3s) and *B. agri* (DHPBa). Lines above the sequence indicate the SGL regions described in Cheon *et al.* 2002.)

The catalytic site of the hydantoinase enzyme consists of six strictly conserved amino acids involved in coordination of the metal ions. The first zinc ion is coordinated by a carboxylated lysine residue (Lys^{150}), His^{183}, His^{239}, and the oxygen atoms of the hydroxide ion (-OH_3) and water. The second zinc ion is coordinated by Lys^{150}, His^{59}, His^{61}, -OH_3 and Asp^{315}

(Abendroth *et al*. 2002a). These amino acids are strictly conserved, including in DHP$_{KM3s}$, regardless of enantiospecificity (Figure 6.8, red boxes) implying that the mechanism of hydantoin hydrolysis is conserved regardless of the enantiospecificity of the enzyme (Cheon *et al*. 2002).

There are two components to substrate interaction with the hydantoinase: recognition of the functional amide groups thereby controlling the orientation of the substrate, whilst the stereochemistry of the hydantoin substrates depends on the recognition of the exocyclic substituents. The residues proposed to be involved in hydrogen-bond formation with the hydantoin ring include Ser^{288} (adjacent to a hairpin loop supported by *cis*-Pro^{289}), Asn^{336}, Tyr^{155}, and His^{183} (Abendroth *et al*. 2002a) and are highlighted in Figure 6.8 by blue boxes. Again, these residues are highly conserved throughout the hydantoinases and dihydropyrimidinases (Figure 6.8).

The recognition of the exocyclic side chain of the hydantoin substrate occurs in buried hydrophobic pockets. The hydrophobic nature of this pocket in Dhyd$_{Th}$ and Dhyd$_{Bs}$ implies that this enzyme interacts only with hydrophobic amino acid residues on hydantoins, but not charged residues. The residues forming this pocket vary between the hydantoinases reported (Figure 6.8, green boxes). In Dhyd$_{BS}$ from *B. stearothermophilus* SD-1 (Cheon *et al.* 2002), the residues that form this pocket include Met^{63}, Leu^{65}, Phe^{152}, Phe^{159} and Tyr^{155} and are located in three loops called stereochemistry gate loops or SGLs. These loops, SGL-1 (residues 62-72) SGL-2 (residues 93-100) and SGL-3 (residues 153-162) according to Cheon *et al.* (2002) are highly conserved. Conversely, while Dhyd$_{Th}$, Dhyd$_{Bs}$, $_{DHPKM3s}$ and Dhyd$_{Pp}$ are fairly homologous within these regions, Lhyd$_{Aa}$, Dhyd$_{Bp}$ and $_{DHPBa}$ show significant variability (Figure 6.8).

The amino acid residues attributed to the hydrophobic pocket in DHyd$_{Th}$ include Leu^{64}, Cys^{95}, Phe^{152}, Tyr^{155}, Phe^{159} (Abendroth *et al.* 2002a). With respect to the exocyclic substituent recognition residues in DHyd$_{BP}$, except for Phe^{150} and Tyr^{153}, the other residues differ. Both Dhyd$_{Th}$ and Dhyd$_{Bs}$ have hydrophobic residues at these positions while Dhyd$_{Bp}$ has hydrophilic residues (Thr^{62}, Ser^{64}, Gln^{93}, Asn^{157}) (Xu *et al.* 2003a) (Figure 6.8). The interaction of these suggested amino acid residues with the exocyclic residue of hydantoin substrates has been proposed to affect the substrate selectivity of the enzymes. Dhyd$_{Th}$ preferentially hydrolyses phenylic substituted hydantoin while benzylic hydantoins are hydrolysed with much lower efficiency. It is suggested that the hydrophobic pocket in Dhyd$_{Th}$ can accommodate phenylic side chains whereas benzylic or polar side chains lead to less productive binding (Abendroth *et al*. 2002a). $_{DHPKM3s}$ differs from Dhyd$_{Th}$ with an Ile^{159} instead of Phe^{159} and Ile^{95} instead of Cys^{95}. Replacement of the polar Cys with a non-polar Ile may provide an explanation for the hydrolysis of polar hydroxyphenylhydantoin by this

strain. This is supported by $_{DHPBa}$ and Dhyd$_{Bs}$ which have leucine residues in these positions and are also able to hydrolyse hydroxyphenylhydantoin (Kao and Hsu 2003, Lee *et al.* 1995). Hydroxyphenylhydantoin specificities for the Dhyd$_{Pp}$ and Lhyd$_{Aa}$, which also have leucine or isoleucine residues at this position, have not been reported. Hydantoin substrates with short side chains, such as methylhydantoin, are hydrolysed non-stereospecifically, as is the case with $_{DHPKM3s}$ (Chapter 2, Table 2.1), because neither enantiomer causes any steric clashes with the protein (Abendroth *et al.* 2002a).

6.4 DISCUSSION

A dihydropyrimidinase, encoded by *dhp*, and a β-ureidopropionase, encoded by *bup*, catalyse the ring opening hydrolysis of hydantoin and the conversion of the resultant *N*-carbamoyl amino acids to L-amino acids respectively in *P. putida* RU-KM3$_S$. A third open reading frame, ORF1, was identified between the *bup* and *dhp* gene and, based on nucleotide sequence similarity, may be involved in transport of hydantoin derivatives across the cell membrane. However, biocatalytic assays done with resting cells of a mutant strain, in which ORF1 was insertionally inactivated, indicated no decrease in the activity of the dihydropyrimidinase relative to the wild type. This implies one of two possibilities: either the protein coded for by ORF1 is not involved in transport of hydantoin or there is more than one permease pathway through which hydantoin can pass into the cell. As ORF1 and *bup* appear to be expressed as a polycistronic mRNA, which implies linked functions of the encoded proteins, the second theory is more likely. This is supported by the total genome of *P. putida* KT2440 in which ~350 cytoplasmic membrane transport systems have been found including a large repertoire of ABC amino acid transporters, 15% more than that found in *P. aeruginosa* PAO1 (Nelson *et al*. 2002). While transport of hydantoin substrate into the cell did occur when ORF1 was inactivated, it would be interesting to see if knockout of this putative transport protein would affect transport of more complex hydantoin-derivatives across the cell membrane. This would be of particularly import if the natural host is used in a biotransformation process for the production of complex amino acids from hydantoin substrates.

Excluding *P. putida* RU-KM3$_S$, the only other bacterial pyrimidine catabolism gene cluster reported to date is from *Brevibacillus agri* NCHU1002 (Kao and Hsu 2003). However, not only does the gene arrangement between these two clusters differ considerably, but the amino acid sequence of the β-ureidopropionases from these two strains do not have any similarity and, from phylogenetic analysis, are evolutionarily divergent with the β-ureidopropionase from RU-KM3$_S$ more closely related to the L-carbamoylases and the β-ureidopropionase from *B. agri* to the D-carbamoylases. Furthermore, the substrate

selectivity of the β-ureidopropionase from *B. agri* differs considerably from that of RU-KM3$_S$ with an inability to hydrolyse *N*-carbamoyl-D,L-amino acids (Kao and Hsu 2003). Moreover, despite the reasonably high levels of similarity between the dihydropyrimidinase of *B. agri* and the dihydropyrimidinase from RU-KM3$_S$, the dihydropyrimidinase enzyme from *B. agri* is unable to hydrolyse *N*-butylhydantoin or *N*-methylhydantoin (Kao and Hsu 2003) which RU-KM3$_S$, in contrast, hydrolyses very effectively (Buchanan *et al*. 2001). However, no significant differences were observed between the dihydropyrimidinases from RU-KM3$_S$ and *B. agri* with respect to the amino acid residues proposed to be responsible for substrate selectivity. This suggests there may be residues involved in interaction with the exocyclic substituents of hydantoin derivatives which have not yet been identified.

The highest amino acid sequence identity to the β-ureidopropionase from RU-KM3$_S$ was obtained with the β-ureidopropionases from *P. putida* KT2440 and *P. aeruginosa* PAO1 amino acid sequences which were both obtained from total genome projects. To date, only two β-ureidopropionases have been isolated and characterized from aerobic bacteria, viz. from *P. putida* IFO 12996 (Ogawa and Shimizu 1994) and *B. agri* NCHU1002 (Kao and Hsu 2003). As already established, the β-ureidopropionase from *B. agri* showed no amino acid sequence similarity with the β-ureidopropionase from RU-KM3$_S$. The primary amino acid sequence of the RU-KM3$_S$ β-ureidopropionase enzyme also lacked identity to several β-ureidopropionases from alternative sources. Whilst similarity to β-ureidopropionases from other kingdoms such as plant, animal, and archea bacteria is perhaps understandable, the lack of similarity to some bacterial β-ureidopropionases was somewhat surprising to discover. The β-ureidopropionase from *P. putida* IFO 12996 differs significantly to that of *B. agri* in terms of substrate selectivity as, unlike *B. agri*, it is able to hydrolyse *N*-carbamoyl-β, γ, and α-amino acids (Ogawa and Shimizu 1994). The β-ureidopropionase from RU-KM3$_S$ has been shown to hydrolyse a range of *N*-carbamoyl-α-amino acids (Buchanan *et al.* 2001) and based on its ability to convert the intermediate of dihydrouracil degradation to alanine, is capable of *N*-carbamoyl-β-amino acid hydrolysis as well. Hydrolysis of *N*-carbamoyl-α-amino acids by the β-ureidopropionase from IFO12996 is strictly L-enantiospecific (Ogawa and Shimizu 1994), a characteristic which the RU-KM3$_S$ β-ureidopropionase also exhibits with regards to *N*-carbamoyl-α-alanine (Chapter 2). It would be interesting to see if the RU-KM3$_S$ β-ureidopropionase further mimics the β-ureidopropionase from IFO12996 in L-enantioselectivity regardless of substrate utilized and in its ability to hydrolyse *N*-carbamoyl-γ-amino acids. Comparison of the N-terminal amino acid sequence of the β-ureidopropionases from IFO12996 and RU-KM3$_S$ resulted in an 80% identity match. However, the amino acid profiles of these two β-ureidopropionase enzymes do differ

somewhat and the β-ureidopropionase from IFO 12996 appears to be 12 amino acids shorter than the β-ureidopropionase from RU-KM3$_S$.

D-enantioselective *N*-carbamoylases have been shown to have some amino acid sequence identity, including strict conservation of residues proposed to be involved in the catalytic site, with the β-ureidopropionase from *Rattus norvegicus* (rat) (Nakai *et al*. 2000). However, the β-ureidopropionase from RU-KM3$_S$ showed no significant amino acid sequence identity to the D-enantiospecific *N*-carbamoylases from *Agrobacterium* sp. IP I-671, NRRL B11291, KNK712 (Hils *et al*. 2001, Grifantini *et al*. 1998, Nanba *et al*. 1998) or *Pseudomonas* sp. KNK003A (Ikenaka *et al*. 1998a). Neither do the amino acid sequences of the *N*-terminal region of the D-carbamoylases from *Comamonas* sp. EC22C (Ogawa *et al*. 1993) and *Blastobacter* sp. A17p-4 (Ogawa *et al*. 1994b) exhibit any similarity to that of β-ureidopropionase from RU-KM3$_S$. This lack of identity between the amino acid sequences of D-carbamoylases and the β-ureidopropionase from RU-KM3$_S$ is not entirely surprising as the β-ureidopropionase from *Pseudomonas* sp. (Ogawa and Shimizu 1994) has been shown to strictly L-enantiospecific, as opposed to D-enantiospecific. In addition, the inability of D-carbamoylases to hydrolyse the natural substrate of β-ureidopropionase, namely β-ureidopropionic acid (Nakai *et al*. 2000, Ogawa *et al.* 1994b) has been documented. It is interesting to note that the L-*N*-carbamoylases from *Pseudomonas* sp. NS671, *A. aurescens* DSM 3747, and *Bacillus kaustophilus,* to which β-ureidopropionase from RU-KM3$_S$ exhibits ≥34% identity, are unable to hydrolyse the natural substrate of this enzyme namely β-ureidopropionic acid (Ishikawa *et al*. 1996, Hu *et al*. 2003, Wilms *et al*. 1999). The remaining L-*N*-carbamoylases described in Table 6.3 were not analysed for the ability to hydrolyse β-ureidopropionic acid.

Phylogenetic analysis of D-carbamoylases, L-carbamoylases, and β-ureidopropionases revealed two distinct sub-families of D-carbamoylases and L-carbamoylases with β-ureidopropionases co-grouping with both sub-families. The β-ureidopropionase from RU-KM3$_S$ showed no significant amino acid sequence similarity to D-carbamoylases or the β-ureidopropionases grouped in the same sub-family. By contrast, similarity to all the L-carbamoylases, albeit low, and all the β-ureidopropionases grouped with L-carbamoylases to the β-ureidopropionase from RU-KM3$_S$ was observed.

The dihydropyrimidinase from *P. putida* RU-KM3$_{S\ (DHPKM3s)}$ showed high identity with D-enantiospecific hydantoinases, especially those from *P. putida* strains, and to a lesser degree an L-enantiospecific hydantoinase from *Arthrobacter aurescens* DSM 3745. The crystal structures of three D-hydantoinases and one L-hydantoinase to which DHP$_{KM3s}$

exhibits identity have been solved (Abendroth *et al*. 2002a, Cheon *et al.* 2002, Xu *et al.* 2003a, Abendroth *et al*. 2002b).

The amino acid residues involved in stereospecific recognition, binding and catalytic cleavage of 5-monosubstituted hydantoin derivatives have been identified using the determined crystal structures and homology to the catalytic action of a related enzyme, dihydroorotase (Abendroth *et al*. 2002a, Cheon *et al.* 2002, Xu *et al.* 2003a, Abendroth *et al*. 2002b). The amino acids (Lys^{150}, His^{183}, His^{239}, His^{59}, His^{61}, Asp^{315}) and the metal ions involved in the catalytic site are strictly conserved irrespective of the stereo- or substrate-specificity of the enzyme. The residues responsible for interaction with the hydantoin ring are also highly conserved throughout. However, differences do occur in the hydrophobic pocket proposed to be involved in recognition of the exocyclic side chain of the hydantoin substrate. These discrepancies in amino acid residues may provide an explanation for differences in substrate-selectivity between these enzymes, however, site-directed mutagenesis of these residues needs to be done in order to conclusively identify these residues as responsible for substrate-selectivity. It would be interesting to see if, by changing these selected amino acid residues to the corresponding amino acids in other hydantoinase enzymes, substrate selectivity would be consistent with that of the model enzyme.

Another potential target area for further analysis is the C-termini of the hydantoinase and dihydropyrimidinase enzymes. The C-terminus of the dihydropyrimidinase from RU-KM3$_S$ and the D-hydantoinase from *P. putida* CCRC12857 are significantly longer than the remaining aligned sequences by 18 to 19 and 34 to 35 amino acid residues respectively. Deletion analysis of the D-hydantoinase from *P. putida* CCRC 12857 indicated that the last 32 amino acid residues from the C-terminal end of the enzyme are essential for activity (Chien *et al*. 1998). Furthermore, D-hydantoinases from *B. stearothermophilus* strains SD-1 and NS1122A were remarkably similar in amino acid sequence (88% amino acid similarity) but differed significantly in the C-terminus (Kim *et al.* 1997). However, the hydantoinase from *B. stearothermophilus* SD-1 is reported to be strictly D-enantiospecific whilst *B. stearothermophilus* NS1122A hydantoinase is non-stereoselective implying that the C-terminal region plays an important role in determining the biocatalytic properties of these enzymes (Kim *et al.* 1997). The C-terminus is also implicated in the quaternary structure of the hydantoinase enzyme as deletion of this region in the hydantoinase from *B. stearothermophilus* GH2 resulted in the formation of a dimer instead of a tetramer as is the case with the wild type enzyme (Kim and Kim 1998a). Cheon *et al.* (2002) reported that the dimers of *B. stearothermophilus* SD-1 are further dimerized to form tetramers using the N-terminal β-sheet which includes the N- and C-termini. It would be interesting to see what

effect the deletion or alteration of the C-terminus of the dihydropyrimidinase from RU-KM3$_S$ would have on the activity, specificity, and/or structure of the enzyme.

This is the first report of a dihydropyrimidinase and β-ureidopropionase enzyme working in tandem to hydrolyse hydantoin derivatives to the corresponding amino acids. While the amino acid sequence of the dihydropyrimidinase from RU-KM3$_S$ corresponded well with those reported in literature, the biophysical characteristics of the respective enzymes differed. Of greater interest is the β-ureidopropionase which is significantly different to β-ureidopropionases and *N*-carbamoylases reported in literature and, due to its L-enantioselectivity, is of considerable interest for the production of L-amino acids.

The biocatalytic production of enantiomerically pure amino acids from hydantoin derivatives is finding increasing application in industry requiring enzyme systems with improved or novel biocatalytic activities. Thus, strain RU-KM3$_S$, isolated from the environment and found to express high levels of hydantoin- and *N*-carbamylglycine-hydrolysing activity, was selected for further study. The principle objective was to determine the industrial potential of the hydantoin-hydrolysing enzyme system of RU-KM3$_S$ in terms of the biocatalytic potential and distinctiveness of the system. Thus the first step was to determine the broad biocatalytic properties of the enzyme system (substrate selectivity, enantioselectivity, optimal reaction parameters, etc.). *P. putida* strain RU-KM3$_S$ was selected for this study due to the apparent L-selectivity and preference for aliphatic substrates of the enzyme system. The overriding focus of the research described in this thesis was to confirm that the enzymes differed from those reported in the literature through molecular determination of their genes.

7.1 Hydantoin-hydrolysing activities in *Pseudomonas* isolates

To date, only three *Pseudomonas* isolates have been reported with both hydantoinase and *N*-carbamoylase activities. *Pseudomonas* sp. AJ-11220 which expresses a D-hydantoinase and D-carbamoylase (Yokozeki *et al.* 1987b,c), *Pseudomonas* sp. NS671 with a non-enantioselective hydantoinase and L-enantioselective *N*-carbamoylase (Ishikawa *et al.* 1993), and *Pseudomonas putida* IFO 12996 from which a D-hydantoinase and a β-ureidopropionase have been purified (Ogawa and Shimizu 1994, Ogawa *et al.* 1994c). While some biochemical characteristics of these enzymes overlap with those of the hydantoin-hydrolysing enzyme system in RU-KM3$_S$, significant dissimilarities occur in all cases particularly with respect to substrate selectivities. Furthermore, the genes coding for the hydantoin-hydrolysing enzyme system have only been elucidated for *Pseudomonas* sp. NS671 to which the dihydropyrimidinase from RU-KM3$_S$ exhibited no similarity and the β-ureidopropionase showed minimal similarity (37% amino acid sequence identity). Thus, this study is the first report of a complete gene cluster, containing a dihydropyrimidinase and β-ureidopropionase, which are responsible for the hydrolysis of hydantoin to amino acids.

Analysis of the complete genome of *P. aeruginosa* PAO1 revealed a similar gene cluster to that of RU-KM3$_S$ while the corresponding operon in *P. putida* KT2440 contains a confirmed frameshift in the *dhp* gene (Stover *et al.* 2000, Nelson *et al.* 2002). In addition, the genes flanking this operon in *P. putida* strain KT2440 and RU-KM3$_S$ differ. This reflects the plasticity of bacterial genomes and that of *P. putida* KT2440 in particular which contains an additional 36 putative transposable elements in comparison to that found in the genome of *P. aeruginosa* PAO1 (Nelson *et al.* 2002). As dihydropyrimidinase and β-ureidopropionase are involved in pyrimidine metabolism and are ubiquitous in bacteria, it may be surprising that

these enzymes have not been isolated for the purpose of hydantoin-hydrolysis more frequently. This may be due to the substrate-selectivity of these enzymes as, for example, not all β-ureidopropionases are capable of hydrolysing *N*-carbamyl-α-amino acids (Kao and Hsu 2003). Alternatively, as observed in RU-KM3$_S$, the regulation of this operon may be complex and, under conditions used to screen for hydantoin-hydrolysing organisms, may be repressed.

7.1.1 Comparative analysis of the RU-KM3$_S$ dihydropyrimidinases

Of the hydantoinase enzymes isolated from *Pseudomonas* species, all exhibit D-enantioselectivity barring that of *Pseudomonas* sp. NS671 with a non-enantioselective hydantoinase (Watabe *et al.* 1992a). However, this hydantoinase differs considerably from the corresponding enzyme in RU-KM3$_S$ in that it is reported to consist of two subunits, encoded on a large plasmid, and to be ATP-dependent (Ishikawa *et al*. 1993, Watabe *et al.* 1992a). Comparative analysis of the amino acid sequence of the dihydropyrimidinase isolated from RU-KM3$_S$ with hydantoinases reported in literature revealed a high percentage of identity with the D-hydantoinases from *P. putida* CCR 12857 (Chien *et al.* 1998) and *P. putida* DSM 84 (LaPointe *et al*. 1994) with amino acid sequence identities of 92% and 74% respectively. However, except for cloning the gene encoding the D-hydantoinase and expression in *E. coli*, no extensive fundamental biochemical characterization of the D-hydantoinase from *P. putida* CCRC 12857 has been reported in literature. With respect to the D-hydantoinase from *P. putida* DSM 84, differences when compared to the dihydropyrimidinase from RU-KM3$_S$ in terms of metal ions affecting enzyme activity, optimal temperature and pH for hydrolytic activity, and substrate preferences were observed (Morin *et al*. 1986b).

The enantioselectivity of the dihydropyrimidinase from RU-KM3$_S$ was determined based on hydrolysis of D- or L-methylhydantoin. However, analysis of the crystal structure of the dihydropyrimidinase (D-hydantoinase) from *Thermus* sp., to which the dihydropyrimidinase from RU-KM3$_S$ exhibited 40% identity and 55% similarity in amino acid sequence, suggests that methylhydantoin is hydrolysed non-stereoselecitively, due to the lack of steric hindrance, while derivatives with larger exocyclic substituents are hydrolysed D-enantioselectively (Abendroth *et al.* 2002a). This implies that for hydantoin substrates with large side chains, such as hydroxyphenylhydantoin, hydrolysis occurs D-enantioselectively in RU-KM3$_S$ cells. However, hydroxyphenylhydantoin is hydrolysed both to the intermediate as well as the hydroxyphenylgycine end product by RU-KM3$_S$ (Buchanan *et al*. 2001). This suggests that either the hydantoinase is indeed non-stereoselective or the enantioselectivity of the β-ureidopropionase is substrate dependent allowing for hydrolysis of D-*N*-carbamylhydroxyphenylglycine. The former option is most likely for two reasons: firstly, *N*-

carbamoylases have been found to be strictly D- or L-enantioselective with no substrate-dependent enantioselectivities reported, and secondly, the β-ureidopropionase from RU-KM3$_S$ only exhibited amino acid sequence homology with L-carbamoylases and some β-ureidopropionases whilst the dihydropyrimidinase exhibited similarity to both D-, L-, and non-enantioselective hydantoinases. In addition, the only β-ureidopropionase for which stereoselectivity in terms of *N*-carbamylamino acid-hydrolysis has been determined is that from *Pseudomonas putida* IFO 12996 which was shown to have strict L-enantioselectivity (Ogawa and Shimizu 1994).

The amino acid residues identified by Abendroth *et al*. (2002a,b), Cheon *et al.* (2002), and Xu *et al*. (2003) as responsible for the catalytic activity of the enzymes, as well the orientation of the substrate, are conserved in the dihydropyrimidinase from RU-KM3$_S$. According to Cheon *et al.* (2002), the residues which form the hydrophobic pocket attributed with recognition and binding of the exocyclic side chain of the hydantoin derivatives, and thus control substrate selectivity and enantioselectivity, are located in three stereochemistry gate loops (SGL1, SGL2, SGL3). Analysis of the amino acid residues proposed to be responsible for substrate selectivity of the hydantoinase enzymes revealed two residues within SGL2 and SGL3, at positions 159 and 95, which differ between the enzymes from *Thermus*, *B. strearothermophilus* SD-1, and RU-KM3$_S$ and which may account for the varying abilities of these enzymes to hydrolyse hydroxyphenylhydantoin. Site-directed mutagenesis of these residues would conclusively determine if this is true. Furthermore, by replacing the entire SGL region from one enzyme by that belonging to another with alternative substrate preferences, and determining if the substrate preference of the constructed enzyme would mimic that of the enzyme from which the SGL regions originated, would also be informative.

7.1.2 Comparative analysis of the RU-KM3$_S$ β-ureidopropionase

The β-ureidopropionase isolated from RU-KM3$_S$ showed no primary amino acid structure similarity to any of the D-carbamoylases reported in literature whilst varying degrees of similarity was observed with L-carbamoylases. The highest similarity of the RU-KM3$_S$ β-ureidopropionase was observed with β-ureidopropionases from other bacterial sources, which were predominantly identified from total genome sequence data and were not analysed for *N*-carbamylamino acid hydrolysing activity. Interestingly, unlike hydantoinases, phylogenetic analysis of the β-ureidopropionases, D- and L-carbamoylases revealed a clear subdivision of D-carbamoylases and L-carbamoylases. This formation of “sub-families” could be useful for establishing the probable enantioselectivities of *N*-carbamoylase sequences mined from genomic libraries.

While the β-ureidopropionases from *P. putida* IFO 12996 and RU-KM3$_S$ do have significant similarities, some differences can be observed when comparing their biochemical characteristics suggesting that these two enzymes are distinct from one another. It should be noted however that the β-ureidopropionase from *P. putida* IFO 12996 was characterised as a purified protein whilst RU-KM3$_S$ β-ureidopropionase activity was analysed in the context of whole cells. The differing environments under which these enzymes were tested may have had some effect on the response of the respective enzymes to the biocatalytic parameters analysed. However, analysis of the N-terminal amino acid sequence and the total amino acid composition supports that the β-ureidopropionases from RU-KM3$_S$ and IFO 12996 are not identical.

The β-ureidopropionase purified from *P. putida* IFO 12996 was shown to have L-enantioselective *N*-carbamylamino acid hydrolytic activity proving that β-ureidopropionase is not synonymous with D-carbamoylase as was at first thought (Ogawa and Shimizu 1994). Data obtained with the β-ureidopropionase from RU-KM3$_S$ supports this. However, it would be interesting to see if the β-ureidopropionases which showed similarity with the D-carbamoylases, based on phylogenetic analysis, would not perhaps be D-enantioselective with respect to *N*-carbamylamino acid hydrolysis.

7.2 Potential industrial application

Of the two enzymes isolated from RU-KM3$_S$, the β-ureidopropionase is of greater interest with respect to potential industrial application. Not only does it differ from reported enzymes but, the literature does not report that β-ureidopropionases have been utilized in industry to produce amino acids. As such, the β-ureidopropionase from RU-KM3$_S$ is of interest. In addition, the β-ureidopropionase from RU-KM3$_S$ is capable of hydrolysing *N*-carbamyl-α-amino acids and, as preliminary data suggests, *N*-carbamyl-β-amino acids as well. This could be useful for the production of amino acids with chiral centres at the α- and β-carbon (e.g. threonine and isoleucine) which occur as four stereoisomers and are therefore very difficult to synthesize chemically and purify to an optically pure form (Ogawa *et al.* 1999). The β-ureidopropionase from *P. putida* IFO 12996 was also observed to hydrolyse *N*-carbamyl-γ-amino acids (Ogawa and Shimizu 1994). If this is true for the β-ureidopropionase from RU-KM3$_S$, it would further extend the range of applications of this enzyme.

In RU-KM3$_S$ cells, the β-ureidopropionase activity is limited as it is dependent on the *N*-carbamylamino acid intermediate produced by the dihydropyrimidinase. By co-expression or fusion of the β-ureidopropionase with an L-enantioselective hydantoinase the productivity of the β-ureidopropionase may be greatly enhanced.

The mutant strains of RU-KM3$_S$ in which the *dhp* or *bup* genes have been insertionally inactivated were shown to exhibit complete loss of hydantoin-hydrolysing activity. These mutants may therefore be valuable, as an alternative to *E. coli*, for the screening of genomic libraries for hydantoin-hydrolysing genes. Using *P. putida* RU-KM3$_S$ as a heterologous host for the expression of hydantoinase and/or *N*-carbamoylase genes is advantageous as the strain is more robust than *E. coli*, and, as evidenced by the high levels of native expression of *dhp* and *bup*, it is capable of surviving over-expression of pyrimidine-degrading enzymes within the cell.

7.3 Limitations of traditional methods for the isolation of genes encoding hydantoin-hydrolysing enzymes

Isolation of the genes encoding *dhp* and *bup* in RU-KM3$_S$ by complementation studies in *E. coli* proved to be unsuccessful. This may be attributed to several factors including: a) over-expression of enzymes responsible for nucleotide degradation could potentially be highly toxic to the cell, b) screening criteria selected against metabolically burdened recombinant cells which exhibited reduced growth rates, c) poor expression of *Pseudomonas* genes in *E. coli*, d) instability of the insert DNA resulting in loss of genetic information. The instability of genes heterologously expressed in *E. coli* was observed by loss of insert, or deletions of DNA segments within the insert of the recombinant plasmid, not only in this study but in similar studies done in *A. tumefaciens* RU-OR as well (Hartley 2001). Plasticity of the genomic regions encoding hydantoin-hydrolysing enzymes is further illustrated by the inactivation of the *dhp* in *P. putida* KT2440 due to a frameshift mutation (which was not a sequencing artefact) (Nelson *et al*. 2002). Hils *et al*. (2001) also identified ORFs with similarities to transpositional elements flanking the gene involved in hydantoin utilization in *Agrobacterium* sp. IP I-671.

Transposon mutagenesis bypasses these negative drawbacks allowing for isolation of the genes coding for the hydantoin-hydrolysing enzymes in RU-KM3$_S$. However, at the time of screening of the transposon generated mutants, the regulatory mechanism affecting expression of the *bup* and *dhp* genes was unknown. Thus the enrichment and screening was done in minimal medium with hydantoin and glucose as nitrogen and carbon sources respectively. As a result, mutants which were isolated predominantly comprised of those with mutations in the global Ntr pathway which resulted in an inability to utilize nitrogen sources optimally. However, subsequent studies revealed that *dhp* and *bup* are regulated by CCR. By screening in the presence of glucose, mutants in which the CCR pathway was inactivated, resulting in derepression of the *dhp* and *bup*, would be selected against. This would explain why no mutants in which the CCR pathway regulating expression of these

genes was interrupted were isolated. In hindsight, glycerol would have served better as a carbon source.

7.4 Regulation of catabolic enzymes in *Pseudomonas*

In the process of isolating the *dhp* and *bup* genes in RU-KM3$_S$, several mutants were isolated which shed light on the mechanism by which the hydantoin-hydrolysing pathway is regulated in this strain. In contrast to the regulation of the hydantoin-hydrolysing enzyme system in *A. tumefaciens* RU-OR (Hartley *et al*. 2001), neither the expression or activity of the β-ureidopropionase or dihydropyrimidinase was directly affected by the nitrogen status of the cell as demonstrated by wild type activities in cells grown in good nitrogen sources and mutants strains in which key elements of the global Ntr pathway had been inactivated (i.e. NtrB, NtrC, pII uridylyltransferase).

Considering that the hydantoin-hydrolysing pathway is generally thought to be responsible for hydrolysis of a potential nitrogen source for the production of amino acids, it is surprising that the regulation of hydantoin-hydrolysing pathway in RU-KM3$_S$ was found to be directly linked to carbon catabolite repression (CCR). This was evidenced by the decreased activity levels of β-ureidopropionase and dihydropyrimidinase in medium supplemented with succinate or glucose, in addition to decreased activities subsequent to inactivation of a component of the TCA cycle. Analysis of the intergenic region between the *dhp* and ORF1/*bup* genes revealed a putative CRP-binding site which was found to function as such in *E. coli*. However, cAMP levels in *Pseudomonas* do not vary, regardless of the carbon source supplied, and CRP does not function in *Pseudomonas* as it does in *E. coli* (Collier *et al.* 1996). Thus an alternative protein which functions in a similar manner to CRP must be present in RU-KM3$_S$.

A homologue of the *E. coli* CRP protein, designated Vfr, has been isolated from *P. aeruginosa* and is 67% identical and 91% similar at the amino acid level to the *E. coli* CRP protein (West *et al.* 1994). Characterization of this protein by Suh *et al*. (2002) indicated that the Vfr binds cAMP with a similar dissociation constant as that of CRP. In addition, Vfr-cAMP complex resulted in similar repressive activities on the *E. coli lac* promoter as CRP-cAMP signifying that, in *E. coli*, Vfr functions in a similar manner to CRP. However, while Vfr functions as a global regulator of gene expression, it does not appear to be involved in CCR in *P. aeruginosa* as succinate-repression of mannitol dehydrogenase, amidase, and urocanase was not relieved by inactivation of the *vfr* gene (Suh *et al.* 2002). Conversely, the presence of a functional CRP-binding site within the promoter region of the *dhp* in RU-KM3$_S$ suggests that a protein such as Vfr, which has been shown to function in a similar manner to CRP when expressed in *E. coli*, is involved in CCR of the hydantoin-hydrolysing enzyme

system in *P. putida* RU-KM3$_S$. It would be interesting to see if inactivation of the *Vfr* gene in RU-KM3$_S$ would result in a concomitant release of the *dhp* and *bup* from CCR which would also prove that, contrary to research to date, Vfr is involved in CCR. Also, while the CRP-binding site is active in *E. coli*, deletion of the CRP-binding site within the promoter region of *dhp* in wild type RU-KM3$_S$ would confirm that the site is functional in regulating expression.

To date, the only protein shown to be directly involved in CCR in *Pseudomonas* is Crc which has been implicated in repression of genes involved in metabolism of both sugars and nitrogenated compounds (Collier *et al.* 1996). However, CCR observed in *Pseudomonas* cannot be completely attributed to the activity of Crc. This was demonstrated in *P. putida* GPo1 containing an inactivated *crc* gene which resulted in repression relief of the alkane degradation pathway observed in exponential phase of growth in rich medium. But the Crc$^-$ phenotype had no effect on the repression caused when the cells were grown in defined media with pyruvate or succinate as a carbon source (Yuste and Rojo 2001). Expression of the genes coding for the proteins in this pathway may therefore by regulated by at least two regulatory mechanisms, one of which is Crc-dependent (Yuste and Rojo 2001). A similar result was obtained with the operon involved in histidine utilization where a *crc*$^-$ genotype did not relieve CCR caused by succinate (Collier *et al.* 1996). Furthermore, while inactivation of the *crc* gene reduced repression of the alkane degradation pathway in rich medium by 6-fold, this relief was only partial (Yuste and Rojo 2001). When RU-KM3$_S$ cells were cultured in complete medium, expression of the dihydropyrimidinase and β-ureidopropionase occurred only once stationary phase of growth had been reached. As more than one mechanism can be involved in the CCR of a particular pathway, as evidenced by the alkane degradation pathway in *P. putida*, inactivation of the *crc* gene, in addition to the *vfr* gene, might shed light on this regulatory pathway.

The questions that remain are: what activates CCR pathways and how is CCR linked to nitrogen metabolism (i.e. hydantoin-hydrolysis)? Collier *et al.* (1996) proposed that CCR may be controlled by a common effector which may be in the form of intermediates of a metabolic pathway and/or a more general indicator of the metabolic state of the cell (e.g. proton motive force, availability of high energy phosphodiester bonds, etc). Studies by Dinamarca *et al.* (2002) suggest that regulation of CCR is linked to the energy status of the cell as inactivation of cytochrome *o* ubiquinol oxidase, a component of the electron transport chain, reduced the CCR observed with respect to the alkane degradation pathway in *P. putida*. However, this inactivation reduced but did not eliminate CCR which indicates that CCR in *Pseudomonas* is dependent on more than just the electron transport chain (Dinamarca *et al.* 2002).

Pseudomonads are renowned for their ability to colonise a wide diversity of ecological niches due to their capacity to utilize a vast range of substrates, including some very complex organic compounds and xenobiotics, for their growth (Stover *et al*. 2000, Nelson *et al.* 2002). While such diversity of metabolic pathways is beneficial, in order to survive in the natural environment and be competitive, expression and activity of these enzymes must be carefully controlled. The intricacy of the regulation of metabolic pathways in Pseudomonads, as compared to *E. coli* for example, is reflected by their genetic complexity. Analysis of the complete genome of *Pseudomonas aeruginosa* revealed the highest percentage (8.4%) of the total number of genes devoted to command and control systems observed in a bacterial genome (Stover *et al*. 2000).

Not only is expression of the hydantoin-hydrolysing pathway in RU-KM3$_S$ regulated by CCR but it is also dependent on induction by an inducer. In order to simplify culture conditions and decrease production costs, an attempt was made to isolate a mutant strain that exhibited inducer-independent hydantoin-hydrolysing activity. Isolated mutants GMP1 and GMP2 showed increased levels of dihydropyrimidinase activity but which were still inducible. The increased activity in mutants strains GMP1 and GMP2 under uninduced conditions cannot be ascribed to an increase in expression or activity of a second hydantoinase as *dhp* knockout mutants GMP12 and GMP13 established the dihydropyrimidinase enzyme to be solely responsible for hydantoin hydrolysis in these strains. Alternatively, the increase in activity observed in GMP1 and GMP2 may be due to an indirect mutation in a regulatory pathway or directly as a result of mutation of the *dhp* gene/promoter. However, the alignment of the promoter region of GMP1 and wild type RU-KM3$_S$ resulted in 100% identity between these two sequences. The *dhp* genes of GMP1 did contain a single mutation, Q143R, where a polar glutamine was replaced by an positive arginine residue both of which are hydrophylic. However, crystallographic analysis of dihydropyrimidinase enzymes from *Thermus* sp. (Abendroth *et al.* 2002a) does not suggest that this amino acid residue is of significant importance. This suggests that the mutation encoded in GMP1 and GMP2 resulting in the observed increased hydantoin hydrolysis is most likely due to a mutation in a pathway involved in regulation of the dihydropyrimidinase expression or activity. Screening for GMP1 and GMP2 was done in complete medium and minimal medium with glucose as a carbon source respectively which may have skewed the selection of mutant strains toward those in which CCR had been affected. As regulation of metabolic pathways in *Pseudomonas* appears to occur via more than one pathway, it would be interesting to see if a similar phenotype to GMP1/GMP2 could be achieved subsequent to inactivation of a single factor regulating CCR in RU-KM3$_S$ (e.g. Vfr or Crc).

7.5 Concluding remarks

Transposon mutagenesis proved to be a versatile and effective way in which the structural genes involved in hydantoin-hydrolysis could be elucidated. Of the genes isolated, *bup* is of particular interest due to its substrate selectivity. In addition to the structural genes, the use of transposon mutagenesis also facilitated in understanding the regulatory components of the hydantoin-hydrolysing pathway in RU-KM3$_S$. Application of this knowledge would allow for deregulation, and thus increased production, of the dihydropyrimidinase and β-ureidopropionase in the wild type strain which negates the difficulties encountered with heterologous expression systems.

Not only does elucidation of the regulatory pathways in *Pseudomonas* directly apply to hydantoin-hydrolysis but it is of interest with respect to other applications as well. Pseudomonads are metabolically extremely versatile and due to their ability to degrade a diverse range of substrates, including complex xenobiotics, have important application in bioremediation (Stover *et al*. 2000). While rapid degradation of complex compounds by *Pseudomonas* isolates can be observed in the laboratory, actual biodegradation rates of xenobiotics in the natural environment may be significantly reduced due to the presence of a more readily metabolizable substrate which results in repression of the required enzymes systems for degradation of the pollutant. Catabolite repression in *Pseudomonas* isolates has been reported for several hydrolytic pathways for hydrocarbons and aromatic compounds (Yuste and Rojo 2001). Studies done by Duetz *et al.* (1996) revealed that the TOL pathway, which is involved in the degradation of toluene and *m*- and *p*-xylene, in *P. putida* was not significantly affected when phosphate or sulphate was limited. However, under conditions of oxygen or carbon and energy limitation, high levels of expression occurred whereas ammonium-limiting conditions resulted in intermediate levels of expression (Duetz *et al*. 1996).

In conclusion, CCR in *Pseudomonas* is complex and appears to be regulated by several factors/pathways functioning independently of one another and at present is poorly understood. Elucidation of the CCR of the hydantoin hydrolysing system in *P. putida* RU-KM3$_S$ would contribute toward an improved understanding of this intricate regulatory mechanism. The mutants already isolated in this study, as well as the identification of a potential site for CCR in the *bup/dhp* promoter of RU-KM3$_S$, provides a good foundation for further analysis of CCR in this strain which can then be used as a model for other isolates.

APPENDIX 1

Minimal media

Basic minimal medium supplemented with different nitrogen sources was composed of the following :

Solution*	Volume / 1 litre	Final concentration
10x M9 Salts§	100 ml	1x
40% Glucose	25 ml	1%
Trace elements¶	10 ml	
1M $MgSO_4$	200 µl	100 µM
1M $CaCl_2$	200 µl	100 µM
4% Hydantoin❖	250 ml	1%
dddH_2O	615 ml	

For agar plates, 20g bacteriological agar or ultrapure agar was added per litre.

∗ Components autoclaved separately (20 minutes at 15 psi pressure – 121°C).

❖ Alternative nitrogen sources include 1% methylhydantoin, 1% *N*-carbamylglycine, 1% *N*-carbamylalanine, 1% glycine, 1% uracil, or 0.25% $(NH4)2SO4$ (final concentration).

§ **10x M9 Salts (per 1 litre)**

Na_2HPO_4	60 g
KH_2PO_4	30 g
NaCl	5 g

¶ **Trace elements (per 1 litre)**

Boric acid	50 mg
$MnSO_4.2H_2O$	40 mg
$ZnSO_4$	40 mg
$(NH_4)_6MO_2O_{24}.4H_2O$	20 mg
KI	10 mg
$CuSO_4$	4 mg
$FeCl_3$*	20 mg

(∗ Autoclaved separately and added to the solution when cool)

APPENDIX 2

Growth and biocatalytic assays for analysis of hydantoinase and *N*-carbamoylase activities

2.1 Resting cell biocatalytic assay

2.1.1 Culture conditions

Seed cultures were prepared by inoculation of a single colony of *P. putida* strain RU-KM3$_S$ from a hydantoin (1%) minimal medium agar plate, into 50ml minimal medium with 1% hydantoin as a sole source of nitrogen. The seed culture was then incubated at 28^{o}C, at 200rpm, for approximately 4 days. When analysing mutant strains which were unable to utilize hydantoin as a sole source of nitrogen, 5ml nutrient broth inoculated and grown overnight as above was used as a seed culture.

Once saturated, the seed culture was inoculated into nutrient broth, containing 0.1% hydantoin as an inducer (where required), such that an $_{OD600}$ of 0.02 was achieved. The cultures were then incubated at 28^{o}C, shaking, for approximately 20 hours until early stationary phase of growth was reached $_{(OD600}$ 2.5 - 3).

2.1.2 Biocatalytic assay

The cells were harvested by centrifugation at 7 500g for 10 minutes in pre-weighed centrifuge tubes. The supernatant was discarded and the cells washed in half the original culture volume with cold potassium phosphate buffer (0.1M, pH 8). After re-centrifugation as above, the wet cell mass of the resultant pellet was determined and the pellet resuspended such that a final concentration of 40mg wet cell mass/ml was achieved. This cell suspension was used to form reaction mixes as follows :

Table A2.1 Reaction components for biocatalytic assay

Components	Buffer blank (x 1)	Substrate blank (x 1)	Cell blank (x 1)	Samples (x 3)
Phosphate buffer (0.1M, pH 8)	5ml	2.5ml	2.5ml	-
Substrate dissolved in phosphate buffer (0.1M, pH 8)	-	2.5ml	-	2.5ml
Cells	-	-	2.5ml	2.5ml

The reaction mixtures were then incubated at 40^{o}C for 3 hours (unless otherwise specified) with constant shaking after which the mixtures were transferred to 1.5ml eppendorfs and centrifuged at maximum speed (13 000rpm) in a Heraeus microfuge for 3 minutes to pellet the cells. The resultant supernatant was analysed for *N*-carbamylamino acids and amino

acids using Ehrlichs and Ninhydrin colorimetric assays respectively. Units of activity were measured as µ mol/ml of product per 20mg wet cell mass per ml, and expressed as an average of 3 replicates. Hydantoinase activity was calculated as the total µ mol/ml of *N*-carbamylamino acid and amino acid produced from a hydantoin substrate whilst *N*-carbamoylase activity was expressed as µ mol/ml of amino acid produced from the *N*-carbamylamino acid intermediate.

2.1.3 Ehrlichs assay for quantification of *N*-carbamylamino acids

1ml of the supernatant was aliquoted into a test tube and 0.5ml 12% trichloroacetic acid added to stop microbial conversion of the *N*-carbamylamino acids to amino acids. The mixture was then vortexed briefly and 0.5ml Ehrlichs reagent (10% p-di-methylaminobenzaldehyde in 6N HCl) added, followed by 3ml triple distilled water. After incubation at room temperature for 20 minutes, the absorbance at 570nm was determined and the concentration of the product calculated using a standard curve of 0 – 50mM *N*-carbamylglycine or 3-ureidopropionate (Figure A2.1).

(A)

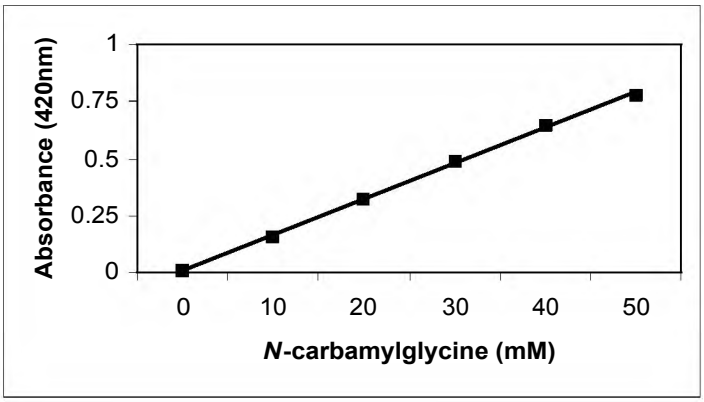

(C)

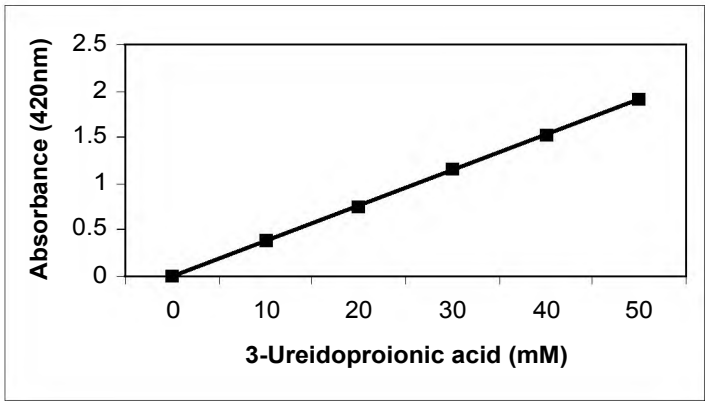

Figure A2.1 Typical standard curves for 0-50mM *N*-carbamylglycine **(A)** and 3-ureidopropionic acid **(B)** with Ehrlichs reagent

2.1.4 Ninhydrin assay for quantification of amino acids

20µ l of the reaction supernatant was aliquoted into test tubes with 0.980µ l potassium phosphate buffer (0.1M, pH 8) and 1ml ninhydrin reagent (0.8g ninhydrin and 0.12g hydrindantin dissolved in 30ml 2-methoxyethanol, before addition of 10ml 4M sodium acetate buffer, pH 5.5) was added. The samples were then placed in a boiling water bath for 15 minutes. After cooling to room temperature, 3ml 50% ethanol was added and the samples incubated for 15 minutes at room temperature. The absorbance at 570nm was then ascertained and the concentration of amino acid determined using a standard curve of 0 – 0.5mM glycine or alanine (Figure A2.2).

(Note : Ninhydrin reagent was freshly prepared for each assay and stored in a dark glass container due to its sensitivity to light)

(A)

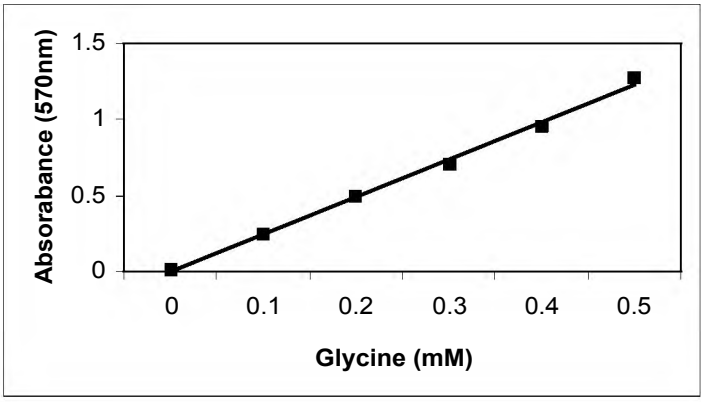

(B)

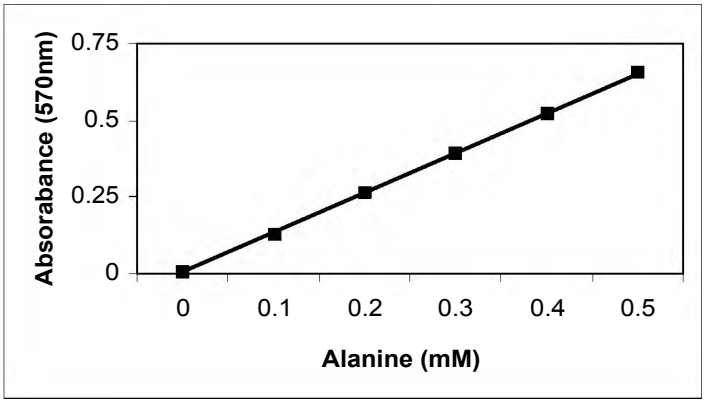

Figure A2.2 Typical standard curves for 0-25mM glycine **(A)** and alanine **(B)** with Ninhydrin reagent

2.2 Biocatalytic assays in microtitre plates

Isolates to be assayed for hydantoinase or *N*-carbamoylase activity were inoculated directly into microtitre plate wells containing 150µ l Luria broth supplemented with the appropriate antibiotic and an inducer (1mM IPTG for heterologous expression in *E. coli* and 0.1% hydantoin for *P. putida* strains) where necessary. The microtitre plates were then incubated overnight at the optimum growth temperature of the strain. Alternatively, the strains were cultured in 5ml Luria broth, overnight, at the optimal temperature for growth (37^{o}C for *E. coli* and 28^{o}C for RU-KM3$_S$) and then 200µ l aliquoted into the relevant wells in the microtitre plates.

Harvesting the resting cells was accomplished by centrifugation of the microtitre plates at 4000rpm for 15 minutes in a Megafuge 1.0R (Heraeus) (rotor/bucket cat. #: 2705/2708). The supernatant was then gently flicked out of the wells and the pellets resuspended in 200µ l 50mM hydantoin, dihydrouracil, or *N*-carbamylglycine in 0.1M phosphate buffer (pH 8) as substrates (resuspension with 0.1M phosphate buffer alone functioned as a cell blank control). The plates were then incubated at 40^{o}C for 3 hours with shaking (100rpm) after which the cells were pelleted once more by centrifugation as described above.

2.2.1 Ehrlich's assay in microtitre plates

To determine the production of *N*-carbamylamino acid, 100µ l of the biocatalytic reaction supernatant was transferred to a clean microtitre plate and 30µ l Ehrlich's reagent (10% *p*-dimethylaminobenzaldehyde in 6N HCl) added. After dilution with 100µ l distilled water, the absorbance at a wavelength of 420nm was determined on the PowerwaveX Microtitre Plate Reader (Bio-Tek Instruments, Inc.) and the *N*-carbamylamino acid concentration calculated as µ mol/ml utilizing a standard curve of *N*-carbamylglycine (10 – 50 mM) prepared via same method as the samples.

2.2.2 Ninhydrin assay in microtitre plates

Production of amino acids from the respective substrates was determined by aliquoting 10µ l of the biocatalytic reaction supernatant from each well into a fresh microtitre plate to which 40µ l 0.1M phosphate buffer (pH 8) and 50µ l 4M sodium acetate buffer (pH 5.5) were added. The plate was then incubated at 60^{o}C for 5 minutes before adding 50µ l freshly prepared ninhydrin solution (0.17g ninhydrin, 0.17g hydrindantin dissolved in 20ml 2-methoxyethanol). Following incubation at 60^{o}C for a further 20 minutes, 100µ l 50% ethanol was added to each sample and the absorbance at a wavelength of 570nm was determined using the PowerwaveX Microtitre Plate Reader. The amino acid concentration of each of the samples was calculated as µ mol/ml utilizing a standard curve of glycine (0.1 – 0.5 mM) prepared via the same method as the samples.

APPENDIX 3

Primers, plasmids, and strains utilized in this study

Table A3.1 Primers utilized in this study

Primer	Description	Sense (+) /Antisense(-)	Sequence
CH1	Primer for the 16s rRNA gene of *Pseudomonas putida*	+	GCG GAT CCGCCT AAC ACA TGC AAG TCG AAC GG
CH2	Primer for the 16s rRNA gene of *Pseudomonas putida*	-	GCG GAT CCG CGA TTA CTA GCG ATT CCA GCT TA
prGM11	Sequencing primer for pTnMod-OKm plasposon	-	TTT ACG GTT CCT GGC CTT T
prGM12	Sequencing primer for pTnMod-OKm plasposon	+	TGA GAC ACA ACG TGG CTT TC
prGM16	Internal primer for NCAAH from KM3s	+	GCG GCA AGT TCG ATG GCT GCT TCG G
prGM19	Primer for tetracycline gene from pTnMod-OTc	-	ACA ACC GCG GCC GCA CTA GTC TAG ATT T
prGM20	Primer for tetracycline gene from pTnMod-OTc	+	TTC TCC GCG GGA ATT GAT TGG CTC CAA TTC
prGM21	Primer for DHP from KM3s (with Nde site)	+	CAT ATG TCC CTG TTG ATC CGT GGC
prGM22	Primer for DHP from KM3s (with Eco RI site)	-	GAAT TCA GCG CTG AAC GGG CGT
prGM24	Primer for NCAAH from KM3s (with Nde site)	+	CAT ATG ACC CCA GCC CAG CAT
prGM25	Primer for NCAAH from KM3s (Eco RI site)	-	GAA TTC TAC GCC GCC AAG CGC CCG CT
prGM28	Sequencing primer for DHP from KM3s	+	ACA GCA CCG CCA TGC GGT CTT
prGM30	Primer for the *dhp* and *bup* promoter region	+	CGG CGG CGA TGT CGT GGT TGT A
pUCF	Primer specific for the plasmids pUC18 and pGEMT-Easy	+	CGC CAG GGT TTT CCC AGT CAC GAC
pUCR	Primer specific for the plasmids pUC18 and pGEMT-Easy	-	TCA CAC AGG AAA CAG CTA TGA C
pT7-7F	Primer specific for the plasmid pT7-7	+	GGG AGA CCA CAA CGG TTT CCC
pT7-7R	Primer specific for the plasmid pT7-7	-	CGC TGA GAT AGG TGC CTC AC

Table A3.2 *Escherichia coli* strains utilized in this study

Strain	Description	Reference
DH5α	*supE44* Δ*lac*U169(∅80*lacZ*ΔM15)*hsdR17 recA1 endA1 gyrA96 thi-1 relA1*	Sambrook *et al*. 1989
XLOLR	Δ(*mcrA*)183Δ(*mcrCB-hsdSMR-mrr*)173 *endA1 thi-1 recA1 gyrA96 relA1 lac*[F'*proAB lacI*^{q}ZΔM15 Tn10(Tet^{r})] Su^{-} (nonsuppressing) λ^{r} (Lambda resistant)	ZAP Express Predigested Gigapack Cloning Kit – Instruction manual
XL1 Blue	Δ(*mcrA*)183Δ(*mcrCB-hsdSMR-mrr*)173 *endA1 supE44 thi-1 recA1 gyrA96 relA1 lac*[F'*proAB lacI*^{q}ZΔM15 Tn10(Tet^{r})]	ZAP Express Predigested Gigapack Cloning Kit – Instruction manual
HB101	*SupE44 hsdS20*($r_B^- m_B^-$)*recA13 ara-14 proA2 lacY1 galK2 rspL20 xyl-5 mtl-1*	Sambrook *et al*. 1989

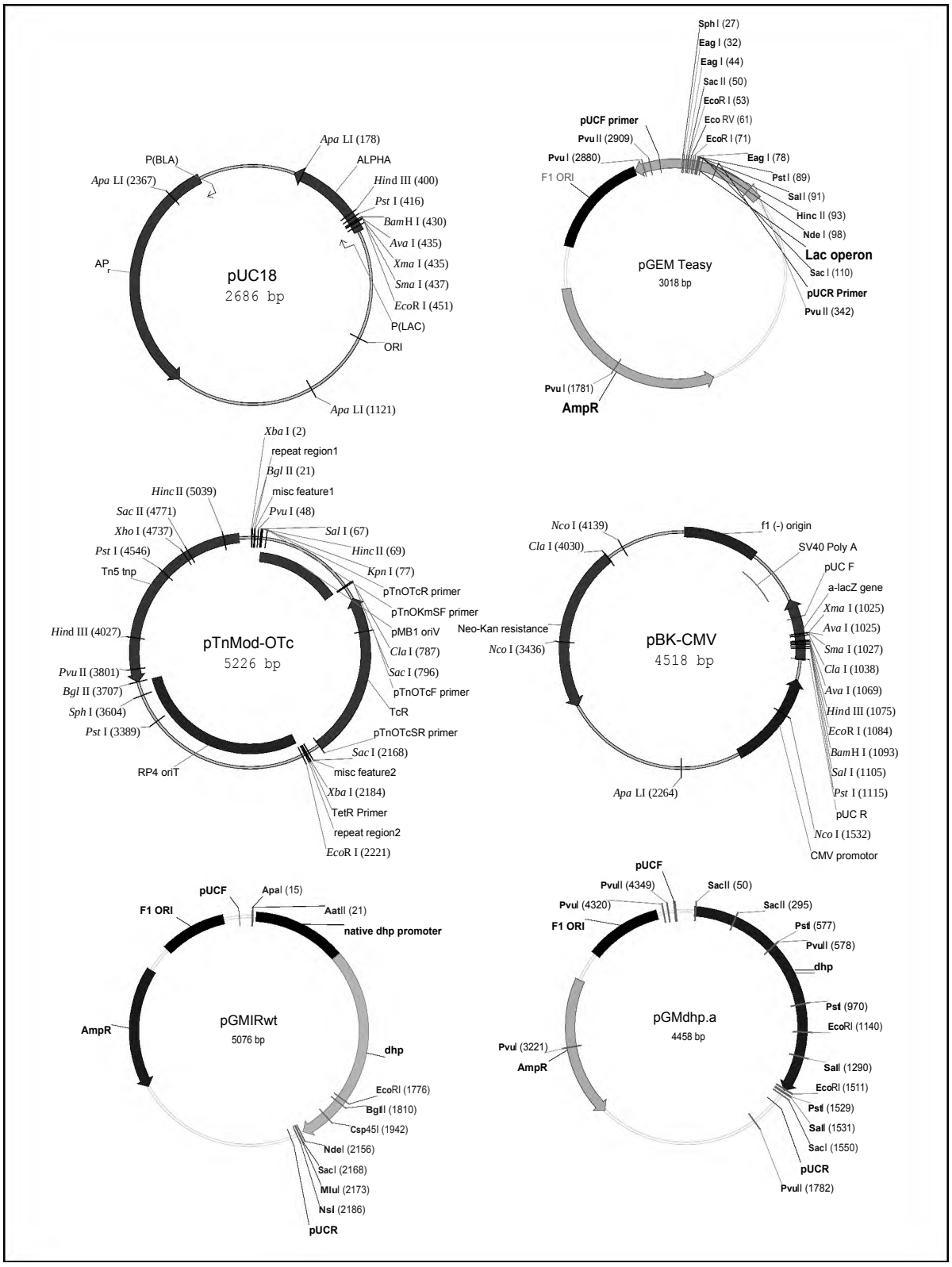

Figure A3.1 Plasmid maps of some of the constructs and vectors utilized in this study

APPENDIX 4

Preparation and transformation of competent *E. coli* cells

4.1 Preparation of competent *Escherichia coli* cells

A test tube containing 5ml of Luria broth was inoculated with the appropriate strain of *E. coli* and grown to confluence overnight at 37°C, shaking at 200rpm. Four Erlenmeyer flasks, containing 100ml Luria broth each, were then inoculated with 1.5, 1.0, 0.7, and 0.3ml of the overnight culture respectively and incubated at 37°C for approximately 2 hours until an OD_{600} of 0.6-0.8 was obtained with the culture pre-inoculated with 1.5ml overnight culture. The flasks were then cooled for 5 to 10 minutes on ice, after which the flask contents were processed separately until the final step. The flask contents were centrifuged in a Beckman centrifuge (JA14 rotor) at 5000rpm, for 10 minutes, at 4°C. The supernatant was discarded and the pellet resuspended in 50ml RF1 (100mM KCl, 50mM $MnCl_2$, 30mM CH_3COOK, 10mM $CaCl_2$, 15% glycerol, pH5.8), followed by a further 20 minute incubation on ice. The cells were once again pelleted by centrifugation as above and the supernatant discarded. All four pellets were then resuspended together in a final volume of 4ml of RF2 (10mM MOPS, 10mM KCl, 75 mM $CaCl_2$, 15% glycerol, pH 6.8). The resuspended cells were frozen and stored at –80°C in 500µ l aliquots until required.

4.2 Transformation of competent *E. coli* cells

Once thawed on ice, 150µ l competent *E. coli* cells were mixed with the plasmid DNA in a sterile eppendorf and incubated on ice for 20 minutes. The cells were then subjected to heat-shock by incubation at 42°C for 45 seconds immediately followed by placement on ice for a further 5 minutes. 1ml cold Luria broth was then added and the cells incubated at 37°C for 1 hour after which the cells were spread plated onto the appropriate selective medium.

APPENDIX 5

DNA manipulation

5.1 Plasmid DNA extraction

For initial screening purposes, selected recombinant *E. coli* colonies were cultured overnight at 37°C, with shaking, in 5ml Luria broth supplemented with the appropriate antibiotic. Plasmid DNA was extracted from these confluent cultures by the "Easyprep" method as described in Berghammer and Auer (1993). Screening for the correct plasmid construct was done by diagnostic restriction endonuclease digestion and electophoretic separation of the resultant fragments through a 1% agarose gel containing 0.5µ g/ml ethidium bromide. The buffer used for preparation and running of the agarose gel was 1x TAE (50x TAE (1L): 242g Tris HCl, 57.1ml glacial acetic acid, 100ml 0.5M Na_2EDTA, pH 8.0). Visualization of the DNA was achieved by fluorescence of the DNA bound ethidium bromide under UV light and an image captured using the Kodak DC 120 Gel Imaging System. Once a suitable culture containing the correct plasmid construct was identified, high quality plasmid DNA was extracted using the High Pure Plasmid Isolation Kit (Roche) or the Quantum Prep Plasmid Midipreps (Qiagen) according to the manufacturers specifications. This pure DNA was then used for in depth analysis and further manipulation.

5.2 Genomic DNA extraction

Genomic DNA was extracted by the detergent lysis/CTAB and organic solvent extraction method as described by Ausubel *et al.* (1983). The resultant extract was then treated with 10µ g/ml RNase A to degrade contaminating RNA and the remaining DNA precipitated by addition of 0.1 volume 3M sodium acetate (pH 5.2) and 2 volumes ice cold 96% rectified ethanol at –20°C for 18 hours. The precipitated DNA was pelleted by centrifugation (13,000rpm in a Heraeus microfuge) for 10 minutes, washed two to three times with ice cold (-20°C) 70% ethanol and the pellet dried by vacuum centrifugation (Speedvac concentrator, Savant) before being resuspended in 50 to 100µ l TE buffer (pH 7). The extracted chromosomal DNA concentration was estimated by visual comparison to phage Lambda DNA standards after electrophoresis in a 1% agarose gel containing 0.5µ g/ml ethidium bromide and visualization by UV light using the Kodak DC 120 Digital Imaging System.

5.3 PCR thermal cycling paramerters

Initial denaturation:	94°C	90s	X1
Denaturation:	94°C	45s	X30
Annealing:	X°C	45s	
Extension:	72°C	60s	
Final extension:	72°C	2min	X1

X°C : Annealing temperatures – 63°C (Chapter 2, Section 2.2.5)
57°C (Chapter 3, Section 3.2.6)
45°C (Chapter 5, Section 5.2.3)
(primers prGM24, prGM11, prGM28)
60°C (Chapter 5, Section 5.2.3)
(primers prGM19, prGM20)
55°C (Chapter 5, Section 5.2.4)

5.4 Determination of DNA sequence

The nucleotide sequence of DNA was determined from double stranded plasmid DNA by the dideoxy-chain termination method (Sanger, 1987) using the ABI Prism Big Dye Terminator Cycle Sequencing Ready Reaction Kit v1.0, v2.0, or v3.1 (PE Applied Biosystems). Sequencing primers utilized are listed in Appendix 3. The thermal cycling reaction parameters were performed according to the manufacturers instruction for the GeneAmp PCR System 9700 thermal cycler. Resultant extension products were purified by ion exchange chromatography using the DNA Clean and Concentrator columns (Zymo), and the sample dried by vacuum centrifugation (Speedvac concentrator, Savant). Pellets were resuspended in Template Suppression Reagent and the nucleotide extension products separated by capillary electrophoresis using an ABI Prism 3100 Genetic Analyser (Hitachi, Applied Biosystems) and POP6 polymer in a 30cm or 50cm capillary.

APPENDIX 6

Nucleotide and amino acid sequences of the dihydropyrimidinase, β-ureidopropionase, and ORF1 from RU-KM3$_S$

```
   1 ttcaagcagc tgattttgca tggaaaatct tgaccaattt ggcatcttgt
  51  caagtgcgtc aaaatggtga acagcctcac cattttggt g aacgccaata
 101 tatttctata aatatcaggt agttacgata gttataagct cataaattat
 151 tttcttgatc aatccatgat cagcaactag attccattct tgtcaggtct
 201 gacaggattg aaatccatcc tccagccact ggcccataac aatttcaaga
                                                 M  S  L  L  I
 251 accggcccag accggtcagc ctgcgaggaa gacggcatgt ccctgttgat
       R  G  A  T  V  V  T  H  E  E  S  Y  P  A  D  V
 301  ccgtggcgcc accgtggtaa cccatgaaga gagctatccc gctgatgtcc
      L  C  V  D  G  Q  I  R  A  I  G  K  D  L  E  P  P
 351  tgtgtgtcga tggccagatc cgcgccattg gcaaagacct cgaaccgccc
       T  D  C  E  I  L  D  G  S  G  Q  Y  L  M  P  G  G
 401  accgactgcg agatcctcga cggcagcggc cagtacctga tgcccggcgg
        I  D  P  H  T  H  M  Q  L  P  F  M  G  T  V  A
 451  catcgacccg cacacccaca tgcagttgcc cttcatgggc accgtggcca
      S  E  D  F  F  S  G  T  A  A  G  L  A  G  G  T  T
 501  gcgaagactt cttcagcggc accgccgcgg ggttggccgg cggcaccacc
       S  I  I  D  F  V  I  P  N  P  Q  Q  S  L  M  E  A
 551  tcgatcatcg acttcgtcat ccccaacccg cagcagtcac tgatggaagc
         F  H  T  W  R  G  W  A  Q  K  S  A  S  D  Y  G
 601  cttccacacc tggcgcggct gggcgcagaa gagcgcgtcc gactatggct
      F  H  V  A  I  T  W  W  S  E  Q  V  A  E  E  M  G
 651  tccacgtcgc catcacctgg tggagcgagc aggtggccga ggaaatgggc
       E  L  V  T  Q  H  G  V  N  S  F  K  H  F  M  A  Y
 701  gagctggtga cccagcacgg ggtcaacagc ttcaagcact tcatggccta
        K  N  A  I  M  A  A  D  D  T  L  V  A  S  F  E
 751  caagaacgcc atcatggccg ccgacgacac cctggtggcc agcttcgagc
      R  C  L  Q  L  G  A  V  P  T  V  H  A  E  N  G  E
 801  gctgcctgca gctgggcgcg gtgcccaccg tgcatgccga gaacggcgag
       L  V  Y  H  L  Q  Q  K  L  L  A  Q  G  M  T  G  P
 851  ctggtctacc acctgcaaca gaaactgctc gcccagggga tgaccggccc
         E  A  H  P  L  S  R  P  S  Q  V  E  G  E  A  A
 901  ggaagcacac ccgctgtcac gcccctcgca agtcgaaggc gaggctgcca
      S  R  A  I  R  I  A  E  T  I  G  T  P  L  Y  V  V
 951  gccgcgctat ccgcatcgcc gaaaccatcg gcacgccgct gtacgtggtg
       H  I  S  S  R  E  A  L  D  E  I  S  Y  A  R  A  K
1001  cacatctcca gccgcgaagc gctggatgaa atcagctatg cccgtgccaa
        G  Q  P  V  Y  G  E  V  L  P  G  H  L  L  I  D
1051  gggccagccg gtgtacggcg aagtgctgcc cggccacctg ctgatcgacg
      D  S  V  Y  R  H  P  D  W  S  T  A  A  G  Y  V  M
1101  acagcgtcta ccgccacccg gactggtcca ctgccgccgg ctacgtgatg
       S  P  P  F  R  P  R  E  H  Q  E  A  L  W  R  G  L
1151  agcccgccgt tccgcccgcg cgagcaccag gaggcgctgt ggcgtggcct
        Q  S  G  N  L  H  T  T  A  T  D  H  C  C  F  C
1201  gcagtcgggc aacctgcaca ccaccgccac cgaccactgc tgcttctgcg
      A  E  Q  K  A  M  G  R  N  D  F  S  R  I  P  N  G
1251  ccgaacagaa agccatgggc cgcaacgact tcagccgtat ccccaacggc
       T  A  G  I  E  D  R  M  A  V  L  W  D  A  G  V  N
1301  acggccggca tcgaagaccg catggcggtg ctgtgggatg cgggggtcaa
        N  G  R  L  S  M  H  E  F  V  A  L  T  S  T  N
1351  caacgggcgc ctgtcgatgc acgaattcgt cgcgctgacc tccaccaaca
      T  A  K  I  F  N  L  F  P  R  K  G  A  I  R  V  G
1401  cggcgaagat cttcaacctg ttcccgcgca agggcgccat tcgcgtgggc
```

```
      A  D  A  D  L  V  L  W  D  P  Q  G  T  R  T  I  S
1451  gccgacgccg acctggtgct gtgggacccg cagggcacgc gcacgatctc
        A  Q  T  H  H  Q  R  V  D  F  N  I  F  E  G  R
1501  tgcgcagacc caccaccagc gcgtcgactt caacattttc gaaggccgca
      T  V  R  G  I  P  S  H  T  I  S  Q  G  R  V  V  W
1551  ccgtgcgcgg cattccgagc cacaccatca gccagggtcg cgtggtatgg
       A  D  G  D  L  R  A  E  P  G  A  G  R  Y  V  E  R
1601  gccgatggcg acctgcgcgc ggagccaggc gcaggccggt atgtggaacg
        P  A  Y  P  S  V  Y  E  V  L  G  R  R  A  E  Q
1651  tccggcctac ccctcggtgt acgaggtgtt gggccgacgc gccgagcagc
      Q  R  P  T  P  V  Q  R  *
1701  agcgccccgac gcccgttcag cgctga
```

Figure A6.1 Nucleotide and amino acid sequence of the *P. putida* RU-KM3$_S$ dihydropyrimidinase and the upstream promoter region. (The open reading frame for *dhp* is underlined, with the initiation and termination codons in bold typeface, and the deduced amino acid sequence illustrated above the nucleotide sequence. The putative Shine-Dalgarno is written in bold italic typeface, the putative –10 and –35 consensus sequences (bold typeface) are double underlined while the possible CRP-binding site is blocked. The numbers on the left indicate nucleotide positions.)

```
   1 agattttcca tgcaaaatca gctgcttgaa tcctggcttc gaggcgctgg
  51 ccgcgccact gaaaaaccag gctgcaccaa ggtgaaaccg ggtgtggggg
 101 ccagggccgg cccagggcgg cgcgaatacc cggcgaaggc atcagcgtgc
 151 cttcgccggg cgcagttgaa agccttgcag atcagttgat tacctccggt
 201 cggcggcggc cgtcgggcag gcccaggcca acccggcacg caaattgagt
 251 acggccacaa ccgccaggcc ggaccggagg tgcagtactg gtggtgtaga
 301 gactccggcc atcgcattag cccgatgagc gaacaattag aaaaatctgg
               M  Q  Q  S  R  S  E  V  V  E  Q  D  G
 351  agaaggcccc atgcaacaga gcagatcggn nnnnnnnnnn nnnnnnnnnn
      L  F  E  L  S  S  G  S  D  V  L  D  S  P  R  Y  N
 401  nnntcgagct gtcgtcgggc agtgacgtgc tcgacagccc acgttacaac
       H  D  X  A  A  D  Q  V  C  T  S  A  P  G  N  K
 451  cacgacntcg ccgccgacca agtgtgcacc agcgcacctg gaaacaaatg
        A  H  H  P  R  C  G  W  A  C  P  S  A  W  P  T
 501  ggcacatcac ccgcgctgtg ggtgggcatg tccatctgcg tggcccacct
      Y  T  L  G  G  V  L  T  A  Y  F  G  L  S  V  G  E
 551  acaccctggg cggtgttctc acagcctact tcggcttgag cgtgggcgag
       A  L  L  A  I  L  T  G  Q  P  D  R  P  D  P  A
 601  gcgctgctgg cgatcctgac tggccaacct gatcgtcctg atcccgctga
        A  Q  C  L  P  R  H  Q  V  R  H  T  V  P  R  T
 651  cgctcaatgc cttccccggc accaagtacg gcataccgtt ccccgtactg
      A  A  V  L  V  R  H  P  W  V  Q  R  A  L  P  D  P
 701  ctgcggtcct cgttcggcat ccttgggtcc aacgtgcctt gcctgatccg
       R  G  G  R  L  W  L  V  R  H  P  D  D  V  R  R
 751  cgcggtggtc gcctgtggct ggttcggcat ccagacgatg ttcggcggct
        G  H  P  P  V  P  H  L  F  L  G  S  V  F  D  G
 801  tggccatcca cctgttcctn nnnnnnnnnn nnnnnnnnnn nnnnnnnnnn
      W  K  A  L  G  G  T  G  E  V  I  G  F  M  V  F  W
 851  nnnnnnccct gggcggcacc ggcgaagtga tcggcttcat ggtgttctgg
       A  L  N  L  W  V  V  L  R  G  A  E  S  I  K  W
 901  gcgctcaacc tgtgggtggt actgcgcggc gccgagtcga tcaaatggct
        E  T  L  S  A  P  L  L  V  A  V  G  F  G  L  L
 951  tgagacgctc tcggcgccgc tgctggtggc cgtgggcttt ggcctgctgt
      F  W  A  L  P  H  M  S  M  T  E  L  L  A  Q  P  P
1001  tctgggcctt gccgcacatg tcgatgaccg agttgctggc ccagccgccc
```

```
       K  R  P  E  G  A  S  V  V  S  Y  F  C  A  G  L
1051   aagcgcccgg aaggggcgag cgtggtcagc tacttctgcg ctgggctcac
         A  M  V  G  F  W  A  T  L  S  L  N  I  P  D  F
1101   ggcgatggtc ggcttctggg ccacgctgtc gctgaacatc ccggacttca
       S  R  Y  A  K  S  Q  K  D  Q  I  L  G  Q  I  F  G
1151   gccgctatgc caaaagccag aaggaccaga tcctcgggca gatcttcggc
         L  P  L  T  M  F  L  F  A  A  L  G  V  V  M  T
1201   ctgccgctga ccatgttcct gttcgcggcg ctgggtgtgg tgatgaccgc
         A  S  A  S  L  V  G  E  T  V  S  D  P  V  S  L
1251   cgcctcggcg tcgctggtgg gcgaaacggt gtcggatccg gtgagcctga
       I  G  K  I  Q  S  P  G  W  V  A  L  A  M  A  L  I
1301   tcggcaagat ccagagcccg gggtgggtag cgttggccat ggcgctgatc
         V  I  A  T  L  S  T  T  P  R  A  T  S  C  H  R
1351   gtcatcgcca cgctgtcgac cacaccgcgg gcaacatcgt gtcaccgacc
         T  T  S  R  T  S  P  A  P  D  R  A  Q  P  R  G
1401   aacgacttcc agaacatcgc ccgcgcctga tcgggcgcaa ccgcgcggtg
       V  A  X  R  L  H  R  S  G  A  D  G  L  K  K  L  G
1451   tggctgancg gcttcatcgg tctggngctg atggnnnnnn nnnnnnnnnn
         L  I  V  S  D  L  S  L  E  S  V  Y  S  N  W  L
1501 nnnnnnnnnn nnnnnnnnnn nnnnnnnnnn nnnnnnnnnn nnnnnnnnnn
         L  G  Y  S  F  X  P  A  X  A  D  C  R  N  H  G
1551   nnnnnnnngg ntattccanc ctgctngggc cgattgccgg aatcatggtg
       G  G  L  L  P  D  P  A  X  E  A  G  P  G  R  V  V
1601   gtggactact tcctgatccg gcgncagaag ctggacctgg ccgggttgta
         P  R  R  R  L  P  G  L  E  L  G  G  F  A  A  F
1651   ccgcgacgac gtctacccgg cctggaactg ggcggctttg ccgccttcgg
         V  P  V  T  L  T  V  M  A  I  G  N  S  S  F  S
1701   cgtgccggtg acgctgaccg tgatggccat tggcaacagc agtttcagct
       W  F  Y  D  Y  G  W  F  T  G  S  L  L  G  G  A  L
1751   ggttctacga ctatggctgg tttaccggct cgctgctcgg gggcgcgttg
         Y  Y  A  L  G  G  V  A  V  R  G  A  A  R  L  A
1801   tactacgccc tgggggggcgt ggcggtgcgt ggggcggcgc ggttggccaa
         P  L  P  *
1851   gccgttgccc tga
```

Figure A6.2 Nucleotide and amino acid sequence of the putative transport protein (ORF1) from *P. putida* RU-KM3$_S$ and the upstream promoter region. (The open reading frame for ORF1 is underlined, with the initiation and termination codons in bold typeface, and the deduced amino acid sequence illustrated above the nucleotide sequence. The putative Shine-Dalgarno is written in bold italic typeface, the putative –10 and –35 consensus sequences (bold typeface) are double underlined, the amino acid sequence from the corresponding putative transport protein in *P. putida* KT2440 is written in grey where sequence data for ORF1 was unavailable. The numbers on the left indicate nucleotide positions.)

```
   1  tgataccgcg ttggccccat cgccggcaag ccggctccca caaggtcagc
  51 gatgttccct ttgggagccg gcttgctggc gatgaggccc gaaaatgaat
                                        M  T  P  A  Q
 101 gcagataaca aaaacgcctg aggagacaac ccaatgaccc cagcccagca
       V  L  Q  S  T  D  H  H  V  D  S  A  R  L  W  Q
 151   tgtcctgcaa tccaccgacc accatgtcga cagcgcccgc ctgtggcaat
       S  L  M  D  L  A  R  L  G  A  T  A  K  G  G  V  C
 201   cgctgatgga cctggcgcgc cttggcgcca ccgccaaggg cggcgtatgc
         R  L  A  L  T  D  L  D  R  Q  A  R  D  L  F  V
 251   cgcctggccc tgaccgacct cgaccgccag gcccgcgacc tgttcgtcga
         W  C  E  A  A  G  C  S  V  S  V  D  A  V  G  N
```

```
301  atggtgcgaa gccgctggct gcagcgtcag cgtcgatgcg gtgggcaaca
       I  F  A  R  R  P  G  R  N  P  K  L  P  P  V  M  T
351  tcttcgcccg ccggccggga cgcaacccca agctgccgcc cgtgatgacg
        G  S  H  I  D  T  Q  P  T  G  G  K  F  D  G  C
401  ggcagccaca tcgacaccca gcccaccggc ggcaagttcg atggctgctt
          G  V  M  A  G  L  E  V  I  R  T  L  N  D  L  G
451  cggggtgatg gcgggcctgg aagtgatccg caccctcaac gacctgggca
       I  E  T  E  A  P  L  E  V  V  V  W  T  N  E  E  G
501  tcgagaccga agcccccctg gaagtggtgg tgtggaccaa cgaagagggc
        S  R  F  A  P  C  M  M  G  S  G  V  F  A  G  K
551  tcccgctttg cgccgtgcat gatgggttcg ggcgtattcg ccggcaagtt
          T  L  E  E  T  L  A  K  R  D  A  Q  G  V  S  M
601  caccctggag gaaaccctgg ccaagcgcga cgcccagggg gtcagcatgg
       G  E  A  L  N  A  I  G  Y  A  G  Q  R  A  V  L  G
651  gcgaggccct caatgccatc ggctatgccg gccagcgtgc ggtgcttggc
        H  P  V  G  A  Y  F  E  A  H  I  E  Q  G  P  I
701  cacccggtgg gggcttactt cgaagcgcat atcgaacagg ggccgatcct
          E  D  Q  A  K  T  I  G  V  V  L  G  A  L  G  Q
751  cgaagaccag gccaagacca tcggcgtggt gctgggggca ctgggccaga
       K  W  F  D  L  T  L  R  G  V  E  A  H  A  G  P  T
801  agtggttcga cctgaccctg cgtggcgtcg aagcccacgc cggcccgacg
        P  M  H  L  R  K  D  A  L  V  G  A  A  A  V  V
851  ccgatgcacc tgcgcaagga cgccctggtc ggcgctgcgg cggtggtcga
          A  V  N  R  A  A  L  G  H  Q  P  H  A  C  G  T
901  ggcggtcaat cgggctgcgc tcggccatca gccgcatgcc tgcggcaccg
       V  G  C  L  Q  A  Y  P  G  S  R  N  V  I  P  G  E
951  tgggttgcct gcaggcctat ccgggttccc gcaacgtgat accgggcgag
        V  R  M  T  L  D  F  R  H  L  E  G  D  R  L  D
1001 gtgcgcatga ccttggactt ccgccacctg gagggcgatc gactggattc
          M  I  K  D  V  R  A  V  I  E  A  T  C  A  K  H
1051 gatgatcaaa gacgtgcgcg cggtgatcga ggcgacctgt gccaagcatg
       G  L  T  H  E  L  I  P  T  A  D  F  P  A  L  Y  F
1101 gtcttaccca tgagctgatt cccacggccg atttcccggc gctgtacttc
        D  R  G  C  V  D  A  V  R  D  S  A  R  T  L  G
1151 gaccgtggtt gcgtcgatgc cgtgcgcgac tcggcgcgca ccctgggctt
          P  Y  M  D  I  V  S  G  A  G  H  D  A  I  F  L
1201 gccgtacatg gacatcgtca gcggggcagg gcatgacgcg atcttcctgg
       A  E  M  G  P  A  G  M  I  F  V  P  C  E  N  G  I
1251 ccgaaatggg gccggcgggg atgatcttcg taccgtgcga aaacggcatc
        S  H  N  E  I  E  N  A  T  P  Q  D  L  A  A  G
1301 agccacaacg agatcgagaa cgccacgccg caagacctgg cggcggggtg
          A  V  L  L  R  A  M  L  A  A  S  E  A  I  A  S
1351 tgcggtgttg ttgcgggcga tgctggcggc gtcggaggcg atcgccagcg
       G  R  L  A  A  *
1401 ggcgcttggc ggcgtag
```

Figure A6.3 Nucleotide and amino acid sequence of the β-ureidopropionase from *P. putida* RU-KM3$_S$. **(**The open reading frame for *bup* is underlined, with the initiation and termination codons in bold typeface, and the deduced amino acid sequence illustrated above the nucleotide sequence. The numbers on the left indicate nucleotide positions.)

APPENDIX 7

Table A7.1 Accession numbers and references for the enzymes depicted in the phylogenetic tree (Figure 6.5)

Organism	Enzyme	NCBI Accession number	Reference
A. tumefaciens C58	BUP	NP_357528	Goodner *et al*. 2001
A. tumefaciens NRRLB11291	D-NCAAH	CAA62550	Buson *et al.* 1996
Agrobacterium sp. IP I-671	D-NCAAH	AAL73200	Hils *et al*. 2001
Agrobacterium sp. KNK712	D-NCAAH	Q44185	Nanba *et al.* 1998
Arabidopsis thaliana	BUP	Q8H183~	
Arthrobacter aurescens DSM 3747	L-NCAAH	AAG02131	Wiese *et al*. 2000
Arthrobacter crystallopoietes DSM 20117	L-NCAAH, D-NACCH	AAO24769, AAO24770	Werner *et al.* 2002 (unp.)*
B. kaustophilus CCRC11223	L-NCAAH	AAN31517	Hu *et al*. 2003
B. stearothermophilus NCIB8224	L-NCAAH	CAA69999	Batisse *et al*. 1997
B. stearothermophilus NS1122A	L-NCAAH	JN0885	Mukohara *et al.* 1993
Bacteroides thetaiotaomicron VPI-5482	BUP	NP_809788	Xu *et al*. 2003b
Bradyrhizobium japonitum USDA110	BUP	BAC48588	Kaneko *et al*. 2002
Brevibacillus agri NCHU1002	BUP	AAO66293	Kao and Hsu 2003
Brucella melintensis	BUP	Q8YJA1~	
Dictyostelium discoideum	BUP	AAK60519	Gojkovic *et al*. 2001
Drosophila melanogaster	BUP	Q9VI04~~	
Homo sapiens	BUP	Q9UBR1	Vreken *et al.* 1999
Lycopersicon esculentum	BUP	CAB45873	Chevalier *et al.* (1999) (unp.)*
Mesorhizobium loti	BUP	NP_103174	Kaneko *et al*. 2000
P. aeruginosa PAO1	BUP	NP-249135	Stover *et al.* 2000
P. putida KT2440	BUP	NP-746162	Nelson *et al.* 2002
Pseudomonas sp. KNK003A	D-NCAAH	JW0083	Ikenaka *et al*. 1998a
Pseudomonas sp. NS671	L-NCAAH	Q01264	Watabe *et al*. 1992a
Pyrococcus abyssi	BUP	CAB50304	Gaspin *et al*. 2000
Rattus norvegicus	BUP	NP_446297	Kvalnes-Krick and Traut 1993
Rhodopseudomonas palustris CGA009	BUP	CAE27186	Larimer *et al*. (unp.)*
S. kluyveri	BUP	AAK60518	Gojkovic *et al*. 2001
Streptococcus pneumoniae R6	BUP	NP_358417	Hoskins *et al*. 2001

(*: Unpublished, ~: Accession numbers for sequences obtained from BRENDA)

REFERENCES

Abendroth J., Chatterjee S., & Schomburg D. (2000a) Purification of a D-hydantoinase using a laboratory-scale streamline phenyl column as the initial step. *Journal of Chromatography B* 737, 187-194.

Abendroth J., Niefind K., Chatterjee S., & Schomburg D. (2000b) Crystallization, preliminary X-ray analysis of a native and selenomethioneine D-hydantoinase from *Thermus* sp. *Acta Crystallographica* D56, 1166-1169.

Abendroth J., Niefind K., & Schomburg D. (2002a) X-ray structure of a dihydropyrimidinase from *Thermus* sp. at 1.3 A resolution. *Journal of Molecular Biology* 320, 143-156.

Abendroth J., Niefind K., May O., Siemann M., Syldatk C., & Schomburg D. (2002b) The structure of L-hydantoinase from *Arthrobacter aurescens* leads to an understanding of dihydropyrimidinase substrate and enantio selectivity. *Biochemistry* 41, 8589-8597

Achary A., Hariharan K.A., Bandhyopadhyaya S., Ramachandran R., & Jayaraman K. (1997) Application of numerical modelling for the development of optimised complex medium for D-hydantoinase production from *Agrobacterium radiobacter* NRRL B 11291. *Biotechnology and Bioengineering* 55, 148-154.

Altenbuchner J., Siemann-Herzberg M., & Syldatk C. (2001) Hydantoinases and related enzymes as biocatalysts for the synthesis of unnatural chiral amino acids. *Current Opinion in Biotechnology* 12, 559-563.

Altschul S.F., Gish W., Miller W., Myers E.W. & Lipman D.J. (1990) Basic local alignment search tool. *Journal of Molecular Biology* 215, 403-410

Arnold F.H. & Moore J.C. (1997) Optimisation industrial enzymes by directed evolution. *Biochemical Engineering/Biotechnology* 58, 1-14.

Ausubel F.M., Brent R., Kingston R.E., Moore D.D., Seidman J.G., Smith J.A. & Struhl K. (1983) Current protocols in molecular biology. Third Edition. Wiley-Interscience. New York.

Azerad R. (1995) Application of biocatalysis in organic synthesis. *Bulletin de la Societe Chimique de France* 132, 17-51

Baneyx F. (1999) Recombinant protein expression in *Escherichia coli. Current Opinion in Biotechnology.* 10, 411-421

Batisse N., Weigel P., Lecocq M., & Sakanyan V. (1997) Two amino acid amidohydrolase genes encoding L-stereospecific carbamoylase and aminoacylase are organised in a common operon in *Bacillus stearothermophilus*. *Applied and Environmental Microbiology* 63, 763-766.

Bentley S.D., Chater K.F., Cerdeno-Tarraga A.M., Challis G.L., Thomson N.R., James K.D., Harris D.E., Quail M.A., Kieser H., Harper D., Bateman A., Brown S., Chandra G., Chen C.W., Collins M., Cronin A., Fraser A., Goble A., Hidalgo J., Hornsby T., Howarth S., Huang C.H., Kieser T., Larke L., Murphy L., Oliver K., O'Neil S., Rabbinowitsch E., Rajandream M.A., Rutherford K., Rutter S., Seeger K., Saunders D., Sharp S., Squares R., Squares S., Taylor K., Warren T., Wietzorrek A., Woodward J., Barrell B.G., Parkhill J., & Hopwood D.A. (2002) Complete genome sequence of the model actinomycete *Streptomyces coelicolor* A3(2). *Nature* 417, 141-147

Berghammer H. & Auer B. (1993) "Easypreps" : Fast and easy plasmid minipreparation for analysis of recombinant clones in *E. coli*. *Biotechniques* 14, 527-528.

Bernheim F. & Bernheim M.L. (1946) The hydrolysis of hydantoin by various tissues. *Journal of Biological Chemistry* 163, 683-685.

Bommarius A.S., Schwarm M., & Drauz K. (1998) Biocatalysis to amino acid-based chiralpharmacueticals - examples and perspectives. *Journal of Molecular Catalysis B: Enzymatic* 5, 1-11.

Brunk C.F., Avaniss-Aghajani E., & Brunk C.A. (1996) A computer analysis of primer and probe hybridisation potential with bacterial small-subunit rRNA sequences. *Applied and Environmental Microbiology.* 62, 872-879.

Buchanan K. (1996) Optimisation of hydantoin biotransformations by RU-KM3$_S$ resting cells. Honours thesis, Rhodes University

Buchanan K., Burton S., Dorrington R., Matcher G., Skepu Z. (2001) A novel *Pseudomonas putida* strain with high levels of hydantoin-converting activity, producing L-amino acids. *Journal of Molecular Catalysis B: Enzymatic* 11,397-406

Buell C.R., Joardar V., Lindeberg M., Selengut J., Paulsen I.T., Gwinn M.L., Dodson R.J., Deboy R.T., Durkin A.S., Kolonay J.F., Madupu R., Daugherty S., Brinkac L., Beanan M.J., Haft D.H., Nelson W.C., Davidsen T., Zafar N., Zhou L., Liu J., Yuan Q., Khouri H., Fedorova N., Tran B., Russell D., Berry K., Utterback T., Van Aken S.E., Feldblyum T.V., D'Ascenzo M., Deng W.L., Ramos A.R., Alfano J.R., Cartinhour S., Chatterjee A.K., Delaney T.P., Lazarowitz S.G., Martin G.B., Schneider D.J., Tang X., Bender C.L., White O., Fraser C.M. & Collmer A. (2003) The complete genome sequence of the Arabidopsis and tomato pathogen *Pseudomonas syringae* pv. tomato DC3000. *Proceedings Of The National Academy Of Sciences Of The United States Of America* 100,10181-10186.

Burton S.G., Dorrington R.A., Hartley C., Kirchmann S., Matcher G., & Phehane V. (1998) Production of enantiomerically pure amino acids: characterization of South African hydantoinases and hydantoinase-producing bacteria. *Journal of Molecular Catalysis B: Enzymatic* 5, 301-305

Buson A., Negro A., Grassato L., Tagliaro M., Basaglia M., Grandi C., Fontana A., & Nuti M.P. (1996) Identification, sequencing and mutagenesis of the gene for a D-carbamoylase from *Agrobacterium radiobacter*. *FEMS Microbiology Letters* 145, 55-62.

Campbell L.L. (1958) Reductive degradation of pyrimidines. IV. Purification and properties of dihydrouracil hydrase. *Journal of Biological Chemistryl* 233, 1236-1240

Capela D., Barloy-Hubler F., Gouzy J., Bothe G., Ampe F., Batut J., Boistard P., Becker A., Boutry M., Cadieu E., Dreano S., Gloux S., Godrie T., Goffeau A., Kahn D., Kiss E., Lelaure V., Masuy D., Pohl T., Portetelle D., Puehler A., Purnelle B., Ramsperger U., Renard C., Thebault P., Vandenbol M., Weidner S. & Galibert F. (2001) Analysis of the chromosome sequence of the legume symbiont *Sinorhizobium meliloti* strain 1021. *Proceedings Of The National Academy Of Sciences Of The United States Of America.* 98, 9877-9882

Cecere F., Galli G., & Morisi F. (1975) Substrate and steric specificity of hydropyrimidine hydrase. *FEBS Letters* 57 , 192-194.

Chao Y.P., Juang T., Chern J., & Lee C. (1999a) Production of D-p-hydroxyphenylglycine by *N*-carbamoyl-D-amino acid amidohydrolase-overproducing *Escherichia coli* strains. *Biotechnology Progress* 15, 603-607.

Chao Y.P., Fu H., Lo T.E., Chen P.T., & Wang J. (1999b) One-step production of D-p-hydroxyphenylglycine by recombinant *Escherichia coli* strains. *Biotechnology Progress* 15, 1039-1045.

Chao Y.P., Chiang C.J., Lo T.E., & Fu H. (2000a) Overproduction of D-hydantoinase and carbamoylase in a soluble form in *Escherichia coli*. *Applied Microbiology and Biotechnology* 54, 348-353.

Chao Y.P., Chiang C.J., & Chen P.T. (2000b) Optimum ration of D-carbamoylase to D-hydantoinase for maximizing D-*p*-hydroxyphenylglycine productivity. *Biotechnology Letters* 99-103.

Chen H. & Tsai H. (1998) Cloning, sequencing and expression in *Escherichia coli* of D-hydantoinase gene from *Pseudomonas putida*. *Annals of the New York Academy of Sciences* 864, 234-237.

Chen C., Chiu W., Liu J., Hsu W., & Wang W. (2003) Structural basis for catalysis and substrate specificity of *Agrobacterium radiobacter N*-carbamoyl-D-amino acid amidohydrolase. *Journal of Biological Chemistry* 278, 26194-26201.

Chevalier C., Joubes J., Petit J. & Raymond P. (1999) Isolation and characterization of a cDNA clone for a putative beta-alanine synthase from tomato (*Lycopersicon esculentum* Mill.)developing fruits. Unpublished

Cheon Y.H., Kim H.S., Han K.H., Abendroth J., Niefind K., Schomburg D., Wang J., & Kim Y. (2002) Crystal structure of D-hydantoinase from *Bacillus stearothermophilus* :Insight into the stereochemistry of enantioselectivity. *Biochemistry* 41, 9410-9417.

Chien H.R., Jih Y., Yang W., & Hsu W. (1998) Identification of the open reading frame for the *Pseudomonas putida* D-hydantoinase gene and expression of the gene in *Escherichia coli*. *Biochimica et Biophysica Acta* 1395, 68-77.

Chung J., Back J., Lim J., Park Y., & Han Y. (2002) Thermostable hydantoinase from a hyperthermophilic archeon, *Methanococcus jannaschii* . *Enzyme and Microbial Technology* 30, 874.

Cole J, Chai B, Marsh T, Farris R, Wang Q, Kulam S, Chandra S, McGarrell D, Schmidt T, Garrity G, Tiedje J (2003) The Ribosomal Database Project (RDP-II): Previewing a new autoaligner that allows regular updates and the new prokaryotic taxonomy. *Nucleic Acids Research* 31:442-443

Collier D.N., Hager P.W. & Phibbs P.V. (1996) Catabolite repression control in the *Pseudomonads*. *Research in Microbiology* 147:551-561

Collier D., Spence C., Cox M. & Phibbs P. (2001) Isolation and phenotypic characterization of *Pseudomonas aeruginosa* pseudorevertants containing suppressors of the catabolite repression control-defective *crc-10* allele. *FEMS Microbiology Letters* 196:87-92

Deepa S., Sivasankar B., & Jayaraman K. (1993) Enzymatic production and isolation of D-amino acids from the corresponding 5-substituted hydantoins. *Process Biochemistry* 28, 447-452.

DeLorenzo V. & Timmis K. (1994) Analysis and construction of stable phenotypes in gram-negative bacteria with Tn5- and Tn10-derived minitransposons in *Methods in Enzymology*, Eds. Clark V.L. and Bavoil P.M. Academic Press, San Diego 235:386-405

Demain A. L. (2000) Small bugs, big business: The economic power of the microbe. *Biotechnology Advances* 18, 499-514

Dennis J. & Zylstra G. (1998) Plasposons: Modular self-cloning minitransposon derivatives for rapid genetic analysis of gram-negative bacterial genomes. *Applied and Environmental Microbiology* 64:2710-2715

Dinamarca M.A., Ruiz-Manzano A., & Rojo F. (2002) Inactivation of cytochrome *o* ubiquinol oxidase relieves catabolic repression of the *Pseudomonas putida* GPo1 Alkane degradation pathway. *Journal of Bacteriology* 184, 3784-3793

Drauz K. (1997) Chiral amino acids: a versatile tool in the synthesis of pharmaceuticals and fine chemicals. *Chimia* 51, 310-314.

Duetz W.A., Marques S., Wind B., Ramos J.L., & van Andel J.G. (1996) Catabolite repression of the toluene degradation pathway in *Pseudomonas putida* harbouring pWW0 under various conditions of nutrient limitation in chemostat culture. *Applied and Environmental Microbiology* 62, 601-606

Durham D.R. & Weber J.E. (1995) Properties of D-hydantoinase from *Agrobacterium tumefaciens* and its use for the preparation of *N*-carbamyl D-amino acids. *Biochemical and Biophysical Research Communications* 216, 1095-1100.

Eadie G.S., Bernheim F., & Bernheim M.L.C. (1949) The partial purification and properties of animal and plant hydantoinases. *Journal of Biological Chemistry* 181, 449-458

Eberl L., Ammendola A., Rothballer M.H., Givskov M., Strenberg C., Kilstrup M., Schleifer K. & Molin S. (2000) Inactivation of *gltB* abolishes expression of the assimilatory nitrate reductase gene (*nasB*) in *Pseudomonas putida* KT2442. *Journal of Bacteriology* 182, 3368-3376

Freifelder D. (1987) Regulation of the activity of genes and gene production in prokaryotes. In: Molecular Biology, Eds. Freifelder Jones and Bartlett, Boston

Gaspin C., Cavaille J., Erauso G. & Bachellerie J.P. (2000) Archaeal homologs of eukaryotic methylation guide small nucleolar RNAs: lessons from the *Pyrococcus* genomes. *Journal of Molecular Biology* 297: 895-906

Gojkovic Z., Sandrini M.P. & Piskur J. (2001) Eukaryotic beta-alanine synthases are functionally related but have a high degree of structural diversity. *Genetics* 158: 999-1011

Gokhale D.V., Bastawde K.B., Patil S.G., Kalkote U.R., Joshi R.R., Joshi R.A., Ravindranathan T., Gaikwad B.G., Jogdand V.V., & Nene S. (1996) Chemoenzymatic synthesis of D-phenylglycine using hydantoinase of *Pseudomonas desmolyticum* resting cells. *Enzyme Microbial Technology* 18, 353-357.

Goodner B., Hinkle G., Gattung S., Miller N., Blanchard M., Qurollo B., Goldman B.S., Cao Y., Askenazi M., Halling C., Mullin L., Houmiel K., Gordon J., Vaudin M., Iartchouk O., Epp A., Liu F., Wollam C., Allinger M., Doughty D., Scott C., Lappas C., Markelz B., Flanagan C., Crowell C., Gurson J., Lomo C., Sear C., Strub G., Cielo C. & Slater S. (2001) Genome sequence of the plant pathogen and biotechnology agent Agrobacterium tumefaciens C58. *Science* 294: 2323-2328

Grabherr R. & Bayer K. (2002) Impact of targeted vector design on ColE1 plasmid replication. *Trends in Biotechnology* 20, 257-260

Grifantini R., Pratesi C., Galli G., & Grandi G. (1996) Topological mapping of the cysteine residues of *N*-carbamyl-D-amino acid amidohydrolase and their role in enzymatic activity *Journal of Biological Chemistry* 16, 9326-9331.

Grifantini R., Galli G., Carpani G., Pratesi C., Frascotti G., & Grandi G. (1998) Efficient conversion of 5-substituted hydantoins to D-α-amino acids using recombinant *Escherichia coli* strains. *Microbiology* 144, 947-954.

Gross C., Syldatk C., Mackowiak V., & Wagner F. (1990) Production of L-tryptophan from D,L-5-indolylmethylhydantoin by resting cells of a mutant of *Arthrobacter* species (DSM 3747). *Journal of Biotechnology* 14, 363-376.

Haas B.J., Volfovsky N., Town C.D., Troukhan M., Alexandrov N., Feldmann K.A., Flavell R.B., White O., & Salzberg,S.L. (2002) Full-length messenger RNA sequences greatly improve genome annotation. *Genome Biology* 3, RESEARCH0029

Hartley C.J., Kirchmann S., Burton S.G., & Dorrington R.A. (1998) Production of D-amino acids from D,L-5-substituted hydantoins by an *Agrobacterium tumefaciens* strain and isolation of a mutant with inducer-independent expression of hydantoin-hydrolysing activity. *Biotechnology Letters* 20, 707-711.

Hartley C.J., Manford F., Burton S.G., & Dorrington R.A. (2001) Over-production of hydantoinase and *N*-carbamylamino acid amidohydrolase enzymes by regulatory mutants of *Agrobacterium tumefaciens*. *Applied Microbiology and Biotechnology* 57, 43-49.

Hartley C.J. (2001) Elucidation and manipulation of the hydantoin-hydrolysing enzyme system *of Agrobacterium tumefaciens* RU-OR for the biocatalytic production of D-amino acids. PhD Thesis, Rhodes University

Henikoff S (1984) Unidirectional digestion with exonuclease III creates targeted breakpoints for DNA sequencing. *Gene* 28:351

Hester K., Lehman J., Najar F., Song L., Roe B., MacGregor C., Hager P., Phibbs P., Sokatch J. (2000) Crc is involved in catabolite repression control in the *bkd* operons of *Pseudomonas putida* and *Pseudomonas aeruginosa. Journal of Bacteriology* 182:1144-1149.

Hils M., Munch P., Altenbuchner J., Syldatk C., & Mattes R. (2001) Cloning and characterization of genes from *Agrobacterium* sp. IP I-671 involved in hydantoin degradation. *Applied Microbiology and Biotechnology* 57, 680-688.

Hockney R.C. (1994) Recent developments in heterologous protein production in *Escherichia coli*. *TIBTECH* 12, 456-463.

Hoskins J.A., Alborn W. Jr., Arnold J., Blaszczak L., Burgett S., DeHoff B.S., Estrem S., Fritz L., Fu D.J., Fuller W., Geringer C., Gilmour R., Glass J.S., Khoja H., Kraft A., LaGace R., LeBlanc D.J., Lee L.N., Lefkowitz E.J., Lu J., Matsushima P., McAhren S., McHenney M., McLeaster K., Mundy C., Nicas T.I., Norris F.H., O'Gara M., Peery R., Robertson G.T., Rockey P., Sun P.-M., Winkler M.E., Yang Y., Young-Bellido M., Zhao G., Zook C., Baltz R.H., Jaskunas S.R., Rosteck P.R. Jr., Skatrud P.L. & Glass J.I. (2001) Genome of the bacterium *Streptococcus pneumoniae* strain R6. *Journal of Bacteriol*ogy 183: 5709-5717

Hsu W., Chien F., Hsu C., Wang T., Yaun H., & Wang W. (1999) Expression, crystallization and preliminary X-ray diffraction studies of *N*-carbamyl-D-amino acid amidohydrolase from *Agrobacterium radiobacter*. *Acta Crystallographica* D55, 694-695.

Hu H., Hsu W., & Chien H. (2003) Characterization and phylogenetic analysis of a thermostable *N*-carbamoyl-L-amino acid amidohydrolase from *Bacillus kaustophilus* CCRC11223. *Archives of Microbiology* 179, 250-257.

Ikenaka Y., Nanba H., Yamada Y., Yajima K., Takano M., & Takahashi S. (1998a) Screening, Characterization, and cloning of the gene for *N*-carbamyl-D-amino acid amidohydrolase from thermotolerant soil bacteria. *Bioscience Biotechnology and Biochemistry* 62, 882-886.

Ikenaka Y., Nanba H., Yajima K., Yamada Y., Takano M., & Takahashi S. (1999) Thermostability reinforcement through a combination of thermostability-related mutations of *N*-carbamyl-D-amino acid amidohydrolase. *Bioscience Biotechnology and Biochemistry* 63, 91-95.

Ishikawa T., Watabe K., Mukohara Y., Kobayashi S., & Nakamura H. (1993) Microbial conversion of DL-5-substituted hydantoins to the corresponding L-amino acids by *Pseudomonas* sp. strain NS671. *Bioscience Biotechnology and Biochemistry* 57, 982-986.

Ishikawa T., Mukohara Y., Watabe K., Kobayashi S., & Nakamura H. (1994) Microbial conversion of DL-5-substituted hydantoins to the corresponding L-amino acids by *Bacillus stearothermophilus* NS1122A. *Bioscience Biotechnology and Biochemistry* 58, 265-270.

Ishikawa T., Watabe K., Mukohara Y., & Nakamura H. (1996) *N*-carbamyl-L-amino acid amidohydrolase of *Pseudomonas* sp. strain NS671 : Purification and some properties of the enzyme expressed in *Escherichia coli*. *Bioscience Biotechnology and Biochemistry* 60, 612-615.

Ishikawa T., Watabe K., Mukohara Y., & Nakamura H. (1997) Mechanism of stereospecific conversion of DL-5-substituted hydantoins to the corresponding L-amino acids by *Pseudomonas* sp. strain NS671. *Bioscience Biotechnology and Biochemistry* 61, 185-187.

Janssen D.B., op den Camp H.J.M., Leene P.J.M., & van der Drift C. (1980) The enzymes of the ammonia assimilation in *Pseudomonas aeruginosa. Archives of Microbiology* 124, 197-203

Janssen D.B., Herst P.M., Joosten H.M.L.J., & van der Drift C. (1981) Nitrogen control in *Pseudomonas aeruginosa*: A role for glutamine in the regulation of the synthesis of NADP-dependent glutamate dehydrogenase, urease and histidase. *Archives of Microbiology* 128, 398-402

Janssen D.B., & van der Drift C. (1983) Catabolite repression and nitrogen control of allantoin-degrading enzymes in *Pseudomonas aeruginosa. Antonie van Leeuwenhoek* 49, 501-508

Judson N., & Mekalanos J. (2000) Transposon-based approaches to identify essential bacterial genes. *Trends in Microbiology* 8, 521-526.

Kaneko T., Nakamura Y., Sato S., Asamizu E., Kato T., Sasamoto S., Watanabe A., Idesawa K., Ishikawa A., Kawashima K., Kimura T., Kishida Y., Kiyokawa C., Kohara M., Matsumoto M., Matsuno A., Mochizuki Y., Nakayama S., Nakazaki N., Shimpo S., Sugimoto M., Takeuchi C., Yamada M., & Tabata S. (2000) Complete genome structure of the nitrogen-fixing symbiotic bacterium *Mesorhizobium loti. DNA Research* 7: 331-338

Kaneko T., Nakamura Y., Sato S., Minamisawa K., Uchiumi T., Sasamoto S., Watanabe A., Idesawa K., Iriguchi M., Kawashima K., Kohara M., Matsumoto M., Shimpo S., Tsuruoka H., Wada T., Yamada M. & Tabata S. (2002) Complete genomic sequence of nitrogen-fixing symbiotic bacterium *Bradyrhizobium japonicum* USDA110. *DNA Research* 9: 189-197

Kao C. & Hsu W. (2003) A gene cluster involved in pyrimidine reductive catabolism from *Brevibacillus agri* NCHU1002. *Biochemical and Biophysical Research Communications*. 303, 848-854

Kim D.M. & Kim H.S. (1993) Enzymatic synthesis of D-*p*-hydroxyphenylglycine from DL-*p*-hydroxyphenyl-hydantoin in the presence of organic cosolvent. *Enzyme and Microbial Technology* 15, 530-534.

Kim G.J. & Kim H.S. (1995) Optimisation of the enzymatic synthesis of D-*p*-hydroxyphenylglycine from DL-5-substituted hydantoin using D-hydantoinase and *N*-carbamoylase. *Enzyme and Microbial Technology* 17, 63-67.

Kim G.J., Park J.H., Lee D.C., Ro H.S., & Kim H.S. (1997) Primary structure, sequence analysis, and expression of the thermostable D-hydantoinase from *Bacillus stearothermophilus* SD-1. *Molecular and General Genetics* 255, 152-156.

Kim G.J. & Kim H.S. (1998) C-terminal regions of D-hydantoinase are nonessential for catalysis, but affect the oligomeric structure. *Biochemical and Biophysical Research Communications* 243, 96-100.

Kim G.J., Cheon Y.H., & Kim H.S. (2000a) Directed evolution of a novel *N*-carbamoylase/D-hydantoinase fusion enzyme for functional expression with enhanced stability. *Biotechnology and Bioengineering* 68, 211-217.

Kim G.J., Lee D.E., & Kim H.S. (2000b) Construction and evaluation of a novel bifunctionl *N*-carbamoylase-D-hydantoinase fusion enzyme. *Applied and Environmental Microbiology* 66, 2133-2138.

Kim G.J., Lee D.E., & Kim H.S. (2000c) Functional expression and characterization of the two cyclic amidohydrolase enzymes, allontoinase and a novel phenylhydantoinase, from *Escherichia coli*. *Journal of Bacteriology* 182, 7021-7028.

Koeller K.M. & Wong C. (2001) Enzymes for chemical synthesis. *Nature* 409, 232-240.

Kraulis P. (1991) Molscript: a program to produce both detailed and schematic plots of protein structures. *Journal of Applied Crystallography* 24, 946-950

Kvalnes-Krick K.L. & Traut T.W. (1993) Cloning, sequencing, and expression of a cDNA encoding beta-alanine synthase from rat liver. *Journal of Biological Chemistry* 268: 5686-5693

Larimer F.W., Chain P., Hauser L., Lamerdin J., Malfatti S., Do L., Land M.L., Pelletier D.A., Beatty T.J., Lang A.S., Tabita F.R., Gibson J.L., Hanson T.E., Torres y Torres J., Peres C., Harrison F.H., Gibson J. & Harwood C.S. Complete genome sequence of the metabolically versatile photosynthetic bacterium *Rhodopseudomonas palustris*. Unpublished

LaPointe G., Viau S., Leblanc D., Robert N., & Morin A. (1994) Cloning, sequencing, and expression in *Escherichia coli* of the D-hydantoinase gene from *Pseudomonas putida* and distribution of homologous genes in other microorganisms. *Applied and Environmental Microbiology* 60, 888-895.

Las Heras-Vazquez F., Martinez-Rodriguez S., Mingorance-Cazorla L., Clemente-Jimenez J., & Rodriguez-Vico F. (2003) Overexpression and characterization of hydantoin racemase from *Agrobacterium tumefaciens* C58. *Biochemical and Biophysical Research Communications* 303, 541-547.

Lee S.G., Lee D.C., Sung M.H., & Kim H.S. (1994) Isolation of thermostable D-hydantoinase-producing thermophilic *Bacillus* sp. SD-1. *Biotechnology Letters* 16, 461-466.

Lee S.G., Lee D.C., Hong S.P., Sung M.H., & Kim H.S. (1995) Thermostable D-hydantoinase from thermophilc *Bacillus stearothermophilus* SD-1 :characteristics of purified enzyme. *Applied Microbiology and Biotechnology* 43, 270-276.

Lee D.C., Lee S.G., Hong S.P., Sung M.H., & Kim H.S. (1996) Cloning and overexpression of thermostable D-hydantoinase from thermophile in *E. coli* and its application to the synthesis of optically active D-amino acids. *Annals of the New York Academy of Sciences* 799, 401-405.

Liese A. & Fliho M.V. (1999) Production of fine chemicals using biocatalysis. *Current Opinion in Biotechnology.* 10, 595-603

Louwrier A. & Knowles C.J. (1996) The purification and characterization of a novel D(-)-specific carbamoylase enzyme from an *Agrobacterium* sp. *Enzyme and Microbial Technology* 19, 562-571.

Louwrier A. & Knowles C.J. (1997) The aim of industrial enzymatic amoxycillin production: characterization of a novel carbamoylase enzyme in the form of a crude, cell-free extract. *Biotechnology and Applied Biochemistry* 25, 143-149.

Luksa V., Starkuviene V., Starkuviene B., & Dagys R. (1997) Purification and characterization of the D-hydantoinase from *Bacillus circulans*. *Applied Biochemistry and Biotechnology* 62, 219-231.

Madigan M., Matinko J. & Parker J. (1984) Brock Biology of Microorganisms. 8th Ed. Prentice Hall International Inc, New Jersey

Maidak B, Cole J, Lilburn T, Parker C, Saxman P, Farris R, Garrity G, Olsen G, Schmidt T, Tiedje J (2001) The RDP-II (Ribosomal Database Project). NAR 29:173-174

Maier N.M., Franco P., Lindner W. (2001) Separation of enantiomers: needs, challenges, perspectives. *Journal of Chromatography A*, 906, 3-33

Malay S.R., Cronan J.E., & Freifelder D. (1994) Transposable elements. *Microbial Genetics* 2nd edition, Jones and Bartlett Publishers, Boston.

May O., Siemann M., Pietzsch M., Kiess M., Mattes R., & Syldatk C. (1998a) Substrate-dependent enantioselectivity of a novel hydantoinase from *Arthrobacter aurescens* DSM 3745 : Purification and characterization as new member of cyclic amidases. *Journal of Biotechnology* 61, 1-13.

May O., Siemann M., Siemann M.G., & Syldatk C. (1998b) Catalytic and structural function of zinc for the hydantoinase from *Arthrobacter aurescens* DSM 3745. *Journal of Molecular Catalysis B: Enzymatic* 4, 211-218.

May O., Siemann M., Siemann M.G., & Syldatk C. (1998c) The hydantoin amidohydrolase from *Arthrobacter aurescens* DSM 3745 is a zinc metalloenzyme. *Journal of Molecular Catalysis B: Enzymatic* 5, 367-370.

May O., Habenicht A., Mattes R., Syldatk C., & Siemann M. (1998d) Molecular evolution of hydantoinases. *Biological Chemistry* 379, 743-747.

May O., Siemann M., & Syldatk C. (1998e) A new method for the detection of hydantoinases with respect to their enantioselectivity on acrylamide gels based on enzyme activity stain. *Biotechnology Techniques* 12, 309-312.

May O., Nguyen P.T., & Arnold F.H. (2000) Inverting enantioselectivity by directed evolution of hydantoinase for improved production of L-methionine. *Nature Biotechnology* 18, 317-320.

Merrick M.J. & Edwards R.A. (1995) Nitrogen control in bacteria. *Microbiological Reviews* 59, 604-622

Michal G. (1999) Biochemical pathways- an atlas of biochemistry and molecular biology. Wiley, New York

Miller J. (1992) A short course in bacterial genetics : A laboratory manual and handbook for *Escherichia coli* and related bacteria. Cold Spring Harbor Laboratory Press, New York

Moller C., Syldatk C., Schulze M., & Wagner F. (1988) Stereo- and substrate-specificity of D-hydantoinase and a D-*N*-carbamyl-amino acid amidohydrolase of *Arthrobacter crystallopoietes* AM 2. *Enzyme and Microbial Technology* 10, 618-625.

Morett E., Segovia L. (1993) The σ^{54} bacterial enhancer-binding protein family: Mechanism of action and phylogenetic relationship of their functional domains. *Journal of Bacteriology* 175:6067-6074

Morin A., Hummel W., & Kula M. (1986a) Production of hydantoinase from *Pseudomonas fluorescens* strain DSM 84. *Applied Microbiology and Biotechnology* 25, 91-96.

Morin A., Hummel W., Schutte H., & Kula M. (1986b) Characterization of hydantoinase from *Pseudomonas fluorescens* strain DSM 84. *Biotechnology and Applied Biochemistry* 8, 564-574.

Morin A. (1993) Use of D-hydantoinase extracted from legumes to produce *N*-cabamyl D-amino acids. *Enzyme and Microbial Technology* 15, 208-214.

Mukohara Y., Ishikawa T., Watabe K., & Nakamura H. (1993) Molecular cloning and sequencing of the gene for a thermostable *N*-carbamyl-L-amino acid amidohydrolase from *Bacillus stearothermophilus* strain NS1122A. *Bioscience, Biotechnology, and Biochemistry* 57, 1935-1937.

Mukohara Y., Ishikawa T., Watabe K., & Nakamura H. (1994) A thermostable hydantoinase of *Bacillus stearothermophilus* NS1122A:Cloning, sequencing, and high expression of the enzyme gene, and some properties of the expressed enzyme. *Bioscience, Biotechnology, and Biochemistry* 58, 1621-1626.

Nakai T., Hasegawa T., Yamashita E., Yamamoto M., Kumasaka T., Ueki T., Nanba H., Ikenaka Y., Takahashi S., Sato M., & Tsukihara T. (2000) Crystal structure of *N*-carbamyl-D-amino acid amidohydrolase with a novel catalytic framework common to amidohydrolases. *Structure* 8, 729-737.

Nanba H., Ikenaka Y., Yamada Y., Yajima K., Takano M., & Takahashi S. (1998) Isolation of *Agrobacterium* sp. strain KNK712 that produces *N*-carbamyl-D-amino amidohydrolase, cloning of the gene for this enzyme, and properties of the enzyme. *Bioscience Biotechnology and Biochemistry* 62, 875-881.

Nelson K., Paulsen I., Weinel C., Dodson R., Hilbert H., Fouts D., Gill S., Pop M., Martins Dos Santos V., Holmes M., Brinkac L., Beanan M., DeBoy R., Daugherty S., Kolonay J., Madupu R., Nelson W., White O., Peterson J., Khouri H., Hance I., Lee P., Holtzapple E., Scanlan D., Tran K., Moazzez A., Utterback T., Rizzo M., Lee K., Kosack D., Moestl D., Wedler H., Lauber J., Hoheisel J., Straetz M., Heim S., Kiewitz C., Eisen J., Timmis K., Duesterhoft A., Tummler B., Fraser C. (2002) Complete genome sequence and comparative analysis of the metabolically versatile *Pseudomonas putida* KT2440. *Environmental Microbiology* 4:799-808

Nishida Y., Nakamichi K., Nabe K., & Tosa T. (1987) Enzymatic production of L-tryptophan from DL-5-indolylmethylhydantoin by *Flavobacterium* sp. *Enzyme and Microbial Technology* 9, 721-725.

Ogawa J., Shimizu S., & Yamada H. (1993) *N*-Carbamoyl-D-amino acid amidohydrolase from *Comamonas* sp. E222c - Purification and characterization. *European Journal of Biochemistry* 212, 684-691.

Ogawa J. & Shimizu S. (1994) β-Ureidopropionase with *N*-carbamoyl-α-L-amino acid amidohydrolase activity from an aerobic bacterium, *Pseudomonas putida* IFO 12996. *European Journal of Biochemistry* 223, 625-630.

Ogawa J., Chung M., Hida S., Yamada H., & Shimizu S. (1994b) Thermostable *N*-carbamyl-D-amino acid amidohydrolase: screening, purification and characterization. *Journal of Biotechnology* 38, 11-19.

Ogawa J., Kaimura T., Yamada H., & Shimizu S. (1994c) Evaluation of pyrimidine- and hydantoin-degrading enzyme activities in aerobic bacteria. *FEMS Microbiology Letters* 122, 55-60.

Ogawa J., Min Kim J., Nirdnoy W., Amano Y., Yamada H., & Shimizu S. (1995a) Purification and characterization of an ATP-dependent amidohydrolase, *N*-methylhydantoin amidohydrolase, from *Pseudomonas putida* 77. *European Journal of Biochemistry* 229, 284-290.

Ogawa J., Honda M., Soong C., & Shimizu S. (1995b) Diversity of cyclic uriede compound-,dihydropyrimidine-, and hydantoin-hydrolysing enzymes in *Blastobacter* sp. A17p-4. *Bioscience Biotechnology and Biochemistry* 59, 1960-1962.

Ogawa J., Miyake H., & Shimizu S. (1995c) Purification and characterization of *N*-carbamoyl-L-amino acid amidohydrolase with broad substrate specificity from *Alcaligenes xylosoxidans*. *Applied and Environmental Microbiology* 43, 1039-1043.

Ogawa J. & Shimizu S. (1997) Diversity and versatility of microbial hydantoin-transforming enzymes. *Journal of Molecular Catalysis B: Enzymatic* 2, 163-176.

Ogawa J., Ryono A., Xie S., Vohra R., Indrati R., Miyakawa H., Ueno T., Ikenaka Y., Nanba H., Takahashi S., & Shimizu S. (1999a) β-carbon stereoselectivity of *N*-carbamoyl-D-α-amino acid amidohydrolase for α,β-diastereomeric amino acids. *Applied Microbiology and Biotechnology* 52, 801.

Ogawa J., Ryouno A., Xie S., Rakesh V., Indrati R., Miyakawa H., Ueno T., & Shimizu S. (1999b) Simultaneous recognition of two chiral centres in α,β-diastereomeric amino acids by an *N*-carbamoyl-L-α-amino acid amidohydrolase from *Alcaligenes xylosoxidans*. *Biotechnology Letters* 21, 711-713.

Ogawa J., Ryono A., Xie S., Vohra R., Indrati R., Akamatsu M., Miyagawa H., Ueno T., & Shimizu S. (2001) Separative preparation of the four stereoisomers of β-methylphenylalanine with *N*-carbamoyl amino acid amidohydrolases. *Journal of Molecular Catalysis B: Enzymatic* 12, 71-75.

Ogawa J. & Shimizu S. (2002) Industrial microbial enzymes: their discovery by screening and use in large-scale production of useful chemicals in Japan. *Current Opinion in Biotechnology* 13, 367-375.

Oh K., Nam S., & Kim H.S. (2002a) Improvement of oxidative and thermostability of *N*-carbamyl-D-amino acid amidohydrolase by directed evolution. *Protein Engineering* 15, 689-695.

Oh K., Nam S., & Kim H.S. (2002b) Directed evolution of *N*-carbamyl-D-amino acid amidohydrolase for simultaneous improvement of oxidative and thermal stability. *Biotechnology Progress* 18, 413-417.

Olivieri R., Fascetti E., Angelini L., & Degan L. (1979) Enzymatic conversion of N-carbamoyl-D-amino acids to D-amino acids. *Enzyme and Microbial Technology* 1, 201-204.

Olivieri R., Fascetti E., Angelini L., & Degan L. (1981) Microbial transformation of racemic hydantoins to D-amino acids. *Biotechnology and Bioengineering* 23, 2173-2183.

Omura S., Ikeda H., Ishikawa J., Hanamoto A., Takahashi C., Shinose M., Takahashi Y., Horikawa H., Nakazawa H., Osonoe T., Kikuchi H., Shiba T., Sakaki Y., & Hattori M. (2001) Genome sequence of an industrial microorganism *Streptomyces avermitilis*: deducing the ability of producing secondary metabolites. *Proceedings Of The National Academy Of Sciences Of The United States Of America* 98, 12215-12220

Page R.D.M (1996) Tree-view: An application to display phylogenetic trees on personal computers. *Computer Application in Biosciences* 12:357-358

Palmer J.A., Hatter K. & Sokatch J.R. (1991) Cloning and sequence analysis of the LPD-glc structural gene of *Pseudomonas putida. Journal of Bacteriology* 173, 3109-3116

Park J.H., Kim G.J., Lee S.G., & Kim H.S. (1998) Biochemical properties of thermostable D-hydantoinase from *Bacillus thermocatenulatus* GH-2. *Annals of the New York Academy of Sciences* 864, 337-340.

Park J.H., Kim G.J., & Kim H.S. (2000) Production of D-amino acid using whole cells of recombinant *Escherichia coli* with separately and coexpressed D-hydantoinase and *N*-carbamoylase. *Biotechnology Progress* 16, 564-570.

Paulsen I., Seshadri R., Nelson K.E., Eisen J.A., Heidelberg J.F., Read T.D., Dodson R.J., Umayam L.A., Brinkac L.M., Beanan M.J., Daugherty S.C., Deboy R., Durkin A.S., Kolonay J.F., Madupu R., Nelson W.C., Ayodeji B., Kraul M., Shetty J., Malek J.A., Van Aken S.E., Riedmuller S., Tettelin H., Gill S., White O., Salzberg S.L., Hoover D.L., Lindler L., Halling S.M., Boyle S.M. & Fraser C.M. (2002) The *Brucella suis* genome reveals fundamental similarities between animal and plant pathogens and symbionts. *Proceedings Of The National Academy Of Sciences Of The United States Of America*. 99, 13148-13153

Petruschka L., Adolf K., Burchhardt G., Dernedde J., Jorgensen J. & Herrmann H. (2002) Analysis of the *zwf-pgl-eda*-operon in *Pseudomonas putida* strains H and KT2440. *FEMS Microbiology Letters* 215:89-95

Pietzsch M., Wiese A., Ragnitz K., Wilms B., Altenbuchner J., Mattes R., & Syldatk C. (2000) Purification of recombinant hydantoinase and L-*N*-carbamoylase from *Arthrobacter aurescens* expressed in *Escherichia coli* : comparison of wild-type and genetically modified proteins. *Journal of Chromatography B* 737, 179-186.

Pozo C., Rodelas B., de la Escalera S., & Gonzalez-Lopez J. (2002) D,L-hydantoinase activity of an *Ochrobactrum anthropi* strain. *Journal of Applied Microbiology* 92, 1028-1034.

Ragnitz K., Syldatk C., & Pietzsch M. (2001) Optimisation of the immobilized parameters and operational stability of immobilized hydantoinase and L-*N*-carbamoylase from *Arthrobacter aurescens* for the production of optically pure L-amino acids. *Enzyme and Microbial Technology* 28, 713-720.

Reitzer L. (2003) Nitrogen assimilation and global regulation in *Escherichia coli. Annual Review of Microbiology* 57, 155-176

Rossello-Mora R. & Amann R. (2001) The species concept for prokaryotes. *FEMS Microbiology Reviews* 25:39-67

Runser S. & Ohleyer E. (1990) Properties of the hydantoinase from *Agrobacterium* sp. IP I-671. *Biotechnology Letters* 12, 259-264.

Runser S. & Meyer P.C. (1993) Purification and biochemical characterization of the hydantoin hydrolysing enzyme system from *Agrobacterium species*. *European Journal of Biochemistry* 213, 1315-1324.

Sanchez S. & Demain A. (2002) Metabolic regulation of fermentation processes. *Enzyme and Microbial Technology* 31, 895-906.

Sanger F., Nicklen S. & Coulson A.R. (1977) DNA sequencing with chain-terminating inhibitors. *Proceedings Of The National Academy Of Sciences Of The United States Of America* 74, 5463–5467

Sano K., Yokozeki K., Eguchi C., Kagawa T., Noda I., & Mitsugi K. (1977) Enzymatic production of L-tryptophan from L- and DL-5-indolylmethylhydantoin by newly isolated bacterium. *Agricultural and Biological Chemistry* 41, 819-825.

Santos P., Bartolo I., Blatny J., Zennaro E. & Valla S. (2001) New broad-host-range promoter probe vectors based on the plasmid RK2 replicon. *FEMS Microbiological Letters.* 195:91-96

Sareen D., Sharma R., Nandanwar H., & Vohra R. (2001a) Two-step purification of D(-)-specific carbamoylase from *Agrobacterium tumefaciens* AM 10. *Protein Expression and Purification* 21, 170-175.

Sareen D., Sharma R., & Vohra R. (2001b) Chaperone-assisted overexpression of an active D-carbamoylase from *Agrobacterium tumefaciens* AM 10. *Protein Expression and Purification* 23, 374-379.

Schmid A., Dordick J.S., Hauer B., Kiener A., Wubbolts M., & Witholt B. (2001) Industrial biocatalysis today and tomorrow. *Nature* 409, 258-268.

Schulze B. & Wubbolts M. (1999) Biocatalysis for industrial production of fine chemicals. *Chemical Biotechnology* 10, 609-615.

Schweizer H. (2001) Vectors to express foreign genes and techniques to monitor gene expression in Pseudomonads. *Current Opinion in Biotechnology* 12, 439-445.

Sharma R. & Vohra R. (1997) A thermostable D-hydantoinase isolated from a mesophilic *Bacillus* sp. AR9. *Biochemical and Biophysical Research Communications* 234, 485-488.

Sheibani N. (1999) Prokaryote gene fusion expression systems and their use in structural and functional studies. *Preparative biochemistry and biotechnology* 29, 77-90

Shi Y., Li H., Yuan J., Qi Y., & Li J. (2001) Purification and some properties of D-hydantoinase produced by *Pseudomonas* 2262. *Wei Sheng Wu Xue Bao* 41, 605-610.

Siemann M., Alvarado-Marin A., Pietzsch M., & Syldatk C. (1999) A D-specific hydantoin amidohydrolase : properties of the metalloenzyme purified from *Arthrobacter crystallopoietes*. *Journal of Molecular Catalysis B: Enzymatic* 6, 387-397.

Skepu Z. (2000) Characterization of amide bond hydrolysis in novel hydantoinase-producing bacteria. Masters Thesis, Rhodes University

Smith R., Pietzsch M., Waniek T., Syldatk C., & Bienz S. (2001) Enzymatic synthesis of enantiomerically enriched D- and L-3-silated alanines by deracemization of DL-5-silylmethylated hydantoins. *Tetrahedron: Asymmetry* 12, 157-165.

Snyder L, & Champness W (2003) Molecular Genetics of Bacteria. 2nd Ed. ASM Press, Washington, D.C. pg 187-207

Soong C., Ogawa J., Honda M., & Shimizu S. (1999) Cyclic-imide-hydrolysing activity of D-hydantoinase from *Blastobacter* sp. strain A17p-4. *Applied and Environmental Microbiology* 65, 1459-1462.

Soong C., Ogawa J., & Shimizu S. (2001) Novel amidohydrolytic reactions in oxidative pyrimidine metabolism: Analysis of the barbiturase reaction and discovery of a novel enzyme, ureidomalonase. *Biochemical and Biophysical Research Communications* 286, 222-226.

Stover C., Pham X., Erwin A., Mizoguchi S., Warrener P., Hickey M., Brinkman F., Hufnagle W., Kowalik D., Lagrou M., Garber R., Tolentino E., Westbrook-Wadman S., Yuan Y., Brody L., Coulter S., Folger K., Kas A., Larbig K., Lim R., Smith K., Spencer D., Wong G., Wu Z., Paulsen I., Saier M., Hancock R., Lory S., Olson M. (2000) Complete genome sequence of Pseudomonas aeruginosa PAO1, an opportunistic pathogen. *Nature* 406:959-964

Sudge S.S., Bastawde K.B., Gokhale D.V., Kalkote U.R., & Ravindranathan T. (1998) Production of D-hydantoinase by halophiilic *Pseudomonas* sp. NCIM 5109. *Applied Microbiology and Biotechnology* 49, 594-599.

Suh S., Runyen-Janecky L., Maleniak T., Hager P., MacGregor C., Zielinski-Mozny N., Phibbs P. & West S. (2002) Effect of *vfr* mutation on global gene expression and catabolite repression control of *Pseudomonas aeruginosa. Microbiology*. 148:1561-1569

Syldatk C., Cotoras D., Dombach G., Grob C., Kallwab H., & Wagner F. (1987) Substrate- and stereospecificity, induction and metallo-dependence of a microbial hydantoinase. *Biotechnology Letters* 9, 25-30.

Syldatk C., Laufer A., Muller R., & Hoke H. (1990a) Production of optically pure D- and L−α-amino acids by bioconversion of D,L-5-monosubstituted hydantoin derivatives. *Adv.Biochem.Eng.Biotechnol.* 41, 29-75.

Syldatk C., Mackowiak V., Hoke H., Gross C., Dombach G., & Wagner F. (1990b) Cell growth and enzyme synthesis of a mutant of *Arthrobacter* sp. (DSM 3747)used for the production of L-amino acids from D,L-5-monosubstituted hydantoins. *Journal of Biotechnology* 14, 345-362.

Syldatk C., Muller R., Siemann M., Krohn K., & Wagner F. (1992a) Microbial and enzymatic production of D-amino acids from DL-5-monosubstituted hydantoins. *Biocatalytic production of amino acids and derivatives* Hanser Publishers, Munich, 77-206.

Syldatk C., Muller R., Pietzsch M., & Wagner F. (1992b) Microbial and enzymatic production of L-amino acids from DL-5-monosubstituted hydantoins. *Biocatalytic production of amino acids and derivatives* Hanser Publishers, Munich, 131-175.

Syldatk C., May O., Altenbuchner J., Mattes R., & Siemann M. (1999) Microbial hydantoinases - industrial enzymes from the origin of life? *Applied Microbiology and Biotechnology* 51, 293-309.

Syldatk C. & Pietzsch M. (1995) Hydrolysis and formation of hydantoins. in Enzyme catalysis in organic synthesis – A comprehensive handbook. Vol. 1. Eds. Drauz K. & Waldmann H., VCH Publishers Inc. Weinheim, pg 409-431

Takahashi S., Kii Y., Kumagai H., & Yamada H. (1978) Purification, Crystallization and properties of hydantoinase from *Pseudomonas striata*. *Journal of Fermentation Technology* 56, 492-498.

Tanner M.E., Gallo K.A., & Knowles J.R. (1993) Isotope effects and the identification of catalytic residues in the reaction catalysed by glutamate racemase. *Biochemistry* 32, 3998-4006

Thompson J.D., Higgins D.G. & Gibson T.J. (1994) ClustalW: Improving the sensitivity of progressive multiple sequence alignment through sequence weighting, position, specific gap penalties, and weight matrix choice. *Nucleic Acids Research* 22, 4679-4680

Towner K.J. & Cockayne A. (1993) Molecular methods for microbial identification and typing. Chapman &Hall, London

Volkel D. & Wagner F. (1995) Reaction mechanism for the conversion of 5-monosubstituted hydantoins to enantiomerically pure L-amino acids. *Annals of the New York Academy of Sciences* 750, 1-9.

Vreken P., van Kuilenburg A.B., Hamajima N., Meinsma R., van Lenthe H., Gohlich-Ratmann G., Assmann B.E., Wevers R.A. & van Gennip A.H. (1999) cDNA cloning, genomic structure and chromosomal localization of the human BUP-1 gene encoding beta-ureidopropionase. *Biochimica Et Biophysica Acta* 1447: 251-257

Wada M. (1934) Uber die bildung des harnstoffs aus uraminosauren. Hydantoinen und aus eiweisskorpern durch einwirkung von enzymen (reduktasen) in neutraler losung. *Proc. Imp. Acad. Jpn. 10, 17-20*

Wagner T., Hantke B., & Wagner F. (1996) Production of L-methionine from D,L-5-(2-methylthioethyl)hydantoin by resting cells of a new mutant strain of *Arthrobacter* species DSM 7330. *Journal of Biotechnology* 46, 63-68.

Wang W., Hsu W., Chien F., & Chen C. (2001) Crystal structure and site-directed mutagenesis studies of *N*-carbamoyl-D-amino acid amidohydrolase from *Agrobacterium radiobacter* reveals a homotetramer and insight into a catalytic cleft. *Journal of Molecular Biology* 306, 251-261.

Ware E. (1950) The chemistry of hydantoins. *Chem Rev.* 46, 403-470

Warner J.B. & Lolkema J.S. (2003) CcpA-dependent carbon catabolite repression in bacteria. *Microbiology and Molecular Biology Reviews* 67, 475-490

Watabe K., Ishikawa T., Mukohara Y., & Nakamura H. (1992a) Cloning and sequencing of the genes involved in the conversion of 5-substituted hydantoins to the corresponding L-amino acids from the native plasmid of *Pseudomonas* sp. strain NS671. *Journal of Bacteriology* 174, 962-969.

Watabe K., Ishikawa T., Mukohara Y., & Nakamura H. (1992b) Identification and sequencing of a gene encoding a hydantoin racemase from the native plasmid of *Pseudomonas* sp. strain NS671. *Journal of Bacteriology* 174, 3461-3466.

Watabe K., Ishikawa T., Mukohara Y., & Nakamura H. (1992c) Purification and characterization of the hydantoin racemase of *Pseudomonas* sp. Strain NS671 expressed in *Escherichia coli*. *Journal of Bacteriology* 174, 7989-7995.

Weickert M.J., Doherty D.H., Best E.A., & Olins P.O. (1996) Optimisation of heterologous protein production in *Escherichia coli* . *Current Opinion in Biotechnology*. 7, 494-499.

Werner M., Fritz C., Altenbuchner J., Siemann M. and Syldatk C. (2002) Hydantoin utilization genes of Arthrobacter crystallopoietes DSM 20117. Unpublished

West S., Sample A. & Runyen-Janecky L. (1994) The *vfr* gene product, required for *Pseudomonas aeruginosa* exotoxin A and protease production, belongs to the cyclic AMP receptor protein family. *Journal of Bacteriology* 176:7532-7542

Wiese A., Pietzsch M., Syldatk C., Mattes R., & Altenbuchner J. (2000) Hydantoin racemase from *Arthrobacter aurescens* DSM 3747 : Heterologous expression, purification and characterization. *Journal of Biotechnology* 80, 217-230.

Wiese A., Syldatk C., Mattes R., & Altenbuchner J. (2001) Organization of genes responsible for the stereospecific conversion of hydantoins to *a*-amino acids in *Arthrobacter aurescens* DSM 3747. *Archives of Microbiology* 176, 187-196.

Wilms B., Wiese A., Syldatk C., Mattes R., Altenbuchner J., & Pietzsch M. (1999) Cloning, nucleotide sequence and expression of a new L-N-carbamoylase gene from *Arthrobacter aurescens* DSM 3747 in *E. coli*. *Journal of Biotechnology* 68, 101-113.

Wilms B., Hauck A., Reuss M., Syldatk C., Mattes R., Siemann M., & Altenbuchner J. (2001a) High-cell-density fermentation for production of L-*N*-carbamoylase using an expression system based on the *Escherichia coli* rhaBAD promoter. *Biotechnology and Bioengineering* 73, 95-103.

Wilms B., Wiese A., Syldatk C., Mattes R., & Altenbuchner J. (2001b) Development of an *Escherichia coli* whole cell biocatalyst for the production of L-amino acids. *Journal of Biotechnology* 86, 19-30.

Xu G. & West T.P. (1994) Characterization of dihydropyrimidinase from *Pseudomonas stutzeri*. *Archives of Microbiology* 161, 70-74.

Xu Z., Liu Y., Yang Y., Jiang W., Arnold E., & Ding J. (2003a) Crystal structure of D-hydantoinase from *Burkholderia pickettii* at a resolution of 2.7 angstroms: Insights into the molecular basis of enzyme thermostability. *Journal of Bacteriology* 185, 4038-4049.

Xu J., Bjursell M.K., Himrod J., Deng S., Carmichael L.K., Chiang H.C., Hooper L.V. & Gordon J.I. (2003b) A Genomic View of the Human-Bacteroides thetaiotaomicron Symbiosis. *Science* 299: 2074-2076

Yagasaki M., Iwata K., Ishino S., Azuma M, & Ozaki A. (1995) Cloning, purification, and properties of a co-factor-independent glutamate racemase from *Lactobacillus brevis* ATCC 8287. *Bioscience, Biotechnology, and Biochemistry* 59, 610-614

Yagasaki M. & Ozaki A. (1998) Industrial biotransformations for the production of D-amino acids. *Journal of Molecular Catalysis B: Enzymatic* 4, 1-11.

Yamanaka H., Kawamoto T., & Tanaka A. (1997) Efficient preparation of optically active p-trimethylsilylphenylalanine by using cell-free extract of *Blastobacter* sp. A17p-4. *Journal of Fermentation and Bioengineering* 84, 181-184.

Yamashiro A., Yokozeki K., Kano H., & Kubota K. (1988) Enzymatic production of L-amino acids from the corresponding 5-substituted hydantoins by a newly isolated bacterium, *Bacillus brevis* AJ-12299. *Agricultural and Biological Chemistry* 52, 2851-2856.

Yokozeki K., Nakamori S., Eguchi C., Yajima K., & Mitsugi K. (1987a) Screening of microorganisms producing D-p-hydroxyphenylglycine from DL-5-(p-hydroxyphenyl)hydantoin. *Agricultural and Biological Chemistry* 51, 355-362.

Yokozeki K., Nakamori S., Yamanaka S., Eguchi C., Mitsugi K., & Yoshinaga F. (1987b) Optimal conditions for the enzymatic production of D-amino acids from the corresponding 5-substituted hydantoins. *Agricultural and Biological Chemistry* 51, 715-719.

Yokozeki K. & Kubota K. (1987c) Mechanism of asymmetric production of D-amino acids from the corresponding hydantoins by *Pseudomonas* sp. *Agricultural and Biological Chemistry* 51, 721-728.

Yokozeki K., Sano K., Eguchi C., Yamada K., & Mitsugi K. (1987d) Enzymatic production of L-tryptophan from DL-5-indolylmethylhydantoin by mutants of *Flavobacterium* sp. T-523. *Agricultural and Biological Chemistry* 51, 363-369.

Yokozeki K., Hirose Y., & Kubota K. (1987e) Mechanism of assemetric production of L-aromatic amino acids from the corresponding hydantoins by *Flavobacterium* sp. *Agricultural and Biological Chemistry* 51, 737-746

Yuste L. & Rojo F. (2001) Role of the *crc* gene in catabolic repression of the *Pseudomonas putida* Gpo1 alkane degradation pathway. *Journal of Bacteriology* 183:6197-6206

Zaks A. & Dodds D.R. (1997) Application of biocatalysis and biotransformations to the synthesis of pharmaceuticals. *Drug Discovery Today* 2, 513-531

Zhao H., Chockalingam K., & Chen Z. (2002) Directed evolution of enzymes and pathways for industrial biocatalysis. *Current Opinion in Biotechnology* 13, 104-110